UNIVERSITY OF CALIFORNIA
RIVERSIDE

# Estimation in Networked Systems: Power Grid Security and Distributed Hybrid Information Fusion Algorithm

A Dissertation submitted in partial satisfaction
of the requirements for the degree of

Doctor of Philosophy

in

Mechanical Engineering

by

Shaocheng Wang

March 2017

Dissertation Committee:

Dr. Wei Ren, Chairperson
Dr. Elisa Franco
Dr. Fabio Pasqualetti

The Dissertation of Shaocheng Wang is approved:

---

---

---

Committee Chairperson

University of California, Riverside

## Acknowledgments

First and the foremost, I am sincerely grateful to my advisor Prof. Wei Ren. This dissertation would not have been possible without his guidance and supports. I always felt extremely lucky to be his student. In the research, he patiently taught me from scratch and was always willing to help me with any question. His insightful thinking process and rigourous academic attitude have always been affecting me throughout the entire Ph.D. program, and have been offering me the skills of problem solving, innovation and critical thinking. These skills will continue to benefit in my future career. In life, his humble personality reminds me to be always modest and never stop making progress. This will also guide me in the rest of my life to be not only a good researcher, but also a nice person.

I would like to thank Prof. Elisa Franco and Prof. Fabio Pasqualetti, not only for being me committee members and reviewing my dissertation, but also for their help on the way of this journey. Prof. Elisa Franco provided me many opportunities to work as her teaching assistant, from which I obtained tons of teaching experiences and learned how to better present ideas. Prof. Fabio Pasqualetti helped me a lot especially in the early stage of my PhD study, and gave me insightful comments.

I would like to also thank my smart and nice lab colleagues, Sheida Ghapani, Salar Rahili, Peng Wang, Jiahui Lu, Hao Wang and all the visiting scholars. I enjoyed working with them and have learned a lot from them through the discussions and interactions with them. Also thanks to Prof. Qi Zhu's research group members. It was fun to share the research lab with them and to discuss many different interesting topics.

Many thanks to my friends in UCR, Peng Deng, Vaibhav Ghadiok, Shouxu Zhang, Lei Chen, Qiang Wang, Stewart Contreras, Ehsan Tarkesh, Arnab Chowdhury, Vahid Mardanlou. We had so much fun and shared tons of fantastic memories. They made my life in UCR enriched and also help me from many different aspects.

Special thanks to the Foo's family, namely, Helen, Alex and Crystal, for treating me and my families as their own. They help me so much and I would not have got here without their help.

I was very lucky to be born and raised up in a large family. Deep thanks to my relatives in China for their years of endless cares. Specifically, this dissertation is also in memory of my paternal grandmother and my maternal grandfather, who cannot make to witness this moment.

Thanks to my dear wife, Dr. Xie, for not only accompanying and taking care of me during this entire journey, but also providing technical suggestions whenever I encountered difficulties in research. She has always been very supportive and encouraging and has definitely sacrificed a lot to take me here. I would like to also thank her parents for the trust and support.

Finally but most importantly, to my parents, who gave me my life, raised me up and always supported me by providing the best they could have, even with their sacrifices. They expect nothing back from me and only want me to be happy. They are my best friends and life mentors. I was very very lucky to be their son.

To my beloved parents Keqin and Aiping

To my dear son Calman

# ABSTRACT OF THE DISSERTATION

Estimation in Networked Systems: Power Grid Security and Distributed Hybrid Information Fusion Algorithm

by

Shaocheng Wang

Doctor of Philosophy, Graduate Program in Mechanical Engineering
University of California, Riverside, March 2017
Dr. Wei Ren, Chairperson

This dissertation studies two topics related to the problem of estimation in networked systems, namely, the problem of secure state estimation against possible stealthy false data injection attacks in electric power network, and the problem of distributed dynamic state estimation using networked local multi-agents. The two topics are, respectively, presented in Part I and Part II.

The study in Part I is motivated by the importance of the state estimation in electric power systems as many applications such as Optimal Power Flow, Automatic Generation Control and Contingency Analysis are highly dependent on the state estimation. Therefore, it is critical to have an accurate and reliable estimate of the states as bad estimates will offer the system operator with inaccurate information about the system, which may cause wrong decisions and finally, cause malfunction or even power blackout in the network. The stealthy attack, as a strategically designed false data injection attack against the power system state estimation mechanism, is able to let the corrupted measurements bypass residue-based bad data detectors with the same probability as that of uncorrupted measurements, and to fool the system operator with the deviated estimates. While most of the existing articles assume the network topology to be fixed, the effects of switching topolo-

gies on such an attack is shown in this work. In Part I, a new mechanism is proposed to eliminate the possibility of such an attack via strategically shutting down some preselected transmission lines by turns and therefore switching the network topologies. The necessary and sufficient condition to achieve such elimination, as well as the general form of possible attacks when the elimination is impossible, are both formulated. The case where the attack is only stealthy in a subset of the preselected is also studied. The general form of the possible estimate deviations caused by this "partially" stealthy attack is derived. Simulations and case studies are provided using different IEEE bus systems to show the efficiency of the proposed strategy, to discuss the countermeasures in the case when there always exist possible stealthy attacks, and to show how the possible deviations introduced by a "partially" stealthy attack could be affected by the decisions made by both the attacker and the system operator.

Part II studies the problem of distributed dynamic state estimation using networked local agents with sensing and communication abilities. This problem has become a popular research area in recent years due to its wide range of applications such as target tracking, region monitoring and area surveillance. Specifically, Part II considers the scenario where the local agents take local measurements and communicate with only their nearby neighbors to estimate the state of interest in a cooperative and fully distributed manner. A *distributed hybrid information fusion* (DHIF) algorithm is proposed in the scenario where the process model of the target and the sensing models of the local agents are linear and time varying. The proposed DHIF algorithm is shown to be fully distributed and hence scalable, to be run in an automated manner and hence adaptive to locally unknown changes in the network, to have agents communicate for only once during each sampling time interval and hence inexpensive in communication, and to be able to track the interested state

with uniformly upper bounded estimate error covariance. It is also explored the very mild conditions on general directed time-varying graphs and joint network observability/detectability to guarantee the stochastic stability of the proposed algorithm. Then the DHIF algorithm is extended to two more general scenarios, namely, the scenario with nonlinearities involved in both the process and the sensing models, and the scenario with uncertain process models. In the former scenario, a nonlinear DHIF algorithm is proposed by adopting the unscented transformation approach. In the latter one, two algorithms are proposed by following the two well-known multiple model (MM) paradigms, namely, the first order generalized pseudo Bayesian and the interacting MM approaches. The extended algorithms in both scenarios inherit the aforementioned advantages of the original DHIF algorithm. The stability is also rigorously analyzed in each extended case with sufficient conditions formulated.

# Contents

# List of Figures

# List of Tables

# Part I

# Effects of Switching Network Topologies on Stealthy False Data Injection Attacks Against State Estimation in Power Grids

# Chapter 1

# Introduction

## 1.1 Overview & Related Works

The electric power system, as arguably one of the most complicated engineered systems, plays a vital role in the modern life. As a result, its reliability becomes a big concern. The Supervisory Control and Data Acquisition (SCADA) system is in charge of monitoring and controlling the power system. The SCADA system obtains measurements through the remote terminal units (RTUs), and then sends them to a state estimator. The state estimator processes these measurements, which are usually redundant, and estimates the unknown states in the network. The system operator uses these estimated states as a critical reference to gain knowledge of the system and make next-step decisions. Some applications such as Optimal Power Flow, Automatic Generation Control and Contingency Analysis are highly dependent on the state estimation [1]. Therefore, it is critical to have an accurate and reliable estimate of the states. Bad estimates will offer the system operator with inaccurate information about the system, which may cause wrong decisions and finally, cause malfunction or even power blackout in the network.

The idea of the smart grid has gained significant attention and is regarded as the future tendency of the current electric power network. While it has the advantage of providing a better "situational awareness" by using communications and intelligent technologies [17, 51], its expansion of the information infrastructures also brings vulnerabilities and shortcomings [54]. The false data injection attack (FDIA) in power systems, which injects malicious data into the measurements in order to fool the system operator with the deviated state estimates, was first proposed and studied in [50]. However, since a power system is usually equipped with a residue-based bad data alarm, in general, injected false data with a significant magnitude will easily drive the value of the residue function above the predefined threshold and therefore trigger the alarm. Therefore, the stealthy attack, which is a strategically designed FDIA whose injection is able to bypass the residue-based bad data alarm whenever the uncorrupted measurements are able to pass it, has gained significant attention [12,16,41,63,66,67,69]. The authors in [12] considered from the system operator's perspective and showed the possibility to disable the stealthy attack by either protecting a set of measurements or independently verifying a set of states. However, such strategies can be costly since with an increasing size of the network, they will require an increasing number of either protections on the measurements or independent verifications of the states.

One of the most well-known topics in the studies of stealthy attacks is the *security index* problem first studied in [66]. The security index is a benchmark to quantify the least effort required in order to corrupt each measurement by stealthy attacks. The authors in [16] proposed algorithms to maximize the system security against such attacks with a limited encryption source. In [67], the authors formulated the *k-tuple* problem, and proved its equivalence with the security index problem under appropriate assumptions. Both the security index and the k-tuple problems are essentially

cardinality minimization problems. Due to the non-convexity of such problems, no solution has been found that is both accurate and computationally efficient. The authors in [41] accurately characterized the security index via a graphical approach, but it was computationally expensive. An exact solution via the $\ell_1$-relaxation was provided in [69], but it was only for a special case where no power injection measurements were considered. In [67], two approaches, namely, the *minimum-cut* and the *mixed integer linear programming* (MILP), were offered to solve the k-tuple problem. The former method was computationally efficient but only gave a suboptimal solution while the latter one returned an exact result but was computationally expensive.

Besides the security index like problems, the authors in [68] proposed schemes to detect and identify stealthy attacks by considering the information from both active and reactive power measurements. The possibilities of the stealthy attacks with uncertain knowledge of some transmission line admittances were studied in [63]. In [86] and [28], the authors showed that the FDIA was able to lead to financial misconduct in electric market operations and can be used to make profits. Besides the FDIA, some other attacks aimed to waste as much energy as possible are proposed in [62].

## 1.2 Motivation

Although most results in the existing literature assume a fixed topology for the power network, the topology can be changed for multiple reasons. The positions of the transformer taps may change from time to time, which change the admittance on the transmission lines (see for example [63]). The connections among the buses can be changed either intentionally (switching on/off the circuit breakers) or passively (line failures). In recent years, with the trend of including

more distributed energy sources, the concept of microgrids was proposed. This motivates the study of intentionally scheduled connection/isolation of the microgrids to/from the main grid (see for examples [25, 42]).

## 1.3 Contributions

In Part I of this dissertation, it is assumed that an attacker aims to fool the system operator with deviated state estimates by launching a stealthy attack. A novel approach is characterized to eliminate the possibility of such an attack by intentionally switching on/off some preselected transmission lines by turns and therefore changing the network topologies by expanding on our preliminary results reported in [78, 79]. Here we assume that the transient stability of the system can be guaranteed during the alternations among the preselected topologies, and only consider the network at the steady state for each topology. The necessary and sufficient conditions that the topologies selected by the system operator have to satisfy to eliminate the existence of stealthy attacks, are proposed. In the case when these conditions are not satisfied, the general form of all possible stealthy attacks is formulated. In the case when these conditions are satisfied, a scenario, where the attacker makes a concession and launches an attack that is only stealthy in some of the preselected topologies, is further considered. It is analytically shown that as this attack is stealthy in more topologies, it has increasingly limited flexibilities in deviating the state estimates. The general form of feasible deviations that can be introduced by this partially stealthy attack is also formulated. In the end, simulations are provided to show the efficiency of the proposed defense strategy against stealthy attacks. Several cases are studied to show how the limitation on the deviations that could

be possibly introduced by the stealthy attacks, is related to the decisions made by both the attacker and the system operator.

## 1.4 Organization

The rest of Part I is organized as follows. Chapter 2 provides some preliminary knowledge on the graph theory, state estimator and attack detections, and formulates the problem of interest. Chapter 3 proposes a new mechanism to eliminate the possibility of a mutually stealthy attack in all preselected topologies, and formulates the necessary and sufficient condition to achieve such an elimination. The impacts of the proposed strategy of switching topologies on the power generation cost is also discussed. The case where the attack is only stealthy in a subset of the preselected is then studied in Chapter 4, where the general form of the possible estimate deviations caused by this "partially" stealthy attack is derived. Simulations and case studies are provided in Chapter 5 to illustrate the results proposed in Chapter 3 and 4.

# Chapter 2

# Background

**Notations**. Throughout Part I, the notations are defined as follow. The MATLAB traditions are used to denote the entries of a matrix/vector. For example, $\mathbf{X}(i,j)$ is the $i$th row, $j$th column of matrix $\mathbf{X}$. $\mathbf{X}(:,j)$ is the $j$th column of matrix $\mathbf{X}$. $\mathbf{y}(i)$ is the $i$th entry of vector $\mathbf{y}$. $\mathbf{0}_n \in \mathbb{R}^n$ is a zero vector. $\mathbf{0}$ is a zero matrix with appropriate size. $\mathbf{1}$ is an all-one vector with appropriate dimension. $|\cdot|$ denotes the cardinality of a set. blkdiag$(\cdot)$ denotes the block diagonal matrix formed by input matrices. "$\sim$" denotes the elementary row/column operations of matrices.

## 2.1 Preliminaries

### 2.1.1 Graph Theory Background

The topology of a power network can be described by a graph $\mathscr{G}(\mathscr{V},\mathscr{E})$, where $\mathscr{V}$ and $\mathscr{E} \subseteq \mathscr{V} \times \mathscr{V}$ are, respectively, the set of vertices/nodes which stands for the buses, and the set of edges/links which stands for the transmission lines. Throughout Part I, the terms bus and node will be used interchangeably. The terms link and transmission line will also be used interchangeably.

Due to the fact that power delivered on each transmission line is bidirectional, the graph for describing the power network is undirected. A *path* from node $v_{i_0}$ to node $v_{i_k}$ is a sequence of nodes $v_{i_0},\ldots,v_{i_k}$ such that $(v_{i_j},v_{i_{j+1}})\in\mathscr{E}$ for $0\leq j<k$. A *circle* is a path that starts and ends at the same node. A graph is *connected* if there exists at least one path from every node to every other node. A graph is *disconnected* if it is not connected. A *spanning tree*[1] is a minimal set of links that connect all nodes. A graph $\mathscr{G}(\mathscr{V}',\mathscr{E}')$ is a *subgraph* of $\mathscr{G}(\mathscr{V},\mathscr{E})$ if $\mathscr{V}'\subseteq\mathscr{V}$ and $\mathscr{E}'\subseteq\mathscr{E}$. A *component* of $\mathscr{G}(\mathscr{V},\mathscr{E})$ is a subgraph of $\mathscr{G}(\mathscr{V},\mathscr{E})$ that is maximal with respect to the property of being connected.

Besides the above well-known concepts used in graph theory, the following two definitions will also be used later on.

**Definition 2.1 (Bridge link)** *A link $e_i$ is a* bridge link *if the graph $\mathscr{G}(\mathscr{V},\mathscr{E})$ has fewer components than $\mathscr{G}(\mathscr{V},\mathscr{E}\setminus\{e_i\})$.*

**Definition 2.2 (Cycle graph [24])** *A graph is a* cycle graph *if it contains the same number of nodes and links, all on a single circle.*

For instance, the graph shown in Figure 2.1(a) is a cycle graph. For another instance, in the graph shown in Figure 2.1(b), $e_8$ is a bridge link as removing $e_8$ breaks the graph into two components.

Throughout out Part I, without loss of generality, it is assumed that the power network associated with $\mathscr{G}(\mathscr{V},\mathscr{E})$ contains $n+1$ buses and $l$ transmission lines. Therefore, $\mathscr{V}=\{v_1,\ldots,v_{n+1}\}$ and $\mathscr{E}=\{e_1,\ldots,e_l\}$. A directed incidence matrix $\mathbf{A}_0\in\mathbb{R}^{(n+1)\times l}$ can be defined to describe the topology. After arbitrarily assigning the direction of each transmission line (without loss of generality), the entries of $\mathbf{A}_0$ are determined in the following way. For each link $e_j$, the entry in the $i$th

[1] Here we focus on the spanning tree in an undirected graph.

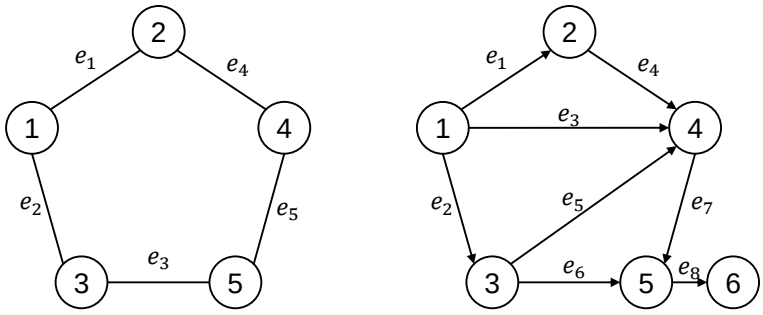


(a) cycle graph (b) graph with bridge link

Figure 2.1: Examples of network topologies

row and $j$th column of $\mathbf{A}_0$ is $\mathbf{A}_0(i,j) = 1$ if the direction of $e_j$ starts at bus $i$, $\mathbf{A}_0(i,j) = -1$ if the direction of $e_j$ ends at bus $i$, and $\mathbf{A}_0(i,j) = 0$ otherwise.

In the power network, in order to study the phase angle of each bus, one bus is required to be arbitrarily selected as the reference bus. The phase angle of the reference bus is assumed to be zero so that the phase angles of the other buses are measured with respect to the reference bus. Then the truncated incidence matrix $\mathbf{A} \in \mathbb{R}^{n \times l}$ is defined by removing the row of $\mathbf{A}_0$ corresponding to the reference bus.

Using the topology shown in Figure 2.1(b) as an example, where $n = 5$ and $l = 8$. Let the direction of each link be assigned as shown in the figure. Then the incidence matrix $\mathbf{A}_0$ can be written as

$$\mathbf{A}_0 = \left[\begin{array}{cccccccc} 1 & 1 & 1 & 0 & 0 & 0 & 0 & 0 \\ \hline -1 & 0 & 0 & 1 & 0 & 0 & 0 & 0 \\ 0 & -1 & 0 & 0 & 1 & 1 & 0 & 0 \\ 0 & 0 & -1 & -1 & -1 & 0 & 1 & 0 \\ 0 & 0 & 0 & 0 & 0 & -1 & -1 & 1 \\ 0 & 0 & 0 & 0 & 0 & 0 & 0 & -1 \end{array}\right].$$

Let bus 1 be the reference bus. The truncated incidence matrix can be obtained by removing the first row of $\mathbf{A}_0$ shown above.

Some fundamental properties of $\mathbf{A}$ and $\mathbf{A}_0$ are listed in the following lemma.

**Lemma 2.3 (properties of A and $\mathbf{A}_0$)**

*i)* *rank*$(\mathbf{A}_0) =$ *rank*$(\mathbf{A})$, *where rank*$(\cdot)$ *denotes the rank of a matrix;*

*ii)* $\mathbf{1} \in$ *Null*$(\mathbf{A}_0^\top)$, *where* $\mathbf{1} \in \mathbb{R}^{|\mathscr{V}|}$ *is an all one vector, and Null*$(\cdot)$ *denotes the null space of a matrix;*

*iii)* $\mathscr{G}(\mathscr{V},\mathscr{E})$ *is connected* if and only if *rank*$(\mathbf{A}_0) = n$;

*iv)* $\mathscr{G}(\mathscr{V},\mathscr{E})$ *is disconnected with k components* if and only if *rank*$(\mathbf{A}_0) = n-k+1$.

### 2.1.2 State Estimation in the DC Power Model

The DC power model, which is derived from the AC power model with appropriate assumptions [1], is commonly adopted for the study of power systems [12, 16, 41, 50, 66, 67, 69]. Let $\mathbf{x} \in \mathbb{R}^n$ be the collection of states of all buses except for the reference bus. Specifically, the states are the phase angles of all other buses relative to the reference bus. Let $\mathbf{z} \in \mathbb{R}^m$ be the collection of measurements including both the power flow on each transmission line and the power injection or load at each bus except for the reference bus. Let $\mathbf{H} \in \mathbb{R}^{m\times n}$ be the measurement matrix associated with the graph $\mathscr{G}(\mathscr{V},\mathscr{E})$. Then the relation between the states and the measurements can be written as

$$\mathbf{z} = \mathbf{H}\mathbf{x} + \mathbf{w},$$

where $\mathbf{w} \in \mathbb{R}^m$ stands for the measurement noise. In this work, it is assumed that only one measurement can be obtained on each transmission line or bus and hence $m = l + n$. Let $\mathbf{D} = \text{diag}(d_1, \ldots, d_l) \in \mathbb{R}^{l \times l}$ be a diagonal matrix with nonzero diagonal entries $d_i$. Here $d_i$ describes the admittance of the $i$th transmission line, $\forall i \in \{1, \ldots, l\}$. Then the measurement matrix $\mathbf{H}$ associated with the graph $\mathscr{G}(\mathscr{V}, \mathscr{E})$ has the form of

$$\mathbf{H} \triangleq \begin{bmatrix} \mathbf{DA}^\top \\ \\ \mathbf{ADA}^\top \end{bmatrix}. \tag{2.1}$$

The following lemma shows the relation between the ranks of $\mathbf{H}$ and $\mathbf{A}$.

**Lemma 2.4** *rank*$(\mathbf{H}) =$ *rank*$(\mathbf{A})$.

**Proof.** It is clear that each row of $\mathbf{ADA}^\top$ is linear dependent on the rows of $\mathbf{DA}^\top$. Thus it follows that $\text{rank}(\mathbf{H}) = \text{rank}(\mathbf{DA}^\top)$. Since $\mathbf{D}$ is nonsingular, it follows that $\text{rank}(\mathbf{DA}^\top) = \text{rank}(\mathbf{A}^\top) = \text{rank}(\mathbf{A})$. ■

Assume that $\mathbf{w}$ is a white Gaussian noise with its covariance matrix $\mathbf{R}$. The weighted least-square, minimum variance and maximum likelihood estimation criteria will yield the same estimator as

$$\hat{\mathbf{x}} = (\mathbf{H}^\top \mathbf{W} \mathbf{H})^{-1} \mathbf{H}^\top \mathbf{W} \mathbf{z},$$

where $\hat{\mathbf{x}} \in \mathbb{R}^n$ is the estimate of $\mathbf{x}$ and $\mathbf{W} = \mathbf{R}^{-1}$ is the weighting matrix.

### 2.1.3 Stealthy Attack against Bad Data Detection

A bad data detector is designed to defend against bad data that may be caused by multiple reasons such as meter failures or malicious attacks. The residue-based bad data detectors are usually

denoted as a function $\mathfrak{J}(\mathbf{r})$, where $\mathbf{r}$ is the residue defined as $\mathbf{r} \triangleq \mathbf{z} - \mathbf{H}\hat{\mathbf{x}}$. Examples include the $\chi^2$-detector or the largest normalized residual test (LNRT). The residue-based detectors are proposed based on the intuition that abnormal data will drive the estimated states away from their true values. That is, the alarm is triggered if $\mathfrak{J}(\mathbf{r}) \geq \tau$, where the threshold $\tau$ is designed according to the desired percentage of the false alarm rate. When false data are injected to the measurement observed by the system operator [50], instead of observing the true measurement $\mathbf{z}$, the operator is only able to observe the corrupted measurement $\mathbf{z}_{\text{bad}} \triangleq \mathbf{z} + \mathbf{z}_a$, where $\mathbf{z}_a$ is the injected false data. Let $\hat{\mathbf{x}}_{\text{bad}}$ be the corrupted estimate of $\mathbf{x}$. Let $\Delta\hat{\mathbf{x}}$ be the estimation deviation introduced by the attacker, *i.e.,* $\Delta\hat{\mathbf{x}} = \hat{\mathbf{x}}_{\text{bad}} - \hat{\mathbf{x}}$. The stealthy attack is defined as a special case of the FDIA when the attacker selects $\mathbf{z}_a = \mathbf{H}\delta$, where $\delta \in \mathbb{R}^n$ is an arbitrary vector selected by the attacker. It follows that

$$\begin{aligned}\Delta\hat{\mathbf{x}} = \hat{\mathbf{x}}_{\text{bad}} - \hat{\mathbf{x}} &= (\mathbf{H}^\top\mathbf{W}\mathbf{H})^{-1}\mathbf{H}^\top\mathbf{W}\mathbf{z}_{\text{bad}} - (\mathbf{H}^\top\mathbf{W}\mathbf{H})^{-1}\mathbf{H}^\top\mathbf{W}\mathbf{z} \\ &= (\mathbf{H}^\top\mathbf{W}\mathbf{H})^{-1}\mathbf{H}^\top\mathbf{W}\mathbf{z}_a = (\mathbf{H}^\top\mathbf{W}\mathbf{H})^{-1}\mathbf{H}^\top\mathbf{W}\mathbf{H}\delta = \delta.\end{aligned}$$

That is, by injecting the false data $\mathbf{z}_a$ such that $\mathbf{z}_a = \mathbf{H}\delta$, the attacker is able to deviate the estimated states away from the uncorrupted estimates by $\Delta\hat{\mathbf{x}} = \delta$. Let $\mathbf{r}_{\text{bad}} \triangleq \mathbf{z}_{\text{bad}} - \mathbf{H}\hat{\mathbf{x}}_{\text{bad}}$ be the residue when the measurement is corrupted by the attack. It follows that for any residue-based detector,

$$\mathfrak{J}(\mathbf{r}_{\text{bad}}) = \mathfrak{J}(\mathbf{z}_{\text{bad}} - \mathbf{H}\hat{\mathbf{x}}_{\text{bad}}) = \mathfrak{J}\left[(\mathbf{z} + \mathbf{z}_a) - \mathbf{H}(\hat{\mathbf{x}} + \Delta\hat{\mathbf{x}})\right] = \mathfrak{J}\left(\mathbf{z} - \mathbf{H}\hat{\mathbf{x}}\right) = \mathfrak{J}\left(\mathbf{r}\right).$$

This implies that $\mathbf{z}_{\text{bad}}$ will have the same possibility of triggering the bad data alarm, as that of $\mathbf{z}$. In summary, a stealthy attack requires $\mathbf{z}_a \in \text{Im}(\mathbf{H})$, where $\text{Im}(\cdot)$ stands for the column space of a matrix.

## 2.2 Problem Formulation

### 2.2.1 Switching Topology Scenario

While the network topology is assumed to be fixed in most existing articles, the scenario where the network topologies are switching, is considered in this work. In this work, it is assumed that the system operator is able to purposely switch on/off some of the selected transmission lines by turns. Therefore, the network topologies can be different over time. Considering the potential issues on the generation-demand balance that might be caused by switching off some transmission lines, we do not allow multiple lines to be switched off simultaneously.

Let $\mathscr{E}_{\backslash i} \triangleq \mathscr{E} \setminus \{e_i\}$. Then $\mathscr{G}(\mathscr{V}, \mathscr{E}_{\backslash i})$ is the graph of the network when the $i$th transmission line is switched off. Therefore its associated truncated incidence matrix $\mathbf{A}_{\backslash i}$ should have one less column than $\mathbf{A}$. However, to simplify the proof later on, without loss of generality, let $\mathbf{A}_{\backslash i}$ be the same as $\mathbf{A}$ except that the $i$th column has all zeros. With $\mathbf{A}_{\backslash i}$ playing the role of $\mathbf{A}$ in Eq. (2.1), the measurement matrix $\mathbf{H}_{\backslash i}$ associated with $\mathscr{G}(\mathscr{V}, \mathscr{E}_{\backslash i})$ can be defined analogously. Note that the $i$th row of $\mathbf{H}_{\backslash i}$ has all zeros.

### 2.2.2 Assumptions & Objectives

In this work, the system operator is assumed to be able to switch the network topologies by switching off one of the preselected transmission lines (*i.e.,* cutting off one of the preselected links in $\mathscr{G}(\mathscr{V}, \mathscr{E})$). To the best of the authors' knowledge, this is the first work to consider the case where the network topology of the power system is switching. As the first step to study this scenario, it is assumed that the transient stability of the system can be guaranteed during the alternations among preselected topologies, and only consider the network at the steady state for each topology.

From the attacker's perspective, it is assumed that the attacker has full knowledge of all preselected topologies, but does not know which topology is being adopted. Besides the knowledge of all possible topologies, the attacker is also able launch an attack by compromising a set of measurements that are not encrypted [12].

Throughout Part I, let $\mathfrak{p} = \{i_1, \cdots, i_p\}$ be a set of link indices such that $\mathscr{E}_{\mathfrak{p}} \triangleq \{e_i | i \in \mathfrak{p}\}$ denotes the set of links preselected by the operator to cut by turns. Since the attacker does not know which topology is being adopted, it has to guarantee that $\mathbf{z}_a \in \mathrm{Im}(\mathbf{H}_{\setminus i})$, $\forall i \in \mathfrak{p}$, or equivalently, $\mathbf{z}_a \in \bigcap_{i\in\mathfrak{p}} \mathrm{Im}(\mathbf{H}_{\setminus i})$. It is clear that if $\mathbf{z}_a \in \bigcap_{i\in\mathfrak{p}} \mathrm{Im}(\mathbf{H}_{\setminus i})$, the corrupted measurements are able to pass the residue-based false data detector whenever the uncorrupted measurements could pass it, regardless of which topology is being adopted. Therefore, from the system operator's perspective, in order to guarantee that no such $\mathbf{z}_a$ exists, it has to guarantee the satisfaction of the following condition:

$$\dim\left(\bigcap_{i\in\mathfrak{p}} \mathrm{Im}(\mathbf{H}_{\setminus i})\right) = 0, \tag{2.2}$$

where $\dim(\cdot)$ stands for the dimension of a matrix subspace. Therefore, the selection of the link set $\mathscr{E}_{\mathfrak{p}}$ is critical for the system operator. The following questions are considered.

a) Is it possible to find a set of measurement matrices such that Eq. (2.2) can be satisfied? If yes, what are the conditions on the set of topologies associated with this set of measurement matrices; and what if the attacker launches only a "partially" stealthy attack? If no, what are the vulnerable measurements; and whether there exists any countermeasure?

b) In either cases (yes or no), what are the possible estimation deviations?

# Chapter 3

# Stealthy Attack in Power Networks with Switching Topologies

This chapter studies that under what condition(s) there exists an attack that is stealthy in all preselected switching topologies. It also discusses the impacts of the proposed switching topologies on the power generation cost.

## 3.1 Existence of Stealthy Attack in Power Networks with Switching Topologies

The necessary and sufficient condition for the possibility of a mutually stealthy attack in all preselected topologies, is formulated in this section. Several lemmas that will be used later on are stated first.

**Lemma 3.1 ( [71])** *The dimension of the intersected column space among k measurement matrices can be computed by*

$$dim\left(\bigcap_{i=j_1}^{j_k} Im(\mathbf{H}_{\backslash i})\right) = \sum_{i=j_1}^{j_k} rank(\mathbf{H}_{\backslash i}) - rank\left(\mathbb{H}\right), \tag{3.1}$$

*where*

$$\mathbb{H} \triangleq \left[\begin{array}{c|ccc} \mathbf{H}_{\backslash j_1} & \mathbf{H}_{\backslash j_2} & & \\ \vdots & & \ddots & \\ \mathbf{H}_{\backslash j_1} & & & \mathbf{H}_{\backslash j_k} \end{array}\right].$$

The proof of Lemma 3.1 follows from [71]. This lemma is a generalization of the well-known formula $\dim(\mathrm{Im}(\mathbf{X} \cap \mathrm{Im}(\mathbf{Y})) = \mathrm{rank}(\mathbf{X}) + \mathrm{rank}(\mathbf{Y}) - \mathrm{rank}([\mathbf{X}|\mathbf{Y}])$, which computes the dimension of intersected column spaces of two matrices $\mathbf{X}$ and $\mathbf{Y}$. Lemma 3.1 offers an efficient tool for proving our main theorem.

**Lemma 3.2** $rank([\mathbf{H}_{\backslash i}|\mathbf{H}_{\backslash j}]) = rank([\mathbf{A}^\top_{\backslash i}|\mathbf{A}^\top_{\backslash j}])$.

**Proof.** Let $\mathbf{a}_i$ be the $i$th column of the truncated incidence matrix $\mathbf{A}$, *i.e.,* $\mathbf{a}_i \triangleq \mathbf{A}(:,i)$. Note that

$$\mathbf{A}_{\backslash i}\mathbf{D}\mathbf{A}^\top_{\backslash i} = \sum_{k=1,k\neq i}^{l} d_k \mathbf{a}_k \mathbf{a}_k^\top = \sum_{k=1,k\neq i}^{l} d_k \mathbf{a}_k \mathbf{a}_k^\top + d_i \mathbf{a}_i \mathbf{0}_n^\top = \mathbf{A}\mathbf{D}\mathbf{A}^\top_{\backslash i}.$$

Therefore, it follows from the definition in Eq. (2.1) that,

$$\left[\mathbf{H}_{\backslash i}|\mathbf{H}_{\backslash j}\right] = \left[\begin{array}{c|c} \mathbf{D}\mathbf{A}^\top_{\backslash i} & \mathbf{D}\mathbf{A}^\top_{\backslash j} \\ \mathbf{A}_{\backslash i}\mathbf{D}\mathbf{A}^\top_{\backslash i} & \mathbf{A}_{\backslash j}\mathbf{D}\mathbf{A}^\top_{\backslash j} \end{array}\right] = \left[\begin{array}{c|c} \mathbf{D}\mathbf{A}^\top_{\backslash i} & \mathbf{D}\mathbf{A}^\top_{\backslash j} \\ \mathbf{A}\mathbf{D}\mathbf{A}^\top_{\backslash i} & \mathbf{A}\mathbf{D}\mathbf{A}^\top_{\backslash j} \end{array}\right].$$

By left multiplying $-\mathbf{A}$ to the first row block, and adding the obtained row block to the second row block, it follows that

$$\left[\begin{array}{c|c} \mathbf{D}\mathbf{A}^\top_{\backslash i} & \mathbf{D}\mathbf{A}^\top_{\backslash j} \\ \mathbf{A}\mathbf{D}\mathbf{A}^\top_{\backslash i} & \mathbf{A}\mathbf{D}\mathbf{A}^\top_{\backslash j} \end{array}\right] \sim \left[\begin{array}{c|c} \mathbf{D}\mathbf{A}^\top_{\backslash i} & \mathbf{D}\mathbf{A}^\top_{\backslash j} \\ \mathbf{0} & \mathbf{0} \end{array}\right].$$

As $\mathbf{D}$ is a diagonal matrix with nonzero diagonal entries and therefore full rank, it follows that

$$\text{rank}([\mathbf{H}_{\setminus i}|\mathbf{H}_{\setminus j}]) = \text{rank}([\mathbf{D}\mathbf{A}_{\setminus i}^{\top}|\mathbf{D}\mathbf{A}_{\setminus j}^{\top}]) = \text{rank}(\mathbf{D}[\mathbf{A}_{\setminus i}^{\top}|\mathbf{A}_{\setminus j}^{\top}]) = \text{rank}([\mathbf{A}_{\setminus i}^{\top}|\mathbf{A}_{\setminus j}^{\top}]),$$

where the fact that, $\text{rank}(\mathbf{XY}) = \text{rank}(\mathbf{Y})$ for any arbitrary matrix $\mathbf{Y}$ and full-rank square matrix $\mathbf{X}$, is used to obtain the last equality. ■

**Lemma 3.3** *Let $\mathbb{H}$ be the matrix defined in Lemma 3.1. Then rank$(\mathbb{H})$ = rank$(\mathbb{A})$, where*

$$\mathbb{A} \triangleq \left[\begin{array}{c|ccc} \mathbf{A}_{\setminus j_1}^{\top} & \mathbf{A}_{\setminus j_2}^{\top} & & \\ \vdots & & \ddots & \\ \mathbf{A}_{\setminus j_1}^{\top} & & & \mathbf{A}_{\setminus j_k}^{\top} \end{array}\right].$$

The proof of Lemma 3.3 can be obtained by applying similar row operations to each row block of $\mathbb{A}$ as in the proof of Lemma 3.2 and is hence omitted here.

Throughout this work, $\mathscr{G}(\mathscr{V},\mathscr{E})$ is assumed to be connected. We also define a set of link indices $\mathfrak{b} \subseteq \{1,\cdots,l\}$ such that, $\forall i \in \{1,\cdots,l\}$, $i \in \mathfrak{b}$ if $e_i$ is a bridge link and $i \notin \mathfrak{b}$ otherwise. Note that if $i \notin \mathfrak{b}$, the graph $\mathscr{G}(\mathscr{V},\mathscr{E}_{\setminus i})$ is still connected. Therefore, according to Lemma 2.3, $\text{rank}(\mathbf{A}_{\setminus i}) = \text{rank}(\mathbf{A})$, $\forall i \notin \mathfrak{b}$. Now the main result is stated as follows.

**Theorem 3.4** *Suppose that $\mathscr{G}(\mathscr{V},\mathscr{E})$ is not a cycle graph. Then* $\dim\left(\bigcap_{i\in\mathfrak{p}} Im(\mathbf{H}_{\setminus i})\right) = 0$ if and only if $\mathscr{E}_{\mathfrak{p}}$ *contains a spanning tree of $\mathscr{G}(\mathscr{V},\mathscr{E})$.*

**Proof.** (Sufficiency). Suppose that $\mathscr{E}_{\mathfrak{p}}$ contains a spanning tree of $\mathscr{G}(\mathscr{V},\mathscr{E})$, it follows that $p \geq n$. Therefore the sufficiency part can be proved by showing $\dim\left(\bigcap_{i\in\mathfrak{n}} \text{Im}(\mathbf{H}_{\setminus i})\right) = 0$, where $\mathfrak{n} \subseteq \mathfrak{p}$ is an index set such that $|\mathfrak{n}| = n$ and $\mathscr{E}_{\mathfrak{n}} \triangleq \{e_i | i \in \mathfrak{n}\}$ forms a spanning tree in $\mathscr{G}(\mathscr{V},\mathscr{E})$. Let $\mathfrak{n} = \{j_1,\cdots,j_n\}$. Let $\mathbb{H}$ and $\mathbb{A}$ be the matrices defined in, respectively, Lemma 3.1 and Lemma 3.3 with $n$ playing the role of $k$. By applying Lemma 2.4 with $\mathbf{H}_{\setminus i}$ and $\mathbf{A}_{\setminus i}$ playing the roles of, respectively, $\mathbf{H}$

and $\mathbf{A}$, one can obtain that $\operatorname{rank}(\mathbf{H}_{\setminus i}) = \operatorname{rank}(\mathbf{A}_{\setminus i})$. By Lemma 3.3, $\operatorname{rank}(\mathbb{A}) = \operatorname{rank}(\mathbb{H})$. Therefore, by Lemma 3.1, the sufficiency part can be proved by showing $\sum_{i\in\mathfrak{n}} \operatorname{rank}(\mathbf{A}_{\setminus i}) = \operatorname{rank}(\mathbb{A})$. This is achieved by three steps.

(Step 1: Elementary row/column operations on $\mathbb{A}$). By subtracting the first column block of $\mathbb{A}$ by its $i$th block column, for each $i \in \{j_2, \cdots, j_n\}$, it follows that

$$\mathbb{A} \sim \left[\begin{array}{c|ccc} \mathbf{A}_{\setminus j_1}^\top - \mathbf{A}_{\setminus j_2}^\top & \mathbf{A}_{\setminus j_2}^\top & & \\ \vdots & & \ddots & \\ \mathbf{A}_{\setminus j_1}^\top - \mathbf{A}_{\setminus j_n}^\top & & & \mathbf{A}_{\setminus j_n}^\top \end{array}\right] \triangleq \mathbb{A}'.$$

Note that for each $i \in \{j_2, \cdots, j_n\}$, $\mathbf{A}_{\setminus j_1}^\top - \mathbf{A}_{\setminus j_i}^\top$ contains only two nonzero rows. Specifically, it has its first row being $-\mathbf{a}_{j_1}^\top$ and the $i$th row being $\mathbf{a}_i^\top$, where $\mathbf{a}_i$ is defined in the proof of Lemma 3.2. Meanwhile, for each $i \in \{j_2, \cdots, j_n\}$, it is satisfied that $\mathbf{A}_{\setminus i}(:, j_1) = \mathbf{a}_{j_1}$ and $\mathbf{A}_{\setminus i}(:, i) = \mathbf{0}_n$. Let $\mathbf{B}_{\setminus i} \in \mathbb{R}^{n\times(l-2)}$ be the matrix obtained by removing the $j_1$th and the $i$th columns of $\mathbf{A}_{\setminus i}$, $\forall i \in \{j_2, \cdots, j_n\}$. Therefore, by collecting the rows in $\mathbb{A}'$ correspond to the $j_1$th and $i$th row of $\mathbf{A}_{\setminus 1}^\top - \mathbf{A}_{\setminus i}^\top$, for each $i \in \{j_2, \cdots, j_n\}$, and rearranging the order of the rows, it follows that

$$\mathbb{A}' \sim \left[\begin{array}{c|ccc} -\mathbf{a}_{j_1}^\top & \mathbf{a}_{j_1}^\top & & \\ \vdots & & \ddots & \\ -\mathbf{a}_{j_1}^\top & & & \mathbf{a}_{j_1}^\top \\ \hline \mathbf{a}_{j_2}^\top & & & \\ \vdots & & \mathbf{0} & \\ \mathbf{a}_{j_n}^\top & & & \\ \hline & \mathbf{B}_{\setminus j_2}^\top & & \\ \mathbf{0} & & \ddots & \\ & & & \mathbf{B}_{\setminus j_n}^\top \end{array}\right] \triangleq \left[\begin{array}{c|c} \mathbb{A}_{11} & \mathbb{A}_{12} \\ \hline \mathbb{A}_{21} & \mathbf{0} \\ \hline \mathbf{0} & \mathbb{A}_{33} \end{array}\right], \tag{3.2}$$

where $\mathbb{A}_{11}$, $\mathbb{A}_{12}$, $\mathbb{A}_{21}$ and $\mathbb{A}_{33}$ are defined by, respectively, each block as shown in Eq. (3.2). Let $\mathbb{A}_1$ and $\mathbb{A}_2$ be defined as, respectively, $\mathbb{A}_1 \triangleq [\mathbb{A}_{11}|\mathbb{A}_{12}]$ and $\mathbb{A}_2 \triangleq \text{blkdiag}(\mathbb{A}_{21}, \mathbb{A}_{33})$. In the proof later on, a set of $k$-dimensional vectors, namely, $\mathbf{x}_1, \cdots, \mathbf{x}_q$, are referred as *mutually not in* $\text{Im}(\mathbf{X})$, where $\mathbf{X} \in \mathbb{R}^{k\times r}$ is an arbitrary matrix, if $\text{rank}([\mathbf{X}, \mathbf{x}_1, \cdots, \mathbf{x}_q]) = \text{rank}(\mathbf{X}) + q$. Note that $\mathbb{A}_1$ is full rank due to the block diagonal structure of $\mathbb{A}_{12}$. Therefore, the rank of $\mathbb{A}'$ can be computed by adding the rank of $\mathbb{A}_2$ to the number of rows in $\mathbb{A}_1$ which are mutually not in $\text{Im}(\mathbb{A}_2^\top)$, denoted as $\ell$. It follows that

$$\begin{aligned}\text{rank}(\mathbb{A}) =& \text{rank}(\mathbb{A}') = \text{rank}(\mathbb{A}_2) + \ell \\ =& \text{rank}(\mathbb{A}_{21}) + \text{rank}(\mathbb{A}_{33}) + \ell = \text{rank}(\mathbb{A}_{21}) + \sum_{i\in\mathfrak{n}\setminus\{j_1\}} \text{rank}(\mathbf{B}_{\setminus i}) + \ell. \end{aligned} \tag{3.3}$$

(Step 2: Computation of $\sum_{i\in\mathfrak{n}\setminus\{j_1\}} \text{rank}(\mathbf{B}_{\setminus i})$). Let $\mathfrak{x}_1$ and $\mathfrak{x}_2$ be, respectively, the index sets defined as $\mathfrak{x}_1 \triangleq \{i|\mathbf{a}_1 \notin \text{Im}(\mathbf{B}_{\setminus i})\}$ and $\mathfrak{x}_2 \triangleq \{i|\mathbf{a}_1 \in \text{Im}(\mathbf{B}_{\setminus i})\}$. It follows that $\mathfrak{x}_1 \cup \mathfrak{x}_2 = \{j_2, \cdots, j_n\}$. Note that the rank of $\mathbf{B}_{\setminus i}$, for each $\{j_2, \cdots, j_n\}$, has only two possibilities, namely, $\text{rank}(\mathbf{B}_{\setminus i}) = \text{rank}(\mathbf{A}_{\setminus i}) - 1$ if $i \in \mathfrak{x}_1$, and $\text{rank}(\mathbf{B}_{\setminus i}) = \text{rank}(\mathbf{A}_{\setminus i})$ if $i \in \mathfrak{x}_2$. Therefore, $\sum_{i\in\mathfrak{n}\setminus\{j_1\}} \text{rank}(\mathbf{B}_{\setminus i})$ can be computed as $\sum_{i\in\mathfrak{x}_1} \text{rank}(\mathbf{B}_{\setminus i}) + \sum_{i\in\mathfrak{x}_2} \text{rank}(\mathbf{B}_{\setminus i}) = \sum_{i\in\mathfrak{n}\setminus\{j_1\}} \text{rank}(\mathbf{A}_{\setminus i}) - |\mathfrak{x}_1|$. It follows from Eq. (3.3) that

$$\text{rank}(\mathbb{A}) = \text{rank}(\mathbb{A}_{21}) + \sum_{i\in\mathfrak{n}\setminus\{j_1\}} \text{rank}(\mathbf{A}_{\setminus i}) - |\mathfrak{x}_1| + \ell. \tag{3.4}$$

(Step 3: Computation of $\ell$). Recall that $\ell$ is the number of rows in $\mathbb{A}_1$ which are mutually not in $\text{Im}(\mathbb{A}_2^\top)$. Note that if $\mathscr{E}_\mathfrak{n}$ forms a spanning tree of $\mathscr{G}(\mathscr{V}, \mathscr{E})$, $\text{rank}(\mathbb{A}_{21}) = n-1$ and $\mathbf{a}_1 \notin \text{Im}(\mathbb{A}_{21}^\top)$. Also note that $|\mathfrak{x}_1| + |\mathfrak{x}_2| = n-1$. It follows from Eq. (3.4) that the sufficiency part can be proved by showing

$$\text{rank}(\mathbf{A}_{\setminus j_1}) = \ell + |\mathfrak{x}_2| \tag{3.5}$$

so that $\sum_{i\in\mathfrak{n}}\text{rank}(\mathbf{A}_{\setminus i})=\text{rank}\,(\mathbb{A})$. There are two possible cases.

(Case 1). If there exists a link $e_i$ such that $i\notin\mathfrak{b}$, without loss of generality, we select this link to be $e_{j_1}$. It follows that $\text{rank}(\mathbf{A}_{\setminus j_1})=n$. Note that if $i\in\mathfrak{x}_2$, $\mathbf{a}_1\in\text{Im}(\mathbf{B}_{\setminus i})$. Therefore, each $\mathbf{a}_{j_1}^\top$ in $\mathbb{A}_{12}$ can be eliminated to all zeros through row operations by using the rows of $\mathbf{B}_{\setminus i}^\top$ in the same column block, for each $i\in\mathfrak{x}_2$. Thus, after the aforementioned eliminations, these $|\mathfrak{x}_2|$ rows in $\mathbb{A}_1$ become identical to $\mathbf{a}_{\text{id}}^\top\triangleq[-\mathbf{a}_{j_1}^\top|\mathbf{0}_{n(n-1)}^\top]$, where $-\mathbf{a}_{j_1}^\top$ is from $\mathbb{A}_{11}$. It follows that $|\mathfrak{x}_2|-1$ of these rows are in $\text{Im}([\mathbf{a}_{\text{id}},\mathbb{A}_2]^\top)$. Therefore, if $|\mathfrak{x}_2|\geq 1$, $\ell$ can be computed as $\ell=(n-1)-(|\mathfrak{x}|_2-1)$, where $(n-1)$ is the total number of rows in $\mathbb{A}_1$. This implies that Eq. (3.5) is satisfied.

The last step for this case is to prove that $|\mathfrak{x}_2|\geq 1$ so that $\ell$ can be computed in the aforementioned manner. Since $e_{j_1}$ is selected such that $j_1\notin\mathfrak{b}$, $e_{j_1}$ must belong to at least one circle in $\mathscr{G}(\mathscr{V},\mathscr{E})$. We select any one of the circles that contain $e_{j_1}$, and define a index set $\mathfrak{c}\subset\{1,\cdots,l\}$ which collects the indices of links that form this circle. It is clear that for any $i\notin\mathfrak{c}$, $\mathscr{G}(\mathscr{V},\mathscr{E}_{\setminus\{j_1,i\}})$ has the same number of components as $\mathscr{G}(\mathscr{V},\mathscr{E}_{\setminus i})$. Such an $i$ always exists due to the fact that $\mathscr{G}(\mathscr{V},\mathscr{E})$ is not a cycle graph. Note that $\mathbf{B}_{\setminus i}$ can be regarded as the truncated incidence matrix associated with $\mathscr{G}(\mathscr{V},\mathscr{E}_{\setminus\{j_1,i\}})$, where the reference bus is the same as that of $\mathscr{G}(\mathscr{V},\mathscr{E})$. Therefore, according to Lemma 2.3, there exists $i\in\{j_2,\cdots,j_n\}$ such that $\text{rank}(\mathbf{B}_{\setminus i})=\text{rank}(\mathbf{A}_{\setminus i})$. This implies that $|\mathfrak{x}_2|\geq 1$.

(Case 2). If there exists no link $e_i$ such that $i\notin\mathfrak{b}$, $\mathscr{G}(\mathscr{V},\mathscr{E})$ is a spanning tree itself. In this case, all rows in $\mathbb{A}_1$ are mutually not in $\text{Im}(\mathbb{A}_2^\top)$ and therefore $\ell=n-1$. Moreover, $\mathbf{a}_1\notin\text{Im}(\mathbf{B}_{\setminus i})$, $\forall i\in\{j_2,\cdots,j_n\}$. It follows that $|\mathfrak{x}_2|=0$. Note that $\text{rank}(\mathbf{A}_{\setminus j_1})=n-1$. Therefore, Eq. (3.5) is satisfied.

(Necessity). If $\mathscr{E}_{\mathfrak{p}}$ does not contain a spanning tree of $\mathscr{G}(\mathscr{V},\mathscr{E})$, $\mathscr{G}(\mathscr{V},\mathscr{E}_{\mathfrak{p}})$ is not connected. It follows from Lemma 2.3 that the rank of the matrix formed by each column vector $\mathbf{a}_i$, where $i\in\mathfrak{p}$,

is less than $n$. Therefore, $\text{rank}(\mathbb{A}_{21}) < n-1$. Then by a similar approach to that used in the proof of the sufficiency part, it follows that $\text{rank}(\mathbb{A}) = \text{rank}(\mathbb{A}_{21}) + \sum_{j\in\mathfrak{p}\setminus\{j_1\}} \text{rank}(\mathbf{A}_{\setminus i}) < \sum_{j\in\mathfrak{p}} \text{rank}(\mathbf{A}_{\setminus i})$, where the last inequality is due to the fact that $\text{rank}(\mathbf{A}_{\setminus i}) \geq n-1$ for a connected $\mathscr{G}(\mathscr{V},\mathscr{E})$. It follows from Lemma 3.1 that $\dim\left(\bigcap_{i\in\mathfrak{p}} \text{Im}(\mathbf{H}_{\setminus i})\right) > 0$. ■

Theorem 3.4 formulates the necessary and sufficient condition for the system operator to select a set of transmission lines to switch off by turns so as to eliminate the possibility of the stealthy attack in all selected topologies. It turns out that the selected link set has to contain a spanning tree of $\mathscr{G}(\mathscr{V},\mathscr{E})$. One one hand, Theorem 3.4 provides a benchmark to judge whether the selection of a set of topologies generated by cutting each of the preselected links, is able to eliminate all possible stealthy attacks. Theorem 3.4 also implies that such a selection is usually not unique as the graph can contain multiple spanning trees, especially when the number of links is much greater than that of the nodes. Therefore, more flexibilities are left for the operator to consider from other perspectives, such as the power generation cost, generation-demand or stability issues and select a proper link set.

On the other hand, if the selected link set does not contain a spanning tree, there always exist possible stealthy attacks. In some situations, due to constraints posed by, for example, the network connectivity, or the infeasibility in matching the generation and demand, some links are not allowed to be switched off. If all possible spanning trees of $\mathscr{G}(\mathscr{V},\mathscr{E})$ contain such an unremovable link, there always exists possible stealthy attacks. Later on in Corollary 4.10, we will formulate the general form of possible attacks in such situations, and discuss possible countermeasures.

**Remark 3.5 (Non-conservative assumption on $\mathscr{G}(\mathscr{V},\mathscr{E})$)** *In Theorem 3.4, it is assumed that $\mathscr{G}(\mathscr{V},\mathscr{E})$ is not a cycle graph. This assumption is not conservative as it is automatically satisfied by most of*

*the power networks. Thus, Theorem 3.4 is applicable in most cases. The necessary and sufficient condition for the case when this assumption is violated, is considered by the following corollary. However, as this is a rare case, we focus on the case when the graph is not a cycle graph, in the rest of this work.*

**Corollary 3.6** *Suppose that $\mathscr{G}(\mathscr{V},\mathscr{E})$ is a cycle graph. Then* $\dim\left(\bigcap_{i\in\mathfrak{p}} Im(\mathbf{H}_{\setminus i})\right)=0$ if and only if $\mathscr{E}_{\mathfrak{p}}=\mathscr{E}$.

**Proof.** (Sufficiency). Note that when $\mathscr{G}(\mathscr{V},\mathscr{E})$ is a cycle graph, there are $n+1$ links in total. It follows that $|\mathfrak{p}|=n+1$ if $\mathscr{E}_{\mathfrak{p}}=\mathscr{E}$. Let $\mathbb{A}$, $\mathbb{A}_1$, $\mathbb{A}_2$, $\mathbb{A}_{21}$, $\ell$ and $\mathfrak{r}_1$ be similarly defined as in Theorem 3.4. By following the same steps as in the proof of Theorem 3.4 till Eq. (3.4), it is clear that $|\mathfrak{r}_1|=n$ in the case considered here. Therefore, all rows of $\mathbb{A}_1$ are mutually not in $\mathrm{Im}(\mathbb{A}_2^{\top})$. Since $\mathbb{A}_1\in\mathbb{R}^{n\times n(n-1)}$, it follows that $\ell=n$. Moreover, it is clear that $\mathrm{rank}(\mathbf{A}_{\setminus i})=n$, $\forall i\in\mathfrak{p}$. Therefore, due to the fact that $\mathrm{rank}(\mathbb{A}_{21})=n$, it follows from Eq. (3.4) that $\mathrm{rank}(\mathbb{A})=n+\sum_{i\in\mathfrak{p}\setminus\{j_1\}}\mathrm{rank}(\mathbf{A}_{\setminus i})-n+n=\sum_{i\in\mathfrak{p}}\mathrm{rank}(\mathbf{A}_{\setminus i})$. This implies that $\dim\left(\bigcap_{i\in\mathfrak{p}}\mathrm{Im}(\mathbf{H}_{\setminus i})\right)=0$.

(Necessity). If $\mathscr{E}_{\mathfrak{p}}\subset\mathscr{E}$, $\mathrm{rank}(\mathbb{A}_{21})=|\mathfrak{r}_1|=\ell=|\mathfrak{p}|-1$. It follows from Eq. (3.4) that $\mathrm{rank}(\mathbb{A})=\sum_{i\in\mathfrak{p}}\mathrm{rank}(\mathbf{A}_{\setminus i})-1$. It follows that $\dim\left(\bigcap_{i\in\mathfrak{p}}\mathrm{Im}(\mathbf{H}_{\setminus i})\right)=n-|\mathfrak{p}|+1>0$. ■

## 3.2 Impacts of Switching Topologies on the Power Generation Cost

As shown in the previous section, the key to eliminate all possible stealthy attacks by removing one of the preselected links by turns, is that the selected link set contains a spanning tree of $\mathscr{G}(\mathscr{V},\mathscr{E})$. This leads to multiple options due to the fact that $l>n$ in most cases. Therefore, it is better to have a criterion to judge whether the selection of one specific set of links is better than

another. Motivated by this, in this section, the impact of the switching topologies on the power generation cost, is considered as a criterion.

The economic dispatch problem (EDP) is a fundamental problem which computes the minimum generation cost across the network, while satisfying several constraints such as the supply-demand balance, the generation capacities and the transmission capacities. A typical EDP can be formulated as:

$$\underset{P_i^G}{\text{minimize}} \quad \sum_{i=1}^{n+1} \mathfrak{C}_i(P_i^G), \tag{3.6}$$

$$\text{subject to} \quad \sum_i P_i^G = \sum_i P_i^L; \tag{3.7}$$

$$\underline{P}_i^G \leq P_i^G \leq \overline{P}_i^G, \quad i \in \{1,...,n+1\}; \tag{3.8}$$

$$\underline{P}_{jk} \leq P_{jk} \leq \overline{P}_{jk}, \quad j,k \in \{1,...,l\}. \tag{3.9}$$

Here $\mathfrak{C}_i(\cdot)$ stands for the function that computes the generation cost of bus $i$, $P_i^G$ and $P_i^L$ stand for, respectively, the power generation and load on bus $i$, $\underline{P}_i^G$ and $\overline{P}_i^G$ are, respectively, the lower and upper limit of the power generation, $P_{jk}$ stands for the power flow from bus $j$ to bus $k$, and $\underline{P}_{jk}$ and $\overline{P}_{jk}$ are, respectively, the lower and upper bound of $P_{jk}$.

Assuming a fixed power demand on each bus, the optimal value of Eq. (3.6) for each preselected topology is computed. Intuitively, switching off any transmission line will change the strategy of power generation and distribution in the network, and therefore change the optimal solution of Eq. (3.6). Recall that $\mathfrak{p}$ is the set of indices associated with the links that are selected to be switched off by turns. We compute the ratio between the weighted average generation cost among all preselected topologies, and the optimal solution of Eq. (3.6) under the original fixed

topology by the following equation:

$$\mu = \frac{\sum_{j\in\mathfrak{p}} w_j \sum_{i=1}^{n+1} \mathfrak{C}_i(P_i^{G^*,j})}{\sum_{i=1}^{n+1} \mathfrak{C}_i(P_i^{G^*})}, \tag{3.10}$$

where $w_j$ is the percentage of the time that link $e_j$ is removed (thus, $\sum_{j\in\mathfrak{p}} w_j = 1$), and $\sum_{i=1}^{n+1} \mathfrak{C}_i(P_i^{G^*,j})$ stands for the optimal generation cost of the power network in the topology with link $e_j$ removed, and $\sum_{i=1}^{n+1} \mathfrak{C}_i(P_i^{G^*})$ is the optimal solution of Eq. (3.6) with the original fixed topology. It is straightforward that $\mu$ is highly dependent on the specific cases. If $\mu$ is close to (or even less than) 1, the generation cost under switching topologies is not increased too much (or even decreased) compared to the case of the original fixed topology. Therefore the operator can consider using switching topologies as a strategy to defend against the stealthy attack. In the extreme case when security becomes the most critical issue, the system operator may prefer to choose such a strategy to defend against potential attacks at any expense.

The case that involves time-varying loads can be similarly obtained by repeatedly computing the EDP ahead of time. Different optimal solutions of the EDP with respect to different loads may contribute to the next-step decisions, such as the switching orders and the frequency of the switching actions. We leave this for future work.

# Chapter 4

# Possible Deviations on the State Estimates Caused by Partially Stealthy Attacks

As discussed in Theorem 3.4, if the operator selects a set of links that contains a spanning tree of $\mathscr{G}(\mathscr{V},\mathscr{E})$ to switch off by turns, there exists no feasible stealthy attack. However, it is still possible for a "smart" attacker to design an attack in a way such that the attack is stealthy in the majority of the preselected topologies. This motivates the work presented in this chapter. Here we study the case when the attacker makes a concession and designs an attack that is stealthy only in some of the topologies preselected by the system operator. Note that the probability of being detected is increasing as the attack is stealthy in fewer topologies.

The objective for the attacker to launch a stealthy attack is to fool the system operator with a deviated state estimate, *i.e.,* $\hat{\mathbf{x}}_{\text{bad}}$, instead of the true estimate $\hat{\mathbf{x}}$. From the attacker's perspec-

tive, being stealthy is only to avoid being detected. More importantly, the attacker cares about the deviation, denoted as $\Delta\hat{\mathbf{x}}$, introduced to the system operator because such a deviation is critical for the operator to make wrong decisions. It is assumed that to achieve some destructive objectives, the attacker tries to fool the system operator with consistent deviations of the state estimates by injecting the aforementioned "partially" stealthy (*i.e.,* stealthy in a subset of the topologies preselected by the operator) attack. That is, the deviations of the corrupted estimates from the real estimates of the states are identical among all topologies in which the attack is stealthy. This is preferable from the attacker's point of view, since a consistent deviation from the true state estimates is more likely to fool the operator. Therefore, in this section, the details of the deviations that could be possibly introduced by launching a partially stealthy attack, are studied. The following questions are considered. 1) What is the relation between the estimation deviation and the probability of the attack being detected? 2) What do the deviations look like? 3) What are the countermeasures to minimize the effects caused by such an attack?

## 4.1 Possible Estimation Deviation v.s. Probability of Attack Detection

Since the attacker knows what the preselected topologies are, in this paper, only the scenario in which the attacker tries to launch an attack stealthy in a subset of the topologies preselected by the system operator, is studied. However, it will be shown that the cases in which the launched attack is stealthy in some topologies that are not preselected by the operator, can be converted to the case studied in this section. The detailed explanation is skipped at this point since it requires the conclusion of Corollary 4.7 that will be given later on. To begin stating the main results in this section, two definitions, namely, trivial and nontrivial links are given as follows:

**Definition 4.1 (nontrivial links)** *Let $\mathfrak{s}$ be a set of indices and $\mathscr{E}_\mathfrak{s} \triangleq \{e_i | i \in \mathfrak{s}\}$. $\mathscr{E}_\mathfrak{s}$ is a set of nontrivial links if $\mathscr{E}_\mathfrak{s}$ contains no circle.*

**Definition 4.2 (trivial link)** *Let $\mathscr{E}_\mathfrak{s}$ be a set of nontrivial links. Then $e_k$ is a trivial link spanned by $\mathscr{E}_\mathfrak{s}$, if $\mathscr{E}_\mathfrak{s} \cup e_k$ contains circle.*

In this section, let $\mathscr{E}_\mathfrak{n} \triangleq \{e_i | i \in \mathfrak{n}\}$ with $|\mathfrak{n}| = n$ be a set of $n$ nontrivial links that forms a spanning tree of $\mathscr{G}(\mathscr{V}, \mathscr{E})$. Without loss of generality, let the system operator select these $n$ links and cut by turns. Therefore, according to Theorem 3.4, there exists no stealthy attack in the corresponding $n$ topologies. Let $\mathfrak{s}$ be the set of nontrivial links such that $\mathbf{z}_a \in \mathrm{Im}(\mathbf{H}_{\setminus i})$, $\forall i \in \mathfrak{s}$. The following definition will be frequently used in the rest of this paper.

**Definition 4.3 ($(\mathfrak{s},\mathfrak{n})$-stealthy attack)** *Suppose that $\mathfrak{s} \subset \mathfrak{n}$. Then $\mathbf{z}_a$ is an $(\mathfrak{s},\mathfrak{n})$-stealthy attack if $\mathbf{z}_a \in \cap_{i\in\mathfrak{s}} Im(\mathbf{H}_{\setminus i})$ and $\mathbf{z}_a \notin Im(\mathbf{H}_{\setminus i})$, $\forall i \in \mathfrak{n} \setminus \mathfrak{s}$.*

Note that an $(\mathfrak{s},\mathfrak{n})$-stealthy attack is defined only for the case when $\mathfrak{s} \subset \mathfrak{n}$. The following lemma will be used to prove our main theorem later on.

**Lemma 4.4** *Suppose that $\mathbf{z}_a \in \cap_{i\in\mathfrak{s}} Im(\mathbf{H}_{\setminus i})$. Then $\mathbf{z}_a(i) = 0$, $\forall i \in \mathfrak{s}$.*

**Proof.** If the $i$th link is removed, $\mathbf{A}_{\setminus i}(:,i) = \mathbf{0}_n$. It follows from (2.1) that $\mathbf{H}_{\setminus i}(i,:) = \mathbf{0}_n^\top$. Therefore, if $\mathbf{z}_a \in \mathrm{Im}(\mathbf{H}_{\setminus i})$, $\mathbf{z}_a(i) = 0$. This has to be satisfied for all $i \in \mathfrak{s}$. ■

**Theorem 4.5** *Suppose that the attacker launches an $(\mathfrak{s},\mathfrak{n})$-stealthy attack, where $|\mathfrak{s}| > 1$. Let $\mathbf{A}_\mathfrak{s} \in \mathbb{R}^{n\times s}$ be a matrix which collects the columns of $\mathbf{A}$ whose indices are in $\mathfrak{s}$, i.e., $\mathbf{a}_i, \forall i \in \mathfrak{s}$. Then the resulting deviation of the state estimates $\Delta\hat{\mathbf{x}}$ satisfies $\Delta\hat{\mathbf{x}} \in Null(\mathbf{A}_\mathfrak{s}^\top)$.*

**Proof.** Recall that $\Delta\hat{\mathbf{x}}$ is caused by injecting the stealthy attack $\mathbf{z}_a$. Therefore, $\mathbf{z}_a = \mathbf{H}_{\setminus i}\Delta\hat{\mathbf{x}}$ holds for all $i \in \mathfrak{s}$. From Lemma 4.4, $\mathbf{z}_a(i) = 0$, $\forall i \in \mathfrak{s}$. Let $\mathbf{H}^{\mathfrak{s}}_{\setminus i}$ be the submatrix that collects the rows of $\mathbf{H}_{\setminus i}$ whose indices are in $\mathfrak{s}$, *i.e.,* $\mathbf{H}_{\setminus i}(j,:), \forall j \in \mathfrak{s}$. Therefore, since $\mathbf{H}^{\mathfrak{s}}_{\setminus i}\Delta\hat{\mathbf{x}} = 0$ for each $i \in \mathfrak{s}$, $|\mathfrak{s}|$ independent equations, namely, $d_i\mathbf{a}_i^\top\Delta\hat{\mathbf{x}} = 0, \forall i \in \mathfrak{s}$, can be obtained. Note that this can be done only if $|\mathfrak{s}| > 1$ so that there exist $i, j \in \mathfrak{s}$ and $i \neq j$. Since $d_i \neq 0$, $\forall i$, it follows that $\mathbf{a}_i^\top\Delta\hat{\mathbf{x}} = 0, \forall i \in \mathfrak{s}$. By writing these $|\mathfrak{s}|$ equations into a compact matrix form, it is obtained that $\mathbf{A}_{\mathfrak{s}}^\top\Delta\hat{\mathbf{x}} = 0$. It follows that $\Delta\hat{\mathbf{x}} \in \text{Null}(\mathbf{A}_{\mathfrak{s}}^\top)$. ■

Theorem 4.5 formulates the limitation on the consistent estimation deviation that can be introduced by the attack $\mathbf{z}_a$, which is stealthy in $|\mathfrak{s}|$ topologies generated by removing link in $\mathscr{E}_{\mathfrak{s}}$. It is clear as $|\mathfrak{s}|$ increases, the size of $\mathbf{A}_{\mathfrak{s}}$ also increases. Therefore, $\Delta\hat{\mathbf{x}}$ has to satisfy more constraints as the attack is designed to be stealthy in more topologies.

**Remark 4.6** *When the attack is only stealthy in one of the n preselected topologies ($|\mathfrak{s}| = 1$), $\mathbf{z}_a$ can be designed based on whatever $\Delta\hat{\mathbf{x}}$ the attacker wants. This brings us back to the case in which the topology is fixed. However, this would result in the highest probability of being detected during the alternations among all preselected topologies.*

In summary, there is a trade-off between the flexibility of manipulating the estimation deviation and the number of nontrivial links preselected to be removed to obtain the topologies in which the attack is stealthy. On one hand, the attacker prefers to launch an attack that is less possible to be detected during the alternations among all possible topologies. This requires $\Delta\hat{\mathbf{x}}$ to satisfy more constraints with which the attacker may not be able to fool the system operator in an expected way. On the other hand, to manipulate the estimation deviation in a more flexible manner, the attacker has to take the risk and make the attack be stealthy in fewer topologies.

**Corollary 4.7** *Suppose that the attacker launches an* $(\mathfrak{s},\mathfrak{n})$*-stealthy attack, where* $|\mathfrak{s}|>1$*, and deviates the state estimate by* $\Delta\hat{\mathbf{x}}$*. Then, 1)* $\mathbf{z}_a=\mathbf{H}\Delta\hat{\mathbf{x}}$*. 2) For any trivial link* $e_k$ *spanned by the nontrivial link set* $\mathscr{E}_{\mathfrak{s}}$*,* $\mathbf{z}_a\in Im(\mathbf{H}_{\setminus k})$*.*

**Proof.** Let $\mathbf{A}_{\mathfrak{s}}$ be defined in Theorem 4.5. Define $\mathbf{A}_i\triangleq\mathbf{A}-\mathbf{A}_{\setminus i}$. Let $\mathbf{H}_i$ be defined by (2.1) with $\mathbf{A}_i$ playing the role of $\mathbf{A}$. It follows that $\mathbf{H}_i=\mathbf{H}-\mathbf{H}_{\setminus i}$. Therefore, $\mathbf{z}_a=\mathbf{H}_{\setminus i}\Delta\hat{\mathbf{x}}=(\mathbf{H}-\mathbf{H}_i)\Delta\hat{\mathbf{x}}$, $\forall i\in\mathfrak{s}$. Since $\Delta\hat{\mathbf{x}}\in\text{Null}(\mathbf{A}_{\mathfrak{s}}^\top)$ from Theorem 4.5, $\mathbf{A}_i^\top\Delta\hat{\mathbf{x}}=0,\forall i\in\mathfrak{s}$. Therefore $\mathbf{H}_i\Delta\hat{\mathbf{x}}=0$, which implies that $\mathbf{z}_a=\mathbf{H}\Delta\hat{\mathbf{x}}$.

Since $e_k$ is a trivial link spanned by the nontrivial link set $\mathscr{E}_{\mathfrak{s}}$, $e_k\cup\mathscr{E}_{\mathfrak{s}}$ contains a circle and therefore $\text{rank}\,([\mathbf{A}_{\mathfrak{s}}|\mathbf{a}_k])=\text{rank}(\mathbf{A}_{\mathfrak{s}})$. This implies that $\mathbf{a}_k\in\text{Im}(\mathbf{A}_{\mathfrak{s}})$ and therefore $\text{Null}([\mathbf{A}_{\mathfrak{s}}|\mathbf{a}_k]^\top)=\text{Null}(\mathbf{A}_{\mathfrak{s}}^\top)$, where $\mathbf{a}_k\triangleq\mathbf{A}(:,k)$. By Theorem 4.5, $\Delta\hat{\mathbf{x}}\in\text{Null}(\mathbf{A}_{\mathfrak{s}}^\top)$. It follows that $\Delta\hat{\mathbf{x}}\in\text{Null}([\mathbf{A}_{\mathfrak{s}}|\mathbf{a}_k]^\top)$, and therefore $\mathbf{a}_k^\top\Delta\hat{\mathbf{x}}=0$. Thus, $\mathbf{H}_k\Delta\hat{\mathbf{x}}=0$. As a result, $\mathbf{z}_a=\mathbf{H}\Delta\hat{\mathbf{x}}=(\mathbf{H}-\mathbf{H}_k)\Delta\hat{\mathbf{x}}=\mathbf{H}_{\setminus k}\Delta\hat{\mathbf{x}}$, which implies that $\mathbf{z}_a\in\text{Im}(\mathbf{H}_{\setminus k})$. This is the case for any trivial link spanned by the nontrivial link set $\mathscr{E}_{\mathfrak{s}}$.

■

Corollary 4.7 implies that, if an attack is stealthy in all topologies generated by removing each link of $\mathscr{E}_{\mathfrak{s}}$, it is also stealthy in any topology generated by removing a trivial link spanned by $\mathscr{E}_{\mathfrak{s}}$. We now explain how problems that are not directly considered by our main results can be converted to problems to which our results are applicable. Definition 4.3 is defined based on the assumption that $\mathfrak{s}\subset\mathfrak{n}$, which might not always be the case. For example in Figure 4.1(a), let $\mathfrak{n}=\{3,4,5,6\}$, as shown by the dashed lines, and $\mathfrak{s}=\{1,2,3,4\}$, as shown by the cross marks. It is clear that $\mathfrak{s}\not\subset\mathfrak{n}$ in this case. However, it is equivalent to consider the case as shown in Figure 4.1(b), where $\mathfrak{s}'=\{3,4,5\}$ with $\mathfrak{s}'$ similarly defined as that of $\mathfrak{s}$ in Figure 4.1(a). This is due to the fact that $\{e_2,e_3,e_5\}$ forms a circle and hence $e_2$ is a trivial link spanned by $\{e_3,e_5\}$. Also $\{e_1,e_3,e_4\}$ forms

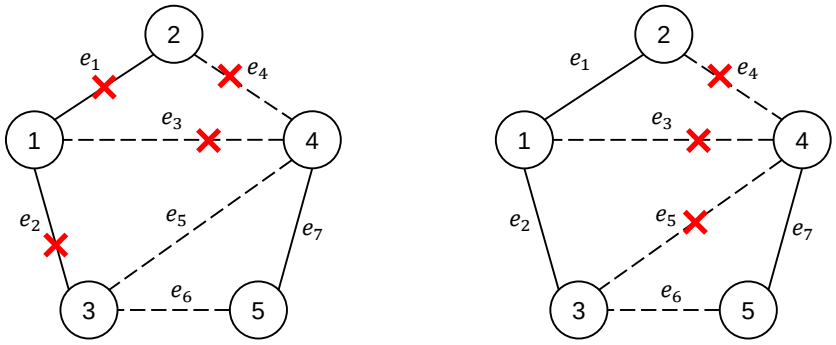


(a) $\mathfrak{s} = \{1,2,3,4\}$ (b) $\mathfrak{s}' = \{3,4,5\}$

Figure 4.1: Example of two equivalent problems with the same $\mathfrak{n} = \{3,4,5,6\}$

a circle and hence $e_1$ is a trivial link spanned by $\{e_3, e_4\}$. It follows from Corollary 4.7 that feasible $\mathbf{z}_a$ such that $\mathbf{z}_a \in \cap_{i\in\mathfrak{s}} \mathrm{Im}(\mathbf{H}_{\setminus i})$ implies that $\mathbf{z}_a \in \cap_{i\in\mathfrak{s}'} \mathrm{Im}(\mathbf{H}_{\setminus i})$. Note that $\mathfrak{s}' \subset \mathfrak{n}$ in this equivalent case so that our main theorem is applicable. In general, if $\mathscr{E}_{\mathfrak{n}}$ forms a spanning tree of $\mathscr{G}(\mathscr{V},\mathscr{E})$, for any $\mathfrak{s}$, one can always find an $\mathfrak{s}'$ such that $\mathfrak{s}' \subset \mathfrak{n}$ as $\mathscr{E}_{\mathfrak{n}}$ is able to span any link $e_i, \forall i \in \{1,\ldots,l\}$. Therefore, our main results, as will be stated in the next section, are applicable to all possible cases.

## 4.2 General Form of Possible Estimation Deviations

**Theorem 4.8** *Suppose that the attacker launches an $(\mathfrak{s},\mathfrak{n})$-stealthy attack. Then $\mathscr{G}(\mathscr{V},\mathscr{E}_{\mathfrak{s}})$ contains $n-s+1$ components. Let $\mathfrak{s}_i$ be the set collects the indices of nodes in the ith component of $\mathscr{G}(\mathscr{V},\mathscr{E}_{\mathfrak{s}})$. Let $\mathfrak{s}_{n-s+1}$ be the component contains the reference node without loss of generality. Then $\Delta\hat{\mathbf{x}}$ has the form of $\Delta\hat{\mathbf{x}} = \sum_{i=1}^{n-s} \alpha_i \mathbf{e}_{\mathfrak{s}_i}$, where $\alpha_i \in \mathbb{R}$ is arbitrary, $\forall i$, and $\mathbf{e}_{\mathfrak{s}_i} \in \mathbb{R}^n$ is a vector each entry of which is one if its index is in $\mathfrak{s}_i$ and zero otherwise.*

**Proof.** Let $\mathbf{A}_{\mathfrak{s}}$ be defined in Theorem 4.5. Since $\mathscr{E}_{\mathfrak{s}}$ a set of nontrivial links, it follows that $\mathrm{rank}(\mathbf{A}_{\mathfrak{s}}) = s$. Note that $\mathbf{A}_{\mathfrak{s}}$ can be regarded as the truncated incidence matrix with respect to

the graph $\mathscr{G}(\mathscr{V},\mathscr{E}_{\mathfrak{s}})$. Let $\mathscr{V}_{\mathfrak{s}_i} \subseteq \mathscr{V}$ and $\mathscr{E}_{\mathfrak{s}_i} \subseteq \mathscr{E}_{\mathfrak{s}}$ be, respectively, the node set and link set of the $i$th component of $\mathscr{G}(\mathscr{V},\mathscr{E}_{\mathfrak{s}})$. Suppose that $\mathscr{G}(\mathscr{V},\mathscr{E}_{\mathfrak{s}})$ contains $k$ components, namely, $\mathscr{G}(\mathscr{V}_{\mathfrak{s}_i},\mathscr{E}_{\mathfrak{s}_i})$, $\forall i \in \{1,\cdots,k\}$. Then according to Lemma 2.3, $s = n-k+1$ and it follows that $k = n-s+1$.

Let $\mathbf{A}_0^{\mathfrak{s}_i}$ be the incidence matrix (similar to $\mathbf{A}_0$) with respect to $\mathscr{G}(\mathscr{V}_{\mathfrak{s}_i},\mathscr{E}_{\mathfrak{s}_i})$, for each $i \in \{1,\ldots,n-s\}$. Let $\mathbf{A}^{\mathfrak{s}_k}$ be the truncated incidence matrix (similar to $\mathbf{A}$) with respect to $\mathscr{G}(\mathscr{V}_{\mathfrak{s}_k},\mathscr{E}_{\mathfrak{s}_k})$ with the reference node selected the same as that of $\mathscr{G}(\mathscr{V},\mathscr{E})$. By appropriately reassigning the indices of buses, without loss of generality, $\mathbf{A}_{\mathfrak{s}}$ can be written as $\mathbf{A}_{\mathfrak{s}} = \text{blkdiag}(\mathbf{A}_0^{\mathfrak{s}_1},\ldots,\mathbf{A}_0^{\mathfrak{s}_{n-s}},\mathbf{A}^{\mathfrak{s}_k})$. Since for each $i \in \{1,\ldots,n-s\}$, $\mathbf{A}_0^{\mathfrak{s}_i}$ is the incidence matrix with respect to the graph $\mathscr{G}(\mathscr{V}_{\mathfrak{s}_i},\mathscr{E}_{\mathfrak{s}_i})$, which is a connected subgraph of $\mathscr{G}(\mathscr{V},\mathscr{E}_{\mathfrak{s}})$. It follows from Lemma 2.3 that $\mathbf{1} \in \text{Null}\left((\mathbf{A}_0^{\mathfrak{s}_i})^\top\right)$ and $\text{rank}(\mathbf{A}_0^{\mathfrak{s}_i}) = |\mathscr{V}_{\mathfrak{s}_i}| - 1$. Thus, $\mathbf{1}$ is the only basis of the left null space of $\mathbf{A}_0^{\mathfrak{s}_i}$, for all $i \in \{1,\ldots,n-s\}$. Since $\mathbf{A}^{\mathfrak{s}_k}$ is the truncated incidence matrix with respect to $\mathscr{G}(\mathscr{V}_{\mathfrak{s}_k},\mathscr{E}_{\mathfrak{s}_k})$. As $\mathscr{G}(\mathscr{V}_{\mathfrak{s}_k},\mathscr{E}_{\mathfrak{s}_k})$ contains only nontrivial links, $\mathbf{A}^{\mathfrak{s}_k}$ is a square matrix with full rank. Therefore $\text{Null}\left((\mathbf{A}^{\mathfrak{s}_k})^\top\right) = \emptyset$. Thus, the general form of the estimation deviation is $\sum_{i=1}^{n-s} \alpha_i \mathbf{e}_{\mathfrak{s}_i}$. ■

Theorem 4.8 describes how exactly the flexibility of manipulating the estimation deviation is limited when the attacker launches an $(\mathfrak{s},\mathfrak{n})$-stealthy attack. It is shown that the flexibility can be judged by checking the graph $\mathscr{G}(\mathscr{V},\mathscr{E}_{\mathfrak{s}})$. It turns out that the deviation vector can only be designed in a "component" sense. That is, for each component in the graph $\mathscr{G}(\mathscr{V},\mathscr{E}_{\mathfrak{s}})$, the corresponding entries of the deviation vector have to be identical. Moreover, for the component that contains the reference bus, as a special case, the corresponding entries of the deviation vector have to be identical to zero. Therefore, even though the attacker takes the risk of being detected and launches an attack that is stealthy in some of the preselected topologies, it has to confront the limited flexibility of designing the deviation vector $\Delta\hat{\mathbf{x}}$, especially when it tries to "hide" in more topologies. This trade-off turns

out to be linear, as proved in Theorem 4.8. The conclusions of Theorem 4.8 instantly leads to the following corollary.

**Corollary 4.9** *The possibility of a specific* $(\mathfrak{s},\mathfrak{n})$*-stealthy attack is zero if there exists at least one independently verifiable bus in each component of* $\mathscr{G}(\mathscr{V},\mathscr{E}_{\mathfrak{s}})$ *that does not contain the reference bus.*

The proof of Corollary 4.9 is straightforward and omitted here for the sake of saving space. This corollary is motivated by the fact that for all buses in the same component of $\mathscr{G}(\mathscr{V},\mathscr{E}_{\mathfrak{s}})$, the corresponding entries of $\mathbf{\Delta\hat{x}}$ have to be identical. Therefore by guaranteeing that at least one state can be independently verified (the state value can be directly obtained by some methods that are independent from the state estimator, see [12] for details), the system operator is able to know whether the estimate of the state is deviated, and further know whether the estimates of all other states in the same component of $\mathscr{G}(\mathscr{V},\mathscr{E}_{\mathfrak{s}})$ are deviated. Therefore, to avoid being detected, the attacker cannot deviate the estimates of the states in any component containing buses corresponding to the independently variable states.

Corollary 4.9 also explains why the estimation deviations of the states that belong to the component containing the reference bus, have to be identically zero. The reason is that the state value of the reference bus is assumed to be fixed (usually zero for convenience) to show the phase angles of other buses relative to it. Therefore, by Theorem 4.8, all states in the same component of $\mathscr{G}(\mathscr{V},\mathscr{E}_{\mathfrak{s}})$ containing the reference bus will have zero deviations. From this perspective, the reference bus plays the role of a verifiable state.

At the end of this chapter, we formulates the general form of the possible stealthy attacks in the case when the system operator fails to find a set of links that contains a spanning tree of $\mathscr{G}(\mathscr{V},\mathscr{E})$, as studied in the previous section.

Let $\mathfrak{n}'$ be a set of indices, where $|\mathfrak{n}'| < n$, such that $\mathscr{E}_{\mathfrak{n}'} \triangleq \{e_i | i \in \mathfrak{n}'\}$ is a set of nontrivial links. Assume that the operator is able to find a nontrivial link set $\mathscr{E}_{\mathfrak{n}}$ that forms a spanning tree of $\mathscr{G}(\mathscr{V}, \mathscr{E})$ and $\mathfrak{n}' \subset \mathfrak{n}$. An $(\mathfrak{n}', \mathfrak{n})$-stealthy attack can be launched. Now suppose that instead of $\mathscr{E}_{\mathfrak{n}}$, the operator is only able to select the nontrivial link set $\mathscr{E}'_{\mathfrak{n}}$ to cut by turns, the aforementioned $(\mathfrak{n}', \mathfrak{n})$-stealthy attack becomes stealthy in all preselected topologies. Therefore, the general form of all possible stealthy attacks in this case can be obtained by combining the conclusions of Corollary 4.7 and Theorem 4.8, and is summarized in the following corollary.

**Corollary 4.10** *Let $\mathfrak{n}'$ be a set of indices where $|\mathfrak{n}'| < n$, such that $\mathscr{E}_{\mathfrak{n}'} \triangleq \{e_i | i \in \mathfrak{n}'\}$ is a set of nontrivial links selected by the system operator to cut by turns. Then the general form of the possible stealthy attack $\mathbf{z}_a$ is $\mathbf{z}_a = \sum_{i=1}^{n-n'} \alpha_i \sum_{j \in \mathfrak{n}'_i} \mathbf{H}(:, j)$, where $\alpha_i$ is an arbitrary scalar and $\mathfrak{n}'_i$ is the set of node indices corresponding to the buses in the ith component of $\mathscr{G}(\mathscr{V}, \mathscr{E}_{\mathfrak{n}'})$ that does not contain the reference bus.*

**Proof.** Let $\mathbf{e}_{\mathfrak{n}'_i} \in \mathbb{R}^n$ be a vector each entry of which is one if its index is in $\mathfrak{n}'_i$ and zero otherwise. It follows from Corollary 4.7 and Theorem 4.8 that $\mathbf{z}_a = \mathbf{H}\Delta\hat{\mathbf{x}} = \mathbf{H}\sum_{i=1}^{n-n'} \alpha_i \mathbf{e}_{\mathfrak{n}'_i} = \sum_{i=1}^{n-n'} \alpha_i \mathbf{H}\mathbf{e}_{\mathfrak{n}'_i} = \sum_{i=1}^{n-n'} \alpha_i \sum_{j \in \mathfrak{n}'_i} \mathbf{H}(:, j)$. ■

The general form of the possible attack vector $\mathbf{z}_a$ shown in Corollary 4.10 can be regarded as a linear combination of a set of basis vectors, each of which is a summation of $\mathbf{H}$'s columns corresponding to the nodes in one component (that does not contain the reference node) of the graph formed by all nodes and the selected links, *i.e.,* $\mathscr{G}(\mathscr{V}, \mathscr{E}_{\mathfrak{n}'})$.

Note that when $\mathfrak{n}' = \emptyset$, *i.e.,* the system operator does not remove any link. In such a case, $\mathscr{G}(\mathscr{V}, \mathscr{E}_{\mathfrak{n}'})$ is a graph with only $n+1$ nodes but no links. Therefore, besides the reference bus, each of the other $n$ buses is a component of $\mathscr{G}(\mathscr{V}, \mathscr{E}_{\mathfrak{n}'})$. By Corollary 4.10, with $\Delta\hat{\mathbf{x}}$ selected as

$\Delta\hat{\mathbf{x}} = [\alpha_1, \cdots, \alpha_n]^\top$, it follows that $\mathbf{z}_a = \mathbf{H}\Delta\hat{\mathbf{x}}$. This brings us back to the case of the fixed topology. Therefore, even though there exists possible stealthy attack when the link set corresponding to the preselected topologies does not forms a spanning tree of $\mathscr{G}(\mathscr{V}, \mathscr{E})$, the proposed scenario puts more constraints on the selection of a possible attack vector $\mathbf{z}_a$ compared to the scenario of the fixed topology. Let the subspace spanned by all possible attack vectors be the attack space. When the topology is fixed, each column of $\mathbf{H}$ is a basis of the attack space. In the proposed scenario, each basis of the attack space is a summation of some columns of $\mathbf{H}$ corresponding to one component of $\mathscr{G}(\mathscr{V}, \mathscr{E}_{\mathfrak{n}'})$. With the increase of the number of the selected links to cut by turns, the dimension of the attack space decreases.

Moreover, the general form of $\mathbf{z}_a$ can be used to locate the set of vulnerable measurements. Each nonzero entry in $\mathbf{z}_a$ implies a measurement that has to be compromised by the attacker in order to launch a stealthy attack. Therefore, one can adopt the measurement protection mechanism [12] as an assisting strategy to eliminate the possibilities of stealthy attacks when the condition in Theorem 3.4 is not satisfied.

# Chapter 5

# Simulations & Case Studies

In this chapter, we show some simulations as well as case studies to illustrate the analytical work shown in the previous two chapters.

## 5.1 Simulation Results

### 5.1.1 Detection of Stealthy Attacks using Switching Topologies

In this subsection, simulation results about the detection of stealthy attacks in the scenario of switching topologies, are shown. The simulation is based on a 5-bus system, where $n = 4$ and $l = 7$ as shown in Figure 5.1(a). Note that there is no bridge link in this 5-bus system, *i.e.,* the graph remains connected with each one of the links removed. Therefore, there are 7 possible topologies generated by switching off each one of the transmission lines (assume that the EDP is feasible when any one of the links is removed). We first show that the strategy for designing the stealthy attack in the scenario of a fixed topology will not be able to launch stealthy attacks in the scenario of

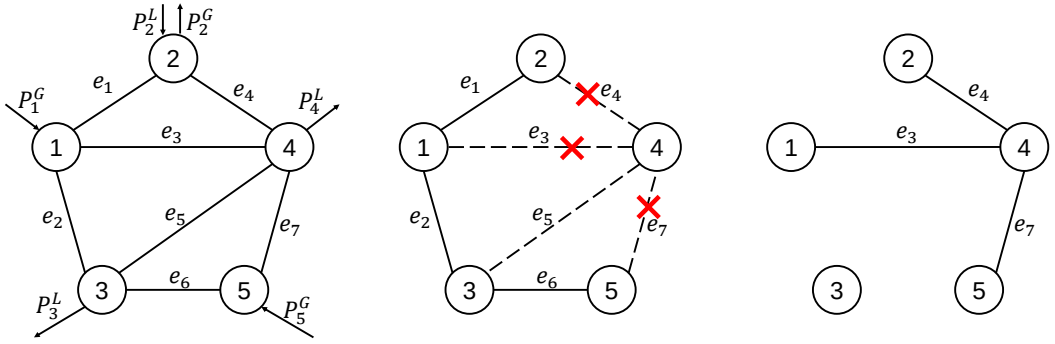


(a) 5-bus System (b) $\mathscr{G}(\mathscr{V},\mathscr{E})$ (c) $\mathscr{G}(\mathscr{V},\mathscr{E}_5)$

Figure 5.1: Figures used for the simulations and case studies

switching topologies in general. We then show that an attack that is stealthy in some topologies will not be able to pass the residue-based detectors in some other topologies. For the sake of convenience in comparison, the index "8" is assigned to the original topology in which no line is switched off, and show the simulation results of all 8 topologies for two tests in Figure 5.2. Let the measurement $\mathbf{z}$, which is originally corrupted with some measurement noise assumed as Gaussian, be further corrupted with an attack $\mathbf{z}_a$, *i.e.,* $\mathbf{z}_{\text{bad}} = \mathbf{H}_{\setminus i}\mathbf{x} + \mathbf{w} + \mathbf{z}_a$ for each $i$ with $\mathbf{w} \sim \mathscr{N}(0, \sigma^2 I)$. Specifically, to be consistent, let $\sigma = 0.5$ and $\|\mathbf{z}_a\|_2 = 100$ in both tests. Note that the false data has much greater magnitude than the measurement noise. The residue-based detector $\mathfrak{J}_i(\mathbf{r})$ for the $\mathscr{G}(\mathscr{V},\mathscr{E}_{\setminus i})$ is defined as $\mathfrak{J}_i(\mathbf{r}) \triangleq \|\mathbf{z}_{\text{bad}} - \mathbf{H}_{\setminus i}\hat{\mathbf{x}}_{\text{bad}}\|_2$. We check the results of residue tests, as well as the estimation deviations on all 4 states in the case of each possible topology.

Test 1 is done by designing $\mathbf{z}_a$ as a random linear combination of the columns of $\mathbf{H}$, *i.e.,* $\mathbf{z}_a \in \text{Im}(\mathbf{H})$. The simulation results are shown in Figure 5.2(a), It is clear that with an appropriately designed threshold $\tau$, even though this attack is stealthy in the original fixed topology (topology 8 in the figure), it will easily trigger the residue-based detector when any transmission line is switched

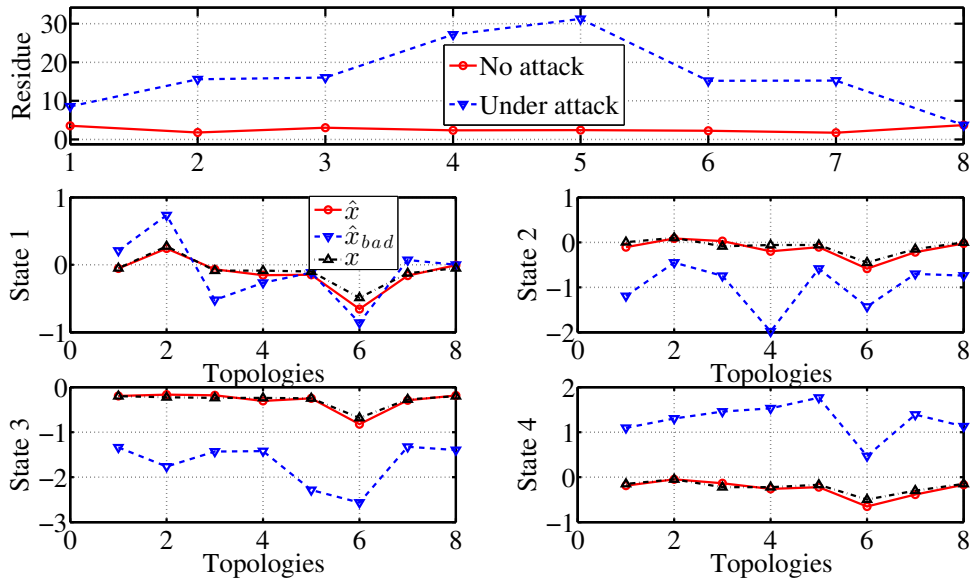


(a) Test 1: $\mathbf{z}_a \in \mathrm{Im}(\mathbf{H})$

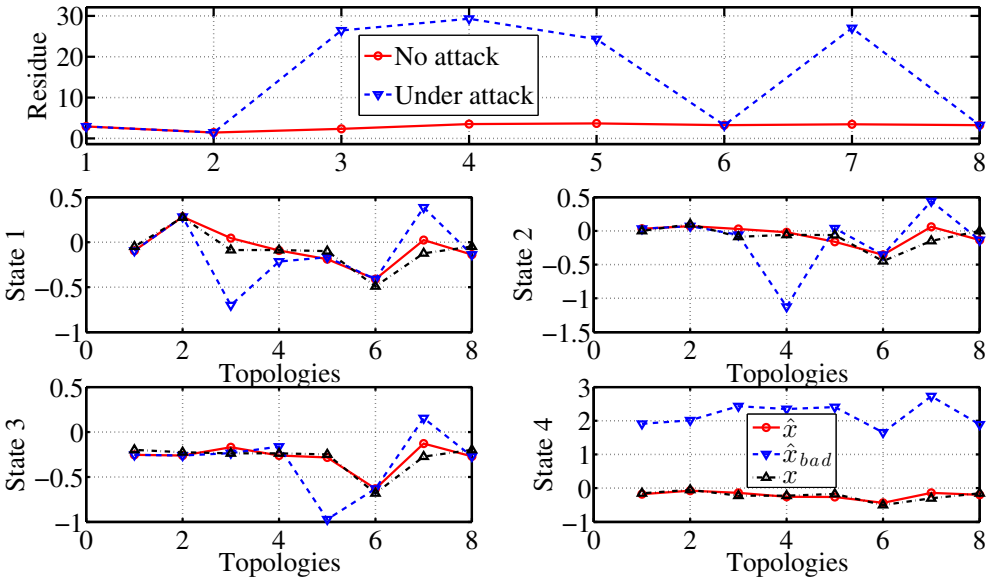


(b) Test 2: $\mathbf{z}_a \in \bigcap_{i\in\{1,2,6\}} \mathrm{Im}(\mathbf{H}_{\setminus i})$

Figure 5.2: Two tests on the residue-based detector and estimation deviations under the same attack with all 8 different topologies (Topology 8 is the original fixed topology)

off. Moreover, for every possible topology, each of the estimated states can be independently deviated from the true estimates, as shown in the bottom 4 sub-figures in Figure 5.2(a).

Test 2 is done by letting the attacker be "smarter" in the sense that it launches an attack that is stealthy in some of the preselected topologies. Specifically, $\mathbf{z}_a \in \bigcap_{i\in\{1,2,6\}} \mathrm{Im}(\mathbf{H}_{\setminus i})$. It can be observed from Figure 5.2(b) that such an attack will pass the residue test if the original fixed topology (topology 8) is selected. Even though such an attack is better designed from the attacker's perspective, it will still trigger the alarm in the case when any link in $\{e_i | i \in \{3,4,5,7\}\}$ is removed. This is because $\{e_i | i \in \{3,4,5,7\}\}$ are not the trivial links spanned by $\{e_i | i \in \{1,2,6\}\}$. Moreover, it can be observed that for the topologies in which $\mathbf{z}_a$ is stealthy, only the estimate of state 4 is deviated. The detailed case studies on the estimation deviations will be given later in this section.

### 5.1.2 Impacts on Power Generation Cost

In this subsection, the impact of switching topologies on the generation cost is shown. To avoid potential infeasibilities of the EDP caused by isolating part of the network, in the simulations presented in this subsection, none bridge link in the graph is allowed to be removed. The following classical quadratic form to compute the generation cost on each bus is adopted:

$$\mathfrak{C}_i(P_i^G) = \varepsilon_i + \beta_i P_i^G + \gamma_i (P_i^G)^2.$$

The first simulation is done on the 5-bus system shown in Figure 5.1(a), where the ratios of the generation cost in each possible topology over that in the original topology are plotted in Figure 5.3(a). The required parameters are adopted from [84] and listed in table 5.1, in which the generation and load are on a 100 MVA base. The admittance on each transmission line is $-10j$.

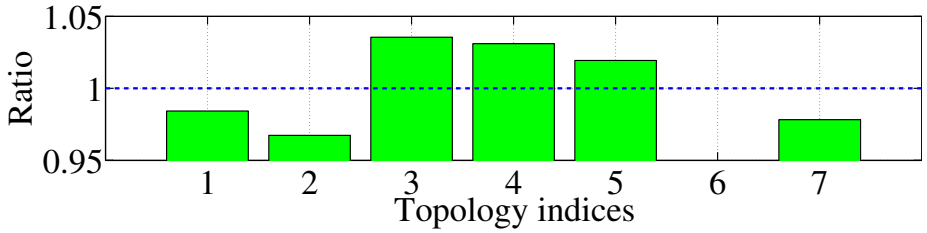


(a) 5-bus system

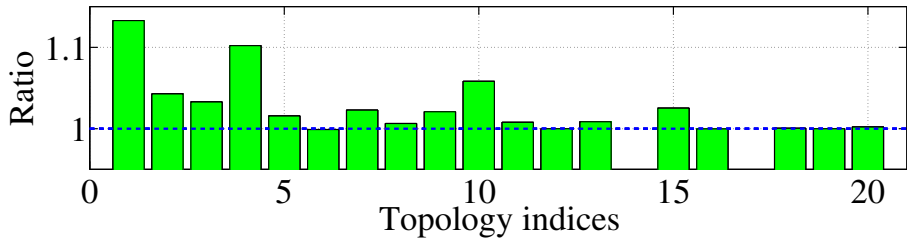


(b) IEEE 14-bus system

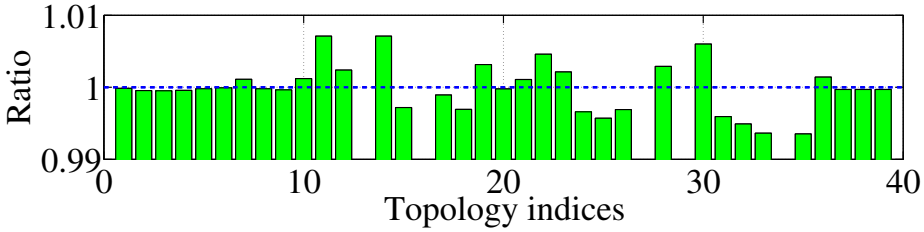


(c) IEEE 30-bus system

Figure 5.3: Ratios of the generation cost in the case of different topologies over that of the original topology in different systems

Table 5.1: Parameters of 5-bus System

| Bus index | $\varepsilon_i$ | $\beta_i$ | $\gamma_i$ | $\underline{P_i^G}$(p.u) | $\overline{P_i^G}$(p.u) | $P_i^L$(p.u) |
|---|---|---|---|---|---|---|
| 1 | 15.62 | 792 | 561 | 1.5 | 5.0 | 0.0 |
| 2 | 19.4 | 785 | 310 | 1.5 | 5.0 | 2.0 |
| 3 | 0.0 | 0.0 | 0.0 | 0.0 | 0.0 | 4.0 |
| 4 | 0.0 | 0.0 | 0.0 | 0.0 | 0.0 | 3.5 |
| 5 | 48.2 | 792 | 78 | 1.5 | 5.0 | 0.0 |

The transmission capacities on $e_2$ and $e_4$ are both 1.5 p.u., and unlimited on other lines. We solve the EDP for each feasible topology using CVX [23]. The ratios of the generation cost when $e_i$ is removed over the cost when no link is removed, for all $i \in \{1, \cdots, l\}$, are computed and shown in the Figure 5.3(a). It can be observed that besides $e_6$, whose removal will cause infeasibility (due to limited transmission capacities) of the EDP, the generation cost is varying when each of the other links is removed. Therefore, assume that each selected topology is adopted with the same length of time, *i.e.,* $w_j = 1/|\mathfrak{p}|$, $\forall j \in \mathfrak{p}$, where $w_j$ is defined in (3.10), among the rest possible link sets (sets without $e_6$) that form a spanning tree of $\mathscr{G}(\mathscr{V}, \mathscr{E})$, the optimal link set $\mathscr{E}_{\mathfrak{p}}^*$ that minimizes the average cost of generation is selected as $\mathscr{E}_{\mathfrak{p}}^* = \{e_1, e_2, e_5, e_7\}$. It follows from (3.10) that $\mu^* = 99.5\%$. This implies that the generation cost is decreased in this case when the topology is switching.

Based on the data adopted from [88], with the MVA ratings of each transmission line adopted from [56], the same simulation is done on the IEEE 14-bus system and the IEEE 30-bus system. The results are shown, respectively, in Figure 5.3(b) and 5.3(c). The topologies of the IEEE 14-bus and IEEE 30-bus system are shown, respectively, in 5.4(a) and 5.4(b), where the bus in red is selected as the reference bus without loss of generality.

In the IEEE 14-bus system, $e_{14}$ is a bridge link. Removing $e_{17}$ will make the EDP infeasible. Therefore, the generation cost for the topologies generated by removing either of these

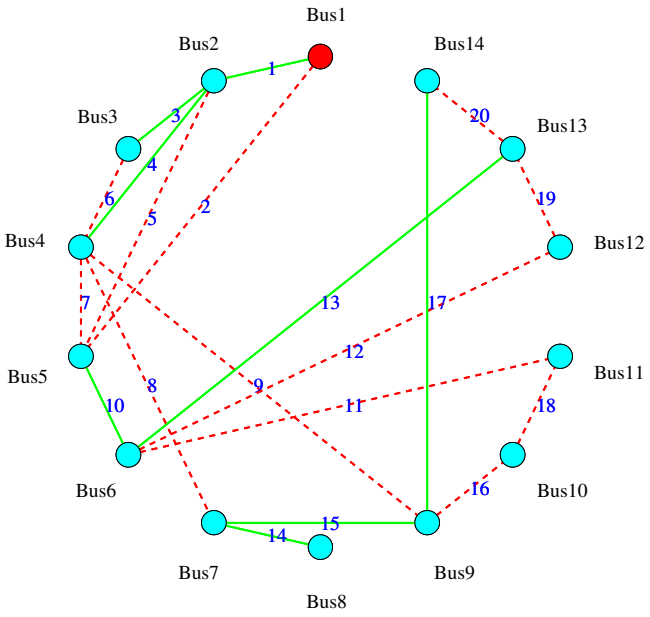


(a) IEEE 14-bus system with Bus 1 being the reference bus

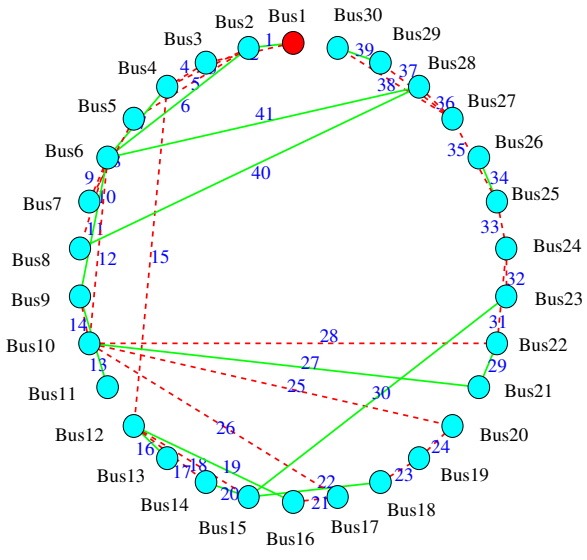


(b) IEEE 30-bus system with Bus 1 being the reference bus

Figure 5.4: IEEE 14-bus and IEEE 30-bus systems with selected links (dashed lines) for topology switching

two links are not shown in Figure 5.3(b). Since $e_{14}$ is a bridge link, all possible spanning trees of $\mathscr{G}(\mathscr{V},\mathscr{E})$ contain $e_{14}$. Therefore, it is always possible to find a stealthy attack according to Theorem 3.4. In such a case, however, it is still possible to find a link set $\mathscr{E}_{\mathfrak{p}}$ contains a spanning tree of $\mathscr{G}(\mathscr{V}\setminus\{v_8\},\mathscr{E}\setminus\{e_{14}\})$. Then it follows from Corollary 4.10 that the dimension of the attack space will be 1. By formulating the general form of this stealthy attack, identifying the vulnerable measurements, and adding protections on these measurements, the possibility of stealthy attacks can be eliminated. The suboptimal link set which forms a spanning tree of $\mathscr{G}(\mathscr{V},\mathscr{E}_{\setminus 14})$ and minimizes the average generation cost among corresponding topologies is shown as dashed lines in Figure 5.4(a). The corresponding $\mu$ is 100.98%.

Similarly, in the IEEE 30-bus system, the bridge link set $\mathfrak{b}=\{13,16,34\}$. Moreover, the removal of $e_{27}$ or $e_{29}$ will make the EDP infeasible. Therefore, the generation cost in the corresponding 5 topologies are not shown in Figure 5.3(c). Similar to the previous case, assuming the equal amount of time for each topology adopted by the operator, the suboptimal link set $\mathscr{E}_{\mathfrak{p}}$ that minimizes the average generation cost among selected topologies can be selected as shown in dashed lines in Figure 5.4(b). The value of $\mu$ corresponding to $\mathscr{E}_{\mathfrak{p}}$ is 99.92%. Similar to the previous case, besides cutting off each link of $\mathscr{E}_{\mathfrak{p}}$ by turns, the system operator should also consider adding protections to some of the vulnerable measurements that located by the general attack form obtained by Corollary 4.10. In this case, the dimension of the attack space is 4. Therefore, by adding protection on at least one measurement in each vulnerable measurement set, which is located by each basis vector of the attack space, the network will be robust against the stealthy attacks. Note that instead of protecting a set of basic measurements (contains 29 measurements in this case) as proposed in [12], only 4 measurements are required to be protected.

Besides adding encrypted measurements, the system operator could also consider verifying some states independently. This strategy will be discussed in the following section.

## 5.2 Case Studies on Estimate Deviations

According to Theorem 4.8, an $(\mathfrak{s},\mathfrak{n})$-stealthy attack is only able to independently deviate $n-s$ components in $\mathscr{G}(\mathscr{V},\mathscr{E}_{\mathfrak{s}})$. However, the number of buses in each component of $\mathscr{G}(\mathscr{V},\mathscr{E}_{\mathfrak{s}})$ is dependent on both the system operator's selection of $\mathfrak{n}$ and the attacker's selection of $\mathfrak{s}$, where $\mathfrak{s}$ and $\mathfrak{n}$ are defined in Section 4. Moreover, since an $(\mathfrak{s},\mathfrak{n})$-stealthy attack is not able to deviate the estimated states of any bus included in the same component with the reference bus, the location of the reference bus in $\mathscr{G}(\mathscr{V},\mathscr{E})$ will also contribute to the limitation as described in Theorem 4.8. Motivated by these intuitions, in this section, we use $\|\Delta\hat{\mathbf{x}}\|_0$, which stands for the number of nonzero entries in $\Delta\hat{\mathbf{x}}$, as a metric to evaluate how the limitation on the estimation deviation vector $\Delta\hat{\mathbf{x}}$ is affected by the selection of $\mathfrak{n}$, $\mathfrak{s}$ and the reference bus in $\mathscr{G}(\mathscr{V},\mathscr{E})$.

### 5.2.1 Scenario without Verifiable State

We first study the scenarios in which the operator is not able to independently verify any state value. The parameters of all cases studied in this scenario are listed in Table 5.2, in which the "Ref" stands for the reference bus for each case. It is assumed that for each case, an $(\mathfrak{s},\mathfrak{n})$-stealthy attack is launched with the listed choice of $\mathfrak{s}$ and $\mathfrak{n}$. $\Delta\hat{x}_i$ denotes the deviation from the normal estimate of the $i$th bus when the measurements are not corrupted by the partially stealthy attack. For example, $\Delta\hat{\mathbf{x}} = [\Delta\hat{x}_1, \Delta\hat{x}_2, \Delta\hat{x}_3, \Delta\hat{x}_5]^\top$ if $v_4$ is selected as the reference bus. Note that this deviation is undefined for the reference bus and therefore marked as "N/A" in the table. $\alpha \in \mathbb{R}$ is arbitrary.

Table 5.2: Parameters of studied cases

| Case # | $\mathfrak{n}$ | Ref | $\mathfrak{s}$ | $\Delta\hat{x}_1$ | $\Delta\hat{x}_2$ | $\Delta\hat{x}_3$ | $\Delta\hat{x}_4$ | $\Delta\hat{x}_5$ |
|---|---|---|---|---|---|---|---|---|
| 1 | 3,4,5,7 | $v_5$ | 3,4,7 | 0 | 0 | $\alpha$ | 0 | N/A |
| 2 | 3,4,5,7 | $v_5$ | 3,4,5 | $\alpha$ | $\alpha$ | $\alpha$ | $\alpha$ | N/A |
| 3 | 3,4,5,7 | $v_4$ | 3,4,5 | 0 | 0 | 0 | N/A | $\alpha$ |
| 4 | 1,2,4,6 | $v_4$ | 1,2,6 | $\alpha$ | $\alpha$ | $\alpha$ | N/A | $\alpha$ |

The details for Case 1 is shown in Figure 5.1 as an example. Similar figures can be easily derived for other cases in Table 5.2 and are omitted here for the interest of space. In Figure 5.1(b), the dashed lines form the link set $\mathscr{E}_{\mathfrak{n}}$, which is decided by the operator. The cross marks show the link set $\mathscr{E}_{\mathfrak{s}}$, which is decided by the attacker. Figure 5.1(c) shows the graph $\mathscr{G}(\mathscr{V},\mathscr{E}_{\mathfrak{s}})$, which is the critical graph used to judge the general form of $\Delta\hat{\mathbf{x}}$.

For all cases in Table 5.2, $|\mathfrak{s}|=3$ and $|\mathfrak{n}|=4$. It follows by Theorem 4.8 that the state estimates of nodes in only one component in $\mathscr{G}(\mathscr{V},\mathscr{E}_{\mathfrak{s}})$ can be deviated. In Case 1, as shown in Figure 5.1(c), bus 3 is the only bus that belongs to the component that does not contain the reference bus $v_5$. Therefore, only $\Delta\hat{x}_3$ can be an arbitrary value $\alpha$. If follows that $\|\Delta\hat{\mathbf{x}}\|_0=1$. The only difference of Case 2 from Case 1 is the selection of $\mathfrak{s}$. As a result, however, the estimated states of all buses (except for the reference bus) are deviated with the same value and therefore $\|\Delta\hat{\mathbf{x}}\|_0=4$. This is because in $\mathscr{G}(\mathscr{V},\mathscr{E}_{\mathfrak{s}})$ of Case 2, the reference bus is isolated from all other buses. Then all buses are included in the component that does not contain the reference bus. Therefore, given the objective of deviating more numbers of states from the attacker's perspective, the selection of $\mathfrak{s}$ in Case 2 is preferred by the attacker. In Case 3, all parameters stay the same as those of Case 2 except that the reference bus is selected as bus 4 instead of bus 5. However, by simply changing the reference bus, only one estimate of states can be deviated. Actually, in this case, any possible $(\mathfrak{s},\mathfrak{n})$-stealthy attack, where $|\mathfrak{s}|=3$ and $|\mathfrak{n}|=4$, is only able to deviate one estimated state since

all buses are directly connected to the reference bus in $\mathscr{G}(\mathscr{V},\mathscr{E}_{\mathfrak{s}})$. Therefore, Case 3 is the most preferable case from the operator's perspective. In Case 4, using the same reference bus as that of Case 3, the selection of $\mathfrak{n}$ is changed. It turns out that by selecting $\mathfrak{s}$ listed in Table 5.2, the estimated states of all buses (except the reference bus) will be deviated, *i.e.,* $\|\Delta\hat{\mathbf{x}}\|_0 = 4$. Thus, this is the least preferable case that the operator should consider.

Therefore, using $\|\Delta\hat{\mathbf{x}}\|_0$ as the metric, the following two criteria are summarized for the system operator to select the location of the reference bus in $\mathscr{G}(\mathscr{V},\mathscr{E})$, and the $n$ links to cut by turns, in the scenario where there is no verifiable state. On one hand, in $\mathscr{G}(\mathscr{V},\mathscr{E}_{\mathfrak{s}})$, the reference bus should be directly connected to as many buses as possible. As shown in the comparison between Case 2 and Case 3. On the other hand, the reference bus should act as the "root" of the spanning tree formed by $\mathscr{E}_{\mathfrak{n}}$. Moreover, each branch of the spanning tree should have as few nodes as possible, as shown in the comparison between Case 3 and Case 4.

### 5.2.2 Scenario with Verifiable State

When there exist independently verifiable states [12], the strategy for the operator to select $\mathfrak{n}$ will be changed significantly. A certain $(\mathfrak{s},\mathfrak{n})$-stealthy attack will be impossible if $n-s$ verifiable buses are added in the way described in Corollary 4.9. However, it is the attacker's decision to select which $|\mathfrak{s}|$ of the $n$ topologies to "hide" in. The comparison between Case 1 and Case 2 in the previous scenario has shown that by selecting different $\mathfrak{s}$ the attacker will significantly change the number of estimated states that could be deviated. Therefore, the operator should try to find a solution to minimize $\|\Delta\hat{\mathbf{x}}\|_0$ regardless of the selection of $\mathfrak{s}$ by the attacker. Suppose that bus 5 is verifiable in Case 4 shown in Table 5.2, $\|\Delta\hat{\mathbf{x}}\|_0 \equiv 0$ for any possible $(\mathfrak{s},\mathfrak{n})$-stealthy attack with $|\mathfrak{s}| = 3$ and $|\mathfrak{n}| = 4$. Note that in the scenario without any verifiable state, Case 4 is one of the

least preferable strategies for the operator to select $\mathfrak{n}$. Case 3 in Table 5.2, however, which is the optimal strategy in the former scenario, becomes the last strategy that operator would consider in this scenario. This is because for the scenario with verifiable states, in order to make $\|\Delta\hat{\mathbf{x}}\|_0 \equiv 0$ hold for any possible $(\mathfrak{s}, \mathfrak{n})$-stealthy attack in Case 3, all buses should be verifiable except for the reference bus. In summary, the existence of the verifiable states can significantly change the strategies for selecting $\mathfrak{n}$ and the reference bus.

# Chapter 6

# Conclusion & Future Work

## 6.1 Conclusion

The existence of possible stealthy attacks in the power system, where the system operator could purposely switch the network topology by rotationally switching off one of the preselected transmission lines, is considered. The effects of such a strategy on the stealthy attacks were shown. It is necessary and sufficient for the system operator to select a set of links to cut by turns while this preselected link set forms a spanning tree of the network topology. The general form of the possible stealthy attacks was formulated in the case when there always exists a possible stealthy attack. The effects on the power generation cost caused by the proposed strategy was also analyzed. Then the scenario in which the attacker launches an attack that is "partially" stealthy in some of the topologies preselected by the operator, is studied. It was shown that there will be a linear trade-off between the flexibility of manipulating the estimation deviation, and the possibility of not being detected. The general form of the possible deviations of the estimated states was also formulated. It turned out that the deviations can only be designed in a "component" sense. Simulations results showed

the efficiency of the proposed strategy in detecting the stealthy attacks, as well as the effects on the power generation cost. The countermeasures for the case when there always exists possible stealthy attacks were discussed. Several cases were studied to show how the deviations can be affected by the decisions made by both the attacker and the system operator.

## 6.2 Future Work

Our future directions include the transient stability during the transition of topologies, the impacts on the generation cost caused by the transition from one topology to another, the optimal order for switching the topologies that maximizes the efficiency of detection from the operator's perspective, and the minimum effort required to learn the current topology from the attacker's perspective. Moreover, we would like to take into account, such as meeting the dynamical applications in the smart grid, in the design of the network switching strategies and study the possible tradeoff or conflicts between different criteria.

## Acknowledgement

I would like to sincerely thank Professor F. Pasqualetti for the insightful discussions and comments.

# Part II

# Fully Distributed Dynamic State Estimation Using Networked Multi-agents

# Chapter 7

# Introduction

## 7.1 Overview & Related Works

The studies of state estimation using networked multi-agents, have a wide range of applications such as target tracking, region monitoring and area surveillance. The traditional centralized approaches usually obtain the optimal solution using the collective measurements from every single sensor in the network. This generally poses heavy burdens in both communication and computation especially as the size of the network increases. In comparison, distributed strategies use a so-called *peer-to-peer* communication schemes and hence, have the advantages of being scalable for large-scale network and being robust against unexpected node or link failures. Therefore, distributed strategies using networked multi-agents with capabilities of sensing and communication, have drawn increasing attention in recent years [2, 7–9, 15, 19, 26, 32, 33, 36, 47, 55, 60, 61, 65]. In exchange of these advantages, however, due to the difficulties in tracking the cross-covariances between each pair of local estimates in a scalable manner, the distributed strategies usually compute

only suboptimal estimates and approximate error covariances due to the difficulties in tracking the cross-covariances between local estimates in a scalable manner.

The consensus algorithm, as a possible tool to solve the distributed state estimation problems, is considered from the Kalman filter's perspective in [65] and [2] to address a static state estimation problem. The Kalman-consensus filter (KCF) [60], with an average-consensus term added in the update steps of the local Kalman filter, aims at asymptotically driving the local estimates of each agent to be identical. The KCF assumes that each agent and its neighbors have joint observability of the state of interest [61]. This is relaxed in [33], where the scenario with locally unobservable agents is considered, and the generalized KCF (GKCF) is considered. The same scenario is also considered in [36], where the authors propose the information-consensus filter (ICF), and analytically show that the ICF is able to asymptotically approach the centralized solution, if the undirected network topology is connected and each agent communicates with its neighbors for infinite iterations before updating its local estimate at each time instant. Further studies of the ICF can be found in [32]. Some other consensus-based filtering algorithms can be founded in [52, 53].

Aside from the consensus-based algorithms, which generally requires multiple communication iterations per time instant, an alternative diffusion-based algorithms, referred as the diffusion Kalman filter (DKF), is first proposed in [15]. In the DKF, each agent first updates its local estimate using its own and neighbors' measurements, and then computes a convex combination of the resulting estimate along with its neighbors'. This requires each agent to communicate only twice instead of a large number of times with its local neighbors before updating its final local estimate at each time instant. The boundedness of local estimate errors obtained by the DKF is shown based on the assumption that the target is jointly detectable in the inclusive neighborhood of every agent.

This assumption is relaxed in [26], where a Covariance Intersection based DKF (CI-DKF) is proposed. Two algorithms are proposed therein to handle, respectively, the scenario where at least one agent has local joint observability, and the scenario where each agent can have at most local joint observability of a subset of state components.

Recently, a notable approach aims at achieving consensus on the probability density functions of local estimates, is proposed in [9], and further studied in detail in [7, 8] for the linear Gaussian case. The stability condition is also investigated for the case of LTI models and a fixed topology. Moreover, the local estimates are guaranteed to be *consistent*, *i.e.*, the approximated error covariance of the local estimate is lower bounded by the true unknown one [27, 30]. It is shown in their later work [8] that, however, such consistent estimates might be too conservative. A countermeasure for such conservatism is also proposed in [8]. However, it might not be applicable to more general scenarios considered in this work (see Section 9.3 for details). As the follow-up work, the algorithm is further extended in [10] to the scenario with nonlinearities involved in both the process and the sensing models. The extended nonlinear filtering algorithm is based on the extended Kalman filter (EKF) paradigm, and is shown to enjoy the local stability properties. Different from the EKF-based approach, the authors in [45, 46] have used the unscented transformation (UT) [29], and designed the solution to the same scenario.

When the process model of the target is uncertain, the multiple model (MM) estimation algorithms [6] have been proposed by using a finite set of candidate models and accordingly computing a bank of Kalman filters in parallel to estimate the state of the target with model uncertainties. By assuming that the exact model at every time instant belongs to a set of finite possible models and follows a Markov process with known probabilities, it is shown that one is able to identify

the underlying model and track the state of interest simultaneously. See [48] for a comprehensive survey and [3, 70] for some further results. Moreover, in recent, distributed approaches in solving the MM estimation problems also become an active research area [19, 47, 55]. Specifically the authors [19, 47] use consensus-based approach and the work in [55] is diffusion-based.

Before moving to the next subsection, it is clarified that this work focuses on the approaches storing only the estimate and associated approximated error covariance at the previous single time instant. The readers are referred to [20] and the references therein for the approaches based on a moving-horizon estimation methodology. Moreover, other than the framework of discrete-time linear systems in which the results of this work are proposed, the readers are referred to [75, 76] and the references therein for works in the framework of continuous-time linear systems.

## 7.2 Motivations

The motivations are discussed in the following with respect to each scenario to be considered by this work.

For the scenario with single linear process and local sensing models, the existing related literature usually makes some of the following assumptions either explicitly or implicitly. a) Every agent and its neighbors have joint observability or at least detectability about the target of interest [15, 61]. b) Some global parameters (the total number of agents, maximum in-degree of the graph, *etc.*) are known to each agent [15,26,32,33,36,61]. c) The agents are able to communicate with their neighbors for multiple (or infinite in the ideal case) iterations before updating their local estimates at every time instant [26,32,33,36,61]. d) The communication graph is connected (in the undirected case) or strongly connected (in the directed case) [7–9, 15, 26, 61] and even also balanced [36]. e)

In the stability analysis, the process model of the target, the sensing model of the local agents, and/or the communication topology are/is assumed to be time invariant [7–9, 15, 52, 53, 61]. In general, these assumptions will impose different limitations in a more realistic scenario (detailed motivations are discussed in Section 9.1.1). This work aims at overcoming these limitations and propose an algorithm, and analyze the stability in a more general scenario without any of the above limitation.

Aside from the scenario with linear process and sensing models, this work also aims at considering the scenario where the models are nonlinear by extending the algorithm proposed in the linear scenario. Different from the EKF-based extension as did in [10], the unscented transformation (UT) is adopted for the extension. The UT is better known for its embed in the Kalman filter as a solution in the case of nonlinear models. Such a solution is referred as the unscented Kalman filter [29] (UKF). The UKF has been regarded as a superior alternative of the EKF especially when the systems are highly nonlinear. Compared to the EKF, it requires no computation of Jacobian matrices at every time instant, and approximates the nonlinear models accurately to the third order [29]. The existing UT-based algorithms ( [45, 46]) for solving the same problem are also consensus-based and hence need multiple communication iterations during every sampling time interval. This would cause heavy communication burdens in general.

While a single model is usually assumed for the target of interest. However, a single model might not be enough to describe the target of interest in some applications. For example, a maneuvering target can move along straight or curved trajectories with the model switching over time. Thus, all single-model based algorithms, either centralized or distributed, will be ineffective in tracking such a target. Another possible difficulty is that the accurate knowledge (noise level,

deterministic input) about the target itself might be hard to obtain. To the best of the author's knowledge, the very first step that applies the MM approach in the distributed estimation framework, is taken by [47]. A consensus-based distributed MM Unscented Kalman Filter is proposed therein to tracking jumping Markov nonlinear systems. A different consensus approach is proposed in [19], which aims at getting satisfactory performance with a smaller number of consensus iterations and also takes into account the presence of local agents without sensing ability. Both consensus-based algorithms intend to have local agents communicate multiple iterations before updating their local estimates as well as the local mode probabilities during each sampling time interval. Again as aforementioned for many times, this might cause too much energy consumption and hence be unrealistic for implementations, as pointed out in [55], where a DKF-based MM adaptive estimation algorithm is proposed to estimate a dynamic complex-value state with a fixed but unknown process model. However, the nature of the DKF implies that the algorithm in [55] also requires each local agent to have joint observability about the target in its inclusive neighborhood. This assumption does not hold in general (see examples in [26, 33, 36, 80, 81]).

## 7.3 Contributions & Organization

Before stating the main contributions of this work, preliminaries are stated in Chapter 8. Then the main contributions, as will be briefly mentioned one by one in the following, are stated in Chapter 9, 10 and 11. The conclusions and future directions are given in Chapter 12.

In Chapter 9, the scenario with linear process and sensing models is considered. A *distributed hybrid information fusion* (DHIF) algorithm, is proposed. The algorithm is unified in the sense that on one hand, it does not need to treat different situations separately (see [26]); on the

other hand, it is able to handle the situation where none of the assumption (discussed at the beginning of Section 7.2) necessarily holds and hence, fits a wide range of scenarios without any ad-hoc modification of the algorithm. By proposing an innovative approach, namely, the (directed) *orderly appearing path* between two agents in a finite time interval, this work explores very mild conditions on general directed switching graphs and joint network observability/detectability to guarantee that the local estimate errors of all agents a) are *uniformly* upper bounded (in the positive definite sense) in finite time; and b) converge to zero asymptotically in expectation. The conditions are shown to be "almost" necessary. Specifically, the conditions are necessary in a special case. The comparisons with existing algorithms are shown both analytically and numerically.

In Chapter 10, In the end, the proposed algorithm is extended to the situation with nonlinearities involved in both the process and the sensing models. A nonlinear DHIF algorithm is proposed by adopting the unscented transformation approach so that no computation of Jacobian matrix is needed. The nonlinear DHIF algorithm requires only one communication iteration between every two consecutive time instants. It is also analytically shown that for the case with linear sensing models, the local estimate errors are bounded in the mean square sense.

In Chapter 11, the DHIF algorithm is further extended to the scenario where the process model of interest is not certain to any local agent. Two algorithms are proposed by following the two well-known multiple model (MM) paradigms, namely, the first order generalized pseudo Bayesian and the interacting MM approaches. The extended algorithms inherit the advantages of the original DHIF algorithm for being fully distributed, being robust against agents not directly sensing the target, and requiring only single communication iteration among agents during each sampling interval. It is shown in the case when the unknown underlying model is fixed, all local

agents are able to asymptotically identify the true underlying model and estimate the state of interest simultaneously. The output local estimate are shown to have uniformly upper bounded estimate error with sufficient conditions formulated. Simulations are shown to illustrate the analytical results as well as the performances of the proposed algorithms.

# Chapter 8

# Preliminaries

## 8.1 Notations

The following notations are defined throughout Part II of this dissertation to avoid possible ambiguities. Denotes $\mathbb{Z}^+$ the set of positive integers. $\mathbb{Z}^* \triangleq \mathbb{Z}^+ \cup \{0\}$. $\mathbb{E}[\cdot]$ denotes the expectation of a random variable. $\Pr(\cdot)$ is the probability function. The symbol "$\otimes$" denotes the Kronecker product. The ceil function is denoted as ceil$\{\cdot\}$. The super-index $k \in \mathbb{Z}^+$ in parenthesis, denoted as $\{\cdot\}^{(k)}$, denotes the variable at the time instant $k$. The interval of time instants $\mathfrak{I}_{k_0}^{k_t}$ is defined as $\mathfrak{I}_{k_0}^{k_t} \triangleq [k_0, \ldots, k_t]$ for some $k_t \geq k_0$, where $k_0,\ k_t \in \mathbb{Z}^+$. The block diagonal operator is denoted as blkdiag$\{\cdot\}$. The 2-norm of a vector is denoted as $\|\cdot\|$.

Moreover, all vectors and matrices are denoted by bold letters in, respectively, lowercase and uppercase. The $n \times n$ identity matrix is denoted as $\mathbf{I}_n$. The notation $\mathbf{0}$ is an all-zero matrix or vector with appropriate dimension according to the context. The notation $\mathbf{1}$ is an all-one vector with appropriate dimension according to the context. The "MATLAB" tradition is used to denote entry/row/column/submatrices of a matrix. For an arbitrary matrix $\mathbf{X}$, $\{\mathbf{X}\}_{(\mathscr{O}_1,\mathscr{O}_2)}$ is the sub-matrix

formed by the entries with the row and column indices in, respectively, $\mathscr{O}_1$ and $\mathscr{O}_2$ for some index sets $\mathscr{O}_1$ and $\mathscr{O}_2$. The index set can be replaced by a single index to denote a specific row/column, or be replaced by ":" to denote all rows/columns. If $\mathbf{X}$ is a square matrix, the trace and the determinant of $\mathbf{X}$ are, respectively, denoted as $\mathrm{tr}(\mathbf{X})$ and $\|\mathbf{X}\|$. If $\mathbf{X}$ is also nonsingular, $\mathbf{X}^{-n\top} \triangleq ((\mathbf{X}^n)^{-1})^\top$ for some $n \in \mathbb{Z}^*$. If it is also satisfied that $\mathbf{X} \succ \mathbf{0}$, it is then defined that $\sqrt{\mathbf{X}} \triangleq \mathbf{Y}$, where $\mathbf{Y}$ fulfills $\mathbf{Y}\mathbf{Y}^\top = \mathbf{X}$. For any arbitrary symmetric matrices $\mathbf{X}_1$ and $\mathbf{X}_2$ with the same dimension, $\mathbf{X}_1 \succeq \mathbf{X}_2$ (respectively, $\mathbf{X}_1 \succ \mathbf{X}_2$) denotes that $\mathbf{X}_1 - \mathbf{X}_2$ is a positive semi-definite (respectively, positive definite) matrix. $\mathbf{X}_1 \geq \mathbf{X}_2$ (respectively, $\mathbf{X}_1 > \mathbf{X}_2$) implies that $\mathbf{X}_1 - \mathbf{X}_2$ is a non-negative (respectively, positive) matrix.

## 8.2 Graph Theory & Adjacency Matrix

A directed graph $\mathscr{G}^{(k)}(\mathscr{V}^{(k)}, \mathscr{E}^{(k)})$ is used to represent the communication topology of a large-scale sensor network, where $\mathscr{V}^{(k)}$ and $\mathscr{E}^{(k)} \subseteq \mathscr{V}^{(k)} \times \mathscr{V}^{(k)}$ are respectively, the set of vertices that stands for the local agents and edges that stands for the communication channels. As the total number of agents will not be involved in any result throughout this work, without loss of generality, it is supposed that there are constantly $N$ agents, *i.e.,* $\mathscr{V}^{(k)} = \mathscr{V} = \{1, \ldots, N\}$, $\forall k$. For simplicity, $\mathscr{G}^{(k)}(\mathscr{V}, \mathscr{E}^{(k)})$ is sometimes denoted as $\mathscr{G}^{(k)}$. An *edge* $(i, j) \in \mathscr{E}^{(k)}$ denotes that $j$ can receive information from $i$ (not necessarily vice versa). Then $i$ is the *parent vertex* of $j$, and $j$ is a *child vertex* of $i$. Let $N_{i,\mathrm{in}}^{(k)} \triangleq \{j | (j,i) \in \mathscr{E}^{(k)},\ \forall j \neq i\}$ and $N_{i,\mathrm{out}}^{(k)} \triangleq \{j | (i,j) \in \mathscr{E}^{(k)},\ \forall j \neq i\}$ be respectively, the set of the *in-neighbors* and *out-neighbors* of agent $i$. Let $J_i^{(k)} \triangleq N_{i,\mathrm{in}}^{(k)} \cup \{i\}$ be the *inclusive neighborhood* of agent $i$. A graph is *complete* if $j \in N_{i,\mathrm{in}}^{(k)}$ for any $i$ and $j$. A *directed path* from vertex $i_0$ to vertex $i_\ell$ is an ordered sequence of vertices $i_0, i_1, \ldots, i_\ell$ such that $(i_{j-1}, i_j) \in \mathscr{E}^{(k)}$

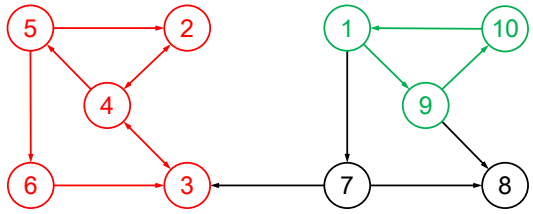


Figure 8.1: Example of strongly connected component and leader component. The subgraph in red is a strongly connected component but not a leader component as it has an incoming edge $(7,3)$. The subgraph in green is a leader component.

for $1 \leq j \leq \ell$. A directed graph is *strongly connected* if there exists at least one directed path from every vertex to every other vertex. A *subgraph* of $\mathcal{G}^{(k)}$, denoted as $\tilde{\mathcal{G}}^{(k)}(\tilde{\mathcal{V}}, \tilde{\mathcal{E}}^{(k)})$, is a graph such that $\tilde{\mathcal{V}}^{(k)} \subseteq \mathcal{V}$ and $\tilde{\mathcal{E}}^{(k)} \subseteq \mathcal{E}^{(k)}$. A graph $\mathcal{G}^{(k)}$ is a *directed spanning tree* if the graph is a directed tree that contains all vertices of $\mathcal{G}^{(k)}$. A graph $\mathcal{G}^{(k)}$ *contains a directed spanning tree* if there exists at least one subgraph of $\mathcal{G}^{(k)}$ that is a directed spanning tree. A *strongly connected component* is a strongly connected subgraph of $\mathcal{G}^{(k)}$ such that no additional edges or vertices from $\mathcal{G}^{(k)}$ can be included in the subgraph without breaking its property of being strongly connected. A *leader component* is a strongly connected component with no incoming edges. The *union graph* over a time interval $\mathfrak{I}$ is defined as $\mathcal{G}[\mathfrak{I}] \triangleq \mathcal{G}(\mathcal{V}, \cup_{k\in\mathfrak{I}}\mathcal{E}^{(k)})$.

The *adjacency matrix*, is used for describing the weights of the edges. Such a matrix and the described graph are referred as being associated with each other. The adjacency matrix $\mathbf{A}^{(k)} \in \mathbb{R}^{N\times N}$ associated with $\mathcal{G}^{(k)}$ is defined as $\{\mathbf{A}^{(k)}\}_{(i,j)} > 0$ if $(j,i) \in \mathcal{E}^{(k)}$, and $\{\mathbf{A}^{(k)}\}_{(i,j)} = 0$ otherwise. For each $i \in \mathcal{V}$, $a_{ij}^{(k)}$ is the weight agent $i$ assigned to the information received from agent $j$ at time instant $k$. In this chapter, self edges are always assumed. Thus, $\{\mathbf{A}^{(k)}\}_{(i,i)} > 0, \forall i \in \mathcal{V}$. A graph is *balanced* if $\sum_{j=1}^{N} a_{ij}^{(k)} = \sum_{j=1}^{N} a_{ji}^{(k)}$. Note that depending on the selections of entries, for a certain graph, there exist an infinite number of associated adjacency matrices, each of which has the

same structure (positive or zero entries). In this work, a special adjacency matrix, denoted as $\mathbf{D}^{(k)}$, is usually adopted such that $\mathbf{D}^{(k)}$ is *row stochastic*, which implies that $\sum_{j\in\mathscr{V}}\{\mathbf{D}^{(k)}\}_{(i,j)} = 1, \forall i \in \mathscr{V}$. A row stochastic matrix is *primitive* if and only if its associated graph is strongly connected. If it also holds that $\sum_i\{D\}_{(i,j)} = 1,\ \forall j$, then $\mathbf{D}^{(k)}$ is a *doubly stochastic matrix*. A row stochastic matrix has its largest eigenvalue being 1.

## 8.3 Consistent Information

In one word, a piece of general information (estimate, measurement *etc.*) is consistent if its approximated error/noise covariance is lower bounded by the true unknown one [27, 30], as defined in the following.

**Definition 8.1 ( [30])** *Let* $\hat{\mathbf{a}}$ *and* $\mathbf{P}_a$ *be, respectively, the approximated mean and covariance of a random variable* $\mathbf{a}$*, where* $\mathbf{a} = \mathbf{H}_b\mathbf{b} + \mathbf{n}$ *with* $\mathbf{b}$ *and* $\mathbf{n}$ *being, respectively, the unknown quantity of interest and the associated error/noise.* $\mathbf{H}_b$ *is a matrix with appropriate dimension. The pair* $(\hat{\mathbf{a}}, \mathbf{P}_a)$ *is* consistent *if* $\mathbf{P}_a \succeq \tilde{\mathbf{P}}_a$*, where* $\tilde{\mathbf{P}}_a \triangleq \mathbb{E}[(\hat{\mathbf{a}} - \mathbf{H}_b\mathbf{b})(\hat{\mathbf{a}} - \mathbf{H}_b\mathbf{b})^\top]$ *is the true error/noise covariance of* $\hat{\mathbf{a}}$.

Note that in Definition 8.1, the pair $(\hat{\mathbf{a}}, \mathbf{P}_a)$ can be either a measurement of $\mathbf{b}$ with $\mathbf{P}_a$ being the approximated noise covariance, or an estimate of $\mathbf{b}$ (*i.e.*, $\mathbf{H}_b$ is identity) with $\mathbf{P}_a$ being the approximated estimate error covariance.

The consistency is a fundamental but critical property that an estimate should have. An inconsistent estimate is over-confident and hence, its approximated error covariance does not realistically imply its uncertainty [18]. This might cause issues when it is further used for the downstream functions (data association *etc.*). The consistency of local estimates is worth paying attention to due

to the fact that the same process noise corrupts the state of interest, and therefore causes significant cross-correlations between each pair of the local estimates. The inconsistency of the local estimates might be caused if such cross-correlations are not well accounted for.

## 8.4 Observability of Discrete LTV System

The observability property of a discrete linear time-varying (LTV) system is stated as follows.

**Definition 8.2 ( [44])** *A discrete LTV system with state propagation matrix* $\mathbf{F}^{(k)}$ *and observation matrix* $\mathbf{H}^{(k)}$ *is observable on the time interval* $\mathfrak{I}_h^l$ *if the matrix* $\mathbf{O}[h,l] \triangleq \sum_{k=h}^{l} (\boldsymbol{\mathscr{F}}_h^k)^\top (\mathbf{H}^{(k)})^\top \mathbf{H}^{(k)} \boldsymbol{\mathscr{F}}_h^k$ *is full rank, where* $\boldsymbol{\mathscr{F}}_h^k$ *is the state transition matrix from h to k and satisfying* $\boldsymbol{\mathscr{F}}_{k'}^{k+1} = \mathbf{F}^{(k)} \boldsymbol{\mathscr{F}}_{k'}^k$ *for some* $k' \leq k$*, and* $\boldsymbol{\mathscr{F}}_k^k$ *is identity.*

## 8.5 Unscented Transformation

The unscented transformation (UT) is a method to approximate the statistics of a random variable undergoing a nonlinear transformation. Given a random variable with known statistics, the UT can be briefly described as follow. A set of so-called *sigma points* are deterministically sampled to parameterize the statistics of this random variable. The details for such parameterizations is omitted at this point as it will be embedded into our algorithm and hence will be elaborated later in this work. It is worth mentioning that such parameterizations is done in the way such that the sample mean and sample covariance coincide with those of the random variable. After the sigma points are determined, they are individually fed into the nonlinear transformation. A set of transformed points

is therefore obtained and is used for characterizing the statistics of the random variable after the nonlinear transformation. The UT has the advantage of being able to characterize the probability distribution with only a very small set of points.

The UT has been adopted as a fundamental component by the authors in [29] to propose the UKF which has equivalent performance to the Kalman filter for linear systems and generalizes to nonlinear systems. Compared to the EKF – a commonly used nonlinear filter, the UKF requires no linearization steps which 1) might bring instabilities especially when the assumption of local linearity is not well fulfilled; 2) requires the derivation of Jacobian matrices that might lead to implementation difficulties. Moreover, it is analytically shown in [29] that the UKF has better expected performance than that of the EKF.

## 8.6 Multiple Model Estimation

The MM approach has been regarded as an efficient estimation method when the target contains both continuous (process noise) and discrete (mode) uncertainties. The MM approach assumes the true model (either fixed or switching over time) to be one of a finite number of models. Each model is separately parameterized and hence can be different in the dynamics, the noise statistics and/or state space.

It is pointed out in [6] that even with the mode switching process following a jumping Markov process, the optimal estimate still requires conditioning on each mode history, the number of which increases exponentially with time. Therefore, suboptimal approaches are used for practical implementations. In this paper, we are interested in two well-known suboptimal approaches, namely, the first-order generalized pseudo-Bayesian (GPB1) MM approach and the interacting multiple

model (IMM) approach. Both account for each possible current mode and associate a Kalman filter to compute the mode-matched estimate. The IMM approach contains all steps of the GPB1 approach with an extra mixing of the previous model-conditioned estimates depending on the current model.

# Chapter 9

# Distributed State Estimation with Linear Process and Local Sensing Models

This chapter studies the problem of distributed state estimation in the scenario where the process model of the target and the local sensing models are linear.

## 9.1 Problem Formulation

### 9.1.1 Motivation

The motivations for relaxing the limitations imposed by the assumptions mentioned in the second paragraph of Section 7.2, are provided in this subsection.

First of all, as large-scale sensor networks are usually deployed to monitor geographically large areas, it is quite common to encounter a situation where the target of interest is not in the sensing ranges of a subset of local agents. As a result, the assumption of local joint observabili-

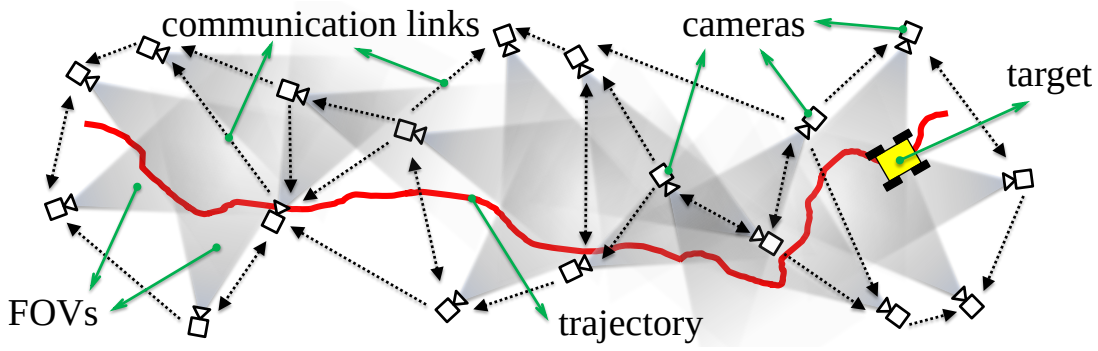


Figure 9.1: Example of time-varying set of agents directly sensing the target. As the target moves along its trajectory, it passes the field-of-views (FOVs) of only a subset of cameras, which might change over time.

ty/detectability at every agent is not satisfied in general. Moreover, the status whether each agent senses the target is generally changing over time, as shown by the example in Figure 9.1.

Second, although some global parameters (total number of agents, graph degree, *etc.*) might be learned in off-line manners, it is still possible for these parameters to change during the filtering process. For example, an unexpected node failure will change the total number of agents and possibly also the degree of the graph. The performance of local agents without knowing such changes might be deteriorated if the algorithm depends on these global parameters.

Third, the assumption on the feasibility of multiple communication iterations per sampling time instant might cause too much energy consumption and hence might not hold with limited energy constraint.

Forth, the assumption of a time-invariant communication topology might not hold in many scenarios. The causes of switching communication topologies might span from positive reasons, such as the pre-scheduled communication schemes, to passive reasons, such as unexpected failures of communication channels, package dropouts, or the changes in the physical distances between mobile agents.

Lastly, a time-varying model for the target is more general. Moreover, the local sensing models can change due to temporary sensor failures or the movement of the target in or out of the sensing ranges of sensors equipped at agents.

### 9.1.2 Models & Assumptions

This chapter considers the following linear dynamic system as the process model of the target of interest:

$$\mathbf{x}^{(k+1)} = \mathbf{F}^{(k)}\mathbf{x}^{(k)} + \mathbf{w}^{(k)}, \tag{9.1}$$

where $\mathbf{x}^{(k)} \in \mathbb{R}^n$ is the state of interest; $\mathbf{F}^{(k)} \in \mathbb{R}^{n\times n}$ is the state propagation matrix. The process noise $\mathbf{w}^{(k)} \in \mathbb{R}^{p_k}$ is assumed to be white Gaussian, *i.e.,* $\mathbf{w}^{(k)} \sim \mathcal{N}(\mathbf{0}, \tilde{\mathbf{Q}}^{(k)})$, $\forall k \in \mathbb{Z}^+$. Here $\tilde{\mathbf{Q}}^{(k)}$ is the true covariance of the process noise at time instant $k$. It is assumed that $\tilde{\mathbf{Q}}^{(k)} \succ \mathbf{0}$, $\forall k \in \mathbb{Z}^+$. Moreover, it is assumed that $\mathbb{E}[\mathbf{x}^{(k')}(\mathbf{w}^{(k)})^\top] = \mathbf{0}$, $\forall k' \in \mathbb{Z}^*$ and $k > k'$.

Each agent $i \in \mathcal{V}$ obtains a local measurement $\mathbf{z}_i^{(k)} \in \mathbb{R}^{m_{i,k}}$, which follows a linear sensing model:

$$\mathbf{z}_i^{(k)} = \mathbf{H}_i^{(k)}\mathbf{x}^{(k)} + \mathbf{v}_i^{(k)}, \tag{9.2}$$

where $\mathbf{H}_i^{(k)} \in \mathbb{R}^{m_{i,k}\times n}$ is the local observation matrix; $\mathbf{v}_i^{(k)} \in \mathbb{R}^{m_{i,k}}$ is the local measurement noise and also assumed to be white Gaussian, *i.e.,* $\mathbf{v}_i^{(k)} \sim \mathcal{N}(\mathbf{0}, \tilde{\mathbf{R}}_i^{(k)})$ with $\tilde{\mathbf{R}}_i^{(k)} \succ \mathbf{0}$ being the true covariance of the measurement noise. The following assumption is made throughout this work.

**Assumption 9.1.1** *For each $k \in \mathbb{Z}^+$, each agent $i \in \mathcal{V}$ knows:*

*(a) the state propagation matrix $\mathbf{F}^{(k)}$;*

*(b) a consistent approximation of the process noise covariance, denoted as $\mathbf{Q}^{(k)}$, i.e., $\mathbf{Q}^{(k)} \succeq \tilde{\mathbf{Q}}^{(k)}$;*

*(c) a consistent approximation of its local measurement noise covariance, denote as* $\mathbf{R}_i^{(k)}$*, i.e.,* $\mathbf{R}_i^{(k)} \succeq \tilde{\mathbf{R}}_i^{(k)}$.

For simplicity, it is assumed in the rest of this chapter that $\mathbf{Q}^{(k)} = \mathbf{Q}$ and $\tilde{\mathbf{Q}}^{(k)} = \tilde{\mathbf{Q}}$, for all $k \in \mathbb{Z}^+$. The same results hold for the case when these variables are time varying. Assumption 9.1.1.(b) and Assumption 9.1.1.(c) are to guarantee that the uncertainty from, respectively, the process noise and the measurement noise, are not underestimated.

At any time instant, if the target is not directly sensed by a certain agent, either due to the target being out of the agent's sensing range, or due to temporary sensor failure at the agent, the following assumption is made.

**Assumption 9.1.2** *If the target of interest is not directly sensed by an agent* $i \in \mathscr{V}$ *at time instant k,* $(\mathbf{R}_i^{(k)})^{-1} = \mathbf{0}$ *and* $\mathbf{z}_i^{(k)}$ *is arbitrary. Moreover,* $\mathbf{H}_i^{(k)} = \mathbf{0}$.

Assumption 9.1.2 essentially states that an agent that does not directly sense the target assumes infinite uncertainties about its local measurement. This also guarantees the consistency of the local measurements and matches Assumption 9.1.1.(c) although it is obviously trivial. It is worth mentioning that assuming $\mathbf{H}_i^{(k)} = \mathbf{0}$ in Assumption 9.1.2 is only for the clarity of the observability condition later in this work. With only a subset of agents directly sensing the target, the concept of *blind agents* is defined as follows.

**Definition 9.1 (Blind agents)** *Let* $\mathscr{B}^{(k)} \subset \mathscr{V}$ *be the set of blind agents across the network at time instant k. Then* $i \in \mathscr{B}^{(k)}$ *if none of* $j \in J_i^{(k)}$ *directly senses the target at time instant k.*

Note that according to Assumption 9.1.2, if $i \in \mathscr{B}^{(k)}$, one has $(\mathbf{R}_j^{(k)})^{-1} = \mathbf{0}$ and $\mathbf{H}_j^{(k)} = \mathbf{0}$, $\forall j \in J_i^{(k)}$. Here we use the term "blind agent". Similar terms have been used in the literature [9, 26, 33, 36].

For example, the "naive agent" in [33, 36], the "communication node" in [9], and the "node with no local uniform observability" in [26]. However, it is assumed therein that the set of agents not directly sensing the target are unchanged with time for the simplicity of the stability analysis. As a result, those terms can be equivalently defined using the time-invariant observability/detectability conditions in the inclusive neighborhood. In this work, however, as we are interested in a more general scenario where the set of such agents might subject to changes with time, the term "blind" is used to reflect only the status whether a certain agent or any of its in-neighbors directly senses the target at a certain time instant. The change of such status of any agent can be regarded as a change of the local sensing model, and hence, will be handled by the formulated unified framework.

### 9.1.3 Objectives

With the motivations provided in Section 9.1.1, the objectives are formulated as follows. It is aimed to design a unified algorithm such that each agent modeled by Eq. (9.2) cooperates with its neighbors through communication, and comes up with an estimate of the target modeled by Eq. (9.1). The local estimates should be as confident as possible while its consistency is guaranteed. The agents can communicate with local neighbors for only once per time instant. No global parameter is allowed. The communication topology among agents is modeled as a general directed time-varying graph. It is aimed to search for very mild conditions to guarantee the convergence of the proposed algorithm in the considered scenario.

## 9.2 Distributed Hybrid Information Fusion (DHIF) Algorithm

At time instant $k$, let $\hat{\mathbf{x}}_i^{k|k-1}$ and $\hat{\mathbf{x}}_i^{k|k}$ be, respectively, the prior and posterior estimate of $\mathbf{x}^{(k)}$. Let $\hat{\boldsymbol{\eta}}_i^{k|k-1} \triangleq \hat{\mathbf{x}}_i^{k|k-1} - \mathbf{x}^{(k)}$ and $\hat{\boldsymbol{\eta}}_i^{k|k} \triangleq \hat{\mathbf{x}}_i^{k|k} - \mathbf{x}^{(k)}$. Let $\hat{\mathbf{P}}_i^{k|k-1}$ and $\hat{\mathbf{P}}_i^{k|k}$ be the approximations of, respectively, $\mathbf{P}_i^{k|k-1}$ and $\mathbf{P}_i^{k|k}$, where $\mathbf{P}_i^{k|k-1} \triangleq \mathbb{E}\left[\hat{\boldsymbol{\eta}}_i^{k|k-1}\left(\hat{\boldsymbol{\eta}}_i^{k|k-1}\right)^\top\right]$ and $\mathbf{P}_i^{k|k} \triangleq \mathbb{E}\left[\hat{\boldsymbol{\eta}}_i^{k|k}\left(\hat{\boldsymbol{\eta}}_i^{k|k}\right)^\top\right]$. The following assumptions are made throughout this work.

**Assumption 9.2.1** *At each $k \in \mathbb{Z}^+$, (a) $\mathbb{E}\left[\mathbf{v}_i^{(k)}\left(\mathbf{v}_j^{(k)}\right)^\top\right] = \mathbf{0}$, $\forall i \neq j$; and (b) $\mathbb{E}\left[\hat{\boldsymbol{\eta}}_i^{k|k-1}\left(\mathbf{v}_j^{(k)}\right)^\top\right] = \mathbf{0}$, $\forall i, j$.*

### 9.2.1 An Information Fusion Perspective

Suppose that at $k \in \mathbb{Z}^+$, agent $i$ aims at updating its local estimate by incorporating the prior local estimate pair, denoted as $\left(\hat{\mathbf{x}}_j^{k|k-1}, \hat{\mathbf{P}}_j^{k|k-1}\right)$, and the local measurement pair, denoted as $\left(\mathbf{z}_j^{(k)}, \mathbf{R}_j^{(k)}\right)$, received from every $j \in N_{i,\text{in}}^{(k)}$. Suppose that $\hat{\mathbf{P}}_j^{k|k-1} \succeq \mathbf{P}_j^{k|k-1}$, $\forall j \in N_{i,\text{in}}^{(k)}$. The proposed updating step can be regarded as a hybrid of two fusion sub-steps.

The first sub-step is to fuse all prior estimate pairs, *i.e.*, $\left(\hat{\mathbf{x}}_j^{k|k-1}, \hat{\mathbf{P}}_j^{k|k-1}\right)$, $\forall j \in N_{i,\text{in}}^{(k)}$, and obtain an intermediate estimate pair, denoted as $\left(\check{\mathbf{x}}_i^{(k)}, \check{\mathbf{P}}_i^{(k)}\right)$. Note that due to the same process noise of the target observed by each local agent, as well as the exchange of local measurements in previous time instants, the local estimates are highly correlated in general. However, such significant correlations are difficult to track in a fully distributed framework. Therefore, the CI algorithm [30] is used for this sub-step to guarantee the consistency of the fused estimate pair. That is,

$$\begin{aligned} \left(\check{\mathbf{P}}_i^{(k)}\right)^{-1} &= \sum\nolimits_{j \in J_i^{(k)}} d_{ij}^{(k)} \left(\hat{\mathbf{P}}_j^{k|k-1}\right)^{-1}, \\ \left(\check{\mathbf{P}}_i^{(k)}\right)^{-1} \check{\mathbf{x}}_i^{(k)} &= \sum\nolimits_{j \in J_i^{(k)}} d_{ij}^{(k)} \left(\hat{\mathbf{P}}_j^{k|k-1}\right)^{-1} \hat{\mathbf{x}}_j^{k|k-1}, \end{aligned} \tag{9.3}$$

where $d_{ij}^{(k)} \geq \underline{d}$ is the weight that agent $i$ assigns to the information received from agent $j \in N_{i,\text{in}}^{(k)}$ at time instant $k$, with $\underline{d} > 0$ being the uniform lower bound for all weights at any time instant. Moreover, $\sum_{j \in J_i^{(k)}} d_{ij}^{(k)} = 1$, $\forall i \in \mathscr{V}$. The selection of the set of weights $\left\{ d_{ij}^{(k)} \right\}_{j \in J_i^{(k)}}$ is critical and will be discussed in detail in Section 9.2.3.

The second sub-step is to fuse all local measurement pairs, $\left( \mathbf{z}_j^{(k)}, \mathbf{R}_j^{(k)} \right)$, $\forall j \in N_{i,\text{in}}^{(k)}$, with the intermediate estimate pair $\left( \check{\mathbf{x}}_i^{(k)}, \check{\mathbf{P}}_i^{(k)} \right)$. The standard optimal fusion strategy is used for this step. This requires the information pairs to have mutually uncorrelated errors, as shown in the following lemma.

**Lemma 9.2** *Let* $\left( \check{\mathbf{x}}_i^{(k)}, \check{\mathbf{P}}_i^{(k)} \right)$ *be defined in Eq.* (9.3)*. Under Assumption 9.2.1,* $\left( \mathbf{z}_j^{(k)}, \mathbf{R}_j^{(k)} \right)$, $\forall j \in J_i^{(k)}$ *and* $\left( \check{\mathbf{x}}_i^{(k)}, \check{\mathbf{P}}_i^{(k)} \right)$ *have mutually uncorrelated errors.*

**Proof.** With Assumption 9.2.1 (i) satisfied, it suffices to show that for each $l \in J_i^{(k)}$,

$$\mathbb{E}\left[ \left( \check{\mathbf{x}}_i^{(k)} - \mathbf{x}^{(k)} \right) \left( \mathbf{v}_l^{(k)} \right)^\top \right] = \mathbf{0}.$$

This can be verified by using Eq. (9.3) to obtain that

$$\begin{aligned}
&\mathbb{E}\left[ \left( \check{\mathbf{x}}_i^{(k)} - \mathbf{x}^{(k)} \right) \left( \mathbf{v}_l^{(k)} \right)^\top \right] \\
=&\mathbb{E}\left[ \left( \check{\mathbf{P}}_i^{(k)} \left( \check{\mathbf{P}}_i^{(k)} \right)^{-1} \check{\mathbf{x}}_i^{(k)} - \check{\mathbf{P}}_i^{(k)} \left( \check{\mathbf{P}}_i^{(k)} \right)^{-1} \mathbf{x}^{(k)} \right) \left( \mathbf{v}_l^{(k)} \right)^\top \right] \\
=&\mathbb{E}\left[ \left\{ \check{\mathbf{P}}_i^{(k)} \left( \sum_{j \in J_i^{(k)}} d_{ij}^{(k)} \left( \hat{\mathbf{P}}_j^{k|k-1} \right)^{-1} \hat{\mathbf{x}}_j^{k|k-1} \right) - \check{\mathbf{P}}_i^{(k)} \left( \sum_{j \in J_i^{(k)}} d_{ij}^{(k)} \left( \hat{\mathbf{P}}_j^{k|k-1} \right)^{-1} \right) \mathbf{x}^{(k)} \right\} \left( \mathbf{v}_l^{(k)} \right)^\top \right] \\
=&\mathbb{E}\left[ \check{\mathbf{P}}_i^{(k)} \sum\nolimits_{j \in J_i^{(k)}} d_{ij}^{(k)} \left( \hat{\mathbf{P}}_j^{k|k-1} \right)^{-1} \left( \hat{\mathbf{x}}_j^{k|k-1} - \mathbf{x}^{(k)} \right) \left( \mathbf{v}_l^{(k)} \right)^\top \right] \\
=&\check{\mathbf{P}}_i^{(k)} \sum\nolimits_{j \in J_i^{(k)}} d_{ij}^{(k)} \left( \hat{\mathbf{P}}_j^{k|k-1} \right)^{-1} \mathbb{E}\left[ \hat{\boldsymbol{\eta}}_j^{k|k-1} \left( \mathbf{v}_l^{(k)} \right)^\top \right] = \mathbf{0},
\end{aligned}$$

where Assumption 9.2.1 (ii) is used for the last equality. ■

Thus, the second sub-step has the following form

$$\left(\hat{\mathbf{P}}_i^{k|k}\right)^{-1} = \left(\check{\mathbf{P}}_i^{(k)}\right)^{-1} + \sum\nolimits_{j\in J_i^{(k)}} \left(\mathbf{H}_j^{(k)}\right)^{\top} \left(\mathbf{R}_j^{(k)}\right)^{-1} \mathbf{H}_j^{(k)}, \tag{9.4}$$
$$\left(\hat{\mathbf{P}}_i^{k|k}\right)^{-1} \hat{\mathbf{x}}_i^{k|k} = \left(\check{\mathbf{P}}_i^{(k)}\right)^{-1} \check{\mathbf{x}}_i^{(k)} + \sum\nolimits_{j\in J_i^{(k)}} \left(\mathbf{H}_j^{(k)}\right)^{\top} \left(\mathbf{R}_j^{(k)}\right)^{-1} \mathbf{z}_j^{(k)}.$$

Combine Eq. (9.3) and Eq. (9.4), the update steps of the proposed algorithm, hereafter referred as the *Distributed Hybrid Information Fusion* (DHIF) algorithm, is obtained. By adding standard prediction steps, the recursive form of the DHIF algorithm is summarized in Algorithm 9.1.

### 9.2.2 Preservation of Consistency

The consistency, as one of the most fundamental but significant properties of estimates, has to be preserved during the information fusion process. The approximated error covariance of an inconsistent estimator is over-confident, and hence does not realistically indicate the uncertainty of the estimate. In this subsection, it is shown that the consistency of the estimates is preserved in each recursion of Algorithm 9.1 with the following assumption satisfied.

**Assumption 9.2.2** *The initialized prior estimate pair of each agent, denoted as* $(\hat{\mathbf{x}}_i^{1|0}, \hat{\mathbf{P}}_i^{1|0})$*, is consistent, i.e.,* $\hat{\mathbf{P}}_i^{1|0} \succeq \mathbb{E}[(\hat{\mathbf{x}}_i^{1|0} - \mathbf{x}^{(1)})(\hat{\mathbf{x}}_i^{1|0} - \mathbf{x}^{(1)})^{\top}]$, $\forall i \in \mathscr{V}$.

Note that Assumption 9.2.2 can be easily satisfied in general. The prior knowledge about the state of interest can be learned in an off-line manner before the fusion process. In the worst case, each agent can simply choose $(\hat{\mathbf{P}}_i^{1|0})^{-1} = \mathbf{0}$, which indicates the infinite local estimate uncertainty at the beginning so that Assumption 9.2.2 is satisfied. The preservation of the estimates consistency is then shown by the following theorem.

**Algorithm 9.1** Linear DHIF algorithm implemented by agent $i$ at time instant $k$

1: **if** $k = 1$ **then**

2: initializes $\hat{\mathbf{x}}_i^{1|0}$ and $\hat{\mathbf{P}}_i^{1|0}$

3: **end if**

4: obtains the local measurement $\mathbf{z}_i^{(k)}$

5: computes $\boldsymbol{\Xi}_i^{(k)} = \left(\hat{\mathbf{P}}_i^{k|k-1}\right)^{-1}$, $\boldsymbol{\xi}_i^{(k)} = \left(\hat{\mathbf{P}}_i^{k|k-1}\right)^{-1} \hat{\mathbf{x}}_i^{k|k-1}$,

6: computes $\mathbf{S}_i^{(k)} = \left(\mathbf{H}_i^{(k)}\right)^{\top} \left(\mathbf{R}_i^{(k)}\right)^{-1} \mathbf{H}_i^{(k)}$, $\mathbf{y}_i^{(k)} = \left(\mathbf{H}_i^{(k)}\right)^{\top} \left(\mathbf{R}_i^{(k)}\right)^{-1} \mathbf{z}_i^{(k)}$

7: sends $\mathbf{S}_i^{(k)}$, $\mathbf{y}_i^{(k)}$, $\boldsymbol{\Xi}_i^{(k)}$ and $\boldsymbol{\xi}_i^{(k)}$ to agent $j$, $\forall j \in N_{i,\text{out}}^{(k)}$

8: receives $\mathbf{S}_j^{(k)}$, $\mathbf{y}_j^{(k)}$, $\boldsymbol{\Xi}_j^{(k)}$ and $\boldsymbol{\xi}_j^{(k)}$ from agent $j$, $\forall j \in N_{i,\text{in}}^{(k)}$

9: selects the set of weights $\{d_{ij}^{(k)}\}_{j \in J_i^{(k)}}$

10: computes $\bar{\mathbf{S}}_j^{(k)} = \sum_{j \in J_i^{(k)}} \mathbf{S}_j^{(k)}$, $\bar{\mathbf{y}}_j^{(k)} = \sum_{j \in J_i^{(k)}} \mathbf{y}_j^{(k)}$, $\bar{\boldsymbol{\Xi}}_i^{(k)} = \sum_{j \in J_i^{(k)}} d_{ij}^{(k)} \boldsymbol{\Xi}_i^{(k)}$ and $\bar{\boldsymbol{\xi}}_i^{(k)} = \sum_{j \in J_i^{(k)}} d_{ij}^{(k)} \boldsymbol{\xi}_i^{(k)}$

11: updates local estimate and approximated covariance

$$\hat{\mathbf{P}}_i^{k|k} = \left(\bar{\mathbf{S}}_j^{(k)} + \bar{\boldsymbol{\Xi}}_i^{(k)}\right)^{-1}, \tag{9.5}$$

$$\hat{\mathbf{x}}_i^{k|k} = \hat{\mathbf{P}}_i^{k|k} \left(\bar{\mathbf{y}}_j^{(k)} + \bar{\boldsymbol{\xi}}_i^{(k)}\right). \tag{9.6}$$

12: predicts local estimate and approximated covariance

$$\hat{\mathbf{P}}_i^{k+1|k} = \mathbf{F}^{(k)} \hat{\mathbf{P}}_i^{k|k} \left(\mathbf{F}^{(k)}\right)^{\top} + \mathbf{Q}, \tag{9.7}$$

$$\hat{\mathbf{x}}_i^{k+1|k} = \mathbf{F}^{(k)} \hat{\mathbf{x}}_i^{k|k}. \tag{9.8}$$

**Theorem 9.3** *Suppose that Assumptions 9.1.1, 9.1.2, 9.2.1 and 9.2.2 hold. Then Algorithm 9.1 preserves the consistency at all time instants, i.e.,* $\hat{\mathbf{P}}_i^{k|k-1} \succeq \mathbf{P}_i^{k|k-1}$ *and* $\hat{\mathbf{P}}_i^{k|k} \succeq \mathbf{P}_i^{k|k}$, $\forall k \in \mathbb{Z}^+$.

**Proof.** Note that one can directly observe that the update steps preserve the consistency as both Eq. (9.3) and Eq. (9.4) preserve the consistency provided consistent estimate and measurement pairs. Then the proof can be shown by induction. When $k = 1$, Assumption implies that 9.2.2 that $\hat{\mathbf{P}}_i^{1|0} \succeq \mathbf{P}_i^{1|0}$. As the update steps preserve the consistency, it follows that $\hat{\mathbf{P}}_i^{1|1} \succeq \mathbf{P}_i^{1|1}$. Suppose that $\hat{\mathbf{P}}_i^{k|k-1} \succeq \mathbf{P}_i^{k|k-1}$ and $\hat{\mathbf{P}}_i^{k|k} \succeq \mathbf{P}_i^{k|k}$ hold for some $k = k' \in \mathbb{Z}^+$. When $k = k' + 1$, if follows that

$$\begin{aligned}
\mathbf{P}_i^{k'+1|k'} &= \mathbb{E}\left[\hat{\boldsymbol{\eta}}_i^{k'+1|k'}(\hat{\boldsymbol{\eta}}_i^{k'+1|k'})^\top\right] \\
&= \mathbb{E}\left[(\mathbf{F}\hat{\boldsymbol{\eta}}_i^{k'|k'} - \mathbf{w}^{(k'+1)})(\mathbf{F}\hat{\boldsymbol{\eta}}_i^{k'|k'} - \mathbf{w}^{(k'+1)})^\top\right] \\
&= \mathbf{F}^{(k')}\mathbf{P}_i^{k'|k'}\left(\mathbf{F}^{(k')}\right)^\top + \tilde{\mathbf{Q}} - \mathbf{F}^{(k')}\mathbb{E}\left[\hat{\boldsymbol{\eta}}_i^{k'|k'}\left(\mathbf{w}^{(k'+1)}\right)^\top\right] - \left(\mathbf{F}^{(k')}\mathbb{E}\left[\hat{\boldsymbol{\eta}}_i^{k'|k'}\left(\mathbf{w}^{(k'+1)}\right)^\top\right]\right)^\top.
\end{aligned}$$

Since $\hat{\boldsymbol{\eta}}_i^{k'|k'}$ in a linear combination of $\mathbf{x}^{(0)}$, $\{\mathbf{w}^{(l)}\}_{l=1}^{k'}$ and $\{\mathbf{v}^{(l)}\}_{l=1}^{k'}$, each of which is uncorrelated with $\mathbf{w}^{(k'+1)}$ under Assumption 9.2.1, it follows that $\mathbb{E}[\hat{\boldsymbol{\eta}}_i^{k'|k'}(\mathbf{w}^{(k'+1)})^\top] = \mathbf{0}$. Therefore, the last two terms in the above equation equal to zeros. Moreover, from Assumption 9.1.1, $\mathbf{Q} \succeq \tilde{\mathbf{Q}}$. It follows from Eq. (9.7) that if $\hat{\mathbf{P}}_i^{k'|k'} \succeq \mathbf{P}_i^{k'|k'}$,

$$\hat{\mathbf{P}}_i^{k'+1|k'} = \mathbf{F}^{(k')}\hat{\mathbf{P}}_i^{k'|k'}\left(\mathbf{F}^{(k')}\right)^\top + \mathbf{Q} \succeq \mathbf{F}^{(k')}\mathbf{P}_i^{k'|k'}\left(\mathbf{F}^{(k')}\right)^\top + \tilde{\mathbf{Q}} = \mathbf{P}_i^{k'+1|k'}.$$

As a result, $\hat{\mathbf{P}}_i^{k'+1|k'+1} \succeq \mathbf{P}_i^{k'+1|k'+1}$. ■

### 9.2.3 Weights Selection

Due to the CI algorithm used in the first fusion step, the update steps in Eq. (9.5) and Eq. (9.6) only give a suboptimal estimate. Provided that this suboptimal estimate is consistent (Theorem 9.3), one should improve the confidence as much as possible. As blind agents could

come up with estimates with very low confidence, if relatively high weights are assigned to such estimates, the fused estimate through the CI algorithm will become less confident. Therefore, the selection of the weights for the embedded CI algorithm in Eq. (9.3) should be determined carefully. This is especially important in the scenario where agents communicate with their neighbors for only once before their local updates, as the advantages of asymptotic properties brought by the average consensus algorithm [36] are lost in such a scenario. The optimal set of nonnegative weights $\{d_{ij}^{(k)}\}_{j\in J_i^{(k)}}$ can be determined by minimizing the trace of $\check{\mathbf{P}}_i^{(k)}$ with $\check{\mathbf{P}}_i^{(k)}$ defined in Eq. (9.3), subject to the constraint that the weights sum up to one. This can be regarded as an *A-optimal experiment design* problem [13], which can be further cast as the following Semi-definite Programming (SDP) problem:

$$\underset{\mathbf{u}\in\mathbb{R}^n}{\text{minimize}}\ \mathbf{u}^\top\mathbf{1}, \tag{9.9}$$

subject to

$$\begin{bmatrix} \sum_{j\in J_i^{(k)}} d_{ij}^{(k)}(\hat{\mathbf{P}}_j^{k|k-1})^{-1} & \mathbf{e}_l \\ \mathbf{e}_l^\top & \mathbf{u}_{(l)} \end{bmatrix} \succeq \mathbf{0},\ l=1,\ldots,n,$$

$$\sum\nolimits_{j\in J_i^{(k)}} d_{ij}^{(k)} = 1,\ 0<\underline{d}_i\le d_{ij}^{(k)}\le 1,\ \forall j\in J_i^{(k)},$$

where $\mathbf{e}_l\in\mathbb{R}^n$ is the canonical basis vector whose $l$th entry is one. The sufficiently small constants $\underline{d}_i$, $\forall i$ are the uniform lower bounds for selecting weights. It will be shown that such a uniform bound is required for each agent when selecting the weights for the information received. Due to the convexity of Eq. (9.9), the set of weights can be determined efficiently. In the case where solving Eq. (9.9) is still considered to be computationally expensive, some suboptimal solutions can be determined by approximations [22, 57, 83].

## 9.3 Comparisons with Existing Algorithms

The comparisons between the proposed DHIF algorithm and some existing algorithms in the literature are shown in this section.

### 9.3.1 Robustness against Blind agents

As one of the objectives formulated in Section 9.1.3, the proposed algorithm is robust against the presence of blind agents. Note that Eq. (9.6) can be written as

$$\begin{aligned}\hat{\mathbf{x}}_i^{k|k} = \hat{\mathbf{x}}_i^{k|k-1} + \hat{\mathbf{P}}_i^{k|k} \sum\nolimits_{j\in J_i^{(k)}} \left(\mathbf{H}_j^{(k)}\right)^{\top} \left(\mathbf{R}_j^{(k)}\right)^{-1} (\mathbf{z}_j^{(k)} - \mathbf{H}_j^{(k)} \hat{\mathbf{x}}_i^{k|k-1}) \\ + \hat{\mathbf{P}}_i^{k|k} \sum\nolimits_{j\in J_i^{(k)}} d_{ij}^{(k)} (\hat{\mathbf{P}}_j^{k|k-1})^{-1} (\hat{\mathbf{x}}_j^{k|k-1} - \hat{\mathbf{x}}_i^{k|k-1}). \end{aligned} \tag{9.10}$$

As observed in Eq. (9.10), the matrix $\hat{\mathbf{P}}_i^{k|k}$, which implies the uncertainty of agent $i$'s local estimate (given guaranteed consistency), is multiplied to both of the last two terms. On one hand, if agent $i$ is more confident about its own local estimate, the last two terms in Eq. (9.10) will be attenuated by a small $\hat{\mathbf{P}}_i^{k|k}$. On the other hand, when agent $i$ is less confident about its own local estimate, its posterior estimate will be pushed to match i) its in-neighbors' measurements; and ii) its in-neighbors' estimate with higher confidence. If the last term in Eq. (9.10) is replaced with $\delta \hat{\mathbf{P}}_i^{k|k} \sum_{j\in J_i^{(k)}} (\hat{\mathbf{x}}_j^{k|k-1} - \hat{\mathbf{x}}_i^{k|k-1})$, with $\delta > 0$ satisfying certain conditions (see [61]), the update step of the local posterior estimates proposed by the KCF is obtained. In the KCF, each agent equally weighs its neighbors' prior estimates regardless of these estimates' confidence. The performance is therefore deteriorated when there exist some blind agents in the neighborhood. In such a situation, even if agent $i$ is able to directly sense the target, its estimate might be driven toward a bad estimate equally. This will gradually degrade the performance of the agents in the entire network. More detailed analysis on the performance of the KCF in presence of blind agents can be found in [33].

### 9.3.2 Consistency

As proved in Theorem 9.3, the DHIF algorithm results in consistent estimates. For the purpose of comparison, let ${}^{\mathrm{i}}\hat{\mathbf{P}}_i^{k|k}$ and ${}^{\mathrm{i}}\hat{\mathbf{P}}_i^{k|k-1}$ be, respectively, the counterpart of $\hat{\mathbf{P}}_i^{k|k}$ and $\hat{\mathbf{P}}_i^{k|k-1}$ obtained by the ICF [36]. In the case where the agents communicate only once before updating their local estimates, the update steps of the ICF proposed in [36] can be written as

$$ {}^{\mathrm{i}}\hat{\mathbf{P}}_i^{k|k} = \big[\textstyle\sum_{j\in J_i^{(k)}} \sigma_{ij}\, ({}^{\mathrm{i}}\hat{\mathbf{P}}_j^{k|k-1})^{-1} + N\sum_{j\in J_i^{(k)}} \sigma_{ij}\mathbf{S}_j^{(k)}\big]^{-1}, \tag{9.11} $$

where $\mathbf{S}_j^{(k)} \triangleq \big(\mathbf{H}_j^{(k)}\big)^\top \big(\mathbf{R}_j^{(k)}\big)^{-1}\mathbf{H}_j^{(k)}$ and $\sigma_{ij}$, $\forall j$ are the weights determined with the knowledge of the maximum in-degree. Therefore, it is possible that

$$ N\sum_{j\in J_i^{(k)}} \sigma_{ij}\mathbf{S}_j^{(k)} \succeq \sum_{j\in J_i^{(k)}} \mathbf{S}_j^{(k)}. \tag{9.12} $$

Note that if $\mathbf{R}_j^{(k)} = \tilde{\mathbf{R}}_j^{(k)}$, $\forall j \in J_i^{(k)}$, the right-hand side of Eq. (9.12) is the total information contained in $\{\mathbf{z}_j^{(k)}\}_{j\in J_i^{(k)}}$. As a result, the information from the measurements in the inclusive neighborhood might be overused and hence, ${}^{\mathrm{i}}\hat{\mathbf{P}}_i^{k|k}$ obtained from Eq. (9.11) is even smaller than the true error covariance of the local posterior estimates. This implies that the estimates are not consistent. This is more likely to be the case when $N \gg |J_i^{(k)}|$, which is usually the case in sparse sensor networks.

### 9.3.3 Confidence

The DHIF algorithm emphasizes the confidence of the estimates. While maintaining the consistency, one would like to come up with an estimate that is as confident as possible. For the purpose of comparison, let ${}^{\mathrm{k}}\hat{\mathbf{P}}_i^{k|k}$ and ${}^{\mathrm{k}}\hat{\mathbf{P}}_i^{k|k-1}$ be, respectively, the counterpart of $\hat{\mathbf{P}}_i^{k|k}$ and $\hat{\mathbf{P}}_i^{k|k-1}$ obtained by the KLA algorithm [9]. In the case where the agents communicate only once before local updates, the update step of the approximated error covariance in the KLA algorithm [9] has

the form of:

$$^{\mathrm{k}}\hat{\mathbf{P}}_i^{k|k} = \big[\sum\nolimits_{j\in J_i^{(k)}} \sigma_{ij}\big((\hat{\mathbf{P}}_j^{k|k-1})^{-1} + \mathbf{S}_j^{(k)}\big)\big]^{-1}, \tag{9.13}$$

where $\sigma_{ij}$, $\forall j$ are the weights and $\mathbf{S}_j^{(k)}$ is defined in Eq. (9.11). In general, given the same set of prior estimates and local measurements from the inclusive neighborhood, the local posterior estimate obtained by Eq. (9.5) is more confident than that obtained by Eq. (9.13). This is because the KLA algorithm does not specify the selection of the weights, which is especially important when only one communication iteration is feasible. More importantly, even if the same set of weights are selected for both fusion processes in Eq. (9.13) and Eq. (9.5), the update steps of the proposed DHIF algorithm are still guaranteed to give more confident estimates since $\sum_{j\in J_i^{(k)}} \mathbf{S}_j^{(k)} \succeq \sum_{j\in J_i^{(k)}} \sigma_{ij}\mathbf{S}_j^{(k)}$, which in turn, implies that $^{\mathrm{k}}\hat{\mathbf{P}}_i^{k|k} \succeq \hat{\mathbf{P}}_i^{k|k}$. This is because when the local measurements are mutually uncorrelated in errors, the update steps of the KLA algorithm makes the estimates unnecessarily conservative. This is also identified in a later work [8]. However, the author would also like to highlight that the KLA algorithm is still guaranteed to give consistent estimates even if the measurements have correlated noises.

### 9.3.4 Unification

We would like to point out that, although considered from a different perspective, the CI-DKF proposed in [26] ends up with a similar structure to the DHIF algorithm. The key difference is on the weight selection strategy (and hence the resulting theoretical analysis), which might seem to only affect the confidence of the fused estimate as long as the weights sum up to one. However, we have to point out that, by simply adopting the prior estimate pair with the highest confidence from the agent in the inclusive neighborhood and discarding those from the rest, a simplified strategy

proposed in [26], the theoretical analysis is simplified but the convergence is not guaranteed when every agent only has at most joint partial detectability. To handle such a situation, another algorithm is proposed therein with extra consensus-based communication iterations embedded until at least one agent has local joint detectability and hence the same theoretical analysis can be applied. Aside from the fact that the communication burden is increased, such a constraint will cause the CI-DKF to be non-unified. In a distributed network, as the blind agents do not know whether there exists any agent with local joint detectability, they have to consider the worst case and, hence, implement the algorithm with multiple communication iterations. In comparison, the DHIF algorithm is unified and only requires one communication iteration per time instant, regardless of whether there exists at least one agent with local joint detectability. Actually when each agent uses the priors of all its in-neighbors, as in the DHIF algorithm, the analysis is more involved. More importantly, instead of requiring the set of blind agents to be fixed, and the graph to be connected all the time as the sufficient conditions formulated in [26], this work aims at formulating very mild conditions on the global joint observability/detectability and the time-varying graphs, and showing the convergence of the proposed unified algorithm.

### 9.3.5 Closure

Before wrapping up this section, the authors would like to identify a recent extension of the KLA algorithm, referred as the *Hybrid Consensus on Measurements - Consensus on Information* (HCMCI) algorithm [8]. Let ${}^{\mathrm{h}}\hat{\mathbf{P}}_i^{k|k}$ and ${}^{\mathrm{h}}\hat{\mathbf{P}}_i^{k|k-1}$ be, respectively, the counterpart of $\hat{\mathbf{P}}_i^{k|k}$ and $\hat{\mathbf{P}}_i^{k|k-1}$ obtained by the HCMCI algorithm [8]. In the scenario considered in this work (single communication

iteration), the update steps of the HCMCI can be written as

$$ {}^{\mathrm{h}}\hat{\mathbf{P}}_i^{k|k} = \left[\sum_{j\in J_i^{(k)}} \sigma_{ij} \left(({}^{\mathrm{h}}\hat{\mathbf{P}}_j^{k|k-1})^{-1} + \omega_i^{(k)} \mathbf{S}_j^{(k)}\right)\right]^{-1}, \tag{9.14} $$

where $\omega_i^{(k)}$ is a parameter selected by agent $i$ to compensate for the possible conservatism caused by the embedded CI algorithm. It is worth mentioning that the HCMCI algorithm mathematically includes a class of distributed filtering algorithms with different selections of $\omega_i^{(k)}$. For instance, one can obtain the KLA algorithm Eq. (9.13) with $\omega_i^{(k)} = 1$, $\forall i,\ k$, or the ICF Eq. (9.11) with $\omega_i = N$, $\forall i$. Note that a small $\omega_i^{(k)}$ might cause unnecessary conservatism but a large $\omega_i^{(k)}$ might cause the loss of consistency. This is as also identified in [8], where a possible countermeasure is proposed. The countermeasure is that each agent runs an additional average consensus algorithm with itself initialized as 1 if directly sensing the target or as 0 otherwise, to obtain the average of the initialized values, which equals to the ratio of the number of agents directly sensing the target to that of the total agents. Each agent $i$ then selects $\omega_i^{(k)}$ as the inverse of this ratio, which improves the confidence and meanwhile guarantees the consistency. Such a countermeasure is valid and computationally efficient. It is worthwhile to point out that to reach such an average consensus, i) multiple communication iterations are generally required between every two consecutive sampling time instants, and ii) additional conditions on the communication graphs $\big($e.g., (jointly) connected undirected graphs or balanced (jointly) strongly connected directed graphs [58]$\big)$ need to be satisfied. Unfortunately, neither i) nor ii) is satisfied in the general scenario considered in this work, namely, the presence of only a single communication iteration per time instant and general directed $\big($not necessarily (jointly) strongly connected balanced$\big)$ graphs. As will be shown in the next section, this work aim at studying very mild conditions on general directed switching graphs. For example, even in the case of a fixed graph, the condition formulated in the corollary does not even require the

existence of a directed spanning tree, not to mention being strongly connected and balanced. Note that in the case of a fixed graph, having a directed spanning tree is a necessary condition to ensure that the agents reach a weighted (not necessarily average) consensus.

It is also worth mentioning that in Eq. (9.14), if each agent $i$ is allowed to assign a different $\omega_i^{(k)}$ for each $j \in J_i^{(k)}$, denoted as $\omega_{ij}^{(k)}$, the DHIF algorithm – although proposed from a different perspective – can be recovered by letting $\omega_{ij} = \sigma_{ij}^{-1}$ with $\sigma_{ij}$ selected at each $k$ as $\sigma_{ij}^{(k)} = d_{ij}^{(k)}$, where $d_{ij}^{(k)}$ can be determined by following Section 9.2.3. Therefore, the DHIF algorithm actually offers a reliable and fully distributed solution in selecting $\omega_i^{(k)}$ in Eq. (9.14) in the more general case with directed time-varying topologies. For the same reason, the convergence analysis in the next section will not only be applicable to the proposed DHIF algorithm, but also to the entire class of algorithms formulated in [8]. Different from the analysis in [8], which assumes a fixed set of blind agents, time-invariant models and a fixed communication topology, the convergence analysis in this work is laid out without any of these assumptions.

In summary, the proposed unified DHIF algorithm enjoys the property of being fully distributed as it does not require any global information (e.g., the maximum degree [36, 61] of the graph or the total number of agents [36]) and hence does not require any parameter determination or tuning. By using only its own and neighbors' information, it is run in an automated manner with a single communication iteration per time instant, and is adaptive to the locally unknown changes in the network. It also deals with the general case of linear time-varying systems with directed switching (not necessarily balanced nor jointly strongly connected) communication graphs, as will be shown in the next section.

## 9.4 Case of Multiple Communication Iterations

Although this work focuses on the scenario where each agent communicates with its neighbors for only once before updating its local posterior estimate, it is still worth exploring the scenario when it is possible to implement multiple communication iterations, and evaluate the performance of the proposed DHIF algorithm. Intuitively, as each agent indirectly obtains information from more agents through multiple communication iterations, the performance of local estimators will be improved in general. In this section, we assume that instead of solving (9.9), the weights are selected such that the graph is strongly connected and balanced. Therefore, an average consensus can be achieved at each time instant with infinite communication iterations [58].

The DHIF algorithm in the case where $T$ multiple communication iterations are possible to be implemented, is summarized in Algorithm 9.2. In Algorithm 9.2, the notation $t$ is the index of the communication iterations before local updates. The weights $\phi_{ij}^{(t)}, \forall j$ are defined similarly to $\omega_{ij}^{(k)}, \forall j$ in the regular DHIF algorithm. As can be observed, the CI algorithm is repeatedly used to fuse the prior estimates for all $t$. Note that the consistency is preserved during this process. Moreover, the CI algorithm is also used to fuse measurements obtained in the inclusive neighborhood when $t \geq 2$. This is also necessary to guarantee the consistency during the fusion process.

Note that if the CI algorithm is used to fuse local measurements starting from $t = 1$, essentially the KLA algorithm is obtained. As analyzed in the Section 9.3, if the local measurements have uncorrelated errors, the KLA gives relatively conservative estimates compare to those given by the DHIF algorithm. This is also true in the scenario of multiple communication iterations. Suppose that the graph is strongly connected and balanced. In the case considered in this section, as $T \to \infty$,

**Algorithm 9.2** DHIF Algorithm Implemented by Agent $i$ at Time $k$

runs Step 1 to Step 6 in Algorithm

computes $\mathbf{S}_{i,t}^{(k)} \triangleq \mathbf{S}_i^{(k)}$, $\mathbf{y}_{i,t}^{(k)} \triangleq \mathbf{y}_i^{(k)}$, $\boldsymbol{\Xi}_{i,t}^{(k)} \triangleq \boldsymbol{\Xi}_i^{(k)}$ and $\boldsymbol{\xi}_{i,t}^{(k)} \triangleq \boldsymbol{\xi}_i^{(k)}$

**for** $(t = 1, t \leq T, t = t + 1)$ **do**

    selects weights $\{\phi_{ij}^{(t)}\}_{j \in J_i^{(k)}}$ such that $\sum_{j \in J_i^{(k)}} \phi_{ij}^{(t)} = 1$

    computes $\boldsymbol{\Xi}_{i,t}^{(k)} = \sum_{j \in J_i^{(k)}} \phi_{ij}^{(t)} \boldsymbol{\Xi}_{i,t-1}^{(k)}$, $\boldsymbol{\xi}_{i,t}^{(k)} = \sum_{j \in J_i^{(k)}} \phi_{ij}^{(t)} \boldsymbol{\xi}_{i,t-1}^{(k)}$

    **if** $t = 1$ **then**

        $\mathbf{y}_{i,t}^{(k)} = \sum_{j \in J_i^{(k)}} \mathbf{y}_{i,t-1}^{(k)}$, $\mathbf{S}_{i,t}^{(k)} = \sum_{j \in J_i^{(k)}} \mathbf{S}_{i,t-1}^{(k)}$

    **else**

        $\mathbf{y}_{i,t}^{(k)} = \sum_{j \in J_i^{(k)}} \phi_{ij}^{(t)} \mathbf{y}_{i,t-1}^{(k)}$, $\mathbf{S}_{i,t}^{(k)} = \sum_{j \in J_i^{(k)}} \phi_{ij}^{(t)} \mathbf{S}_{i,t-1}^{(k)}$

    **end if**

    **if** $t < T$ **then**

        sends $\boldsymbol{\Xi}_{i,t}^{(k)}$, $\boldsymbol{\xi}_{i,t}^{(k)}$, $\mathbf{y}_{i,t}^{(k)}$ and $\mathbf{S}_{i,t}^{(k)}$ to $j \in N_{i,\text{out}}^{(k)}$

        receives $\boldsymbol{\Xi}_{j,t}^{(k)}$, $\boldsymbol{\xi}_{j,t}^{(k)}$, $\mathbf{y}_{j,t}^{(k)}$ and $\mathbf{S}_{j,t}^{(k)}$ from $j \in N_{i,\text{in}}^{(k)}$

    **else**

        computes $\mathbf{S}_i^{(k)} \triangleq \mathbf{S}_{i,T}^{(k)}$, $\mathbf{y}_i^{(k)} \triangleq \mathbf{y}_{i,T}^{(k)}$, $\boldsymbol{\xi}_i^{(k)} \triangleq \boldsymbol{\xi}_{i,T}^{(k)}$, $\boldsymbol{\Xi}_i^{(k)} \triangleq \boldsymbol{\Xi}_{i,T}^{(k)}$

    **end if**

**end for**

runs Step 11 and Step 12 in Algorithm 1

for the DHIF,

$$\hat{\mathbf{P}}_i^{k|k} \to \left[\frac{1}{N}\sum_{j=1}^{N}\left(\hat{\mathbf{P}}_j^{k|k-1}\right)^{-1} + \frac{1}{N}\sum_{j=1}^{N}\left(1+|N_{j,\text{out}}^{(k)}|\right)\left(\mathbf{H}_j^{(k)}\right)^{\top}\left(\mathbf{R}_j^{(k)}\right)^{-1}\mathbf{H}_j^{(k)}\right]^{-1}. \tag{9.15}$$

Therefore, since $|N_{j,\text{out}}^{(k)}| \geq 1$ for any $j$, the approximated posterior estimate error covariance $\hat{\mathbf{P}}_i^{k|k}$ from (9.15) is guaranteed to be smaller than ${}^{\text{k}}\hat{\mathbf{P}}_i^{k|k}$ obtained from (9.13) in the case of infinite communication iterations. This implies that, provided the same set of measurement and communication scheme, the DHIF algorithm is able to obtain a more confident estimate than the one obtained by the KLA algorithm.

Eq. (9.15) also implies that, as the graph becomes denser, *i.e.,* $|N_{j,\text{out}}^{(k)}|$ becomes greater, more differences in confidence between $\hat{\mathbf{P}}_i^{k|k}$ and ${}^{\text{k}}\hat{\mathbf{P}}_i^{k|k}$ can be obtained. In the extreme case where the graph is complete, *i.e.,* $|N_{j,\text{out}}^{(k)}| = N-1,\ \forall j$, Eq. (9.15) yields

$$\hat{\mathbf{P}}_i^{k|k} \to \left[\frac{1}{N}\sum_{j=1}^{N}\left(\hat{\mathbf{P}}_j^{k|k-1}\right)^{-1} + \frac{1}{N}\sum_{j=1}^{N}\left(\mathbf{H}_j^{(k)}\right)^{\top}\left(\mathbf{R}_j^{(k)}\right)^{-1}\mathbf{H}_j^{(k)}\right]^{-1},$$

which has the same form to what (9.11) will yield in the case of multiple communication iterations.

In summary, although shown to be possibly inconsistent in the case of a single communication iteration before local updates, the ICF, as analytically shown in [36], will asymptotically recover the centralized solution with appropriate conditions and therefore, has the best performance in the ideal case where infinite communication iterations might be implemented before local updates. However, one should note that this recovery requires both a strongly connected and balanced communication topology and the correct number of the agents (global knowledge), both of which are subject to possible changes. Using only the local knowledge, the proposed DHIF algorithm, which cannot asymptotically approach the centralized solution in general though, will come up with a more confident estimate than that from the KLA algorithm. This confidence is related to

the density of the graph, as shown above, and the number of non-naive agents, as will be shown analytically in the next section.

## 9.5 Main Results

In this section, the convergence of the proposed DHIF algorithm is analyzed based on none of the assumptions mentioned in Section 7. A key lemma, as one of the main contributions of this work, is first presented. Then using a similar approach used in [9], the sufficient conditions for all local estimates to be *uniformly* upper bounded in finite time, and the local estimate errors to asymptotically converge to zero in expectation, are formulated. The conditions are shown to be very mild and "almost" necessary. In the special time-invariant case, which is the focus of [9] with only sufficient conditions derived, necessary and sufficient conditions are derived here. Then some insights are addressed.

### 9.5.1 Multiplication of Stochastic Adjacency Matrices

The properties of the multiplication of a finite number of stochastic adjacency matrices, is first analyzed in this subsection for the use in the convergence analysis later in this work. A key concept, namely, the *orderly appearing path*, is first defined.

**Definition 9.4** *Let* $\mathfrak{P} \triangleq \{e_1, \ldots, e_p\}$*, where* $e_i \triangleq (j_{i-1}, j_i)$*,* $\forall i = 1, \ldots, p$*, be a directed path. Then* $\mathfrak{P}$ *is an orderly appearing path in* $\mathfrak{I}_{k_0}^{k_t}$*, if there exist* $p$ *time instants* $k_{\ell_1} < k_{\ell_2} < \cdots < k_{\ell_p}$ *in* $\mathfrak{I}_{k_0}^{k_t}$ *such that* $e_i \in \mathscr{E}^{(k_{\ell_i})}$*, where* $i = 1, \ldots, p$*.*

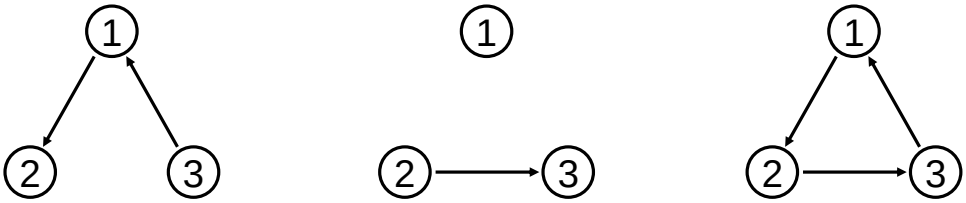


(a) $\mathscr{G}^{(1)}$. (b) $\mathscr{G}^{(2)}$. (c) $\mathscr{G}^{(1)} \cup \mathscr{G}^{(2)}$.

Figure 9.2: Example topologies for orderly appearing path.

Note that according to Definition 9.4, any edge (including self edge) that exists at a certain time instant is naturally an orderly appearing path in a time interval containing that time instant. A simple example is provided below.

**Example 9.5** *Two graphs, namely, $\mathscr{G}^{(1)}$ and $\mathscr{G}^{(2)}$, are shown, respectively, in Figure 9.2(a) and 9.2(b). Then Figure 9.2(c) is the union graph over $\mathfrak{I}_1^2$, where every agent has a directed path to every other agent. The path $\mathfrak{P}_{1\to 3} \triangleq \{(1,2),(2,3)\}$ is an orderly appearing path in $\mathfrak{I}_1^2$. In comparison, the path $\mathfrak{P}_{3\to 2} \triangleq \{(3,1),(1,2)\}$ is not as the edge $(3,1)$ never appears prior to the edge $(1,2)$ in $\mathfrak{I}_1^2$.*

The orderly appearing path in a finite interval can be intuitively understood using a parcel delivery example in analogy. Let $\mathfrak{P}$ and $\mathfrak{I}_{k_0}^{k_t}$ be defined in Definition 9.4. Consider each vertex as a person and imagine that $j_0$ is holding a parcel at $k_0$. At each time instant $k$ with $k \in \mathfrak{I}_{k_0}^{k_t}$, once a certain edge belonging to $\mathfrak{P}$ appears, if the person as the parent vertex of that edge is holding the parcel, must pass it to the person as the child vertex of that edge. By following this rule, if the parcel is delivered to $j_n$ by $k_t$, then $\mathfrak{P}$ is an orderly appearing path in $\mathfrak{I}_{k_0}^{k_t}$.

Two lemmas on the properties of non-negative matrix multiplications are then stated as follows.

**Lemma 9.6** *Suppose that* $\mathbf{M}_1 \geq \mathbf{M}_2 \geq \mathbf{0}$ *and* $\mathbf{M}_3 \geq \mathbf{M}_4 \geq \mathbf{0}$. *Then* $\mathbf{M}_1\mathbf{M}_3 \geq \mathbf{M}_2\mathbf{M}_4 \geq \mathbf{0}$.

**Proof.** Note that for each pair of $i$ and $j$, one has $\{\mathbf{M}_1\}_{(i,j)} \geq \{\mathbf{M}_2\}_{(i,j)} \geq 0$ and $\{\mathbf{M}_3\}_{(i,j)} \geq \{\mathbf{M}_4\}_{(i,j)} \geq 0$. It follows that

$$\{\mathbf{M}_1\mathbf{M}_3\}_{(i,j)} = \sum_l \{\mathbf{M}_1\}_{(i,l)}\{\mathbf{M}_3\}_{(l,j)} \geq \sum_l \{\mathbf{M}_2\}_{(i,l)}\{\mathbf{M}_4\}_{(l,j)} = \{\mathbf{M}_2\mathbf{M}_4\}_{(i,j)} \geq 0.$$

■

**Lemma 9.7** *Let* $p \geq 2$ *be a finite integer and let* $\mathbf{M}_1, \ldots, \mathbf{M}_p$ *be nonnegative square matrices with positive diagonal entries. Then*

$$\boldsymbol{\mathscr{M}}_{1:p} \triangleq \mathbf{M}_1\mathbf{M}_2\cdots\mathbf{M}_p \geq \gamma(\mathbf{M}_{k_1}\mathbf{M}_{k_2}\cdots\mathbf{M}_{k_q}) \triangleq \gamma\boldsymbol{\mathscr{M}}_{k_1:k_q}, \tag{9.16}$$

*where* $\gamma > 0$ *and the integers* $k_1, \ldots, k_q$ *satisfies that* $1 \leq k_1 < \cdots < k_q \leq p$ *for some* $q \leq p$. *Specifically,* $\gamma = 1$ *if* $p = q$; $\gamma = \prod_{j\in\mathscr{K}} \mu_j$ *otherwise with* $\mathscr{K} \triangleq \{1, \ldots, p\} \setminus \{k_1, \ldots, k_q\}$ *and* $\mu_j \triangleq \min_i \{\mathbf{M}_j\}_{(i,i)}$ *for each* $j \in \mathscr{K}$.

**Proof.** The proof for the case when $q = p$ is trivial and hence omitted. When $q \leq p$, one should note that for each $j \in \mathscr{K}$, $\mathbf{M}_j$ can be written as $\mathbf{M}_j = \mu_j\mathbf{I} + \mathbf{M}'_j$, with $\mu_j$ being the minimum diagonal entry of $\mathbf{M}_j$ and $\mathbf{M}'_j$ satisfying $\mathbf{M}'_j \geq \mathbf{0}$. Therefore, if substituting each $\mathbf{M}_j$, $j \in \mathscr{K}$ in the multiplication $\mathbf{M}_1\cdots\mathbf{M}_p$ with $(\mu_j\mathbf{I} + \mathbf{M}'_j)$, the multiplication after expanding all parentheses can be written as

$$\mathbf{M}_1\cdots\mathbf{M}_p = (\prod_{j\in\mathscr{K}} \mu_j)(\mathbf{M}_{k_1}\cdots\mathbf{M}_{k_q}) + \mathbf{K} \geq \gamma(\mathbf{M}_{k_1}\cdots\mathbf{M}_{k_q})$$

, where $\mathbf{K}$ collects all other crossing terms after expanding the parentheses. The last inequality is due to $\mathbf{K} \geq \mathbf{0}$ because all matrices involved in computing $\mathbf{K}$ are nonnegative. Note that the definition of $\mu_j$ implies that $\mu_j > 0, \forall i \in \mathscr{K}$. Also as $\mathscr{K}$ is a set with finite entries. It follows that $\gamma > 0$. This completes the proof. ■

Lemma 9.7 essentially states that the matrix, resulting from the multiplication of multiple nonnegative square matrices with positive diagonal entries, cannot have fewer positive entries than the matrix, resulting from the multiplication of a subset of these nonnegative matrices. Note that the parameter $\gamma$ in Eq. (9.16) can be conservative, *i.e.*, it is possible to replace $\gamma$ with some $\bar{\gamma} > \gamma$ such that Eq. (9.16) still holds. This is caused by ignoring all positive entries of the nonnegative matrix $\mathbf{K}$ when obtaining the inequality in Eq. (9.16), where $\mathbf{K}$ is defined in the proof Lemma 9.7. Also note that as the self edge is always assumed in this work, the stochastic adjacency matrix associated with any graph is nonnegative with positive diagonal entries. Starting from this point, the discussion will be focused on the stochastic adjacency matrices. In the rest of this work, let $\mathscr{G}^{(k)}(\mathscr{V}, \mathscr{E}^{(k)})$ and $\mathbf{D}^{(k)}$ be, respectively, the graph and the associated stochastic adjacency matrix at time instant $k$. For each pair of $i$ and $j$, where $i, j \in \mathscr{V}$, $\{\mathbf{D}^{(k)}\}_{(i,j)} = d_{ij}^{(k)}$ with $d_{ij}^{(k)}$ being the weights from Algorithm 9.1 if $j \in J_i^{(k)}$, and 0 otherwise. Based on Section 9.2.3, the following assumption holds for the rest of the paper.

**Assumption 9.5.1** *For each agent $i \in \mathscr{V}$ at any $k \in \mathbb{Z}^+$, $d_{ij}^{(k)} \geq \underline{d}_i$ with $\underline{d}_i > 0$, $\forall j \in J_i^{(k)}$.*

**Lemma 9.8** *Suppose that Assumption 9.5.1 holds. Also suppose that $\mathfrak{I}_{k_0}^{k_t}$ is finite. Let $\mathfrak{D}_{k_0}^{k_t} \triangleq \mathbf{D}^{(k_t)} \cdots \mathbf{D}^{(k_0+1)} \mathbf{D}^{(k_0)}$. Then $\{\mathfrak{D}_{k_0}^{k_t}\}_{(j_p, j_0)} > 0$* if and only if *there exists an orderly appearing path from $j_0$ to $j_p$ in $\mathfrak{I}_{k_0}^{k_t}$.*

**Proof. (Sufficiency)**. Let $\mathfrak{P} \triangleq \{(j_0, j_1), \ldots, (j_{p-1}, j_p)\}$ be the orderly appearing path in $\mathfrak{I}_{k_0}^{k_t}$. Without loss of generality, let $k'_1, \ldots, k'_p$, where $k'_1 < \cdots < k'_p$, be the $p$ time instants belonging to the time interval $\mathfrak{I}_{k_0}^{k_t}$ such that for each $k'_i$, $(j_{i-1}, j_i) \in \mathscr{E}^{(k'_i)}$. It follows from Lemma 9.7 that

$$\mathfrak{D}_{k_0}^{k_t} = \mathbf{D}^{(k_t)} \cdots \mathbf{D}^{(k_0)} \geq \gamma \mathbf{D}^{(k'_p)} \cdots \mathbf{D}^{(k'_1)},$$

where $\gamma > 0$ can be determined by Lemma 9.7. Thus it suffices to show that $\{\mathfrak{D}_{k_0}^{k_t}\}_{(j_p,j_0)} > 0$ by showing that $\{\mathbf{D}^{(k'_p)} \cdots \mathbf{D}^{(k'_1)}\}_{(j_p,j_0)} > 0$. As Assumption 9.5.1 holds, the fact that $(j_{i-1}, j_i) \in \mathscr{E}^{(k'_i)}$ implies that $j_{i-1} \in J_{j_i}^{(k'_i)}$ and hence $\{\mathbf{D}^{(k'_i)}\}_{(j_i,j_{i-1})} \geq \underline{d}_{j_i}$, where $\underline{d}_{j_i} > 0$, for each $i = 1, \ldots, p$. It follows that

$$\{\mathbf{D}^{(k'_2)}\mathbf{D}^{(k'_1)}\}_{(j_2,j_0)} = \{\mathbf{D}^{(k'_2)}\}_{(j_2,:)}\{\mathbf{D}^{(k'_1)}\}_{(:,j_0)} \geq \{\mathbf{D}^{(k'_2)}\}_{(j_2,j_1)}\{\mathbf{D}^{(k'_1)}\}_{(j_1,j_0)} \geq \underline{d}_{j_1}\underline{d}_{j_2},$$

where the inequality is due to the fact each entry of each matrix is non-negative. Similarly, one can prove that

$$\{\mathbf{D}^{(k'_3)}\mathbf{D}^{(k'_2)}\mathbf{D}^{(k'_1)}\}_{(j_3,j_0)} = \{\mathbf{D}^{(k'_3)}\}_{(j_3,:)}\{\mathbf{D}^{(k'_2)}\mathbf{D}^{(k'_1)}\}_{(:,j_0)} \geq \{\mathbf{D}^{(k'_3)}\}_{(j_3,j_2)}\{\mathbf{D}^{(k'_2)}\mathbf{D}^{(k'_1)}\}_{(j_2,j_0)} \geq \underline{d}_{j_1}\underline{d}_{j_2}\underline{d}_{j_3}.$$

Eventually, it can be shown by induction that $\{\mathbf{D}^{(k'_p)} \cdots \mathbf{D}^{(k'_1)}\}_{(j_p,j_0)} \geq \prod_{i=1}^{p} \underline{d}_{j_i} > 0$, where the last inequality is due to the fact that $\underline{d}_{j_i} > 0$, $\forall i = 1, \ldots, p$ with $p$ being finite.

**(Necessity)**. The proof of necessity contains two parts. Part A shows that a directed path from $j_0$ to $j_p$ in $\mathscr{G}[\mathfrak{I}_{k_0}^{k_t}]$ is necessary. Then it is proved in Part B that the path has to be an orderly appearing path in $\mathfrak{I}_{k_0}^{k_t}$.

(Part A). Suppose that there is no such a path in $\mathscr{G}[\mathfrak{I}_{k_0}^{k_t}]$. Let $\mathscr{O} \subseteq \mathscr{V}$ be the set of vertices that contains $j_0$ and $j_0$ has a path to in $\mathscr{G}[\mathfrak{I}_{k_0}^{k_t}]$. Let $\bar{\mathscr{O}} \triangleq \mathscr{V} \setminus \mathscr{O}$. Then for each $k \in \mathfrak{I}_{k_0}^{k_t}$, with loss of generality, $\mathbf{D}^{(k)}$ can be written as

$$\mathbf{D}^{(k)} = \begin{bmatrix} \mathbf{D}_{\mathscr{O}}^{(k)} & \mathbf{D}_{\mathscr{O}\bar{\mathscr{O}}}^{(k)} \\ \mathbf{0} & \mathbf{D}_{\bar{\mathscr{O}}}^{(k)} \end{bmatrix},$$

where the zero block is because there is no edge from any vertex in $\mathscr{O}$ to any vertex in $\bar{\mathscr{O}}$ at any $k \in \mathfrak{I}_{k_0}^{k_t}$. It follows that

$$\mathfrak{D}_{k_0}^{k_t} = \begin{bmatrix} \mathbf{D}_{\mathscr{O}}^{(k_t)} \cdots \mathbf{D}_{\mathscr{O}}^{(k_0)} & \star \\ \mathbf{0} & \mathbf{D}_{\bar{\mathscr{O}}}^{(k_t)} \cdots \mathbf{D}_{\bar{\mathscr{O}}}^{(k_0)} \end{bmatrix},$$

where the "$\star$" is a matrix block that can be specified. Note that $j_p \in \bar{\mathscr{O}}$. It follows that $\{\mathfrak{D}_{k_0}^{k_t}\}_{(j_p,j_0)} = 0$.

(Part B). Now suppose that there is no orderly appearing path from $j_0$ to $j_p$ in $\mathfrak{I}_{k_0}^{k_t}$. Then for some $k_m$ satisfying $k_0 < k_m \leq k_t$, one has

$$\{\mathfrak{D}_{k_0}^{k_t}\}_{(j_p,j_0)} = \{\mathfrak{D}_{k_m}^{k_t}\mathfrak{D}_{k_0}^{k_m-1}\}_{(j_p,j_0)} = \{\mathfrak{D}_{k_m}^{k_t}\}_{(j_p,:)}\{\mathfrak{D}_{k_0}^{k_m-1}\}_{(:,j_0)}.$$

Let $\mathscr{O}_1$ be the set of vertices that $j_0$ has a directed path to in $\mathscr{G}[\mathfrak{I}_{k_0}^{k_m-1}]$. Let $\bar{\mathscr{O}}_1 = \mathscr{V} \setminus \mathscr{O}_1$. It follows from the conclusion of Part A that $\{\mathfrak{D}_{k_0}^{k_m-1}\}_{(\bar{\mathscr{O}}_1,j_0)} = \mathbf{0}$. Suppose that every vertex in $\mathscr{O}_1$ has an orderly appearing path from $j_0$ in $\mathfrak{I}_{k_0}^{k_m-1}$. The case when this does not hold will be discussed later. It follows from the conclusion of the sufficiency part that $\{\mathfrak{D}_{k_0}^{k_m-1}\}_{(\mathscr{O}_1,j_0)} > \mathbf{0}$. Similarly, let $\mathscr{O}_2$ be the set of vertices that have a path to $j_p$ in $\mathscr{G}[\mathfrak{I}_{k_m}^{k_t}]$. Let $\bar{\mathscr{O}}_2 = \mathscr{V} \setminus \mathscr{O}_2$. It follows from Part A that $\{\mathbf{D}_{k_m}^{k_t}\}_{(\bar{\mathscr{O}}_2,j_0)} = 0$. Similar to $\mathscr{O}_1$, suppose that every vertex in $\mathscr{O}_2$ has an orderly appearing path to $j_p$ in $\mathfrak{I}_{k_m}^{k_t}$. The case when this does not hold will be discussed later. As a result, $\{\mathfrak{D}_{k_m}^{k_t}\}_{(j_p,\mathscr{O}_2)} > \mathbf{0}$. It follows that

$$\{\mathfrak{D}_{k_0}^{k_t}\}_{(j_p,j_0)} = \{\mathfrak{D}_{k_m}^{k_t}\}_{(j_p,:)}\{\mathfrak{D}_{k_0}^{k_m-1}\}_{(:,j_0)} = \{\mathfrak{D}_{k_m}^{k_t}\}_{(j_p,\mathscr{O}_1\cap\mathscr{O}_2)}\{\mathfrak{D}_{k_0}^{k_m-1}\}_{(\mathscr{O}_1\cap\mathscr{O}_2,j_0)}.$$

Therefore, $\{\mathfrak{D}_{k_0}^{k_t}\}_{(j_p,j_0)} > 0$ if and only if there exists any $i \in \mathscr{O}_1 \cap \mathscr{O}_2$ satisfying $\{\mathfrak{D}_{k_m}^{k_t}\}_{(j_p,i)} > 0$ and $\{\mathfrak{D}_{k_0}^{k_m-1}\}_{(i,j_0)} > 0$. As each directed path to $j_p$ (respectively, from $j_0$) in $\mathscr{G}[\mathfrak{I}_{k_m}^{k_t}]$ (respectively, $\mathscr{G}[\mathfrak{I}_{k_0}^{k_m-1}]$) is an orderly appearing path, to satisfy both $\{\mathfrak{D}_{k_m}^{k_t}\}_{(j_p,i)} > 0$ and $\{\mathfrak{D}_{k_0}^{k_m-1}\}_{(i,j_0)} > 0$ at the same time, vertex $i$ must have not only an orderly appearing path to $j_p$ in $\mathfrak{I}_{k_m}^{k_t}$, but also an orderly appearing path from $j_0$ in $\mathfrak{I}_{k_0}^{k_m-1}$. That is, $\{\mathfrak{D}_{k_0}^{k_t}\}_{(j_p,j_0)} > 0$ if and only if there exists an orderly appearing path from $j_0$ to $j_p$ in $\mathfrak{I}_{k_0}^{k_t}$. This is contradictory to the supposition at the beginning of Part B. Therefore, $\{\mathfrak{D}_{k_0}^{k_t}\}_{(j_p,j_0)} = 0$ if there is no orderly appearing path from $j_0$ to $j_p$ in $\mathfrak{I}_{k_0}^{k_t}$.

If there exists any vertex, say $i_1'$, in $\mathscr{O}_1$ that does not have an orderly appearing path from $j_0$ in $\mathfrak{I}_{k_0}^{k_m-1}$, one can further select $k_m' \in (k_0, k_m-1]$ and let $k_m'$, $\mathscr{O}_{11}, \mathscr{O}_{12}$, $(k_m-1)$ and $i_1'$ play the roles of, respectively $k_m$, $\mathscr{O}_1$, $\mathscr{O}_2$, $k_t$ and $j_p$ in the proof above, and again suppose that every vertex in $\mathscr{O}_{11}$ (respectively, $\mathscr{O}_{12}$) has an orderly appearing path from $j_0$ in $\mathfrak{I}_{k_0}^{k_m'-1}$ (respectively, to $i_1'$ in $\mathfrak{I}_{k_m'}^{k_m}$). Then using the same aforementioned approach, it can be shown that $\{\mathfrak{D}_{k_0}^{k'-1}\}_{(i',j_0)} = 0$. Similarly, if there exists any vertex, say $i_2'$, in $\mathscr{O}_2$ that does not have an orderly appearing path to $j_p$ in $\mathfrak{I}_{k_m}^{k_t}$, one can show that $\{\mathfrak{D}_{k_m}^{k_t}\}_{(j_p,i')} = 0$. Whenever the supposition does not hold for any path, a similar discussion can be further addressed on the path by placing the same suppositions on some subintervals, until the suppositions are satisfied. This concludes the proof. ■

**Remark 9.9** *Adopt the notation in Lemma 9.8. Note that Assumption 9.5.1 guarantees that each positive entry of the stochastic adjacency matrices is uniformly lower bounded above 0. As a result, if an interval $\mathfrak{I}_{k_0}^{k_t}$ is uniformly upper bounded in length, any positive entry of the matrix resulting from the multiplication of the stochastic adjacency matrices associated with the graphs in $\mathfrak{I}_{k_0}^{k_t}$, is uniformly lower bounded above 0,* i.e., *$\{\mathfrak{D}_{k_0}^{k_t}\}_{(j_p,j_0)} > 0$ implies that $\{\mathfrak{D}_{k_0}^{k_t}\}_{(j_p,j_0)} \geq \varepsilon$ with $\varepsilon > 0$ being a certain uniform lower bound for all positive entries of $\mathfrak{D}_{k_0}^{k_t}$. Using an example in the proof of sufficiency of Lemma 9.8, a uniform lower bound is $\varepsilon = \gamma \prod_{i=1}^{p} \underline{d}_{j_i}$, which is strictly positive provided that $\mathfrak{I}_{k_0}^{k_t}$ is finite.*

From an intuitive perspective, Lemma 9.8 essentially states the necessary and sufficient condition for one agent to be influenced by another agent within a time interval of finite length, when the communication graph is time varying. Besides a directed path from one to the other, as most would expect, two keys are highlighted. On one hand, it is not necessary for such a path to exist at every time instant within the finite time interval. On the other hand, it is not sufficient for

the union graph over the time interval to contain this path. The path has to be an orderly appearing path within this time interval, as shown in the following example.

**Example 9.10** *Adopt the graphs in Figure 9.2 and notation from Example 9.5 and Lemma 9.8. Let* $\mathbf{D}^{(1)}$ *and* $\mathbf{D}^{(2)}$ *be the stochastic matrices associated with, respectively,* $\mathscr{G}^{(1)}$ *and* $\mathscr{G}^{(2)}$*. Thus,* $\mathfrak{D}_1^2 = \mathbf{D}^{(2)}\mathbf{D}^{(1)}$*. Let "*$*$*" denote the positive entries. It follows that*

$$\mathfrak{D}_1^2 = \begin{bmatrix} * & & \\ & * & \\ & * & * \end{bmatrix} \begin{bmatrix} * & & * \\ * & * & \\ & & * \end{bmatrix} = \begin{bmatrix} * & & * \\ * & * & \\ * & * & * \end{bmatrix}.$$

*Recall that in* $\mathfrak{I}_1^2$*,* $\mathfrak{P}_{1\to 3}$ *is orderly appearing but* $\mathfrak{P}_{3\to 2}$ *is not. This can also be observed from the fact that* $\{\mathfrak{D}_1^2\}_{(3,1)} > 0$ *and* $\{\mathfrak{D}_1^2\}_{(2,3)} = 0$*.*

Here we would like to emphasize the importance of the assumption on the finiteness of $\mathfrak{I}_{k_0}^{k_t}$, under which a theoretic positive uniform lower bound $\varepsilon$, can always be found without any further condition required from the graphs in $\mathfrak{I}_{k_0}^{k_t}$. Although such a uniform lower bound is generally conservative as discussed after Lemma 9.7, it is possible that such a positive uniform lower bound does not exist if $\mathfrak{I}_{k_0}^{k_t}$ has an infinite length. For example, when infinite stochastic matrices are multiplied together, it is possible for some entries to converge to zero, even though the corresponding entries at the same location in each multiplying matrix are positive. In such a case, there exists no positive uniform lower bound.

### 9.5.2 Convergence Analysis

In this subsection, the convergence of the DHIF algorithm is analyzed. Specifically, the sufficient conditions for the local estimates of each agent to be uniformly bounded, and the estimate errors to converge to zero in expectation, are formulated. Then we show that such conditions are very mild and "almost" necessary. Two lemmas are stated before finally formulating the main results. The first lemma is directly obtained following Definition 8.2. The second one is originally proposed in [9] and restated here.

**Lemma 9.11** *Let $\mathcal{V}' \subseteq \mathcal{V}$ be the set of indices corresponding to a subset of all networked agents. The discrete LTV system Eq.* (9.1) *is jointly observable to the agents in $\mathcal{V}'$ on $\mathfrak{I}_{k_0}^{k_t}$ for some integers $0 \leq k_0 \leq k_t$* if and only if $\mathbf{O}_{\mathcal{V}'}[k_0, k_t] \triangleq col\{\mathbf{H}_{\mathcal{V}'}^{(k)} \boldsymbol{\mathscr{F}}_{k_0}^{k}]\}_{k \in \mathfrak{I}_{k_0}^{k_t}}$ *is full rank, where $\mathbf{H}_{\mathcal{V}'}^{(k)} \triangleq col\{\mathbf{H}_j^{(k)}\}_{j \in \mathcal{V}'}$, and $\boldsymbol{\mathscr{F}}_{k'}^{k}$ is defined in Definition 8.2.*

**Proof.** Omitted. ■

**Lemma 9.12 ( [9])** *Let $\mathbf{F}$ be a nonsingular matrix. Then for any $\mathbf{Y} \succ \mathbf{0}$ and $\check{\mathbf{X}} \succeq \mathbf{0}$, there exists a $\beta \in (0,1]$ such that $(\mathbf{F}\mathbf{X}^{-1}\mathbf{F}^{\top} + \mathbf{Y})^{-1} \succeq \beta \mathbf{F}^{-\top}\mathbf{X}\mathbf{F}^{-1}$ for any $\mathbf{X}^{-1} \succeq \check{\mathbf{X}}^{-1}$.*

**Theorem 9.13** *Suppose that Assumption 9.1.1, 9.1.2, 9.2.1, 9.5.1 and 9.2.2 are satisfied. Also suppose that the state propagation matrix $\mathbf{F}^{(k)}$ in Eq.* (9.1) *is nonsingular, $\forall k \in \mathbb{Z}^+$. Then,*

*(i) the approximated error covariance corresponding to the local estimate by each agent is uniformly upper bounded (in the PD sense) in finite time,* i.e., *for each $i \in \mathcal{V}$, there exist $\bar{k} \in \mathbb{Z}^+$ and $\bar{\mathbf{P}}_i \succ \mathbf{0}$, such that $\forall k \geq \bar{k}$, $\hat{\mathbf{P}}_i^{k|k} \preceq \bar{\mathbf{P}}_i$;*

*(ii) the local estimate errors at all agents obtained by Algorithm 9.1 asymptotically converge to zero in expectation,* i.e., *$\forall i \in \mathcal{V}$, $\mathbb{E}[\hat{\boldsymbol{\eta}}_i^{k|k-1}] \to \mathbf{0}$, and $\mathbb{E}[\hat{\boldsymbol{\eta}}_i^{k|k}] \to \mathbf{0}$, as $k \to \infty$,*

*if for each agent $i \in \mathscr{V}$ at $k \geq \bar{k}$, there exists a set of agents with the vertex set $\mathscr{O}_i$, and $\bar{\tau} \leq \bar{k}$ with $\bar{\tau} \geq 0$ being uniformly upper bounded, such that,*

*(a) $\mathscr{O}_i$ has joint observability about the target on $\mathfrak{I}_{k-\bar{\tau}}^{k-\bar{\tau}+p-1}$, where $p \leq \bar{\tau}+1$; and,*

*(b) every agent in $\mathscr{O}_i$ has an orderly appearing path to agent $i$ in $\mathfrak{I}_{k-\bar{\tau}+p-1}^{k}$.*

**Proof.** As the proof follows a similar approach to the main results in [9], only the parts contributed by this work are shown in details in the following.

**Proof of Part (i)**. As stated in Theorem 9.3, if Assumptions 9.1.1, 9.1.2 and 9.2.1 hold, then for any $k \in \mathbb{Z}^+$, $\hat{\mathbf{P}}_i^{k|k} \succeq \mathbf{P}_i^{k|k} \succ \mathbf{0}$. Let $\mathscr{P}_j^{(k)} \triangleq \mathbf{F}^{(k)}\hat{\mathbf{P}}_j^{k|k}(\mathbf{F}^{(k)})^\top$, $\forall k \in \mathbb{Z}^+$. As $\mathbf{Q} \succ \mathbf{0}$, it follows from Lemma 9.12 that $(\mathscr{P}_j^{(k)}+\mathbf{Q})^{-1} \succeq \beta_k\big(\mathscr{P}_j^{(k)}\big)^{-1}$ with $\beta_k \in (0,1]$, $\forall j \in \mathscr{V}$ and $k \in \mathbb{Z}^+$. Let $\mathbf{S}_i^{(k)} \triangleq (\mathbf{H}_i^{(k)})^\top(\mathbf{R}_i^{(k)})^{-1}\mathbf{H}_i^{(k)}$, $\forall k \in \mathbb{Z}^+$. As $\mathbf{S}_j^{(k)} \succeq \mathbf{0}$, $\forall j \in \mathscr{V}$, it follows from Eq. (9.5) that

$$\big(\hat{\mathbf{P}}_i^{k|k}\big)^{-1} \succeq \sum\nolimits_{j\in\mathscr{V}} \bar{d}_{ij}^{(k)}\mathbf{S}_j^{(k)} + \sum\nolimits_{j\in\mathscr{V}} d_{ij}^{(k)}\beta_k(\mathscr{P}_j^{(k-1)})^{-1}, \tag{9.17}$$

where $\bar{d}_{ij}^{(k)} = \text{ceil}\{d_{ij}^{(k)}\}$ and $\beta_k \in (0,1]$. Note that

$$\begin{aligned}(\mathscr{P}_j^{(k-1)})^{-1} \succeq & \sum\nolimits_{l\in\mathscr{V}} \bar{d}_{jl}^{(k-1)}(\mathbf{F}^{(k-1)})^{-\top}\mathbf{S}_l^{(k-1)}(\mathbf{F}^{(k-1)})^{-1} \\ & + \sum\nolimits_{l\in\mathscr{V}} d_{jl}^{(k-1)}\beta_{k-1}(\mathbf{F}^{(k-1)})^{-\top}(\mathscr{P}_j^{(k-2)})^{-1}(\mathbf{F}^{(k-1)})^{-1},\end{aligned} \tag{9.18}$$

where $\beta_{k-1} \in (0,1]$. Let ${}^kB_\tau \triangleq \prod_{i=\tau}^k \beta_i$ for any $k \geq \tau$. Substitute Eq. (9.18) into Eq. (9.17) and recursively using Eq. (9.5) and Lemma 9.12, it follows that

$$\begin{aligned}\big(\hat{\mathbf{P}}_i^{k|k}\big)^{-1} \succeq \sum\nolimits_{\tau=1}^{\bar{\tau}} {}^kB_{k-\tau+1} \sum\nolimits_{j\in\mathscr{V}} \Big[ & \{\mathfrak{D}_{k-\tau}^k\}_{(i,j)}(\mathbf{F}^{(k-1)})^{-\top}\cdots \\ & \cdots(\mathbf{F}^{(k-\tau)})^{-\top}\mathbf{S}_j^{(k-\tau)}(\mathbf{F}^{(k-\tau)})^{-1}\cdots(\mathbf{F}^{(k-1)})^{-1}\Big],\end{aligned} \tag{9.19}$$

where $\mathfrak{D}_{k-\bar{\tau}}^k \triangleq \mathbf{D}^{(k)}\cdots\mathbf{D}^{(k-\bar{\tau}+1)}\bar{\mathbf{D}}^{(k-\bar{\tau})}$ with $\bar{\mathbf{D}}^{(k)} \triangleq \text{ceil}\{\mathbf{D}^{(k)}\}$. Note that Eq. (9.19) can be equivalently written as

$$\big(\hat{\mathbf{P}}_i^{k|k}\big)^{-1} \succeq [\mathbf{F}^{(k-1)}\cdots\mathbf{F}^{(k-\bar{\tau})}]^{-\top}\mathbf{\Phi}[\mathbf{F}^{(k-1)}\cdots\mathbf{F}^{(k-\bar{\tau})}]^{-1},$$

where $\mathbf{\Phi}$ has the form of

$$\mathbf{\Phi} = \sum_{\tau=1}^{\bar{\tau}-p} ({}^{k}B_{k-\tau+1}) \sum_{j\in\mathscr{V}} \Big[ \{\mathfrak{D}_{k-\tau}^{k}\}_{(i,j)} (\mathbf{F}^{(k-\tau-1)} \cdots \mathbf{F}^{(k-\bar{\tau})})^{\top} \mathbf{S}_{j}^{(k-\tau)} (\mathbf{F}^{(k-\tau-1)} \cdots \mathbf{F}^{(k-\bar{\tau})}) \Big] + \mathbf{\Delta}[k_0, k_t].$$

For clarity, let $k_0 \triangleq k - \bar{\tau}$ and $k_t \triangleq k - \bar{\tau} + p - 1$. Let $\mathscr{F}_{k_0}^{k}$, $k \geq k_0$, be defined in Lemma 9.11. The last term $\mathbf{\Delta}[k_0, k_t]$ above can be written as $\mathbf{\Delta}[k_0, k_t] = (\mathbf{O}[k_0, k_t])^{\top} \mathbf{\Psi}[k_0, k_t] \mathbf{O}[k_0, k_t]$, where

$$\mathbf{O}[k_0, k_t] \triangleq \big[ (\mathbf{H}^{(k_t)} \mathscr{F}_{k_0}^{k_t})^{\top}, \cdots, (\mathbf{H}^{(k_0)})^{\top} \big]^{\top}, \ \mathbf{\Psi}[k_0, k_t] \triangleq \mathrm{blkd}\{\mathbf{\Gamma}_q\}_{q=k_0}^{k_t},$$

with $\mathbf{H}^{(q)} \triangleq \mathrm{col}\{\mathbf{H}_j^{(q)}\}_{j\in\mathscr{V}}$ and

$$\mathbf{\Gamma}_q \triangleq {}^{k}B_{q+1} \mathrm{blkd}\big\{ \{\mathfrak{D}_q^{k}\}_{(i,j)} \otimes \mathbf{I}_{m_j} \big\}_{j\in\mathscr{V}} \mathrm{blkd}\{(\mathbf{R}_j^{(q)})^{-1}\}_{j\in\mathscr{V}},$$

for each $q = k_0, \ldots, k_t$. Note that $\mathbf{\Psi}[k_0, k_t] \succeq \mathbf{0}$ due to the special structure of $\mathbf{\Gamma}_q$ and the fact that $(\mathbf{R}_j^{(q)})^{-1} \succeq \mathbf{0}$, for each $q$. Thus, $\mathbf{\Delta}[k_0, k_t] \succeq \mathbf{0}$. Note that this property still holds after removing some rows of $\mathbf{O}[k_0, k_t]$ and the corresponding blocks in $\mathbf{\Psi}[k_0, k_t]$ with respect to a subset of agents at any time instants. Specifically, we are interested in the agents in $\mathscr{O}_i \setminus \mathscr{B}^{(q)}$, at each time instant $q \in \{k_0, \ldots, k_t\}$. By only selecting the blocks corresponding to this subset of agents, it follows that

$$\mathbf{\Delta}[k_0, k_t] \succeq \underbrace{\begin{bmatrix} \tilde{\mathbf{H}}^{(k_t)} \mathscr{F}_{k_0}^{k_t} \\ \vdots \\ \tilde{\mathbf{H}}^{(k_0)} \end{bmatrix}^{\top}}_{(\tilde{\mathbf{O}}[k_0,k_t])^{\top}} \underbrace{\begin{bmatrix} \tilde{\mathbf{\Gamma}}_{k_t} & & \\ & \ddots & \\ & & \tilde{\mathbf{\Gamma}}_{k_0}, \end{bmatrix}}_{\tilde{\mathbf{\Psi}}[k_0,k_t]} \underbrace{\begin{bmatrix} \tilde{\mathbf{H}}^{(k_t)} \mathscr{F}_{k_0}^{k_t} \\ \vdots \\ \tilde{\mathbf{H}}^{(k_0)} \end{bmatrix}}_{\tilde{\mathbf{O}}[k_0,k_t]}$$

where $\tilde{\mathbf{H}}^{(q)} \triangleq \mathrm{col}\{\mathbf{H}_j^{(q)}\}_{j\in\mathscr{O}_i\setminus\mathscr{B}^{(q)}}$. $\tilde{\mathbf{\Gamma}}_q$ is defined similarly to $\mathbf{\Gamma}_q$ by replacing $\mathscr{V}$ with $\mathscr{O}_i \setminus \mathscr{B}^{(q)}$, for each $q = k_0, \ldots, k_t$. If Condition (a) is satisfied, it follows from Lemma 9.11 that $\tilde{\mathbf{O}}[k_0, k_t]$ is full rank. Therefore, it suffices to prove $\mathbf{\Delta}[k_0, k_t] \succ \mathbf{0}$ by showing $\mathbf{\Psi}[k_0, k_t] \succ \mathbf{0}$.

Note that $\mathbf{\Psi}[k_0, k_t]$ has a block diagonal structure. As for each $q = k_0, \ldots, k_t$, it is satisfied that ${}^{k}B_{q+1} > 0$ and $(\mathbf{R}_j^{(q)})^{-1} \succ \mathbf{0}$, $\forall j \in \mathscr{O}_i \setminus \mathscr{B}^{(q)}$. The only possibility for $\mathbf{\Psi}[k_0, k_t]$ to have a zero

diagonal block is when there exists $j \in \mathscr{O}_i \setminus \mathscr{B}^{(q)}$ such that $\{\mathfrak{D}_q^k\}_{(i,j)} = 0$. As $k_t \geq k_0$, it suffices to excluded this possibility by showing that $\{\mathfrak{D}_{k_t}^k\}_{(i,j)}$ is uniformly lower bounded above 0, $\forall j \in \mathscr{O}_i$.

If Condition (b) is satisfied, it follows from Lemma 9.8 that $\{\mathfrak{D}_{k_t}^k\}_{(i,j)} > 0$, $\forall j \in \mathscr{O}_i$. As $\bar{\tau}$ is uniformly upper bound by a finite number, say $\tau_m$, it follows that $\{\mathfrak{D}_{k_t}^k\}_{(i,j)}$, $\forall j \in \mathscr{O}_i$ must be uniformly lower bounded by some $\varepsilon > 0$. This implies that, $\mathbf{\Phi} \succeq \mathbf{\Delta}[k_0, k_t] \succ \mathbf{0}$ and hence, $\left(\hat{\mathbf{P}}_i^{k|k}\right)^{-1} \succ \mathbf{0}$. As this is the case for all $k \geq \bar{k}$ for any $\bar{k} \geq \tau_m$, it follows that there exists a uniform upper bound $\bar{\mathbf{P}}_i \succ \mathbf{0}$, such that $\hat{\mathbf{P}}_i^{k|k} \preceq \bar{\mathbf{P}}_i$, $\forall k \geq \bar{k}$. This concludes the proof of Part (i).

**Proof of Part (ii)**. By following Eq. (9.6), writing $\hat{\boldsymbol{\eta}}_i^{k+1|k}$ in terms of $\hat{\boldsymbol{\eta}}_j^{k|k}$, $j \in J_i^{(k)}$, and taking expectations of both hand-sides of the resulting equation, it follows that

$$\mathbb{E}\left[\hat{\boldsymbol{\eta}}_i^{k+1|k}\right] = \mathbf{F}^{(k)} \hat{\mathbf{P}}_i^{k|k} \sum\nolimits_{j \in J_i^{(k)}} d_{ij}^{(k)} \left(\hat{\mathbf{P}}_j^{k|k-1}\right)^{-1} \mathbb{E}\left[\hat{\boldsymbol{\eta}}_j^{k|k-1}\right].$$

Let $V_i^{(k)} \triangleq \mathbb{E}[(\hat{\boldsymbol{\eta}}_i^{k|k-1})^\top](\hat{\mathbf{P}}_i^{k|k-1})^{-1}\mathbb{E}[\hat{\boldsymbol{\eta}}_i^{k|k-1}]$ be the Lyapnouv function at agent $i$. With Part (i) satisfied, a similar approach to that candidate of Theorem 5 of [9] can be followed to obtain that $V_i^{(k)} \leq \tilde{\beta} \sum_{j \in J_i^{(k)}} d_{ij}^{(k)} V_j^{(k)}$, where $0 < \tilde{\beta} < 1$. Let $\mathscr{L}^{(k)} \triangleq \text{col}\{V_i^{(k)}\}_{i=1}^N$. It follows that $\mathscr{L}^{(k+1)} \leq \tilde{\beta} \mathbf{D}^{(k)} \mathscr{L}^{(k)}$, $k \in \mathbb{Z}^+$. As $\mathbf{D}^{(k)}$ is a stochastic matrix, its spectral radius is 1. Thus for $0 < \tilde{\beta} < 1$, the spectral radius of $\tilde{\beta}\mathbf{D}^{(k)}$ is less than 1. The dynamic system with respect to $\mathscr{L}^{(k)}$ is therefore stable. As a result, $\mathscr{L}^{(k)} \to \mathbf{0}$ as $k \to \infty$. It follows that $\mathbb{E}[\hat{\boldsymbol{\eta}}_i^{k|k-1}] \to \mathbf{0}$ as $k \to \infty$, $\forall i \in \mathscr{V}$. Thus, $\mathbb{E}[\hat{\boldsymbol{\eta}}_i^{k|k}] = (\mathbf{F}^{(k)})^{-1}\mathbb{E}[\hat{\boldsymbol{\eta}}_{i,k+1|k}] \to \mathbf{0}$ as $k \to \infty$, $\forall i \in \mathscr{V}$. This concludes the proof. ■

With the guaranteed consistency as stated in Theorem 9.3, Conclusion (i) of Theorem 9.13 essentially implies that the local estimate errors are uniformly upper bounded at steady state. Moreover, Conclusion (ii) of Theorem 9.13 implies that the local estimates are asymptotically unbiased.

Compared with the main theorems in [9], where the sufficient conditions for the same conclusions are formulated based on the assumptions of a fixed strongly connected graph and time-invariant process/sensing models, it is worth pointing out that, the conditions formulated in Theorem 9.13 are much milder. Similar to the main theorems in [9], the requirement of joint observability instead of detectability in Condition (a) of Theorem 9.13 is to simplify the convergence analysis and will not cause loss of generality. If the system is only jointly detectable but not necessarily observable to the agents in $\mathscr{O}_i$ with $\mathscr{O}_i$ defined in Theorem 9.13 for each $i \in \mathscr{V}$, one can then apply the theorem to the subsystem that is jointly observable to $\mathscr{O}_i$ after applying the observability decomposition (see [9] for more details). Therefore, Condition (a) in 9.13 can be easily relaxed to only require joint detectability. Such a relaxed version of Condition (a) is referred as the "relaxed Condition (a)" hereafter. Moreover, it will be shown in Corollary 9.15 that the sufficient conditions formulated in Theorem 9.13 are "almost" necessary with such a relaxation. Specifically, if considering the same scenario as considered in [9], the relaxed sufficient conditions turn out to be also necessary, as will be shown in Corollary 9.16.

The differences of the conditions in Theorem 9.13 compared to the main theorem in [26] can be stated in threefold. First of all, only the conditions for bounded estimate errors are formulated in [26]. The unbiasedness is not considered therein. Second, the conditions in [26] require the existence of at least one agent with joint observability in its inclusive neighborhood. In comparison, the conditions in Theorem 9.13 does not require the existence of such agent. Last but not least, although the conditions in [26] admit to time-varying undirected communication topologies, the topology at every time instant is required to be connected. In comparison, Theorem 9.13 does not formulate any requirement on the communication topology at a single time instant. It studies the

most general situation where the graph is directed and any communication link is subject to change with time.

Instead of requiring specific conditions hold to guarantee the convergence, as did in some existing literature, Theorem 9.13 studies the essence for the convergence. That is, each agent has to be able to eventually be influenced by the information about the entire state from somewhere. This is achieved by two keys. (i) The knowledge about the entire state. This requires the target state to be jointly observable/detectable by a subset of agents on a time interval. (ii) Each agent recovers the entire state by either directly or indirectly using such knowledge. This requires each agent to have an orderly appearing path from at least one subset of agents satisfying Key (i), in the following time interval with uniformly upper bounded length. Note that for different agents to recover the entire state, each of them can have multiple or different subsets of agents satisfying both keys. For a certain agent to have uniformly bounded error covariance at different time instants, the subsets satisfying both keys can also be different. Even for a certain agent to have uniformly bounded error covariance at a certain time instant, the agents of the subset satisfying Key (i) are not necessary to have directly paths to each other in the union graph over the time interval used for achieving Key (ii). However, each of them should have an orderly appearing path to this certain agent in the time interval satisfying Key (ii). With these two keys satisfied for each agent, the agents directly sensing the target either directly or indirectly influence the other agents so that the target trajectory is cooperatively estimated by each agent with the approximated estimate error covariance being uniformly upper bounded in finite time, and the estimate being asymptotically unbiased.

Essentially, for both conclusions in Theorem 9.13 to hold, it is sufficient to guarantee the existence of a sliding window with uniformly upper bounded size, for each agent. The sliding

window consists of two consecutive sub-windows. The necessary information to recover the entire state has to be obtained by a subset of agents within the first sub-window, and this subset of agents have to be able to influence other agents through orderly appearing paths in the second sub-window. The sizes of both sub-windows, and hence the size of the sliding window, might subject to change over time. Note that if each agent has such a sliding window with uniformly bounded length, it is able to be "frequently" influenced by the information about the entire state from somewhere, and hence, guarantees its local estimates to track the target trajectory with uniformly bounded tracking errors that asymptotically converge to zero in expectation.

**Remark 9.14** *Similar to the discussion after Lemma 9.8, the uniform upper bound for the size of the sliding window is necessary for formulating the uniform upper bound of the local estimate error covariances. Moreover, if the uniform upper bound for the window size is too large, some entries of the matrix resulting from multiplying all stochastic matrices in the corresponding time interval, might be very close to zero. This implies a very large uniform upper bound for the local estimate error covariances.*

**Corollary 9.15** *Under the same assumptions of Theorem 9.13, if for any agent $i \in \mathcal{V}$, either Condition (b) or the relaxed Condition (a) of Theorem 9.13 is not satisfied, $\forall \bar{\tau} \in \mathbb{Z}^+$, then agent i must fails to track at least one component of the state of interest.*

**Proof.** Suppose that only the relaxed Condition (a) is not satisfied. That is, there exists at least one subset of agents with the vertex set $\mathcal{O}_i$, each of which has an orderly appearing path to $i$ within $\mathfrak{I}_{k-\bar{\tau}}^k$. However, the target is not jointly detectable to $\mathcal{O}_i$ over any sub-interval of $\mathfrak{I}_{k-\bar{\tau}}^k$ for any possible $\bar{\tau} \in \mathbb{Z}^+$. In this case, there exists a mode that is neither internally stable nor observable to agents in $\mathcal{O}_i$, for all possible $\mathcal{O}_i$. In this case, even a centralized Kalman filter (CKF) with all measurements

collected from $\mathscr{O}_i$ is not able to track the subspace of the interested state with respect to the unstable and unobservable mode.

Now suppose that only Condition (b) is not satisfied. Without loss of generality, let $\mathscr{O}_i$ be the minimum set of agents to which the target is jointly detectable over any sub-interval of $\mathfrak{I}^k_{k-\bar{\tau}}$ That is, removing any agent in $\mathscr{O}_i$ will cause the rest agents in $\mathscr{O}_i$ the loss of joint detectability about the state of interest. Suppose that there exists agent $j \in \mathscr{O}_i$ with no orderly appearing path to agent $i$ within $\mathfrak{I}^k_{k-\bar{\tau}}$, it follows from the proof of the necessity part of Lemma 9.8 that $\{\mathfrak{D}^k_{k-\bar{\tau}}\}_{(i,j)} = 0$. If this is the case for any $\bar{\tau} \in \mathbb{Z}^+$ (and hence for any $k$ as $\bar{\tau} \leq k$), agent $i$ will never be influenced by agent $j$, which has necessary and unique information contributing to the recovery of the entire state values. Again, with only the measurement collected from $\mathscr{O}_i \setminus \{j\}$, even the CKF is not able to track the subspace of the interested state with respect to the unstable mode that is observable only with the measurement collected by agent $j$.

As in both cases, there exists mode, and hence at least one state component such that the CKF – as the optimal estimator one can has – fails to track, the DHIF algorithm must not able to achieve the same objective as an suboptimal estimator. ■

Corollary 9.15 formulates the situations in which the DHIF algorithm does not work. Essentially, if either the relaxed Condition (a) or Condition (b) in Theorem 9.13 is not satisfied for a certain agent for any $\bar{\tau}$, this agent will not be "frequently" influenced by the information about the state components with respect to a unstable mode. As a matter of fact, the DHIF algorithm fails to track the corresponding state components.

Corollary 9.15 also implies that the relaxed sufficient conditions in Theorem 9.13 are "almost" necessary. As previously mentioned, the uniform upper bound of $\bar{\tau}$ in Theorem 9.13 is

critical for the formulation of the uniform upper bound of the covariances. A limited $\bar{\tau}$ guarantees the agent is influenced by the information of the entire state for at most every $\bar{\tau}$ time instants. Such influences, no matter how less frequent (with a larger $\bar{\tau}$), guarantees a theoretical uniform upper bound for the estimate uncertainties to exist as long as the frequency is uniformly lower bounded. However, if there exists agent that is never (or not any more) influenced by such information ($\bar{\tau} \to \infty$), the algorithm will simply not work. If all factors are time invariant, as considered in [9], the conditions formulated in Theorem 9.13 with Condition (a) relaxed, turn out to be not only sufficient, but also necessary, as stated in the following corollary.

**Corollary 9.16** *Suppose that* $\mathbf{F}^{(k)} = \mathbf{F}$, $\mathscr{G}^{(k)} = \mathscr{G}$, $\mathscr{B}^{(k)} = \mathscr{B}$ *and* $\mathbf{H}_i^{(k)} = \mathbf{H}_i$, *where* $i \in \mathscr{V}$, $\forall k \in \mathbb{Z}^+$. *Also suppose that the same assumptions in Theorem 9.13 hold. Then Conclusion (i) and (ii) in Theorem 9.13 are true if and only if for each leader component with the vertex set* $\mathscr{V}_\ell$, *the LTI system with state propagation* $\mathbf{F}$ *and observation matrix* $\tilde{\mathbf{H}}_\ell$ *is detectable, where* $\tilde{\mathbf{H}}_\ell \triangleq col\{\mathbf{H}_j\}_{j \in \mathscr{V}_\ell \setminus \mathscr{B}}$.

**Proof.** The proof of the sufficiency and necessity part of Corollary 9.16 can be obtained by following the conclusions of, respectively, Theorem 9.13 and Corollary 9.15. ■

Note that according to Corollary 9.16, in the special case with all factors being time invariant, if a certain agent does not have any directed path from any leader component, it forms a leader component itself and hence, must have local detectability in order to track the target. In the extreme case where all agents are isolated, each of them is a leader component. As a result, the state of interest needs to be detectable to every agent. This also shows the importance of cooperation between local agents. By locally cooperating with other agents, the requirement on the local detectability of each agent can be dramatically relaxed.

In summary, the conditions formulated by Theorem 9.13 admit to a much more general and realistic scenario where any of the factors, namely, the process model of the target, the sensing model at local agent, and the communication topology, might subject to changes over time. The sufficient conditions for convergence are much milder compared to those for the algorithms in [9, 15, 26, 61], and "almost" necessary after the relaxation. In the time-invariant case, the relaxed conditions are also necessary.

## 9.6 Simulations

In this section, simulations are used to illustrate the analysis in previous sections. The comparisons with existing algorithms are first shown. Then the main results in section 9.13 are illustrated. The linear dynamic system in Eq. (9.1) is considered, where the parameters at each $k \in \mathbb{Z}^+$ are:

$$\mathbf{F}^{(k)} = \begin{bmatrix} \mathbf{I}_2 & \Delta_T \mathbf{I}_2 \\ \mathbf{0} & \mathbf{I}_2 \end{bmatrix}, \mathbf{Q}^{(k)} = \begin{bmatrix} 5\Delta_T^3 \mathbf{I}_2/3 & 5\Delta_T^2 \mathbf{I}_2/2 \\ 5\Delta_T^2 \mathbf{I}_2/2 & 5\Delta_T \mathbf{I}_2 \end{bmatrix},$$

with $\Delta_T = 0.05$ being the sampling interval. The four state components are, respectively, the positions along $x$ and $y$ directions, and the velocities along $x$ and $y$ directions. A distributed sensor network consisting $N$ agents with circular communication topology, as shown in Figure 9.3, is used to track the state of the target in this subsection. The value of $N$ is different in each simulation, and will be specified.

**Simulation 1**. A time-invariant scenario is selected to show the comparisons with existing algorithms. The circular topology shown in Figure 9.3 is selected with $N = 10$. It is assumed that for all $k \in \mathbb{Z}^+$, $\mathbf{H}_1^{(k)} = [1\ 0\ 0\ 0]$, $\mathbf{H}_6^{(k)} = [0\ 1\ 0\ 0]$, and none of the rest agents can directly

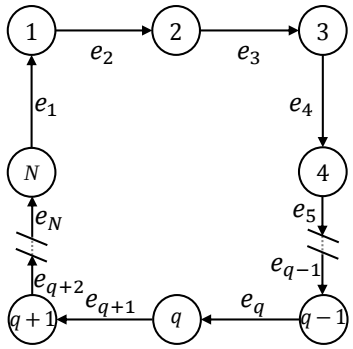


Figure 9.3: Communication graph for simulations

sense the target. It is selected that $\mathbf{R}_1 = \mathbf{R}_6 = 25$. Note that this sensor network has very weak connectivity and poor global observability. Aside from the existence of many blind agents, which makes the KCF [61] and the DKF [15] not work, not a single agent has local joint detectability. As a result, the algorithm in [26] would require multiple consensus-based communication iterations per time instant in this scenario. Therefore, two other distributed estimation algorithms are selected for comparisons. The KLA algorithm, due to its superficially similar form to the proposed DHIF Algorithm, is selected to show the difference in terms of confidence caused by the different fusion philosophies as analyzed in Section 9.3. As the selection of weights is not specified in [9], we let each agent assign equal weights to its in-neighbors' information. The ICF is also selected for comparison due to its better performance than the KCF and GKCF especially in presence of blind agents. The consensus parameter $\epsilon$ used in the ICF is the same to that in [36], *i.e.,* $\epsilon = 0.65/\Delta_{\max}$. The proposed DHIF algorithm is implemented with the weights selected using 3 different strategies, namely, the uniformly equal weights (DHIF1), the Fast CI method [57] (DHIF2), and the optimal weights by Eq. (9.9) (DHIF*). In all distributed algorithms, each agent communicates with its

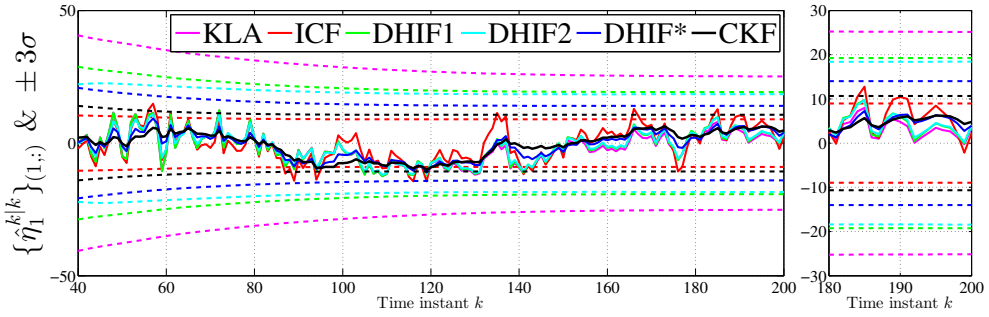


(a) Local posterior estimate error on $x$-position by Agent 1.

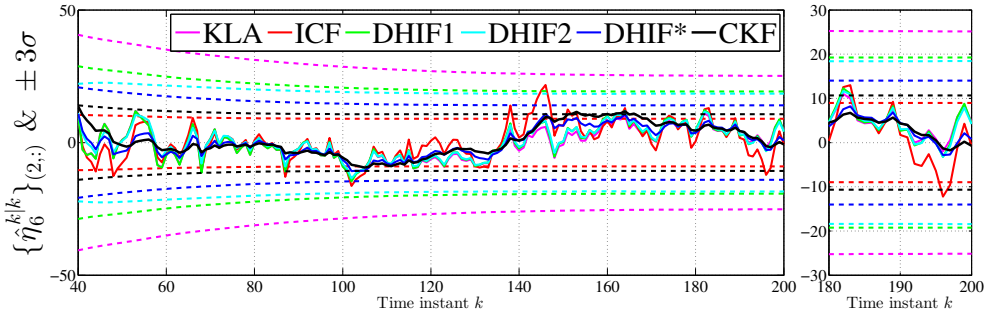


(b) Local posterior estimate error on $y$-position by Agent 6.

Figure 9.4: Local posterior estimate error on state components by local agents.

neighbors for only once before its local updates. A hypothetical CKF with collective measurement across the entire network is used as the benchmark.

The first and the second component of the local posterior estimate errors by, respectively, agent 1 and 6, obtained by each algorithm, are plotted in, respectively, Figure 9.4(a) and Figure 9.4(b). The corresponding (approximated) $3\sigma$-envelope corresponding to each algorithm, is also plotted in the same color but dashed lines. Therefore, for a consistent estimator at the steady state, the error should lie below the $3\sigma$-bound for no less than 99.7% of the time. As observed in both figures, the posterior estimate errors of the ICF's exceed its $3\sigma$-bound frequently. In both figures, the

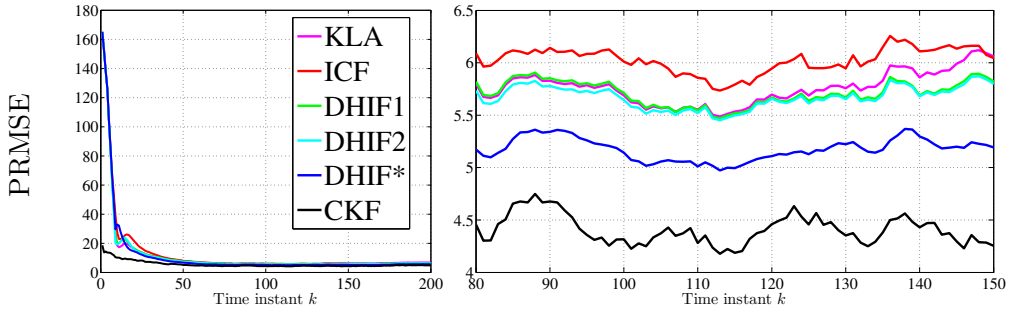


Figure 9.5: The PRMSE averaged over all 200 trails and all 10 agents.

uncertainty of the ICF is even less than the one obtained by the CKF, which provides the minimum possible MSE. Therefore, the ICF can be overconfident when the agents communicate with each other for only once before updating their local estimates, as analyzed in Section 9.3. In both figures, the DHIF algorithms give a tighter $3\sigma$-envelope compare to the KLA algorithm, which implies a more confident estimate. These observations match the analysis in Section 9.3. It is also shown that the DHIF algorithm with the weights by Eq. (9.9) gives the most confident estimates compared with those with uniform or suboptimal weight selection strategies. The same simulation is run for 200 independent Monte Carlo trails. The position root mean square error (PRMSE), averaged over all trails and all 10 agents using each algorithm, is plotted with respect to the time instant $k$ in Figure 9.5. As observed, the DHIF algorithm with the optimal weights gives the lowest average PRMSE.

**Simulation 2**. Now consider an even worse scenario, where the graph shown in Figure 9.3 is only the union communication graph over all time instants, denoted as $\mathscr{G}[\mathfrak{I}]$ with $\mathfrak{I} \triangleq \{k|k \in \mathbb{Z}^+\}$. For any single realization, both the status of whether each edge of $\mathscr{G}[\mathfrak{I}]$ exists, and whether each agent directly senses the target at every time instant, are synthetically generated based on probabilities. Specifically, for each $i = 1,\ldots,N$, and $k \in \mathbb{Z}^+$, $\Pr\left(e_i^{(k)} \in \mathscr{E}^{(k)}\right) = 0.3$ and $\Pr\left(i \in\right.$

$\mathscr{B}^{(k)}\big) = 0.7$. If agent $i$ directly senses the target at $k$, $\mathbf{H}_i^{(k)} = [\mathbf{I}_2 \quad \mathbf{0}]$, $\mathbf{R}_i^{(k)} = 25\mathbf{I}_2$. Some comments about the communication graph in Figure 9.3 are addressed here. On one hand, one should note that even the union graph $\mathscr{G}[\mathfrak{I}]$ has very weak connectivity. For any agent at any time instant, it is only able to receive/send information from/to at most one other agent. On the other hand, even the global joint observability is quite limited. Note that it is possible for none of the agents to directly sense the target at some time instants. Suppose that a certain edge exists at a certain time instant, it is possible that the parent node does not directly sense the target at that time instant so no information about the current state is received by its child node. Similarly, suppose that an agent directly senses the target at a certain time instant, it is still possible that the agent cannot send such most recent information to any other agent. As this chapter aims at studying very mild conditions for the convergence of distributed filtering using sensor networks, we make up this graph with extremely weak connectivity and poor global joint observability at any time.

For clarity, a relatively small $N = 6$ is selected for validating Part (i) of Theorem 9.13. The statuses of whether each possible edge appears and whether each agent directly senses the target at the steady state of a random single trail are generated and, respectively, plotted in Figure 9.6(a) and 9.6(b). For example, none of the 6 agents directly senses the target at $k = 138$ and $k = 140$. When $k = 125$ or $k = 129$, all agents are isolated as none of the 6 possible edges appears. Note that Figure 9.6 shows that both Condition (a) and (b) formulated in Theorem 9.13 are satisfied for each agent. Using agent 5 at $k = 153$ as an example. Agent 4 has observability about the target over $\mathfrak{I}_{146}^{148}$, this satisfies Condition (a). Also $e_5$ appears at $k = 152$ and hence, is an orderly appearing path from agent 4 to agent 5 within $\mathfrak{I}_{148}^{153}$, this satisfies Condition (b). Thus for agent 5 at $k = 153$, one of the intervals satisfy both conditions is $\mathfrak{I}_{146}^{153}$.

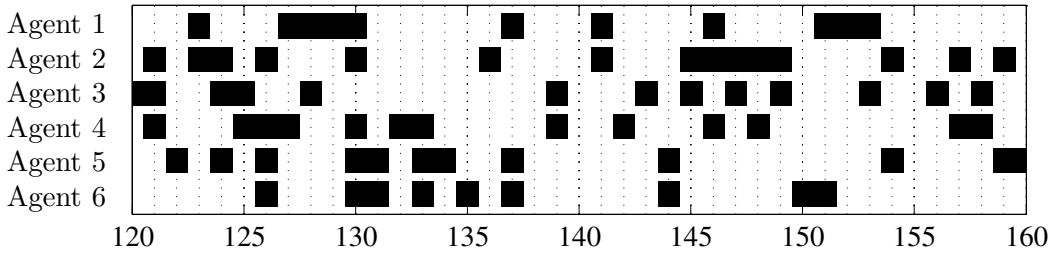


(a) Status of whether each agent directly senses the target at $120 \leq k \leq 160$.

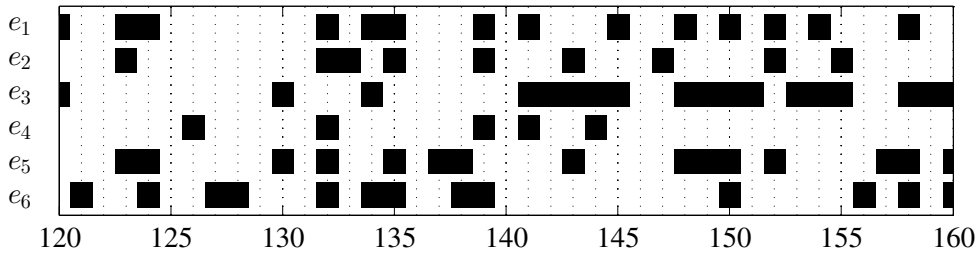


(b) Status of whether each possible edge appears at $120 \leq k \leq 160$.

Figure 9.6: Statuses of network connectivity and local sensing at each time instant: each black square implies a positive status at the corresponding $k$.

The estimated trajectories by local agents and the CKF are plotted along with the true target trajectory in Figure 9.7. For clarity, only the trajectories estimated by agent 1 and agent 5 are plotted. To show the evolution of each trajectory, checkpoints in the same colors are marked for every 40 time instants. It is shown in Figure 9.7 that the local estimates are able to track the true target trajectory. Moreover, the covariance ellipse with the 99.7% confidence of the local estimate at each checkpoint is plotted in dashed lines. As observed, the true location (star in green) at each checkpoint is always enclosed by the corresponding ellipse in red (agent 1) or blue (agent 5). This verifies the consistency of local estimates. The local estimates are more conservative compared to the one by the CKF. This is intuitive as the graph is very weakly connected and each agent has poor joint observability in general.

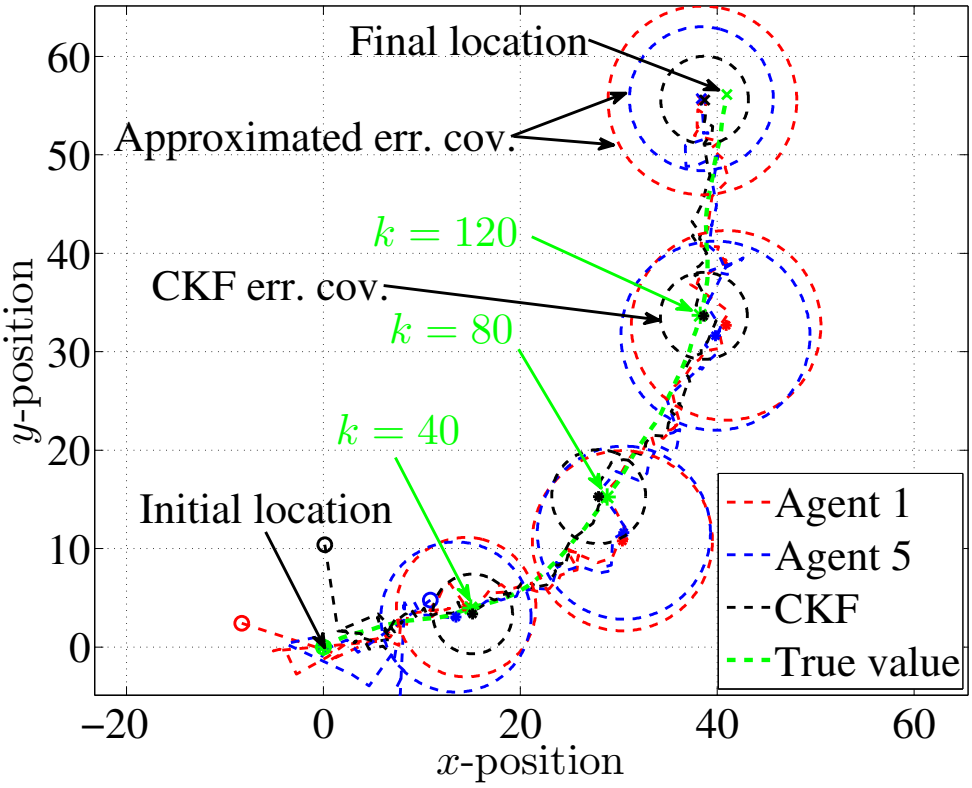


Figure 9.7: 2D target tracking task: DHIF algorithm v.s. CKF.

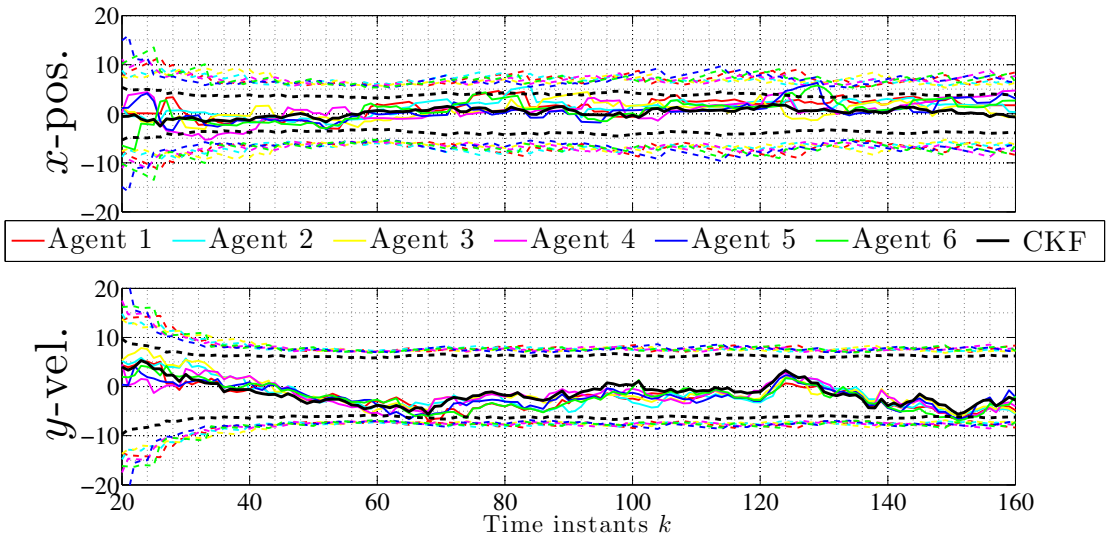


Figure 9.8: Trajectory tracking errors & $\pm 3\sigma$ envelopes: DHIF algorithm v.s. CKF.

In Figure 9.8, the local posterior estimate errors (solid lines in colors), as well as the corresponding $\pm 3\sigma$ envelopes (dashed lines in the same color) at each of the 6 agents, are plotted. As observed in Figure 9.8, the estimate errors by each agent are bounded by the $\pm 3\sigma$ envelopes at the steady-state, which verifies the consistency.

When the agent does not sense the target directly, it can only obtain the information to recover the entire state by communication. Compared to the time-invariant scenario, where each agent continuously obtains such information from some leader component at every time instant, in the time-varying scenario, the agents are only able to obtain such information in a less frequent manner. Such lower frequencies will also cause the information to become more "outdated". This further increases the estimate uncertainties. Therefore, as observed in Figure 9.8, the $3\sigma$-bounds of local estimates have the "saw-like" shapes. This is because the weakly connected graph, as well as the poor collective observability in the network at every time instant, might cause the local estimate

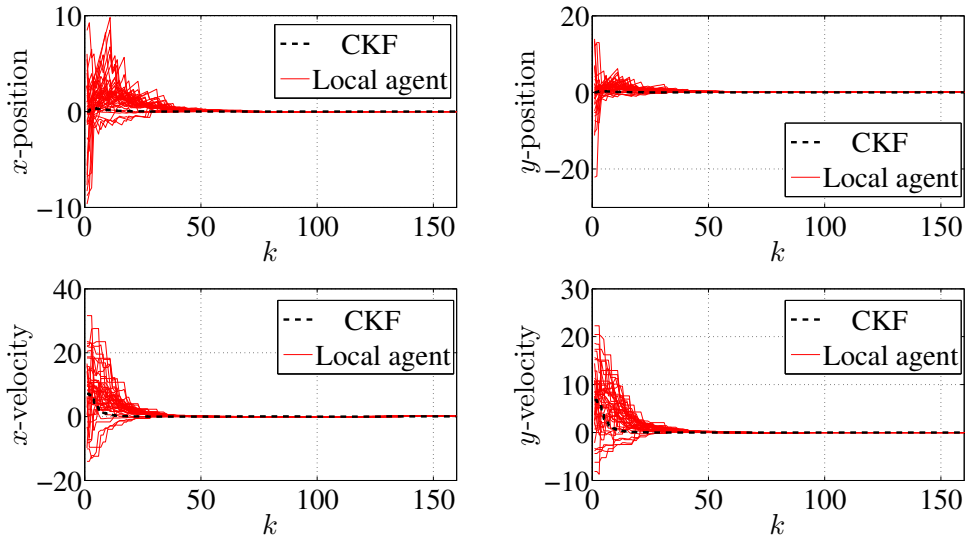


Figure 9.9: Expectations of estimate errors: DHIF algorithm v.s. CKF.

to diverge in short terms. Long-term-wisely, however, as the conditions formulated in Theorem 9.13 are satisfied, the local estimate errors are uniformly bounded.

**Simulation 3**. To illustrate Part (ii) of Theorem 9.13 in this simulation, a larger $N = 40$ is selected. The rest parameters are the same as the previous simulation. The expectations of all 4 state components of the local posterior estimate errors by all 40 agents using the DHIF Algorithm, are plotted along with the one by the CKF in Figure 9.9. Note that similar to the $\pm 3\sigma$ envelopes previously shown, the expectations of the local tracking error on the two position components also turn to have the "saw-like" shape. This is again, due to the overall weak connectivity and poor observabilities as previously explained. As observed in Figure 9.9, however, even in such an extreme scenario, the local estimate errors asymptotically converge to zero in expectations.

## 9.7 Conclusion

In this chapter, the problem of distributed dynamic state estimation using networked multi-agents is considered in the scenario where the process model of the target as well as the local sensing models of the local agents are modeled as linear. A distributed hybrid information fusion algorithm is proposed to solve the problem of dynamic state estimation in the scenario, where the process model of the target, the sensing models of local agents, and the communication topology might subject to change with time. The proposed algorithm requires no global parameter and only one communication iteration at every time instant. It comes up with consistent but confident local estimates with the estimate errors being uniformly upper bounded in finite time, and asymptotically converge to zero in expectation. The sufficient conditions to guarantee such convergence are formulated, and shown to be very mild and "almost" necessary. In the special case where the process/sensing models and the topology are both time invariant, the conditions with certain relaxations are necessary. The outperformance compared with existing algorithms are shown both analytically and numerically.

# Chapter 10

# Distributed State Estimation with Nonlinear Process and Local Sensing Models

In this chapter, the DHIF algorithm proposed in Chapter 9 is extended to the scenario with nonlinear process and local sensing models. The extended nonlinear DHIF algorithm is based on the Unscented Transformation paradigm.

## 10.1 Problem Formulation

### 10.1.1 Models & Assumptions

Consider the interested process model to be a general nonlinear dynamic system shown as follows:

$$\mathbf{x}^{(k+1)} = f(\mathbf{x}^{(k)}, \mathbf{w}^{(k)}), \tag{10.1}$$

where $\mathbf{x}^{(k)} \in \mathbb{R}^{n_x}$ and $\mathbf{w}^{(k)} \in \mathbb{R}^{n_w}$ are, respectively, the state of interest and the process noise. Being assumed to be known to all agents, the function $f : \mathbb{R}^{n_x} \times \mathbb{R}^{n_w} \to \mathbb{R}^{n_x}$ is the transform modeling the dynamics of the state of interest. It is assumed that for all time instants $k \in \mathbb{Z}^+$, $\mathbf{w}^{(k)} \sim \mathcal{N}(\mathbf{0}, \mathbf{Q}^{(k)})$ with $\mathbf{Q}^{(k)} \succ \mathbf{0}$ known to all agents as well. As $\mathbf{Q}^{(k)}$ is known to all local agents, for simplicity, we let $\mathbf{Q}^{(k)} = \mathbf{Q}$, $\forall k \in \mathbb{Z}^+$. It is also assumed that $\mathbb{E}[\mathbf{x}^{(k')}(\mathbf{w}^{(k)})^\top] = \mathbf{0}$, $\forall k' \in \mathbb{Z}^*$ and $k > k'$.

Let $m_i$ be the dimension[1] of the local measurement obtained by agent $i$, denoted as $\mathbf{z}_i^{(k)}$. The local sensing model at each agent $i \in \mathcal{V}$ is modeled as follows:

$$\mathbf{z}_i^{(k)} = h_i(\mathbf{x}^{(k)}) + \mathbf{v}_i^{(k)}, \tag{10.2}$$

where $\mathbf{v}_i^{(k)} \in \mathbb{R}^{m_i}$ is the associated sensing noise. It is assumed that $\forall k \in \mathbb{Z}^+$, $\mathbf{v}^{(k)} \sim \mathcal{N}(\mathbf{0}, \mathbf{R}^{(k)})$ with $\mathbf{R}^{(k)} \succ \mathbf{0}$. $h_i : \mathbb{R}^{n_x} \to \mathbb{R}^{m_i}$ is the transform modeling the sensing process of agent $i$.

As discussed in previous chapters of Part II, the networked agents are usually geographically located in many applications of distributed estimation, it is common to encounter the situation where the state of interest is directly observed by only a subset of local agents. Moreover, this subset changes over time in general. Therefore, Assumption 9.1.2 is adopted again in this chapter. The definition of blind agent (Definition 9.1) is also adopted in this chapter.

[1] For simplicity, $m_i$ is assumed to be time-invariant with out loss of generality.

### 10.1.2 Motivation & Objective

Although the distributed linear estimation problem has been extensively studied with the conditions for the stochastic stabilities being well formulated, the nonlinear case still draws limited attention. It is intuitive to extend the linear algorithm to their nonlinear analogies using approach similar to that of extending the Kalman filter to the EKF. Such an extension is achieved in [10] with the local stability properties shown analytically. However, the EKF-based extension requires the computation of the Jacobian at every time instant, which might bring difficulties for implementations. Moreover, the estimation performance could be deteriorated if the assumption of the local linearity is not well fulfilled (*e.g.*, bearing sensors *etc.*). An alternative approach to extend the algorithm while avoiding the aforementioned potential drawbacks is to use the Unscented transformation (UT), as adopted in [45, 46]. However, the algorithms therein both require multiple communication iterations during every sampling time interval and hence, bring heavy communication burdens in general. The works also do not explicitly consider the existence of agents sensing no target.

Motivated by the above facts, in this chapter, we aim at extending our previously proposed DHIF algorithm to the scenario where the process model of the target and the sensing model of the local agents are nonlinear. The UT approach is adopted to approximate the statistics of random variables undergoing nonlinear models. The extended algorithm should inherit the advantages of the original DHIF algorithm for requiring only single communication iteration per each sampling time instant. It should also be robust against the presence of agents sensing no target. Aside from extending the DHIF algorithm, we also aim at studying the stochastic stability of the extended algorithm, and formulating the conditions to fulfill in the case if the local sensing models are linear.

## 10.2 The Nonlinear DHIF Algorithm

In this section, we extended the DHIF algorithm to the case with nonlinear models, using the UT approach.

Suppose that at time $k$, each agent has an estimated state at time $k-1$, as well as an approximated error covariance, denoted, respectively as $\hat{\mathbf{x}}_i^{k-1|k-1}$ and $\hat{\mathbf{P}}_i^{k-1|k-1}$. The recursive algorithm implemented by each agent $i \in \mathscr{V}$ at $k$ contains four steps, namely, propagation, packing, communication and update.

**Propagation**. Each agent $i \in \mathscr{V}$ propagates its local posterior estimate from the previous time instant to the current time. This is done by using the UT. Let the augmented state vector as well as the corresponding augmented covariance matrix for each agent be denoted, respectively, as, ${}^a\hat{\mathbf{x}}_i^{(k-1)} \in \mathbb{R}^{n_a}$ and $\mathbf{P}_{i,a}^{(k-1)} \in \mathbb{R}^{n_a \times n_a}$, where $n_a = n_x + n_w$,

$$ {}^a\hat{\mathbf{x}}_i^{(k-1)} \triangleq \begin{bmatrix} \hat{\mathbf{x}}_i^{k-1|k-1} \\ \\ \mathbf{0} \end{bmatrix}, \text{ and } \mathbf{P}_{i,a}^{(k-1)} \triangleq \begin{bmatrix} \hat{\mathbf{P}}_i^{k-1|k-1} & \mathbf{0} \\ \\ \mathbf{0} & \mathbf{Q} \end{bmatrix}. $$

A set of $2n_a+1$ sigma points, denoted as, ${}^a\boldsymbol{\mathscr{X}}_{i,r}^{k-1|k-1}$, $r = 0, \ldots, 2n_a$, are selected by the following:

$$ \begin{aligned} {}^a\boldsymbol{\mathscr{X}}_{i,0}^{k-1|k-1} &= {}^a\hat{\mathbf{x}}_i^{(k-1)}, \\ {}^a\boldsymbol{\mathscr{X}}_{i,r}^{k-1|k-1} &= {}^a\hat{\mathbf{x}}_i^{(k-1)} + \left\{ \sqrt{(n_a+\gamma)\,\mathbf{P}_{i,a}^{(k-1)}} \right\}_{(:,r)}, \text{ if } r \in [1, n_a], \\ {}^a\boldsymbol{\mathscr{X}}_{i,r}^{k-1|k-1} &= {}^a\hat{\mathbf{x}}_i^{(k-1)} - \left\{ \sqrt{(n_a+\gamma)\,\mathbf{P}_{i,a}^{(k-1)}} \right\}_{(:,r-n_a)}, \text{ otherwise.} \end{aligned} $$

Here $\gamma = \alpha^2 (n_a + \kappa) - n_a$ is a scaling parameter with $0 \leq \alpha \leq 1$ and $\kappa \in \mathbb{R}$ being a tuning parameter to be selected. Note that the definition of the sigma points directly implies that

$$ \sum_{r=0}^{2n_a} {}^a\boldsymbol{\mathscr{X}}_{i,r}^{k-1|k-1} = {}^a\boldsymbol{\mathscr{X}}_{i,0}^{k-1|k-1} = {}^a\hat{\mathbf{x}}_i^{(k-1)}, $$

or equivalently,

$$\sum_{r=0}^{2n_a} \boldsymbol{\mathscr{X}}_{i,r}^{k-1|k-1} = \hat{\mathbf{x}}_i^{k-1|k-1}, \quad \sum_{r=0}^{2n_a} \boldsymbol{\mathscr{W}}_{i,r}^{k-1|k-1} = \mathbf{0},$$

where $\boldsymbol{\mathscr{X}}_{i,r}^{k-1|k-1}$ and $\boldsymbol{\mathscr{W}}_{i,r}^{k-1|k-1}$, collect the components of ${}^a\boldsymbol{\mathscr{X}}_{i,r}^{k-1|k-1}$ corresponding to, respectively, $\mathbf{x}^{(k-1)}$ and $\mathbf{w}^{(k-1)}$. The corresponding weights for computing the mean and covariances denoted, respectively as $W_{i,r}^m$ and $W_{i,r}^c$, are computed as

$$W_{i,0}^m = \gamma/(n_a+\gamma),$$

$$W_{i,0}^c = \gamma/(n_a+\gamma) + \left(1-\alpha^2+\beta\right),$$

$$W_{i,r}^m = W_{i,r}^c = 1/2(n_a+\gamma), \quad r = 1,\ldots,2n_a,$$

where $\beta$ is used to incorporate extra higher order effects. Then the prior local estimate of the current state is computed as $\hat{\mathbf{x}}_i^{k|k-1} = \sum_{r=0}^{2n_a} W_{i,r}^m \boldsymbol{\mathscr{X}}_{i,r}^{(k)}$, with

$$\boldsymbol{\mathscr{X}}_{i,r}^{(k)} = f\left(\boldsymbol{\mathscr{X}}_{i,r}^{k-1|k-1}, \boldsymbol{\mathscr{W}}_{i,r}^{k-1|k-1}\right).$$

The corresponding error covariance is computed as

$$\hat{\mathbf{P}}_i^{k|k-1} = \sum_{r=0}^{2n_a} W_{i,r}^c \left(\boldsymbol{\mathscr{X}}_{i,r}^{(k)} - \hat{\mathbf{x}}_i^{k|k-1}\right)\left(\boldsymbol{\mathscr{X}}_{i,r}^{(k)} - \hat{\mathbf{x}}_i^{k|k-1}\right)^\top.$$

**Packing**. After agent $i$ sensing the target and obtaining its local measurement $\mathbf{z}_i^{(k)}$, it packs the local information for the use of transmission in the next step. The local prior estimate pairs can be easily packed as done in the original DHIF algorithm. *i.e.*,

$$\boldsymbol{\Xi}_i^{(k)} = \left(\hat{\mathbf{P}}_i^{k|k-1}\right)^{-1}, \; \boldsymbol{\xi}_i^{(k)} = \left(\hat{\mathbf{P}}_i^{k|k-1}\right)^{-1} \hat{\mathbf{x}}_i^{k|k-1}.$$

On the other hand, however, one should note that the packing for the local measurement pairs are not as straightforward as that of the original DHIF algorithm due to the fact that nonlinearities are involved in the local sensing models. Different from the EKF-based extension [10], where

the Jacobian matrix is used to replace the measurement matrix, a substitution of the measurement matrix does not exist in the UT approach. Therefore, to this end, we adopt the formulation used in the unscented information filter (UIF [43]). That is, each agent $i$ computes,

$$\mathbf{Y}_i^{(k)} = \left(\mathscr{H}_i^{(k)}\right)^\top \left(\mathbf{R}_i^{(k)}\right)^{-1} \mathscr{H}_i^{(k)},$$

$$\mathbf{y}_i^{(k)} = \left(\mathscr{H}_i^{(k)}\right)^\top \left(\mathbf{R}_i^{(k)}\right)^{-1} \left[\mathbf{z}_i^{(k)} - \hat{\mathbf{z}}_i^{(k)} + \mathscr{H}_i^{(k)} \hat{\mathbf{x}}_i^{k|k-1}\right],$$

where $\mathscr{H}_i^{(k)} \triangleq \left(\hat{\mathbf{P}}_{i,k}^{xz}\right)^\top \left(\hat{\mathbf{P}}_i^{k|k-1}\right)^{-1}$ is the pseudo measurement matrix with

$$\hat{\mathbf{P}}_{i,k}^{xz} = \sum_{r=0}^{2n} W_{i,r}^c \left[\mathscr{X}_{i,r}^{(k)} - \hat{\mathbf{x}}_i^{k|k-1}\right] \left[h_i\left(\mathscr{X}_{i,r}^{(k)}\right) - \hat{\mathbf{z}}_i^{(k)}\right]^\top$$

and $\hat{\mathbf{z}}_i^{(k)} = \sum_{r=0}^{2n_a} W_{i,r}^m h_i \mathscr{X}_{i,r}^{(k)}$.

**Communication**. Once the local information is packed, each agent $i \in \mathscr{V}$ sends $\mathbf{Y}_i^{(k)}$, $\mathbf{y}_i^{(k)}$, $\mathbf{\Xi}_i^{(k)}$ and $\boldsymbol{\xi}_i^{(k)}$ to agent $j$, $\forall j \in N_{i,\text{out}}^{(k)}$ and receives $\mathbf{Y}_j^{(k)}$, $\mathbf{y}_j^{(k)}$, $\mathbf{\Xi}_j^{(k)}$ and $\boldsymbol{\xi}_j^{(k)}$ from agent $j$, $\forall j \in N_{i,\text{in}}^{(k)}$.

**Update**. After receiving the information transmitted from its in-neighbors, each agent $i$ selects the set of weights $\{d_{ij}^{(k)}\}_{j \in J_i^{(k)}}$, and updates its local estimate as well as the corresponding approximated covariance as

$$\hat{\mathbf{P}}_i^{k|k} = \left(\sum_{j \in J_i^{(k)}} \mathbf{Y}_j^{(k)} + \sum_{j \in J_i^{(k)}} d_{ij}^{(k)} \mathbf{\Xi}_i^{(k)}\right)^{-1}, \tag{10.3}$$

$$\hat{\mathbf{x}}_i^{k|k} = \hat{\mathbf{P}}_i^{k|k} \left(\sum_{j \in J_i^{(k)}} \mathbf{y}_j^{(k)} + \sum_{j \in J_i^{(k)}} d_{ij}^{(k)} \boldsymbol{\xi}_i^{(k)}\right). \tag{10.4}$$

**Remark 10.1 (Weights selection)** *The weights $\{d_{ij}^{(k)}\}_{j \in J_i^{(k)}}$ are determined locally by agent i without using any global information (total number of agents,* etc.*). The details for determining the weights is not the focus of this chapter (see Chapter 9 for details). Recall that for all time instants, the weights $\{d_{ij}^{(k)}\}_{j \in J_i^{(k)}}$ are uniformly lower bounded above zero and satisfy that $\sum_{j \in J_i^{(k)}} d_{ij}^{(k)} = 1$, $\forall i \in \mathscr{V}$. As a result, the adjacency matrix describing the communication topology at any time instant is row stochastic. For the rest of this chapter, we define $\mathbf{D}^{(k)}$ such that $\{\mathbf{D}\}_{(i,j)} = d_{ij}^{(k)}$.*

## 10.3 Stability Analysis

In this section, the stochastic stability of the proposed algorithm is studied for the scenario where the local sensing models are linear. The stability analysis for the scenario with general nonlinear local sensing models is more mathematically challenging and is left for the future work. In this section, instead of considering the sensing model in Eq. (10.2), the sensing model in Eq. (9.2) is considered. In the case considered in this section, the correspondingly packing steps for the measurement pairs are modified as

$$\mathbf{Y}_i^{(k)} = \left(\mathbf{H}_i^{(k)}\right)^\top \left(\mathbf{R}_i^{(k)}\right)^{-1} \mathbf{H}_i^{(k)},$$
$$\mathbf{y}_i^{(k)} = \left(\mathbf{H}_i^{(k)}\right)^\top \left(\mathbf{R}_i^{(k)}\right)^{-1} \mathbf{z}_i^{(k)}.$$

Specifically, it will be shown in the following that the local prior estimate errors at each agent, as a stochastic process, is bounded in mean square under some sufficient conditions. To this end, the following Lemmas are used.

**Lemma 10.2 ( [64])** *Assume that $\boldsymbol{\xi}^{(k)}$ is a stochastic process and there is a stochastic process $V\left(\boldsymbol{\xi}^{(k)}\right)$ as well as real numbers $v_{min}$, $v_{max} > 0$, $\mu > 0$ and $0 < \lambda \leq 1$ such that the following conditions are fulfilled $\forall k \in \mathbb{Z}^+$.*

$$v_{min}\|\boldsymbol{\xi}^{(k)}\|^2 \leq V\left(\boldsymbol{\xi}^{(k)}\right) \leq v_{max}\|\boldsymbol{\xi}^{(k)}\|^2 \tag{10.5}$$

$$\mathbb{E}[V\left(\boldsymbol{\xi}^{(k)}\right)|\boldsymbol{\xi}^{(k-1)}] - V\left(\boldsymbol{\xi}^{(k-1)}\right) \leq \mu - \lambda V\left(\boldsymbol{\xi}^{(k-1)}\right) \tag{10.6}$$

*Then the stochastic process is bounded in mean square, i.e.,*

$$\mathbb{E}[\|\boldsymbol{\xi}^{(k)}\|^2] \leq \frac{v_{max}}{v_{min}}\mathbb{E}[\|\boldsymbol{\xi}^{(0)}\|^2](1-\lambda)^k + \frac{\mu}{v_{min}}\sum_{i=1}^{k-1}(1-\lambda)^i. \tag{10.7}$$

**Lemma 10.3 ( [9])** *Given N positive definite matrices* $\mathbf{M}_1,\ldots,\mathbf{M}_N$*, and N vectors* $\mathbf{v}_1,\ldots,\mathbf{v}_N$ *with* $N \geq 2$*, the following inequality holds:*

$$\left(\sum_{i=1}^{N}\mathbf{M}_i\mathbf{v}_i\right)^{\top}\left(\sum_{i=1}^{N}\mathbf{M}_i\right)^{-1}\left(\sum_{i=1}^{N}\mathbf{M}_i\mathbf{v}_i\right) \leq \sum_{i=1}^{N}\mathbf{v}_i^{\top}\mathbf{M}_i\mathbf{v}_i.$$

Before stating the main result, some derivations are needed for the notations to be used in the main theorem. Let $\hat{\boldsymbol{\eta}}_i^{k|k} \triangleq \mathbf{x}^{(k)} - \hat{\mathbf{x}}_i^{k|k}$ be the posterior estimate error by agent $i$ at time instant $k$. Note that $\mathbf{x}^{(k+1)}$ can be approximated by the Taylor series about $\left(\hat{\mathbf{x}}_i^{k|k},\mathbf{0}\right)$ up to the first order:

$$\mathbf{x}^{(k+1)} \approx f\left(\hat{\mathbf{x}}_i^{k|k},\mathbf{0}\right) + \nabla_{\mathbf{x}^{(k)}} f\left(\hat{\mathbf{x}}_i^{k|k},\mathbf{0}\right)\hat{\boldsymbol{\eta}}_i^{k|k} + \nabla_{\mathbf{w}^{(k)}} f\left(\hat{\mathbf{x}}_i^{k|k},\mathbf{0}\right)\mathbf{w}^{(k)}.$$

Similarly, each sigma point after the transformation can be approximated using the Taylor series:

$$\boldsymbol{\mathcal{X}}_{i,r}^{(k+1)} \triangleq f\left(\boldsymbol{\mathcal{X}}_{i,r}^{k|k},\boldsymbol{\mathcal{W}}_{i,r}^{k|k}\right) \approx f\left(\hat{\mathbf{x}}_i^{k|k},\mathbf{0}\right) + \nabla_{\mathbf{x}^{(k)}} f\left(\hat{\mathbf{x}}_i^{k|k},\mathbf{0}\right)\left(\boldsymbol{\mathcal{X}}_{i,r}^{k|k} - \hat{\mathbf{x}}_i^{k|k}\right) + \nabla_{\mathbf{w}^{(k)}} f\left(\hat{\mathbf{x}}_i^{k|k},\mathbf{0}\right)\boldsymbol{\mathcal{W}}_{i,r}^{k|k}.$$

As a result, $\hat{\mathbf{x}}_i^{k+1|k}$ can be approximated as

$$\begin{aligned}
\hat{\mathbf{x}}_i^{k+1|k} =& \sum_{r=0}^{2n_a} W_{i,r}^{m} f\left(\boldsymbol{\mathcal{X}}_{i,r}^{k|k},\boldsymbol{\mathcal{W}}_{i,r}^{k|k}\right) \\
\approx& f\left(\hat{\mathbf{x}}_i^{k|k},\mathbf{0}\right) + \nabla_{\mathbf{x}^{(k)}} f\left(\hat{\mathbf{x}}_i^{k|k},\mathbf{0}\right)\left(\sum_{r=0}^{2n_a} W_{i,r}^{m}\boldsymbol{\mathcal{X}}_{i,r}^{k|k} - \hat{\mathbf{x}}_i^{k|k}\right) + \nabla_{\mathbf{w}^{(k)}} f\left(\hat{\mathbf{x}}_i^{k|k},\mathbf{0}\right)\left(\sum_{r=0}^{2n_a} W_{i,r}^{m}\boldsymbol{\mathcal{W}}_{i,r}^{k|k}\right) \\
=& f\left(\hat{\mathbf{x}}_i^{k|k},\mathbf{0}\right).
\end{aligned}$$

Let $\hat{\boldsymbol{\eta}}_i^{k+1|k} \triangleq \mathbf{x}^{(k+1)} - \hat{\mathbf{x}}_i^{k+1|k}$ be the prior estimate error by agent $i$ at time $k+1$. It follows that

$$\hat{\boldsymbol{\eta}}_i^{k+1|k} \approx \mathbf{F}_{i,k}\hat{\boldsymbol{\eta}}_i^{k|k} + \mathbf{B}_{i,k}\mathbf{w}^{(k)},$$

where $\mathbf{F}_{i,k} = \nabla_{\mathbf{x}^{(k)}} f\left(\hat{\mathbf{x}}_i^{k|k},\mathbf{0}\right)$ and $\mathbf{B}_{i,k} = \nabla_{\mathbf{w}^{(k)}} f\left(\hat{\mathbf{x}}_i^{k|k},\mathbf{0}\right)$. Thus, by introducing the unknown instrumental diagonal matrices [87], denoted as $\mathbf{E}_{i,k}^{x} \in \mathbb{R}^{n_x \times n_x}$ and $\mathbf{E}_{i,k}^{w} \in \mathbb{R}^{n_x \times n_x}$, one has

$$\hat{\boldsymbol{\eta}}_i^{k+1|k} = \mathbf{E}_{i,k}^{x}\mathbf{F}_{i,k}\hat{\boldsymbol{\eta}}_i^{k|k} + \mathbf{E}_{i,k}^{w}\mathbf{B}_{i,k}\mathbf{w}^{(k)}. \tag{10.8}$$

The true covariance of the prior estimate error $\hat{\boldsymbol{\eta}}_i^{k+1|k}$, denoted as $\mathbf{P}_i^{k+1|k} \triangleq \mathbb{E}[\hat{\boldsymbol{\eta}}_i^{k+1|k}\left(\hat{\boldsymbol{\eta}}_i^{k+1|k}\right)^\top]$, is

$$\mathbf{P}_i^{k+1|k} = \mathbf{E}_{i,k}^x \mathbf{F}_{i,k} \hat{\mathbf{P}}_i^{k|k} \mathbf{F}_{i,k}^\top \mathbf{E}_{i,k}^x + \Delta \mathbf{P}_i^{k+1|k} + \mathbf{E}_{i,k}^w \mathbf{B}_{i,k} \mathbf{Q}_k \mathbf{B}_{i,k}^\top \mathbf{E}_{i,k}^w,$$

where

$$\Delta \mathbf{P}_i^{k+1|k} = \mathbf{E}_{i,k}^x \mathbf{F}_{i,k} \mathbb{E}[\hat{\boldsymbol{\eta}}_i^{k|k}\left(\hat{\boldsymbol{\eta}}_i^{k|k}\right)^\top] \mathbf{F}_{i,k}^\top \mathbf{E}_{i,k}^x - \mathbf{E}_{i,k}^x \mathbf{F}_{i,k} \hat{\mathbf{P}}_i^{k|k} \mathbf{F}_{i,k}^\top \mathbf{E}_{i,k}^x.$$

Therefore, let $\delta \mathbf{P}_i^{k+1|k} \triangleq \hat{\mathbf{P}}_i^{k+1|k} - \mathbf{P}_i^{k+1|k}$ and

$$\hat{\mathbf{Q}}_{i,k} \triangleq \delta \mathbf{P}_i^{k+1|k} + \Delta \mathbf{P}_i^{k+1|k} + \mathbf{E}_{i,k}^w \mathbf{B}_{i,k} \mathbf{Q}_k \mathbf{B}_{i,k}^\top \mathbf{E}_{i,k}^w, \tag{10.9}$$

one has $\hat{\mathbf{P}}_i^{k+1|k} = \mathbf{E}_{i,k}^x \mathbf{F}_{i,k} \hat{\mathbf{P}}_i^{k|k} \mathbf{F}_{i,k}^\top \mathbf{E}_{i,k}^x + \hat{\mathbf{Q}}_{i,k}$.

**Theorem 10.4** *Let* $\mathbf{F}_{i,k}$, $\mathbf{E}_{i,k}^x$, $\mathbf{E}_{i,k}^w$ *and* $\mathbf{B}_{i,k}$ *be defined in Eq.* (10.8). *Suppose that* $\mathscr{G}^{(k)}$ *is strongly connected,* $\forall k \in \mathbb{Z}^+$. *Then the prior estimate error* $\hat{\boldsymbol{\eta}}_i^{k|k-1}$, $\forall i \in \mathscr{V}$, *is bounded in mean square, on the condition that the following assumptions are fulfilled for each* $i \in \mathscr{V}$*: there exist positive numbers* $p_{\min}$, $p_{\max}$, $f_{\min}$, $f_{\max}$, $e_{x,\min}$, $e_{x,\max}$, $e_{w,\min}$, $e_{,w\max}$, $\hat{q}_{\min}$, $r_{\min}$, *and* $h_{\max}$ *such that for all* $k \in \mathbb{Z}^*$*:*

$$p_{\min}\mathbf{I} \preceq \hat{\mathbf{P}}_i^{k+1|k} \preceq p_{\max}\mathbf{I}, \tag{10.10}$$

$$f_{\min}\mathbf{I} \preceq \mathbf{F}_{i,k}\left(\mathbf{F}_{i,k}\right)^\top \preceq f_{\max}\mathbf{I}, \tag{10.11}$$

$$e_{x,\min}\mathbf{I} \preceq \mathbf{E}_{i,k}^x \left(\mathbf{E}_{i,k}^x\right)^\top \preceq e_{x,\max}\mathbf{I} \tag{10.12}$$

$$e_{w,\min}\mathbf{I} \preceq \mathbf{E}_{i,k}^w \left(\mathbf{E}_{i,k}^w\right)^\top \preceq e_{w,\max}\mathbf{I} \tag{10.13}$$

$$\begin{cases} b_{\min}\mathbf{I} \preceq \mathbf{B}_{i,k}\mathbf{B}_{i,k}^\top \preceq b_{\max}\mathbf{I}\,, \text{if } n_x \geq n_w \\ b_{\min}\mathbf{I} \preceq \mathbf{B}_{i,k}^\top\mathbf{B}_{i,k} \preceq b_{\max}\mathbf{I}\,, \text{if } n_x < n_w \end{cases} \tag{10.14}$$

$$\hat{\mathbf{Q}}_{i,k} \succeq \hat{q}_{\min}\mathbf{I} \tag{10.15}$$

$$\mathbf{R}_i^{(k)} \succeq r_{\min}\mathbf{I} \tag{10.16}$$

$$\mathbf{H}_i^{(k)}\left(\mathbf{H}_i^{(k)}\right)^\top \preceq h_{\max}\mathbf{I} \tag{10.17}$$

**Proof.** Let $\rho_i^{(k)}$ be the $i$th entry of the $\boldsymbol{\rho}^{(k)} \in \mathbb{R}^N$ with $\boldsymbol{\rho}^{(k)}$ being the left-eigenvector associated with the largest eigenvalue (*i.e.*, 1) of the matrix $\mathbf{D}^{(k)}$. As the graph $\mathscr{G}^{(k)}$ is strongly connected, $\rho_i^{(k)} > 0$, $\forall i \in \mathscr{V}$. Let

$$\hat{\boldsymbol{\eta}}^{k+1|k} \triangleq \begin{bmatrix} \hat{\boldsymbol{\eta}}_1^{k+1|k} \\ \vdots \\ \hat{\boldsymbol{\eta}}_N^{k+1|k} \end{bmatrix}, \quad \hat{\mathbf{P}}^{k+1|k} \triangleq \begin{bmatrix} \rho_1^{(k)}\hat{\mathbf{P}}_1^{k+1|k} & & \\ & \ddots & \\ & & \rho_N^{(k)}\hat{\mathbf{P}}_N^{k+1|k} \end{bmatrix},$$

$V_{k+1}(\hat{\boldsymbol{\eta}}^{k+1|k}) \triangleq (\hat{\boldsymbol{\eta}}_i^{k+1|k})^\top(\hat{\mathbf{P}}^{k+1|k})^{-1}(\hat{\boldsymbol{\eta}}^{k+1|k})$ and $V_{i,k+1}(\hat{\boldsymbol{\eta}}_i^{k+1|k}) \triangleq (\hat{\boldsymbol{\eta}}_i^{k+1|k})^\top(\hat{\mathbf{P}}_i^{k+1|k})^{-1}(\hat{\boldsymbol{\eta}}_i^{k+1|k})$. It follows that $V_{k+1} \triangleq \sum_{i\in\mathscr{V}}\rho_i^{(k+1)}V_{i,k+1}$. If Eq. (10.10) is satisfied, it follows from Lemma 10.2 that

$$p_{\max}\|\hat{\boldsymbol{\eta}}^{k+1|k}\|^2 \leq V_{k+1}(\hat{\boldsymbol{\eta}}^{k+1|k}) \leq p_{\min}\|\hat{\boldsymbol{\eta}}^{k+1|k}\|^2.$$

Therefore, $\hat{\boldsymbol{\eta}}^{k+1|k}$ can be shown to be bounded in mean square if it is satisfied that

$$\mathbb{E}\left[V_{k+1}\left(\hat{\boldsymbol{\eta}}^{k+1|k}\right)|\hat{\boldsymbol{\eta}}^{k|k-1}\right] - V_k\left(\hat{\boldsymbol{\eta}}^{k|k-1}\right) \leq \mu - \lambda V_k\left(\hat{\boldsymbol{\eta}}^{k|k-1}\right),$$

for some $\mu > 0$ and $0 < \lambda \leq 1$. The rest of the proof will be focused on showing this.

Note that by Eq. (10.8),

$$\begin{aligned} V_{i,k+1}\left(\hat{\boldsymbol{\eta}}_i^{k+1|k}\right) = &\left(\mathbf{E}_{i,k}^x\mathbf{F}_{i,k}\hat{\boldsymbol{\eta}}_i^{k|k}\right)^\top\left(\hat{\mathbf{P}}_i^{k+1|k}\right)^{-1}\left(\mathbf{E}_{i,k}^x\mathbf{F}_{i,k}\hat{\boldsymbol{\eta}}_i^{k|k}\right) \\ &+\left(\mathbf{E}_{i,k}^w\mathbf{B}_{i,k}\mathbf{w}^{(k)}\right)^\top\left(\hat{\mathbf{P}}_i^{k+1|k}\right)^{-1}\left(\mathbf{E}_{i,k}^w\mathbf{B}_{i,k}\mathbf{w}^{(k)}\right) \\ &+2\left(\mathbf{E}_{i,k}^x\mathbf{F}_{i,k}\hat{\boldsymbol{\eta}}_i^{k|k}\right)^\top\left(\hat{\mathbf{P}}_i^{k+1|k}\right)^{-1}\left(\mathbf{E}_{i,k}^w\mathbf{B}_{i,k}\mathbf{w}^{(k)}\right). \end{aligned} \tag{10.18}$$

Also note that

$$\hat{\boldsymbol{\eta}}_i^{k|k} = \hat{\mathbf{P}}_i^{k|k} \sum_{j \in J_i^{(k)}} d_{ij}^{(k)} \left(\hat{\mathbf{P}}_j^{k|k-1}\right)^{-1} \hat{\boldsymbol{\eta}}_j^{k|k-1} - \hat{\mathbf{P}}_i^{k|k} \sum_{j \in J_i^{(k)}} \left(\mathbf{H}_j^{(k)}\right)^{\top} \left(\mathbf{R}_j^{(k)}\right)^{-1} \mathbf{v}_j^{(k)}. \tag{10.19}$$

Now let us take a look at all three terms on the right-hand side of Eq. (10.18). The expectation of the last term in Eq. (10.18) conditioned on $\hat{\boldsymbol{\eta}}^{k|k-1}$ with Eq. (10.19) being substituted in, has the form of

$$\begin{aligned}
&\mathbb{E}\left[\left(\mathbf{E}_{i,k}^x \mathbf{F}_{i,k} \hat{\boldsymbol{\eta}}_i^{k|k}\right)^{\top} \left(\hat{\mathbf{P}}_i^{k+1|k}\right)^{-1} \left(\mathbf{E}_{i,k}^w \mathbf{B}_{i,k} \mathbf{w}^{(k)}\right) | \hat{\boldsymbol{\eta}}^{k|k-1}\right] \\
=&\mathbb{E}\left[\left(\mathbf{w}^{(k)}\right)^{\top} | \hat{\boldsymbol{\eta}}^{k|k-1}\right] \left(\mathbf{E}_{i,k}^w \mathbf{B}_{i,k}\right)^{\top} \left(\hat{\mathbf{P}}_i^{k+1|k}\right)^{-1} \left(\hat{\mathbf{P}}_i^{k|k} \sum_{j \in J_i^{(k)}} d_{ij}^{(k)} \left(\hat{\mathbf{P}}_j^{k|k-1}\right)^{-1} \hat{\boldsymbol{\eta}}_j^{k|k-1}\right) \\
&-\mathbb{E}\left[\left(\mathbf{w}^{(k)}\right)^{\top} | \hat{\boldsymbol{\eta}}^{k|k-1}\right] \left(\mathbf{E}_{i,k}^w \mathbf{B}_{i,k}\right)^{\top} \left(\hat{\mathbf{P}}_i^{k+1|k}\right)^{-1} \left(\hat{\mathbf{P}}_i^{k|k} \sum_{j \in J_i^{(k)}} \left(\mathbf{H}_j^{(k)}\right)^{\top} \left(\mathbf{R}_j^{(k)}\right)^{-1} \mathbb{E}\left[\mathbf{v}_j^{(k)} | \hat{\boldsymbol{\eta}}^{k|k-1}\right]\right) \\
=&0,
\end{aligned}$$

where the property of mutual independence among $\mathbf{w}^{(k)}$, $\{\mathbf{v}_j^{(k)}\}_{j \in \mathscr{V}}$ and $\hat{\boldsymbol{\eta}}^{k|k-1}$ is used. As each term on the right-hand side of Eq. (10.18) is a scalar and hence equals to its own trace. It follows that the expectation of the second term in Eq. (10.18) conditioned on $\hat{\boldsymbol{\eta}}^{k|k-1}$ can be written as

$$\begin{aligned}
&\mathbb{E}\left[\left(\mathbf{E}_{i,k}^w \mathbf{B}_{i,k} \mathbf{w}^{(k)}\right)^{\top} \left(\hat{\mathbf{P}}_i^{k+1|k}\right)^{-1} \left(\mathbf{E}_{i,k}^w \mathbf{B}_{i,k} \mathbf{w}^{(k)}\right) | \boldsymbol{\eta}^{k|k-1}\right] \\
=&\mathbb{E}\left[\operatorname{tr}\left\{\mathbf{B}_{i,k}^{\top} \left(\mathbf{E}_{i,k}^w\right)^{\top} \left(\hat{\mathbf{P}}_i^{k+1|k}\right)^{-1} \mathbf{E}_{i,k}^w \mathbf{B}_{i,k} \mathbf{w}^{(k)} \left(\mathbf{w}^{(k)}\right)^{\top}\right\} | \boldsymbol{\eta}^{k|k-1}\right] \\
=&\operatorname{tr}\left\{\mathbf{B}_{i,k}^{\top} \left(\mathbf{E}_{i,k}^w\right)^{\top} \left(\hat{\mathbf{P}}_i^{k+1|k}\right)^{-1} \mathbf{E}_{i,k}^w \mathbf{B}_{i,k} \mathbf{Q}\right\},
\end{aligned} \tag{10.20}$$

where the second equality uses again the property of mutual independence.

Now we look at the first term in Eq. (10.18). Note if Eq. (10.11) and Eq. (10.12) are fulfilled, $\mathbf{E}_{i,k}^x \mathbf{F}_{i,k}$ is invertible. Moreover, if Eq. (10.15) is fulfilled, it follows that

$$\begin{aligned}
\left(\hat{\mathbf{P}}_i^{k+1|k}\right)^{-1} &= \left(\mathbf{E}_{i,k}^x \mathbf{F}_{i,k} \hat{\mathbf{P}}_i^{k|k} \mathbf{F}_{i,k}^{\top} \mathbf{E}_{i,k}^x + \hat{\mathbf{Q}}_{i,k}\right)^{-1} \\
&\prec \left(\mathbf{E}_{i,k}^x \mathbf{F}_{i,k} \hat{\mathbf{P}}_i^{k|k} \mathbf{F}_{i,k}^{\top} \mathbf{E}_{i,k}^x\right)^{-1} = \left(\mathbf{F}_{i,k}^{\top} \mathbf{E}_{i,k}^x\right)^{-1} \left(\hat{\mathbf{P}}_i^{k|k}\right)^{-1} \left(\mathbf{E}_{i,k}^x \mathbf{F}_{i,k}\right)^{-1}.
\end{aligned} \tag{10.21}$$

As a result, the first term on the right-hand side of Eq. (10.18) satisfies

$$\begin{aligned}
&\left(\hat{\boldsymbol{\eta}}_i^{k|k}\right)^\top \left(\mathbf{F}_{i,k}\right)^\top \mathbf{E}_{i,k}^x \left(\hat{\mathbf{P}}_i^{k+1|k}\right)^{-1} \mathbf{E}_{i,k}^x \mathbf{F}_{i,k} \hat{\boldsymbol{\eta}}_i^{k|k} \\
&< \left(\hat{\boldsymbol{\eta}}_i^{k|k}\right)^\top \left(\mathbf{F}_{i,k}\right)^\top \mathbf{E}_{i,k}^x \left(\mathbf{F}_{i,k}^\top \mathbf{E}_{i,k}^x\right)^{-1} \left(\hat{\mathbf{P}}_i^{k|k}\right)^{-1} \left(\mathbf{E}_{i,k}^x \mathbf{F}_{i,k}\right)^{-1} \mathbf{E}_{i,k}^x \mathbf{F}_{i,k} \hat{\boldsymbol{\eta}}_i^{k|k} \\
&= \left(\hat{\boldsymbol{\eta}}_i^{k|k}\right)^\top \left(\hat{\mathbf{P}}_i^{k|k}\right)^{-1} \hat{\boldsymbol{\eta}}_i^{k|k}.
\end{aligned}$$

Substitute Eq. (10.19) into the above equation, one has

$$\begin{aligned}
&\left(\hat{\boldsymbol{\eta}}_i^{k|k}\right)^\top \left(\hat{\mathbf{P}}_i^{k|k}\right)^{-1} \hat{\boldsymbol{\eta}}_i^{k|k} \\
=&-2\left(\sum\nolimits_{j\in J_i^{(k)}} \left(\mathbf{H}_j^{(k)}\right)^\top \left(\mathbf{R}_j^{(k)}\right)^{-1} \mathbf{v}_j^{(k)}\right)^\top \hat{\mathbf{P}}_i^{k|k} \left(\sum\nolimits_{j\in J_i^{(k)}} d_{ij}^{(k)} \left(\hat{\mathbf{P}}_j^{k|k-1}\right)^{-1} \hat{\boldsymbol{\eta}}_j^{k|k-1}\right) \\
&+\left(\sum\nolimits_{j\in J_i^{(k)}} \left(\mathbf{H}_j^{(k)}\right)^\top \left(\mathbf{R}_j^{(k)}\right)^{-1} \mathbf{v}_j^{(k)}\right)^\top \hat{\mathbf{P}}_i^{k|k} \left(\sum\nolimits_{j\in J_i^{(k)}} \left(\mathbf{H}_j^{(k)}\right)^\top \left(\mathbf{R}_j^{(k)}\right)^{-1} \mathbf{v}_j^{(k)}\right) \\
&+\left(\sum\nolimits_{j\in J_i^{(k)}} d_{ij}^{(k)} \left(\hat{\mathbf{P}}_j^{k|k-1}\right)^{-1} \hat{\boldsymbol{\eta}}_j^{k|k-1}\right)^\top \hat{\mathbf{P}}_i^{k|k} \left(\sum\nolimits_{j\in J_i^{(k)}} d_{ij}^{(k)} \left(\hat{\mathbf{P}}_j^{k|k-1}\right)^{-1} \hat{\boldsymbol{\eta}}_j^{k|k-1}\right).
\end{aligned} \tag{10.22}$$

Note that due to the mutual independence between any prior estimate errors up to the time (*i.e.*, $\hat{\boldsymbol{\eta}}_j^{k|k-1}, \forall j \in N_{i,\text{in}}^{(k)}$) and all local measurement noises at the time (*i.e.*, $\mathbf{v}_i^{(k)}, \forall i \in \mathcal{V}$), the expectation of the first term in Eq. (10.22) conditioned on $\hat{\boldsymbol{\eta}}^{k|k-1}$ is 0. Moreover, the expectation of the second term in Eq. (10.22) conditioned on $\hat{\boldsymbol{\eta}}^{k|k-1}$ is

$$\begin{aligned}
&\mathbb{E}\left[\left(\sum\nolimits_{j\in J_i^{(k)}} \left(\mathbf{H}_j^{(k)}\right)^\top \left(\mathbf{R}_j^{(k)}\right)^{-1} \mathbf{v}_j^{(k)}\right)^\top \hat{\mathbf{P}}_i^{k|k} \left(\sum\nolimits_{j\in J_i^{(k)}} \left(\mathbf{H}_j^{(k)}\right)^\top \left(\mathbf{R}_j^{(k)}\right)^{-1} \mathbf{v}_j^{(k)}\right) |\boldsymbol{\eta}^{k|k-1}\right] \\
=&\mathbb{E}\left[\sum\nolimits_{j\in J_i^{(k)}} \left(\left(\mathbf{H}_j^{(k)}\right)^\top \left(\mathbf{R}_j^{(k)}\right)^{-1} \mathbf{v}_j^{(k)}\right)^\top \hat{\mathbf{P}}_i^{k|k} \left(\mathbf{H}_j^{(k)}\right)^\top \left(\mathbf{R}_j^{(k)}\right)^{-1} \mathbf{v}_j^{(k)} |\boldsymbol{\eta}^{k|k-1}\right] + 0 \\
=&\sum\nolimits_{j\in J_i^{(k)}} \mathbb{E}\left[\operatorname{tr}\left\{\left(\mathbf{R}_j^{(k)}\right)^{-1} \left(\mathbf{H}_j^{(k)}\right) \hat{\mathbf{P}}_i^{k|k} \left(\mathbf{H}_j^{(k)}\right)^\top \left(\mathbf{R}_j^{(k)}\right)^{-1} \mathbf{v}_j^{(k)} \left(\mathbf{v}_j^{(k)}\right)^\top\right\}\right] \\
=&\sum\nolimits_{j\in J_i^{(k)}} \operatorname{tr}\left\{\left(\mathbf{R}_j^{(k)}\right)^{-1} \left(\mathbf{H}_j^{(k)}\right) \hat{\mathbf{P}}_i^{k|k} \left(\mathbf{H}_j^{(k)}\right)^\top\right\},
\end{aligned} \tag{10.23}$$

where the zero term after the first equality is due to the mutual independence among local measurement noises. Note that the last term in Eq. (10.22) can be written as

$$
\begin{aligned}
&\left[\sum_{j\in J_i^{(k)}} d_{ij}^{(k)} \left[\hat{\mathbf{P}}_j^{k|k-1}\right]^{-1} \hat{\boldsymbol{\eta}}_j^{k|k-1}\right]^{\top} \hat{\mathbf{P}}_i^{k|k} \left[\sum_{j\in J_i^{(k)}} d_{ij}^{(k)} \left[\hat{\mathbf{P}}_j^{k|k-1}\right]^{-1} \hat{\boldsymbol{\eta}}_j^{k|k-1}\right] \\
=&\left[\sum_{j\in J_i^{(k)}} d_{ij}^{(k)} \left[\hat{\mathbf{P}}_j^{k|k-1}\right]^{-1} \hat{\boldsymbol{\eta}}_j^{k|k-1}\right]^{\top} \left[\sum_{j\in J_i^{(k)}} d_{ij}^{(k)} \left[\hat{\mathbf{P}}_j^{k|k-1}\right]^{-1}\right]^{-1} \left[\sum_{j\in J_i^{(k)}} d_{ij}^{(k)} \left[\hat{\mathbf{P}}_j^{k|k-1}\right]^{-1} \hat{\boldsymbol{\eta}}_j^{k|k-1}\right] \\
&+\left[\sum_{j\in J_i^{(k)}} d_{ij}^{(k)} \left[\hat{\mathbf{P}}_j^{k|k-1}\right]^{-1} \hat{\boldsymbol{\eta}}_j^{k|k-1}\right]^{\top} \left[\sum_{j\in J_i^{(k)}} d_{ij}^{(k)} \mathbf{Y}_j^{(k)}\right]^{-1} \left[\sum_{j\in J_i^{(k)}} d_{ij}^{(k)} \left[\hat{\mathbf{P}}_j^{k|k-1}\right]^{-1} \hat{\boldsymbol{\eta}}_j^{k|k-1}\right] \\
\leq&\left[\sum_{j\in J_i^{(k)}} d_{ij}^{(k)} \left[\hat{\mathbf{P}}_j^{k|k-1}\right]^{-1} \hat{\boldsymbol{\eta}}_j^{k|k-1}\right]^{\top} \left[\sum_{j\in J_i^{(k)}} d_{ij}^{(k)} \left[\hat{\mathbf{P}}_j^{k|k-1}\right]^{-1}\right]^{-1} \left[\sum_{j\in J_i^{(k)}} d_{ij}^{(k)} \left[\hat{\mathbf{P}}_j^{k|k-1}\right]^{-1} \hat{\boldsymbol{\eta}}_j^{k|k-1}\right] \\
\leq&\sum_{j\in J_i^{(k)}} d_{ij}^{(k)} \left[\hat{\boldsymbol{\eta}}_j^{k|k-1}\right]^{\top} \left[\hat{\mathbf{P}}_j^{k|k-1}\right]^{-1} \hat{\boldsymbol{\eta}}_j^{k|k-1} \\
=&\sum_{j\in J_i^{(k)}} d_{ij}^{(k)} V_{j,k},
\end{aligned}
\tag{10.24}
$$

where the first inequality is due to Eq. (10.3) and the fact that $\mathbf{Y}_j^{(k)} \succeq \mathbf{0}$, $\forall j \in \mathscr{V}$; and the second inequality is obtained by following Lemma 10.3. Therefore, by collecting the right-hand side of Eq. (10.20), Eq. (10.23) and Eq. (10.24), one can summarize that

$$
\begin{aligned}
&\mathbb{E}\left[V_{k+1}(\hat{\boldsymbol{\eta}}^{k+1|k})|\hat{\boldsymbol{\eta}}^{k|k-1}\right] \\
<&\sum_{i\in\mathscr{V}} \rho_i \mathrm{tr}\left\{\mathbf{B}_{i,k}^{\top}(\mathbf{E}_{i,k}^{w})^{\top}(\hat{\mathbf{P}}_i^{k+1|k})^{-1}\mathbf{E}_{i,k}^{w}\mathbf{B}_{i,k}\mathbf{Q}\right\} + \sum_{i\in\mathscr{V}} \rho_i \sum_{j\in J_i^{(k)}} \mathrm{tr}\left\{\left(\mathbf{R}_j^{(k)}\right)^{-1}\left(\mathbf{H}_j^{(k)}\right)\hat{\mathbf{P}}_i^{k|k}\left(\mathbf{H}_j^{(k)}\right)^{\top}\right\} \\
&+\sum_{i\in\mathscr{V}} \rho_i \sum_{j\in J_i^{(k)}} d_{ij}^{(k)} V_{j,k}.
\end{aligned}
\tag{10.25}
$$

If Eq. (10.10), Eq. (10.13) and Eq. (10.14) are fulfilled, the first term on the right-hind side of Eq. (10.25) can be written as

$$
\begin{aligned}
\sum_{i\in\mathscr{V}} \rho_i \mathrm{tr}\left\{\mathbf{B}_{i,k}^{\top}(\mathbf{E}_{i,k}^{w})^{\top}(\hat{\mathbf{P}}_i^{k+1|k})^{-1}\mathbf{E}_{i,k}^{w}\mathbf{B}_{i,k}\mathbf{Q}\right\} &\leq \sum_{i\in\mathscr{V}} \rho_i \frac{e_{e,\max} b_{\max}}{\hat{p}_{\min}} \min(n_x, n_w)\mathrm{tr}\{\mathbf{Q}\} \\
&= \frac{e_{e,\max} b_{\max}}{\hat{p}_{\min}} \min(n_x, n_w)\mathrm{tr}\{\mathbf{Q}\} \triangleq \mu_1.
\end{aligned}
$$

Note that as $\mathbf{Q} \succ \mathbf{0}$, $\mu_1 > 0$. Eq. (10.10) gives $\left(\hat{\mathbf{P}}_i^{k|k-1}\right)^{-1} \succeq \frac{1}{\hat{p}_{\max}}\mathbf{I}$, which further implies that $\sum_{j\in J_i^{(k)}} d_{ij}^{(k)} \left(\hat{\mathbf{P}}_j^{k|k-1}\right)^{-1} \succeq \frac{1}{\hat{p}_{\max}}\mathbf{I}$ and hence

$$\hat{\mathbf{P}}_i^{k|k} \preceq \left(\sum_{j\in J_i^{(k)}} d_{ij}^{(k)} \left(\hat{\mathbf{P}}_j^{k|k-1}\right)^{-1}\right)^{-1} \preceq \hat{p}_{\max}\mathbf{I}.$$

It follows that the second term on the right-hind side of Eq. (10.25) can be written as

$$\begin{aligned}
&\sum_{i\in\mathscr{V}} \rho_i \sum_{j\in J_i^{(k)}} \mathrm{tr}\left\{\left(\mathbf{R}_j^{(k)}\right)^{-1}\left(\mathbf{H}_j^{(k)}\right)\hat{\mathbf{P}}_i^{k|k}\left(\mathbf{H}_j^{(k)}\right)^{\top}\right\} \\
=&\sum_{i\in\mathscr{V}} \rho_i \sum_{j\in J_i^{(k)}\setminus\mathscr{B}^{(k)}} \mathrm{tr}\left\{\left(\mathbf{R}_j^{(k)}\right)^{-1}\left(\mathbf{H}_j^{(k)}\right)\hat{\mathbf{P}}_i^{k|k}\left(\mathbf{H}_j^{(k)}\right)^{\top}\right\} \\
\leq&\sum_{i\in\mathscr{V}} \rho_i \frac{h_{\max}\hat{p}_{\max}}{r_{\min}} \max_{j\in J_i^{(k)}\setminus\mathscr{B}^{(k)}} \{m_j\} \triangleq \mu_2,
\end{aligned}$$

where the inequality is due to Eq. (10.16), Eq. (10.17). Finally, let $\mathbf{V}_k \triangleq [V_{1,k},\ldots,V_{N,k}]^{\top}$, the last term on the right-hand side of Eq. (10.25) can be written as

$$\sum_{i\in\mathscr{V}} \rho_i \sum_{j\in J_i^{(k)}} d_{ij}^{(k)} V_{j,k} = \boldsymbol{\rho}^{\top}\mathbf{D}^{(k)}\mathbf{V}_k = \boldsymbol{\rho}^{\top}\mathbf{V}_k = V_k.$$

Let $\mu \triangleq \mu_1 + \mu_2$. Then one has $\mu > 0$. It follows from Eq. (10.25) that

$$\mathbb{E}\left[V_{k+1}\left(\hat{\boldsymbol{\eta}}^{k+1|k}\right)|\hat{\boldsymbol{\eta}}^{k|k-1}\right] - V_k\left(\hat{\boldsymbol{\eta}}^{k|k-1}\right) < \mu. \tag{10.26}$$

Note that as Eq. (10.26) holds, we can always define

$$\bar{\lambda} \triangleq \min\left(1, \frac{\mu + V_k\left(\hat{\boldsymbol{\eta}}^{k|k-1}\right) - \mathbb{E}\left[V_{k+1}(\hat{\boldsymbol{\eta}}^{k+1|k})|\hat{\boldsymbol{\eta}}^{k|k-1}\right]}{V_k(\hat{\boldsymbol{\eta}}^{k|k-1})}\right)$$

and select a $\lambda$ satisfying $0 < \lambda \leq \bar{\lambda}$ such that,

$$\mathbb{E}\left[V_{k+1}\left(\hat{\boldsymbol{\eta}}^{k+1|k}\right)|\hat{\boldsymbol{\eta}}^{k|k-1}\right] - V_k\left(\hat{\boldsymbol{\eta}}^{k|k-1}\right) \leq \mu - \lambda V_k\left(\hat{\boldsymbol{\eta}}^{k|k-1}\right).$$

This concludes the proof. ■

Some comments about the conditions formulated in Theorem 10.4 are discussed. In general, the conditions are analogous to the original stability results formulated in [87], which is the first stability analysis on the centralized UKF-based nonlinear filter to the best of the authors' knowledge. However, the assumptions Eq. (10.13) and Eq. (10.14) have no counterparts therein as the process noise therein is assumed to be additive to the state vector rather than going through the nonlinear process model as considered in this chapter. Moreover, the authors would also like to highlight the assumption in Eq. (10.15). Recall from Eq. (10.9) that $\hat{\mathbf{Q}}_{i,k}$ contains three terms. The last term is always positive definite if Eq. (10.13) and Eq. (10.14) are fulfilled. However, the signs for $\delta\mathbf{P}_i^{k+1|k}$ and $\Delta\mathbf{P}_i^{k+1|k}$ could be possibly opposite and hence the sign of their summation is not clear. If the last term is dominant, $\hat{\mathbf{Q}}_{i,k}$ is more likely to be positive definite. Otherwise, to fulfill Eq. (10.15), one can always manually add a positive definite matrix and hence guarantee the stability, as proposed in [77].

Before wrapping up this section, the authors would like to make another point. Note that the conditions in Theorem 10.4 are formulated using Jacobian matrices. Also note that if the matrices in the propagation steps of the original DHIF algorithm are replaced with their corresponding Jacobian matrices, the error dynamics derived from the resulting algorithm will end up with the same forms to those derived at the beginning of Section 10.3. Therefore, as a side product, Theorem 10.4 also applies to the EKF-based extension of the DHIF algorithm.

## 10.4 Simulation

In this section, the effectiveness of the extended nonlinear DHIF algorithm is illustrated using a simulation example.

The target of interest is a unicycle vehicle moving with known constant speed $v_c$ and turning angular velocity $d_c$ in a rectangular region monitored by $N = 49$ agents. It is assumed that $v_c = 0.5$ (m/s) and $d_c = \pi/100$ (rad/s). However, the real speed and turning angular velocity at each time instant, respectively, denoted as, $v_{\text{real}}^{(k)}$ and $d_{\text{real}}^{(k)}$, are subject to uncorrelated white Gaussian process noise, respectively, denoted as, $w_v^{(k)}$ and $w_d^{(k)}$, where $w_v^{(k)} \sim \mathcal{N}(0, 0.02^2)$ and $w_d^{(k)} \sim \mathcal{N}(0, (\frac{\pi}{180})^2)$. As a result, $v_{\text{real}}^{(k)} = v_c + w_v^{(k)}$ and $d_{\text{real}}^{(k)} = d_c + w_d^{(k)}$.

The state vector $\mathbf{x}^{(k)}$ to be estimated contains three entries, namely, $x^{(k)}$, $y^{(k)}$ and $\theta^{(k)}$ representing respectively, the $x$-position, the $y$-position, and the orientation of the vehicle with respect to the global frame. It is assumed that the vehicle is at the origin at the initial time instant. The process model is therefore

$$\mathbf{x}^{(k+1)} \triangleq \begin{bmatrix} x^{(k+1)} \\ y^{(k+1)} \\ \theta^{(k+1)} \end{bmatrix} = \begin{bmatrix} x^{(k)} + \Delta_T \left( v_c + w_v^{(k)} \right) \cos\theta^{(k)} \\ y^{(k)} + \Delta_T \left( v_c + w_v^{(k)} \right) \sin\theta^{(k)} \\ \theta^{(k)} + \Delta_T \left( d_c + w_d^{(k)} \right) \end{bmatrix},$$

where $\Delta_T = 0.5$ (s) is the length of sampling time interval.

The 49 networked agents form a rectangular $7 \times 7$ array, and are geographically distributed as shown in Figure 10.1. Each agent is assumed to be static and equipped with only one ranging sensor with limited sensing radius shown in pink circles in Figure 10.1. The communication links between local agents are bidirectional and shown in sky-blue dash-dot lines. For agent $i$, if the target is in its sensing range at time $k$, it obtains a scalar measurement

$$z_i^{(k)} = h_i(\mathbf{x}^{(k)}) = \left\| \begin{bmatrix} x_i^s \\ y_i^s \end{bmatrix} - \begin{bmatrix} x^{(k)} \\ y^{(k)} \end{bmatrix} \right\| + v_i^{(k)},$$

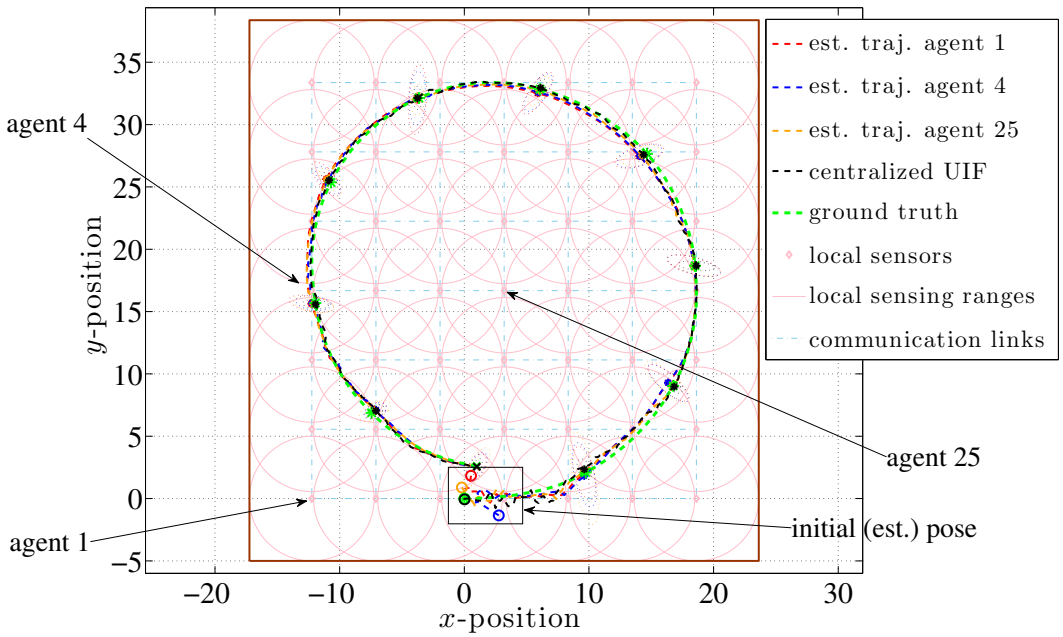


Figure 10.1: Unicycle mobile vehicle tracking task: the nonlinear DHIF algorithm v.s. UIF.

where $[x_i^s \ y_i^s]$ is the global position of agent $i$ and $v_i^{(k)} \sim \mathcal{N}(0,1)$. Note that as a single ranging measurement is not able to recover the vehicle state, not any single agent is able to track the target without cooperating with others. Moreover, at any time instant, the vehicle can be directly sensed by at most 4 agents, which is less that 10% percent of the total number of agents.

The nonlinear DHIF algorithm proposed in Section 10.2 is used with $\alpha = 0.001$, $\kappa = 0$ and $\beta = 2$ for all agents. The prior estimate pairs are initialized as $\hat{\mathbf{x}}_i^{0|0} \sim \mathcal{N}(\mathbf{0}, 10\mathbf{I})$, $\forall i \in \mathcal{V}$. The weights for the update steps are determined using the fast Covariance Intersection method [57]. A hypothetical centralized unscented information filter (UIF) using the collective measurements from all agents at each time instant, is used as the benchmark.

The estimated trajectories by local agents using the nonlinear DHIF algorithm and by the hypothetical centralized UIF are plotted along with the true trajectory in Figure 10.1. For clarity, only the trajectories estimated by three typical agents, namely, agent 1 (corner), agent 4 (side) and agent 25 (center), are plotted. Note that agent 1 and agent 25 never directly sense the target during the entire tracking process. The checkpoints, as well as the approximated covariance ellipses centered at the checkpoints for each estimated trajectory are plotted for every 20 seconds using the same color but dotted lines. As observed in Figure 10.1, the estimated trajectories by local agents are able to track the true target trajectory. In Figure 10.2, The local posterior estimate errors (solid lines in colors) and the corresponding approximated $\pm 3\sigma$ envelopes (dashed lines in the same color) at the aforementioned three agents for $50 \leq k \leq 400$, are plotted. As observed in Figure 10.2, the estimate errors by each agent is bounded by the $\pm 3\sigma$ envelopes at the steady-state.

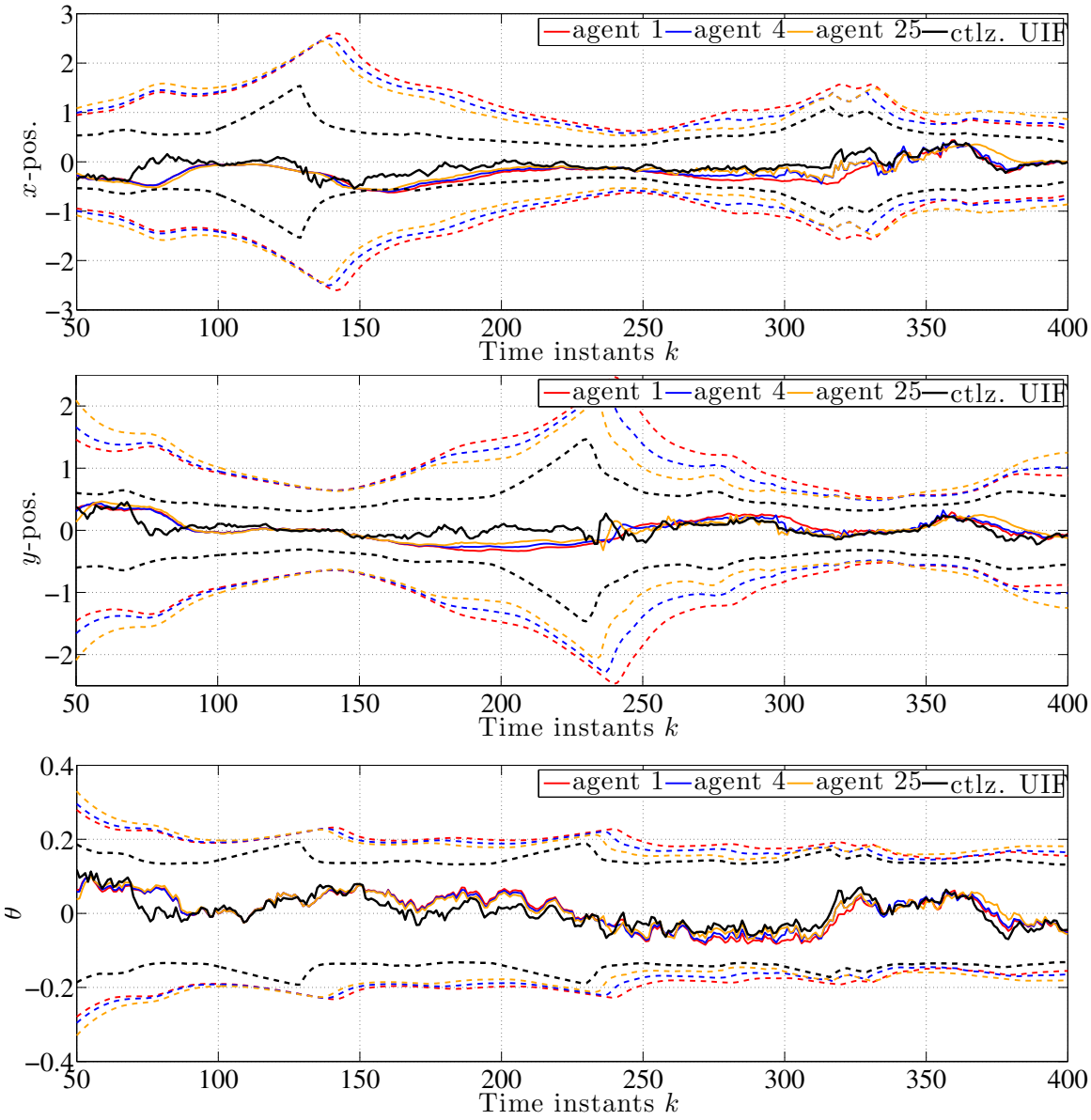


Figure 10.2: Trajectory tracking errors & $\pm 3\sigma$ envelopes in all 3 state components by the nonlinear DHIF algorithm and the centralized (ctlz.) UIF: $x^{(k)}$ (top); $y^{(k)}$ (middle); $\theta^{(k)}$ (bottom).

## 10.5 Conclusion

In this chapter, our nonlinear DHIF algorithm is extended from the algorithm proposed in Chapter 9 to the scenario with nonlinear models. The extension is achieved by embedding the UT approach into our distributed estimation framework. The extended algorithm requires only one communication iteration per sampling time instant and allow the existence of agents sensing no target. Sufficient conditions to guarantee the stochastic stability of the filtering process are formulated for the case in which the sensing models are linear. The effectiveness of the nonlinear DHIF algorithm are also illustrated using a simulation example.

# Chapter 11

# Distributed State Estimation with Uncertain Process Models

In this chapter, the DHIF algorithm proposed in Chapter 9 is extended to the scenario where the process model of the target of interest is not known to any local agent. Instead, it is assumed that the agents only know a finite set of possible underlying process models instead of the exact ones. Two algorithms are proposed based on two well-known centralized MM approaches, namely, the first order generalized pseudo Bayesian (GPB1) and the interacting multiple model (IMM) approaches.

## 11.1 Problem Formulation

### 11.1.1 Models & Assumptions

It is assumed in this chapter that the underlying mode of the process model during each sampling time interval is unknown but belongs to a set of finite possible modes. Throughout the chapter the sub-script $\ell \triangleq \ell^{(k)}$ is used to denote the mode in effect during the time interval starting at $k$. It is assumed that during each time interval,

- $\ell$ takes value from a finite set $\mathscr{M} \triangleq \{1, \ldots, N_m\}$;
- the transition probability between each pair of modes is constant;
- the probability of switching to a certain mode in the following time instant depends only on the mode at the current time instant.

**Assumption 11.1.1** *Every agent $i \in \mathscr{V}$ knows the mode transition matrix $\mathbf{\Pi} \triangleq [\pi_{sr}] \in \mathbb{R}^{N_m \times N_m}$, where $\pi_{sr} \triangleq \Pr\{\ell^{(k+1)} = r | \ell^{(k)} = s\}$ for some $r, s \in \mathscr{M}$ and $\forall k$.*

Let $\mathbf{F}_\ell \in \mathbb{R}^{n \times n}$ be the state transition matrix if mode $\ell$ is in effect. The following process model is considered to model the target of interest in this chapter:

$$\mathbf{x}^{(k)} = \mathbf{F}_\ell \mathbf{x}^{(k-1)} + \mathbf{w}_\ell^{(k-1)}, \tag{11.1}$$

where $\mathbf{x}^{(k)} \in \mathbb{R}^n$ is the state of interest at time $k$ and $\mathbf{w}_\ell^{(k)} \in \mathbb{R}^n$ is the white process noise associated with mode $\ell$ at time $k$. It is assumed that $\mathbf{w}_\ell^{(k)} \sim \mathscr{N}(\mathbf{0}, \mathbf{Q}_\ell)$, where $\mathbf{Q}_\ell \succ \mathbf{0}$. Although $\ell$ is unknown to any local agent, it is assumed that $\mathbf{Q}_\ell, \forall \ell \in \mathscr{M}$ are known to all local agents.

Correspondingly, suppose that at time $k$, each agent $i \in \mathscr{V}$ is able to obtain a local measurement

$$\mathbf{z}_i^{(k)} = \mathbf{H}_{i,\ell}^{(k)} \mathbf{x}^{(k)} + \mathbf{v}_{i,\ell}^{(k)}, \tag{11.2}$$

where $\mathbf{H}_{i,\ell}^{(k)} \in \mathbb{R}^{m_i \times n}$ and $\mathbf{v}_{i,\ell}^{(k)} \in \mathbb{R}^{m_i}$ are, respectively, the local observation matrix and the white local measurement noise of agent $i$ associated with mode $\ell$. It is assumed that for each $\ell \in \mathscr{M}$, $\mathbf{v}_{i,\ell}^{(k)} \sim \mathscr{N}(\mathbf{0}, \mathbf{R}_{i,\ell}^{(k)})$, where $\mathbf{R}_{i,\ell}^{(k)} \succ \mathbf{0}$ is known to agent $i$.

As discussed in Chapter 9, the local agents could be geographically distributed in many applications, it is common that the target of interest is in the sensing range of only a subset of agents in the inclusive neighborhood of every agent. In this chapter, let $\mathscr{S}^{(k)}$ be the set of agents directly sensing the target at time $k$. Let $\bar{\mathscr{S}}^{(k)} \triangleq \mathscr{V} \setminus \mathscr{S}^{(k)}$. The following assumption similar to Assumption 9.1.2 is made throughout this chapter.

**Assumption 11.1.2** *If agent $i \in \bar{\mathscr{S}}^{(k)}$, one has $(\mathbf{R}_{i,\ell}^{(k)})^{-1} = \mathbf{0}$ and an arbitrary $\mathbf{z}_i^{(k)}$, $\forall \ell \in \mathscr{M}$. Moreover, $\mathbf{H}_{i,\ell}^{(k)} = \mathbf{0}$, $\forall \ell \in \mathscr{M}$.*

### 11.1.2 Motivation & Objective

Although distributed strategies in estimating a single known process model problem have been extensively studied. The scenarios with multiple process models or model uncertainties are still not well considered. However, it is not a completely innovative idea to consider the distributed estimation problem in such a scenario [19, 47, 55]. The authors in [47] propose a consensus-based distributed MM Unscented Kalman Filter to track a jumping Markov nonlinear system. The authors in [19] also use the consensus-based approach to propose an algorithm. The work therein takes into account the presence of local agents without sensing ability and meanwhile aims at obtaining

a satisfactory performance with a smaller number of consensus iterations. However, the nature of the consensus algorithms implies that the algorithms in [19, 47] intend to have local agents communicate for multiple times during each sampling time interval. This might be energy consuming and hence becomes unrealistic for implementations. In comparison, the authors in [55] propose a *diffusion Kalman filter* (DKF) based MM adaptive estimation algorithm that is able to estimate a dynamic complex-value state with a fixed but unknown process model. However, the algorithm therein requires the target to be jointly observable to the inclusive neighborhood of each local agent. This assumption might not hold in general (see examples in [26, 33, 36, 80, 81]).

In this chapter, we aim at extending the DHIF algorithm proposed in Chapter 9 by taking into account the uncertainties in the process model/models. The extended algorithms should inherit the advantages of the original DHIF algorithm for being fully distributed and robust against the presence of agents not directly sensing the target. More importantly, different from the consensus-based approaches, the extended algorithm should require only a single communication iteration during each sampling time interval. We also aim at analyzing the convergence of mode probabilities at all agents, and proposing conditions under which the estimate error covariance of the output local estimates are uniformly upper bounded.

## 11.2 Multiple Model DHIF (MM-DHIF) Algorithms

In this section, we extend the DHIF algorithm to handle the scenarios where the target has multiple possible models or model uncertainties.

Suppose that at time instant $k+1$, agent $i \in \mathcal{V}$ has a set of $N_m$ mode-matched estimate pairs $\left(\hat{\mathbf{x}}_{i,\ell}^{k|k}, \hat{\mathbf{P}}_{i,\ell}^{k|k}\right)$, $\ell = 1, \cdots, N_m$, where $\hat{\mathbf{x}}_{i,\ell}^{k|k}$ is the local estimate of agent $i$ assuming $\ell$ is the true

mode. An approximated error covariance $\hat{\mathbf{P}}_{i,\ell}^{k|k}$ is associated with $\hat{\mathbf{x}}_{i,\ell}^{k|k}$, for each $i \in \mathscr{V}$ and $\ell \in \mathscr{M}$. The probability that mode $\ell$ was in effect at time $k$, where $\ell \in \mathscr{M}$, believed by each agent $i \in \mathscr{V}$, referred as the *local mode probability* hereafter in this chapter, is denoted as $\mu_{i,\ell}^{(k)}$. The algorithm executed by a certain agent $i$ at time instant $k$ are shown in the following. Two algorithms are extended from the DHIF algorithm by following, respectively, the GPB1-based and the IMM-based approaches. Specifically, the IMM-based extension has identical steps to the GPB1-based one with extra mixing/interacting steps.

### 11.2.1 GPB1-based DHIF algorithm

**Local estimate propagation**. This step is identical to that of the original DHIF algorithm except that it is run for each possible mode. That is, for each $\ell \in \mathscr{M}$,

$$\begin{aligned} \hat{\mathbf{x}}_{i,\ell}^{k|k-1} &= \mathbf{F}_\ell \hat{\mathbf{x}}_{i,\ell}^{k-1|k-1}, \\ \hat{\mathbf{P}}_{i,\ell}^{k|k-1} &= \mathbf{F}_\ell \hat{\mathbf{P}}_{i,\ell}^{k-1|k-1} (\mathbf{F}_\ell)^\top + \mathbf{Q}_\ell. \end{aligned} \tag{11.3}$$

**Local mode probability update – Step 1**. The update step of the local mode probabilities consists of two steps. Step 1 is executed after a local measurement $\mathbf{z}_i^{(k)}$ is obtained. Each agent $i \in \mathscr{V}$ computes a set of *intermediate local mode probabilities*, denoted as $\bar{\mu}_{i,\ell}^{(k)}$, $\ell = 1, \cdots, N_m$. The computation is done in a way depending on whether it is able to directly sense the target at time instant $k$, *i.e.*, whether $i \in \mathscr{S}^{(k)}$.

If $i \in \mathscr{S}^{(k)}$, the likelihood for each mode $\ell$, denoted as $\Lambda_{i,\ell}^{(k)}$, is computed as:

$$\Lambda_{i,\ell}^{(k)} = (2\pi)^{-\frac{n}{2}} \left|\mathbf{S}_{i,\ell}^{(k)}\right|^{-\frac{1}{2}} \exp\left\{-\frac{1}{2}(\mathbf{r}_{i,\ell}^{(k)})^\top (\mathbf{S}_{i,\ell}^{(k)})^{-1} \mathbf{r}_{i,\ell}^{(k)}\right\}, \tag{11.4}$$

where

$$\begin{aligned}\mathbf{r}_{i,\ell}^{(k)} &\triangleq \mathbf{z}_i^{(k)} - \mathbf{H}_{i,\ell}^{(k)} \hat{\mathbf{x}}_{i,\ell}^{k|k-1}, \\ \mathbf{S}_{i,\ell}^{(k)} &\triangleq \mathbf{H}_{i,\ell}^{(k)} \hat{\mathbf{P}}_{i,\ell}^{k|k-1} (\mathbf{H}_{i,\ell}^{(k)})^\top + \mathbf{R}_{i,\ell}^{(k)}.\end{aligned} \tag{11.5}$$

The pair $\left(\mathbf{r}_{i,\ell}^{(k)}, \mathbf{S}_{i,\ell}^{(k)}\right)$ is referred as the innovation pair hereafter. Note that $\mathbf{S}_{i,\ell}^{(k)}$ is the approximated innovation covariance rather than the true one. However, $\left(\mathbf{r}_{i,\ell}^{(k)}, \mathbf{S}_{i,\ell}^{(k)}\right)$ is consistent as long as $\left(\hat{\mathbf{x}}_{i,\ell}^{k|k-1}, \hat{\mathbf{P}}_{i,\ell}^{k|k-1}\right)$ is consistent, which is guaranteed by the nature of the DHIF algorithm (see [80] for details). As a result, the value of $\Lambda_{i,\ell}^{(k)}$ does realistically imply how much the obtained measurement matches the expected measurement, and hence can be used as the metric for the following computation of the intermediate local mode probabilities:

$$\bar{\mu}_{i,\ell}^{(k)} = c_i^{(k)} \Lambda_{i,\ell}^{(k)} \textstyle\sum_{\ell'=1}^{N_m} \pi_{\ell'\ell} \mu_{i,\ell'}^{(k-1)}, \tag{11.6}$$

where $c_i^{(k)} > 0$ is the normalizing factor and is determined such that $\sum_{\ell \in \mathscr{M}} \bar{\mu}_{i,\ell}^{(k)} = 1$.

On the other hand, if $i \in \bar{\mathscr{S}}^{(k)}$, no meaningful measurement is obtained by agent $i$. Therefore, no mode likelihood can be computed. In this case, the intermediate local mode probabilities are simply computed as:

$$\bar{\mu}_{i,\ell}^{(k)} = \textstyle\sum_{\ell'=1}^{N_m} \pi_{\ell'\ell} \mu_{i,\ell'}^{(k-1)}. \tag{11.7}$$

**Packing & Communication**. The intermediate local mode probabilities are stacked as $\bar{\boldsymbol{\mu}}_i^{(k)} \triangleq \mathrm{col}\{\bar{\mu}_{i,\ell}^{(k)}\}_{\ell \in \mathscr{M}}$. Then $\mathbf{z}_i^{(k)}$ is packed along with the propagated estimate pair with respect to each possible mode $\ell \in \mathscr{M}$, using the following equations:

$$\begin{aligned}\mathbf{Y}_{i,\ell}^{(k)} &\triangleq (\mathbf{H}_{i,\ell}^{(k)})^\top (\mathbf{R}_{i,\ell}^{(k)})^{-1} \mathbf{H}_{i,\ell}^{(k)}, \quad \boldsymbol{\Xi}_{i,\ell}^{(k)} \triangleq (\hat{\mathbf{P}}_{i,\ell}^{k|k-1})^{-1}, \\ \mathbf{y}_{i,\ell}^{(k)} &\triangleq (\mathbf{H}_{i,\ell}^{(k)})^\top (\mathbf{R}_{i,\ell}^{(k)})^{-1} \mathbf{z}_{i,\ell}^{(k)}, \quad \boldsymbol{\xi}_{i,\ell}^{(k)} \triangleq (\hat{\mathbf{P}}_{i,\ell}^{k|k-1})^{-1} \hat{\mathbf{x}}_{i,\ell}^{k|k-1}.\end{aligned} \tag{11.8}$$

After packing, for each $\ell \in \mathscr{M}$, agent $i$ transmits $\mathbf{Y}_{i,\ell}$, $\mathbf{y}_{i,\ell}$, $\boldsymbol{\Xi}_{i,\ell}^{(k)}$, $\boldsymbol{\xi}_{i,\ell}^{(k)}$ and $\bar{\boldsymbol{\mu}}_i^{(k)}$ to agent $j$, $\forall j \in N_{i,\text{out}}^{(k)}$, and receives $\mathbf{Y}_{j,\ell}$, $\mathbf{y}_{j,\ell}$, $\boldsymbol{\Xi}_{j,\ell}^{(k)}$, $\boldsymbol{\xi}_{j,\ell}^{(k)}$ and $\bar{\boldsymbol{\mu}}_j^{(k)}$ from agent $j$, $\forall j \in N_{i,\text{in}}^{(k)}$.

**Local estimate updates**. The update steps of the original DHIF algorithm are used for the estimate updates with respect to each possible mode. That is, for each $\ell \in \mathscr{M}$,

$$\begin{aligned} \hat{\mathbf{P}}_{i,\ell}^{k|k} &= \left[\sum\nolimits_{j\in J_i^{(k)}} \mathbf{Y}_{j,\ell}^{(k)} + \sum\nolimits_{j\in J_i^{(k)}} d_{ij}^{(k)} \boldsymbol{\Xi}_{j,\ell}^{(k)}\right]^{-1}, \\ \hat{\mathbf{x}}_{i,\ell}^{k|k} &= \hat{\mathbf{P}}_{i,\ell}^{k|k} \left[\sum\nolimits_{j\in J_i^{(k)}} \mathbf{y}_{j,\ell}^{(k)} + \sum\nolimits_{j\in J_i^{(k)}} d_{ij}^{(k)} \boldsymbol{\xi}_{j,\ell}^{(k)}\right]. \end{aligned} \tag{11.9}$$

In (11.9), the set of weights $\{d_{ij}^{(k)}\}_{j\in J_i^{(k)}}$ satisfies that $\sum_{j\in J_i^{(k)}} d_{ij}^{(k)} = 1$ and $d_{ij}^{(k)} > 0$, $\forall j \in J_i^{(k)}$. The weights can be determined using different approaches, such as solving an *A-optimal design* problem [80], using some close-form methods [22, 57, 83], or even simply computing a (weighted) average. The methods can be used to determine a set of weights for each possible mode. Although the weight selection is not the focus of this chapter, we would like to emphasize that the weights for all in-neighbors should be uniformly lower bounded above zero.

**Local mode probability update – Step 2**. Each agent updates its local mode probabilities using the previously computed intermediate local mode probabilities from its inclusive neighborhood. Similar to Step 1 of the local mode probability update, each agent also executes different commends in Step 2 depending on whether it is able to directly sense the target, as described in the following.

If $i \in \mathscr{S}^{(k)}$, it simply uses the previously computed intermediate local mode probabilities as the final values, *i.e.*, $\boldsymbol{\mu}_i^{(k)} = \bar{\boldsymbol{\mu}}_i^{(k)}$. On the other hand, if agent $i$ with $i \in \bar{\mathscr{S}}^{(k)}$ also updates in this way, it follows from (11.7) that its local mode probabilities will only follow the trend of the Markov process and simply converge to constant values related to the mode transition matrix. This is obviously not preferred. Therefore, if $i \in \bar{\mathscr{S}}^{(k)}$, agent $i$ is designed to modify its mode probabilities as:

$$\boldsymbol{\mu}_i^{(k)} = \sum\nolimits_{j\in J_i^{(k)}} \omega_{ij}^{(k)} \bar{\boldsymbol{\mu}}_j^{(k)}, \tag{11.10}$$

where the weights satisfy that $\sum_{j\in J_i^{(k)}} \omega_{ij}^{(k)} = 1$ and $\omega_{ij} > 0$, $\forall j \in J_i^{(k)}$. The weights selection is not the focus of this chapter, one simple option is $\omega_{ij}^{(k)} = d_{ij}^{(k)}$, $\forall j \in J_i^{(k)}$.

**Output**. This step is only needed when the overall local estimate is requested. Let $\mu_{i,\ell}^{(k)}$ be the component of $\boldsymbol{\mu}_i^{(k)}$ corresponding to mode $\ell$. The following output is given when requested:

$$\begin{aligned}
\hat{\mathbf{x}}_i^{k|k} &= \sum\nolimits_{\ell\in\mathscr{M}} \mu_{i,\ell}^{(k)} \hat{\mathbf{x}}_{i,\ell}^{k|k}, \\
\hat{\mathbf{P}}_i^{k|k} &= \sum\nolimits_{\ell\in\mathscr{M}} \mu_{i,\ell}^{(k)} \left[\hat{\mathbf{P}}_{i,\ell}^{k|k} + \left(\hat{\mathbf{x}}_{i,\ell}^{k|k} - \hat{\mathbf{x}}_i^{k|k}\right)\left(\hat{\mathbf{x}}_{i,\ell}^{k|k} - \hat{\mathbf{x}}_i^{k|k}\right)^\top\right].
\end{aligned} \tag{11.11}$$

### 11.2.2 IMM-based DHIF algorithm

In addition to the steps in the GPB1-based DHIF algorithm, the IMM-based DHIF algorithm contains the following extra mixing/interacting steps before the local estimate propagation step in (11.3). The following value is first computed for each pair of $\ell'$ and $\ell$, with $\ell', \ell \in \mathscr{M}$:

$$\mu_{i,\ell'|\ell}^{(k-1)} = \frac{\pi_{\ell'\ell}\mu_{i,\ell'}^{(k-1)}}{\sum_{\ell'\in\mathscr{M}} \pi_{\ell'\ell}\mu_{i,\ell'}^{(k-1)}},$$

where $\mu_{i,\ell'|\ell}^{(k-1)}$, referred as the *local mixing probability*, reflects the probability of mode $\ell'$ being in effect at $k-1$ given that mode $\ell$ is in effect at $k$, computed by agent $i$. Then the posterior estimate pairs at $k-1$ are mixed using the following equations for each $\ell \in \mathscr{M}$:

$$\begin{aligned}
\hat{\mathbf{x}}_{i,0\ell}^{k-1|k-1} &= \sum\nolimits_{\ell'\in\mathscr{M}} \mu_{i,\ell'|\ell}^{(k-1)} \hat{\mathbf{x}}_{i,\ell'}^{k-1|k-1}, \\
\hat{\mathbf{P}}_{i,0\ell}^{k-1|k-1} &= \sum\nolimits_{\ell'\in\mathscr{M}} \mu_{i,\ell'|\ell}^{(k-1)} \left[\hat{\mathbf{P}}_{i,\ell'}^{k-1|k-1} + \left(\hat{\mathbf{x}}_{i,\ell'}^{k-1|k-1} - \hat{\mathbf{x}}_{i,0\ell}^{k-1|k-1}\right)\left(\hat{\mathbf{x}}_{i,\ell'}^{k-1|k-1} - \hat{\mathbf{x}}_{i,0\ell}^{k-1|k-1}\right)^\top\right].
\end{aligned} \tag{11.12}$$

With $\hat{\mathbf{x}}_{i,0\ell}^{k-1|k-1}$ and $\hat{\mathbf{P}}_{i,0\ell}^{k-1|k-1}$, respectively, playing the role of $\hat{\mathbf{x}}_{i,\ell}^{k-1|k-1}$ and $\hat{\mathbf{P}}_{i,\ell}^{k-1|k-1}$ in (11.3), for each $\ell \in \mathscr{M}$, the rest steps of the IMM-based DHIF algorithm are identical to those of the GPB1-based one.

### 11.2.3 Comparisons with Existing Algorithms

The extended algorithms in this chapter inherit the advantages of the original DHIF algorithm. One important feature that is worth emphasizing is that the extended algorithms require only one communication iteration between neighboring agents during each sampling time interval. In comparison, the consensus-based algorithms [19, 47] require the agents to communicate for multiple times during each sampling time interval. Such approaches might be expensive in terms of communication and hence might be impractical for implementations in some applications. Moreover, the algorithm in [47] also assumes that the target is directly seen by all agents, the graph is balanced, and the total number of agents is known to all agents. Such assumptions actually limit the algorithms from being fully distributed. For example, if a local agent fails during the estimation process, the overall performance might be deteriorated if such a change is not known to other local agents. In comparison, our algorithms do not need such knowledge and hence will adapt to the locally unknown changes in an automated manner. Different from the consensus-based approaches, an algorithm based on the DKF [15] is proposed in [55] to handle the case where the true model is fixed. One advantage of the algorithm proposed therein compared to those of [19, 47] is that, only two communication iterations are needed during each sampling time interval. However, the main limitation is the requirement of joint local observability at each agent, due to the nature inherited from the original DKF algorithm. This requirement might be difficult to satisfy in many applications (see examples in [26, 33, 36, 80, 81]).

In comparison, our algorithms require only a single communication iteration during each sampling time interval. By cooperatively estimating the state and diffusing the local mode probabilities from the agents directly sensing the target to the rest, our algorithms do not require any

global information and have very mild requirements on the joint global observability conditions. As will see in the following section, it is not necessary for any single agent to have joint local observability about the target. Different from the work in [19, 47], which uses simulations to verify the performance, it is analytically shown in the next section that in the scenario with an unknown but fixed underlying mode, all agents across the network will be able to identify the true underlying mode and track the target of interest with consistent output local estimates. Sufficient conditions are formulated.

## 11.3 Stability Analysis: GPB1-DHIF with the Fixed Unknown Underlying Mode

In this section, the stability properties of the proposed GPB1-based DHIF algorithm is studied. Specifically, we show that if the unknown underlying model is fixed, the output local estimates obtained from (11.11) have the errors uniformly upper bounded in the positive definite sense at the steady state. The proof is shown considering the following conditions.

**C1.** For each mode, the local sensing model of each agent as well as the noise statistics are time invariant, *i.e.*, $\mathbf{H}_{i,\ell}^{(k)} = \mathbf{H}_{i,\ell}$ and $\mathbf{R}_{i,\ell}^{(k)} = \mathbf{R}_{i,\ell}$, for each $\ell \in \mathscr{M}$ and all $k$.

**C2.** The graph is time invariant, *i.e.*, $\mathscr{G}^{(k)} = \mathscr{G}$, $\forall k$.

**C3.** The weights selected by each agent in (11.9) are time invariant, *i.e.*, $\{d_{ij}^{(k)}\}_{j\in J_i} = \{d_{ij}\}_{j\in J_i}$, for each $i \in \mathscr{V}$ and all $k$.

**C4.** For each leader component of $\mathscr{G}$ with vertex set $\mathscr{V}_l$, $(\mathbf{F}_\ell, \tilde{\mathbf{H}}_{l,\ell})$ is detectable pair, for each $\ell \in \mathscr{M}$, where $\tilde{\mathbf{H}}_{l,\ell} \triangleq \text{col}\{\mathbf{H}_{j,\ell}\}_{j\in\mathscr{V}_l}$.

**C5.** Each agent $i \in \mathscr{V}$ selects $(\hat{\mathbf{P}}_{i,\ell}^{0|0})^{-1} = \mathbf{0}$, $\forall \ell \in \mathscr{M}$.

Some comments about the above conditions are given before moving to the proof. Note that Condition C1 implies that the status, whether each agent is directly sensing the target, is time invariant, *i.e.*, $\mathscr{S}^{(k)} = \mathscr{S}$, $\forall k$. Condition C2 also implies that the neighboring relations between agents are time invariant. As a result, the set $J_i$ in Condition C3 is independent of $k$. Essentially, Condition C1, C2 and C3 jointly imply that the entire network has the property of time invariance, which will be used as a key property in the later proof. The same properties has also been used in the analysis in the centralized case [4]. In joint with Condition C4, it follows from Corollary 9.16 that one is able to guarantee the boundedness of the local estimate errors, assuming each possible mode is the true underlying mode. Recall that Condition C4 is very mild in the sense that it requires neither the graph to contain a directed spanning tree, nor any single local agent to have joint observability in its inclusive neighborhood. This attributes to the very mild convergence conditions of the DHIF algorithm. Condition C5 is to guarantee the consistency of the estimate corresponding to the true mode. Such initializations are also selected in [8, 9] in the single-model scenario.

Now we show that for each possible mode, the approximated innovation covariance matrices in (11.5) are asymptotically independent of time.

**Lemma 11.1** *Suppose that Conditions C1 – C5 hold. Also suppose that* $\mathbf{F}_\ell$ *is nonsingular,* $\forall \ell \in \mathscr{M}$. *Then for each possible mode, the innovation covariance matrices approximated by all local agents directly sensing the target, are asymptotically independent of time. That is, as* $k \to \infty$, $\mathbf{S}_{i,\ell}^{(k)} \to \bar{\mathbf{S}}_{i,\ell}$ *with* $\bar{\mathbf{S}}_{i,\ell} \succ \mathbf{0}$ *being constant, for all* $i \in \mathscr{S}$ *and* $\ell \in \mathscr{M}$.

**Proof.** As the conclusion is shown using the same approach for each $\ell \in \mathscr{M}$, the mode index $\ell$ is omitted in this proof for simplicity.

With Condition C1 satisfied, one can observe from (11.5) that to show that $\mathbf{S}_i^{(k)}$, $\forall i \in \mathscr{S}$ are asymptotically time independent, it suffices to shown that $\hat{\mathbf{P}}_i^{k|k-1}$, $\forall i \in \mathscr{S}$ are asymptotically time independent. This can be shown by the following two steps.

The first step is to show that if Condition C5 is satisfied, each $\hat{\mathbf{P}}_i^{k|k}$, $i \in \mathscr{S}$ is asymptotically uniformly bounded in the positive definite (PD) sense from both above and below. The uniform lower bound can be directly observed from (11.3) and the fact that $\mathbf{Q} \succ \mathbf{0}$, which jointly imply the existence of uniform lower bound of $\hat{\mathbf{P}}_i^{k|k-1}$ (and hence $\hat{\mathbf{P}}_i^{k|k}$ due to (11.9) and the fact that $d_{ij} > 0$, $\forall j \in J_i$), $\forall i \in \mathscr{V}$, at all time. On the other hand, as Condition C1, C2 and C4 are satisfied, it follows from Corollary 9.16 that for each $i \in \mathscr{V}$ (hence, $i \in \mathscr{S}$), $\hat{\mathbf{P}}_i^{k|k}$ is also uniformly upper bounded (in the PD sense) in steady state.

The second step is to show that $\hat{\mathbf{P}}_i^{k|k}$ is monotonically non-increasing and hence, must asymptotically approach some finite (due to the uniform upper bound) constant PD (due to the uniform lower bound) matrix. Consider two different solutions of $\hat{\mathbf{P}}_i^{k|k}$ with different initializations, namely, $(\hat{\mathbf{P}}_i^{k_0|k_0})^{-1} = \mathbf{0}$ and $(\hat{\mathbf{P}}_i^{k_0-1|k_0-1})^{-1} = \mathbf{0}$. The two corresponding solutions at any $k$ are distinguished using, respectively, $\hat{\mathbf{P}}_{i[k_0]}^{k|k}$ and $\hat{\mathbf{P}}_{i[k_0-1]}^{k|k}$. Then we aim at showing that $\hat{\mathbf{P}}_{i,[k_0]}^{k|k} \succeq \hat{\mathbf{P}}_{i,[k_0-1]}^{k|k}$, $\forall k$. Due to the non-singular property of both matrices, it suffices to show that

$$(\hat{\mathbf{P}}_{i,[k_0-1]}^{k|k})^{-1} \succeq (\hat{\mathbf{P}}_{i,[k_0]}^{k|k})^{-1}, \ \forall k. \tag{11.13}$$

This is completed by induction. Note if $k = k_0$, $(\hat{\mathbf{P}}_{i,[k_0]}^{k_0|k_0})^{-1} = \mathbf{0}$. It follows from (11.9) and (11.3) that

$$\begin{aligned}(\hat{\mathbf{P}}_{i,[k_0-1]}^{k_0|k_0})^{-1} &= \sum\nolimits_{j\in J_i} \left[ d_{ij}(\mathbf{F}\hat{\mathbf{P}}_{j,[k_0-1]}^{k_0-1|k_0-1}\mathbf{F}^\top + \mathbf{Q})^{-1} + \mathbf{Y}_j \right] \\ &= \sum\nolimits_{j\in J_i} \mathbf{Y}_j \succeq \mathbf{0} = (\hat{\mathbf{P}}_{i,[k_0]}^{k_0|k_0})^{-1},\end{aligned}$$

where the second equality uses the facts that $(\hat{\mathbf{P}}_{i,[k_0-1]}^{k_0-1|k_0-1})^{-1} = \mathbf{0}$, $\forall i \in \mathscr{V}$ and $\mathbf{F}$ is non-singular. Suppose that (11.13) holds for all $i \in \mathscr{V}$ and $k = k_0, \ldots, k_t - 1$. When $k = k_t$,

$$\begin{aligned}\left(\hat{\mathbf{P}}_{i,[k_0-1]}^{k_t|k_t}\right)^{-1} &= \sum\nolimits_{j\in J_i}\left[d_{ij}(\mathbf{F}\hat{\mathbf{P}}_{j,[k_0-1]}^{k_t-1|k_t-1}\mathbf{F}^\top + \mathbf{Q})^{-1} + \mathbf{Y}_j\right] \\ &\succeq \sum\nolimits_{j\in J_i}\left[d_{ij}(\mathbf{F}\hat{\mathbf{P}}_{j,[k_0]}^{k_t-1|k_t-1}\mathbf{F}^\top + \mathbf{Q})^{-1} + \mathbf{Y}_j\right] = \left(\hat{\mathbf{P}}_{i,[k_0]}^{k_t|k_t}\right)^{-1},\end{aligned}$$

where the inequality is due to the induction hypothesis. This proves that (11.13) holds. Due to the property of time-invariance of all quantities in the covariance matrix equation (Conditions C1, C2 and C3), Eq. (11.13) directly implies that $(\hat{\mathbf{P}}_{i,[k_0]}^{k+1|k+1})^{-1} \succeq (\hat{\mathbf{P}}_{i,[k_0]}^{k|k})^{-1}$, $\forall k$. As $k_0$ is arbitrary, this indicates that with Condition C5 satisfied, $\hat{\mathbf{P}}_i^{k|k}$ and hence $\hat{\mathbf{P}}_i^{k|k-1}$ is monotonically non-increasing. Therefore, there exists $\bar{\mathbf{\Sigma}}_i \succ \mathbf{0}$, such that $\hat{\mathbf{P}}_i^{k|k-1} \to \bar{\mathbf{\Sigma}}_i$ as $k \to \infty$. As this is the case for all $i \in \mathscr{V}$, one has

$$\mathbf{S}_{i,\ell}^{(k)} \to \mathbf{H}_{i,\ell}\bar{\mathbf{\Sigma}}_i(\mathbf{H}_{i,\ell})^\top + \mathbf{R}_{i,\ell} \triangleq \bar{\mathbf{S}}_{i,\ell} \succ \mathbf{0},$$

for all $i \in \mathscr{S}$ and $\ell \in \mathscr{M}$, as $k \to \infty$. This concludes the proof. ■

**Remark 11.2** *The original proof of Theorem 9.13 (and hence Corollary 9.16) requires the approximated estimate error covariance $\hat{\mathbf{P}}_i^{k|k}$ to be uniformly lower bounded, and uses the consistency property to satisfy this requirement. However, this is not necessary due to the fact that $\mathbf{Q} \succ \mathbf{0}$ implies a uniform lower bound for $\hat{\mathbf{P}}_i^{k|k-1}$ and hence $\hat{\mathbf{P}}_i^{k|k}$. That is, the conclusion of Theorem 9.13 holds even without the guaranteed consistency properties of the local estimates. However, one should also note that, without consistency, the approximated estimate error covariance no longer implies the actual uncertainty of the estimate and hence, the approximated estimate error covariance being upper bounded no longer guarantees the actual estimate error covariance being upper bounded.*

As shown in Lemma 11.1, the networked system has the property of being asymptotically time independent under certain conditions. Based on this result, we are ready to state the following

main result, assuming ergodicity[1] [4] of the local innovations. As stated in [55], as the local innovation matched to the true underlying mode is uncorrelated and white, one can exploit the fact that the sequence is ergodic. The following lemmas are also used.

**Lemma 11.3 ( [4])** *Let* $\mathbf{A}$, $\mathbf{B}$ *be two* $p \times p$ *positive definite matrices. Then* $p + \ln(|\mathbf{A}|/|\mathbf{B}|) - tr(\mathbf{B}^{-1}\mathbf{A}) \preceq \mathbf{0}$ *with the equality holds if and only if* $\mathbf{A} = \mathbf{B}$.

**Lemma 11.4** *Given positive semi-definite (respectively, definite) matrices* $\mathbf{A}$ *and* $\mathbf{B}$ *with the same size, one has* $tr(\mathbf{AB}) \geq 0$ *(respectively,* $tr(\mathbf{AB}) > 0$*).*

**Proof.** The fact that $\mathbf{A} \succeq \mathbf{0}$ implies that by the Cholesky decomposition, one can write $\mathbf{A}$ as $\mathbf{A} = \mathbf{L}\mathbf{L}^\top$. It follows that $\mathrm{tr}(\mathbf{AB}) = \mathrm{tr}(\mathbf{L}\mathbf{L}^\top\mathbf{B}) = \mathrm{tr}(\mathbf{L}^\top\mathbf{B}\mathbf{L}) \geq 0$, where the last inequality is due to the fact that $\mathbf{B} \succeq \mathbf{0}$. If $\mathbf{A} \succ \mathbf{0}$, $\mathbf{L}$ is a unique lower-triangular matrix with nonzero diagonal entries. It follows that $\mathrm{tr}(\mathbf{L}^\top\mathbf{B}\mathbf{L}) > 0$, where the last inequality is due to the facts that $\mathbf{B} \succ \mathbf{0}$ and $\mathbf{L}$ is full rank.

■

**Theorem 11.5** *Suppose that Condition C1 – C5 hold. Also suppose that* $\mathbf{F}_\ell$ *is nonsingular,* $\forall \ell \in \mathscr{M}$. *Let* $\bar{\mathbf{S}}_{i,\ell}$ *be defined in Lemma 11.1, for each* $\ell \in \mathscr{M}$. *Let* $\tau \in \mathscr{M}$ *be the fixed underlying process model. Then for each* $i \in \mathscr{V}$, $\mu_{i,\tau}^{(k)} \to 1$ *as* $k \to \infty$. *If for each* $\ell \neq \tau$, *for a sufficiently large k, as* $\bar{k} \to \infty$,

$$\frac{1}{\bar{k}} \sum_{\kappa=k}^{k+\bar{k}-1} \mathbf{r}_{i,\ell}^{(\kappa)} (\mathbf{r}_{i,\ell}^{(\kappa)})^\top \succ \bar{\mathbf{S}}_{i,\tau}. \tag{11.14}$$

**Proof.** Note that when the underlying model is fixed, $\mathbf{\Pi} = \mathbf{I}_{N_m}$. Also note that if $i \in \mathscr{S}$, $\mu_{i,\ell}^{(k)} = \bar{\mu}_{i,\ell}^{(k)}$. Thus, with $c_i^{(k)}$ in (11.6) being specified, for each $i \in \mathscr{S}$, one has

$$\mu_{i,\ell}^{(k)} = \frac{\Lambda_{i,\ell}^{(k)} \mu_{i,\ell}^{(k-1)}}{\sum_{\ell' \in \mathscr{M}} \Lambda_{i,\ell'}^{(k)} \mu_{i,\ell'}^{(k-1)}}. \tag{11.15}$$

[1] The same assumption is also made in both the centralized case [4] and the distributed case [55].

Also from Lemma 11.1, for a sufficiently large $k$, $\mathbf{S}_{i,\ell}^{(k)} \to \bar{\mathbf{S}}_{i,\ell}$ for all $i \in \mathscr{S}$ and $\ell \in \mathscr{M}$. Define $\mathscr{L}_{i,\ell}^{(k)} \triangleq (\mu_{i,\ell}^{(k)})/(\mu_{i,\tau}^{(k)})$. One can instantly have $\mathscr{L}_{i,\ell}^{(k)} = \mathscr{L}_{i,\ell}^{(k-1)} \cdot (\Lambda_{i,\ell}^{(k)})/(\Lambda_{i,\tau}^{(k)})$. Suppose that $k$ is sufficiently large. Let $\bar{k}$ be a positive integer and let

$$R_{k-1}^{k+\bar{k}-1} \triangleq \ln\left(\frac{\mathscr{L}_{i,\ell}^{(k+\bar{k}-1)}}{\mathscr{L}_{i,\ell}^{(k-1)}}\right) = \ln\left(\frac{\Lambda_{i,\ell}^{(k+\bar{k}-1)}\Lambda_{i,\ell}^{(k+\bar{k}-2)}\cdots\Lambda_{i,\ell}^{(k)}}{\Lambda_{i,\tau}^{(k+\bar{k}-1)}\Lambda_{i,\tau}^{(k+\bar{k}-2)}\cdots\Lambda_{i,\tau}^{(k)}}\right). \tag{11.16}$$

It follows from (11.4) and (11.15) that

$$\frac{2}{\bar{k}}R_{k-1}^{k+\bar{k}-1} = \ln\frac{|\bar{\mathbf{S}}_{i,\tau}|}{|\bar{\mathbf{S}}_{i,\ell}|} - \mathrm{tr}\left[\frac{1}{\bar{k}}\sum_{\kappa=k}^{k+\bar{k}-1}\mathbf{r}_{i,\ell}^{(\kappa)}(\mathbf{r}_{i,\ell}^{(\kappa)})^{\top}(\bar{\mathbf{S}}_{i,\ell})^{-1}\right] + \mathrm{tr}\left[\frac{1}{\bar{k}}\sum_{\kappa=k}^{k+\bar{k}-1}\mathbf{r}_{i,\tau}^{(\kappa)}(\mathbf{r}_{i,\tau}^{(\kappa)})^{\top}(\bar{\mathbf{S}}_{i,\tau})^{-1}\right]. \tag{11.17}$$

Note that with $\tau$ being the true mode, the ergodicity implies that as $\bar{k} \to \infty$,

$$\frac{1}{\bar{k}}\sum_{\kappa=k}^{k+\bar{k}-1}\mathbf{r}_{i,\tau}^{(\kappa)}(\mathbf{r}_{i,\tau}^{(\kappa)})^{\top} \to \tilde{\mathbf{S}}_{i,\tau},$$

where $\tilde{\mathbf{S}}_{i,\tau}$ is the true covariance matrix of the innovation sequence at the steady state. Let $\mathbb{S}_{i,\tau} \triangleq \bar{\mathbf{S}}_{i,\tau} - \tilde{\mathbf{S}}_{i,\tau}$. Then the last term on the right-hand side of (11.17), with a sufficiently large $\bar{k}$, has the form of

$$\mathrm{tr}[(\bar{\mathbf{S}}_{i,\tau} - \mathbb{S}_{i,\tau})(\bar{\mathbf{S}}_{i,\tau})^{-1}] = m_i - \mathrm{tr}[(\mathbb{S}_{i,\tau})(\bar{\mathbf{S}}_{i,\tau})^{-1}].$$

With this combined with (11.17), one has

$$2\bar{k}^{-1}R_{k-1}^{k+\bar{k}-1} = \alpha + \beta + \gamma,$$

where $\alpha = -\mathrm{tr}\left((\mathbb{S}_{i,\tau})\left(\bar{\mathbf{S}}_{i,\tau}\right)^{-1}\right)$,

$$\beta = \ln\frac{|\bar{\mathbf{S}}_{i,\tau}|}{|\bar{\mathbf{S}}_{i,\ell}|} + m_i - \mathrm{tr}\left((\bar{\mathbf{S}}_{i,\ell})^{-1}(\bar{\mathbf{S}}_{i,\tau})\right),$$

and

$$\gamma = \mathrm{tr}\left(\left[\bar{\mathbf{S}}_{i,\tau} - \frac{1}{\bar{k}}\sum_{\kappa=k}^{k+\bar{k}-1}\mathbf{r}_{i,\ell}^{(\kappa)}\left(\mathbf{r}_{i,\ell}^{(\kappa)}\right)^{\top}\right](\bar{\mathbf{S}}_{i,\ell})^{-1}\right).$$

Note that $\bar{\mathbf{S}}_{i,\ell} \succ \mathbf{0}$, $\forall \ell \in \mathscr{M}$. The guaranteed consistency implies that $\bar{\mathbf{S}}_{i,\tau} \succeq \tilde{\mathbf{S}}_{i,\tau}$, and hence $\mathbb{S}_{i,\tau} \succeq \mathbf{0}$. It follows from Lemma 11.4 that $\alpha \leq 0$. Moreover, it follows from Lemma 11.3 that $\beta \leq 0$. Moreover, if (11.14) holds, it follow from Lemma 11.4 that $\gamma < 0$. It follows from (11.16) and (11.17) that

$$\mathscr{L}_{i,\ell}^{(k+\bar{k}-1)} \to C \exp\left\{-\frac{\bar{k}c}{2}\right\} \mathscr{L}_{i,\ell}^{(k-1)}$$

for some constants $c > 0$ and $C$. Therefore, for each $i \in \mathscr{S}$ and $\ell \neq \tau$, $(\mu_{i,\ell}^{(k)})/(\mu_{i,\tau}^{(k)}) \to 0$ or equivalently, $\mu_{i,\ell}^{(k)} \to 0$. As a result, for each $i \in \mathscr{S}$, $\mu_{i,\tau}^{(k)} \to 1$. The conclusion of $\mu_{i,\tau}^{(k)} \to 1$, $\forall i \in \bar{\mathscr{S}}$ can be directed observed from two facts. One one hand, Condition C4 guarantees that each $i \in \bar{\mathscr{S}}$ must have a directed path from at least one agent in $\mathscr{S}$. One the other hand, as the mode probabilities by each agent in $\mathscr{S}$ are never affected by other agents, the nature of the diffusion step (11.10) indicates that the mode probabilities of all agents in $\bar{\mathscr{S}}$ must eventually approach those of the agents in $\mathscr{S}$. This concludes the proof. ■

Throughout the rest of this section, let $\tau \in \mathscr{M}$ be defined in Theorem 11.5. Some comments about the sufficient condition (11.14) in Theorem 11.5 are provided here. Note that for each mode $\ell \neq \tau$, if it is not even "close" to the true underlying one, the condition is automatically satisfied in general as the local estimates matched to a very wrong model will be erroneous and even divergent. As a result, the summation of the products of the corresponding innovation term with its transpose will be significantly large or even unbounded.

A trickier case is when there exists a certain $\ell \in \mathscr{M}$, denoted as mode $\ell'$, such that $\ell' \neq \tau$ but mode $\ell'$ is "close" to mode $\tau$. For example, mode $\ell'$ can have the same state transition matrix ($\mathbf{F}_{\ell'} = \mathbf{F}_\tau$), but with wrong but close process noise covariance matrix ($\mathbf{Q}_{\ell'} \neq \mathbf{Q}_\ell$). In such cases, the estimates matched to mode $\ell'$ also converge and hence for a sufficiently large $\bar{k}$, one has $\frac{1}{\bar{k}} \sum_{\kappa=k}^{k+\bar{k}-1} \mathbf{r}_{i,\ell'}^{(\kappa)} (\mathbf{r}_{i,\ell'}^{(\kappa)})^\top \to \tilde{\mathbf{S}}_{i,\ell'}$. Then (11.14) might not hold as the innovation covariance matched

to the true mode is only approximated rather than the true one at the first place. As a result, it is possible that $\bar{\mathbf{S}}_{i,\tau} \succeq \tilde{\mathbf{S}}_{i,\ell'}$ although $\tilde{\mathbf{S}}_{i,\tau} \prec \tilde{\mathbf{S}}_{i,\ell'}$, where $\bar{\mathbf{S}}_{i,\tau}$ and $\tilde{\mathbf{S}}_{i,\tau}$ are defined in Theorem 11.5. Note that this would not be an issue in the centralized scenario [4] because (i) the true innovation covariance can be computed directly; and (ii) the mode-matched estimate corresponding to the true mode is the optimal one (due to the optimality of the Kalman filter given accurate models and noise statistics). Also note that, however, if $\bar{\mathbf{S}}_{i,\tau}$ is close to $\tilde{\mathbf{S}}_{i,\tau}$, the sufficient condition (11.14) is more likely to hold. This also emphasizes the importance of improving the estimate confidence [80]. The detailed studies for the case where the proposed sufficient condition do not hold are left for future work.

With the each agent's local mode probability with respect to the true mode converging to one, the output local estimate errors at all agents are asymptotically uniformly upper bounded (in the PD sense), as stated in the following corollary.

**Corollary 11.6** *Let $\tau \in \mathscr{M}$ and $\bar{\mathbf{S}}_{i,\ell}$, $\ell \in \mathscr{M}$ be, respectively, defined in Theorem 11.5 and Lemma 11.1. Suppose that Conditions C1 – C5 hold and $\mathbf{F}_\ell$ is nonsingular, $\forall \ell \in \mathscr{M}$. Also suppose that the sufficient condition* (11.14) *is satisfied. Then, as $k \to \infty$, there exists $\bar{\mathbf{P}} \succ \mathbf{0}$ such that*

$$\mathbb{E}[(\mathbf{x}^{(k)} - \hat{\mathbf{x}}_i^{k|k})(\mathbf{x}^{(k)} - \hat{\mathbf{x}}_i^{k|k})^\top] \preceq \bar{\mathbf{P}},\ \forall i \in \mathscr{V}.$$

**Proof.** The conclusion can be obtained by following (11.11) and the conclusion of Theorem 11.5. Since for each $i \in \mathscr{V}$, $\mu_{i,\tau}^{(k)} \to 1$ as $k \to \infty$. It follows from (11.11) that

$$\hat{\mathbf{x}}_i^{k|k} = \sum\nolimits_{\ell \in \mathscr{M}} \mu_{i,\ell}^{(k)} \hat{\mathbf{x}}_{i,\ell}^{k|k} \to \hat{\mathbf{x}}_{i,\tau}^{k|k}.$$

As a result,

$$\lim_{k\to\infty} \mathbb{E}[(\mathbf{x}^{(k)} - \hat{\mathbf{x}}_i^{k|k})(\mathbf{x}^{(k)} - \hat{\mathbf{x}}_i^{k|k})^\top]$$

$$= \mathbb{E}[(\mathbf{x}^{(k)} - \hat{\mathbf{x}}_{i,\tau}^{k|k})(\mathbf{x}^{(k)} - \hat{\mathbf{x}}_{i,\tau}^{k|k})^\top] \preceq \hat{\mathbf{P}}_{i,\tau}^{k|k},\ \forall i \in \mathscr{V},$$

where the last inequality is due to the guaranteed consistency of the mode-matched local estimate corresponding to the true mode. As $\hat{\mathbf{P}}_{i,\tau}^{k|k} \succ \mathbf{0}$, $\forall i \in \mathscr{V}$, the proof is completed by selecting $\bar{\mathbf{P}}$ such that $\bar{\mathbf{P}} \succeq \hat{\mathbf{P}}_{i,\tau}^{k|k}$, $\forall i \in \mathscr{V}$. ■

Following the discussion in Remark 11.2, when it comes to the scenario of multiple possible underlying modes, as long as the very mild joint detectability condition in Corollary 9.16 is satisfied for each possible mode (Condition C4), a uniform upper bound can always be found for the approximated local estimate error covariance matched to the mode. However, this is not sufficient to show that the actual error covariance of the output local estimate is uniformly upper bounded as the actual error covariances of the local estimates matched to wrong/inaccurate modes are in general not bounded by this uniform bound.

In summary, the uniform upper bound of the actual error covariance of the output local estimates is guaranteed by two keys. On one hand, the guaranteed consistency of the local estimates matched to the true underlying mode implies that its actual estimate error covariance is upper bounded by the approximated one, and hence upper bounded by the uniform upper bound. On the other hand, the guaranteed convergence to the true underlying mode. With these two keys jointly satisfied, the output local estimates are guaranteed to be consistent and therefore the error covariance of the output local estimate is upper bounded by the approximated error covariance, which is further uniformly upper bounded.

## 11.4 Simulations

In this section, simulations are given to show the performance of the extended algorithms, and to illustrate the analytical results in previous sections. The target of interest is assumed to move in the 2D-plane with two possible modes, *i.e.*, $\mathscr{M} = \{1,2\}$. The state vector

$$\mathbf{x}^{(k)} = [x^{(k)}, y^{(k)}, \dot{x}^{(k)}, \dot{y}^{(k)}, \ddot{x}^{(k)}, \ddot{y}^{(k)}]^\top,$$

with $x^{(k)}$ and $y^{(k)}$ being the position at time $k$ along each direction. On each direction, the target moves with a constant velocity if $\ell = 1$, and a constant acceleration if $\ell = 2$. The state transition matrices are therefore given as,

$$\mathbf{F}_1 = \begin{bmatrix} 1 & T \\ 0 & 1 \end{bmatrix} \otimes \mathbf{I}_2, \; \mathbf{F}_2 = \begin{bmatrix} 1 & T & \frac{1}{2}T^2 \\ 0 & 1 & T \\ 0 & 0 & 1 \end{bmatrix} \otimes \mathbf{I}_2,$$

where $T = 0.2$ second is the sampling period. The process noise covariance matrices are, respectively,

$$\mathbf{Q}_1 = \begin{bmatrix} \frac{1}{3}T^3 & \frac{1}{2}T^2 \\ \frac{1}{2}T^2 & T \end{bmatrix} \otimes \mathbf{I}_2, \; \mathbf{Q}_2 = \begin{bmatrix} \frac{1}{20}T^5 & \frac{1}{8}T^4 & \frac{1}{6}T^3 \\ \frac{1}{8}T^4 & \frac{1}{3}T^3 & \frac{1}{2}T^2 \\ \frac{1}{6}T^3 & \frac{1}{2}T^2 & T \end{bmatrix} \otimes \mathbf{I}_2.$$

Note that each mode-matched estimate has different dimension. When outputting the estimate using (11.11), the estimate based on mode 1 will only affect the first four dimensions of the outputting estimate. Two simulations are given.

**Simulation 1**. The first simulation is done for the case where the underlying mode is fixed as mode 2. A set of 8 agents with topology shown on the top of Figure 11.1 are used to track

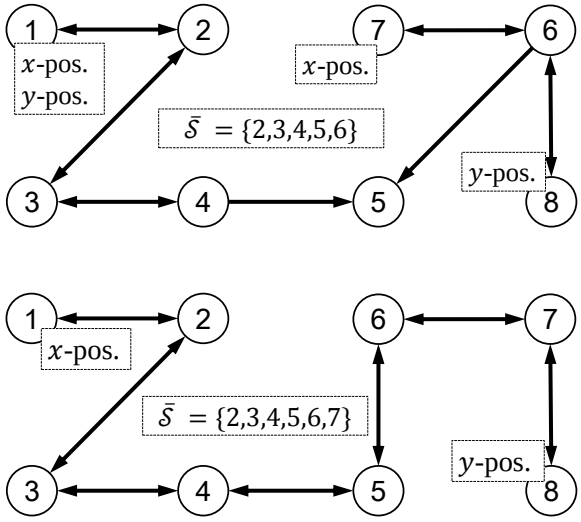


Figure 11.1: Topologies for simulation 1 (top) and 2 (bottom).

the target. Specifically, agent 7 and agent 8 are able to sense only the position of the target along, respectively, the $x$ and $y$ direction; agent 1 is able to sense both. None of the other agents is able to directly sense the target, *i.e.*, $\bar{\mathscr{S}} = \{2,3,4,5,6\}$. Note that there is not even a direct spanning tree in this graph. A hypothetic centralized (ctlz.) GPB1 estimator with all measurements collected from the entire network is used as the benchmark. The trajectories estimated by the centralized GPB1 estimator and the local agents using the GPB1-based DHIF (GPB1-DHIF) algorithm are plotted along with the true trajectory in Figure 11.2. As observed, all local agents successfully track the target. The probabilities of mode 1 being true, computed by the centralized GPB1 and by the GPB1-DHIF algorithm, are plotted in Figure 11.3. As observed, all agents asymptotically identify the underlying mode. The errors of the overall local estimates as well as the corresponding $3\sigma$-envelopes, computed by the centralized GPB1 and by the GPB1-DHIF algorithm, for states 2, 3

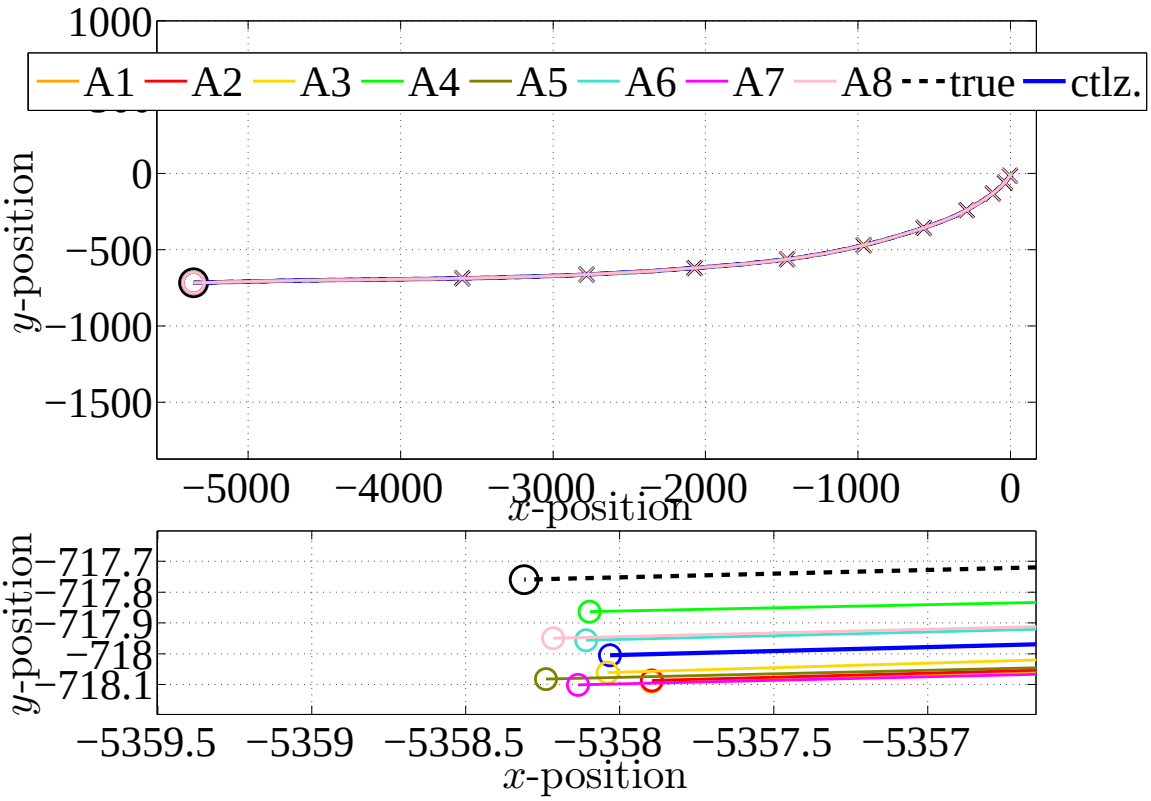


Figure 11.2: True trajectory as well as the trajectories estimated by the centralized GPB1 and the GPB1-DHIF algorithm: overview (top) and zoomed-in view (bottom) at the final location.

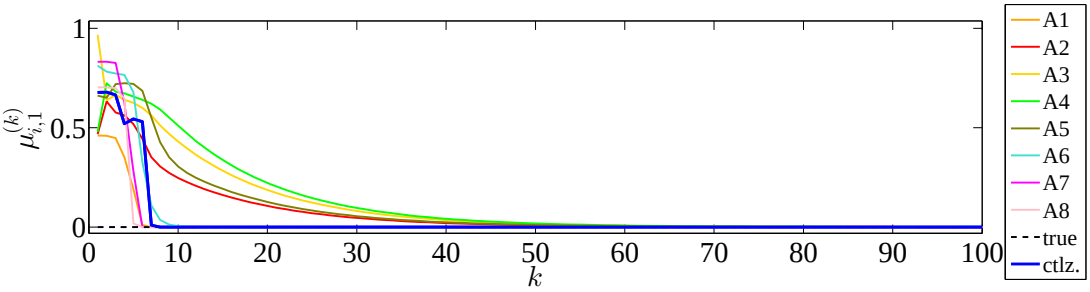


Figure 11.3: Probability of mode 1 computed by the centralized GPB1 and by the GPB1-DHIF algorithm.

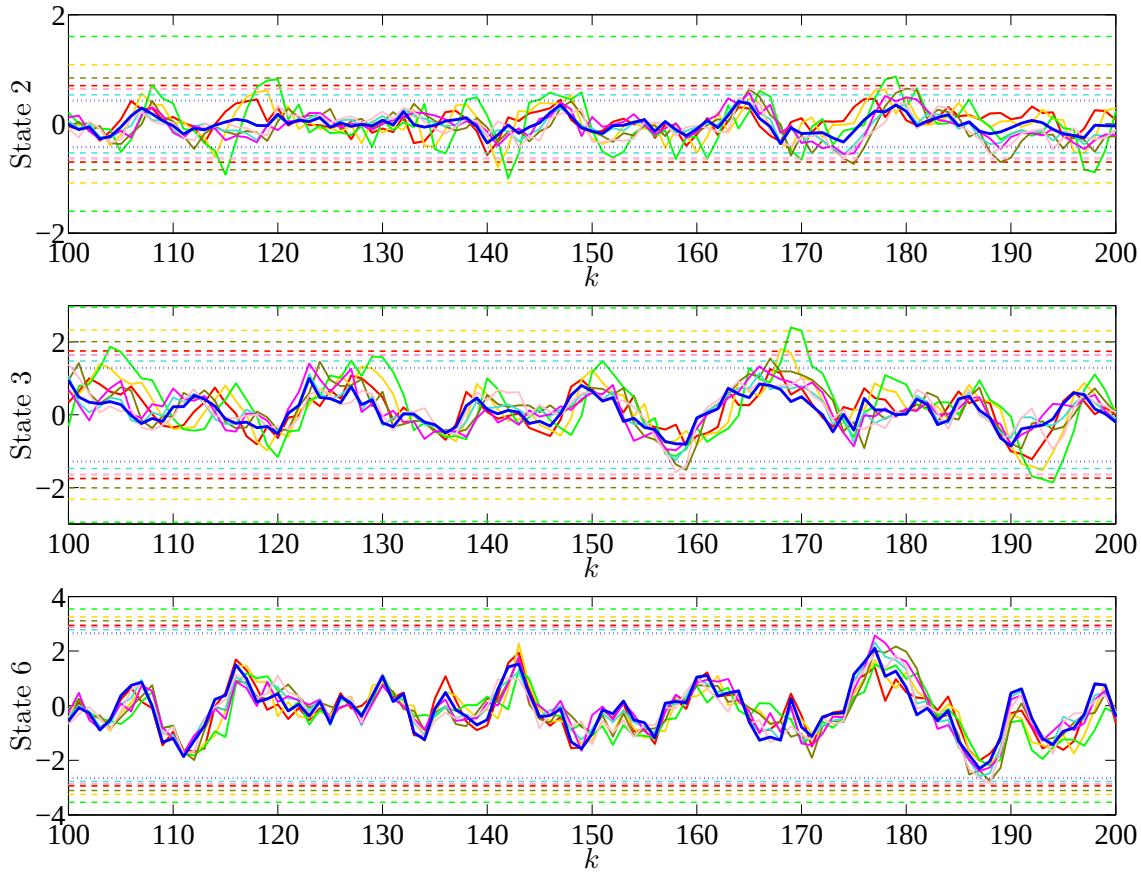


Figure 11.4: Errors of the overall local estimates (solid lines) as well as the corresponding $3\sigma$-envelopes (dashed lines in the same colors) by the GPB1-DHIF algorithm and the centralized GPB1 in steady state: $y$-position (top), $x$-velocity (middle) and $y$-acceleration (bottom). The colors are consistent with Figure 11.3.

and 6 are plotted in Figure 11.4. As observed, the errors are bounded by in the $3\sigma$-envelopes. This verifies the conclusion of Corollary 11.6.

**Simulation 2**. In the second simulation, we let the target have its underlying mode subjected to change over time. The mode transition matrix is

$$\mathbf{\Pi} = \begin{bmatrix} 0.99 & 0.01 \\ 0.01 & 0.99 \end{bmatrix}.$$

A set of 8 agents with topology shown on the right-hand side of Figure 11.1 is used to track the target. Specifically, only agent 1 and agent 8 are able to sense only the position of the target along, respectively, $x$ and $y$ direction. Therefore, $\bar{\mathscr{S}} = \{2,3,4,5,6,7\}$. Note that the network connectivity is very week. Moreover, there is not a single agent with joint observability about the target of interest in its inclusive neighborhood. A hypothetic centralized (ctlz.) IMM estimator with all measurements across the network is used as the benchmark. The trajectories estimated by the centralized IMM and by the local agents using the IMM-based DHIF (IMM-DHIF) algorithm are plotted along with the true trajectory in Figure 11.5. As observed in the figure, all local agents successfully track the target. The probability of mode 1 being true, computed by the centralized IMM and the IMM-DHIF algorithm are plotted along with the true underlying mode in Figure 11.6. As observed that the mode probabilities computed by IMM-DHIF algorithm follow the trend of the true mode switching. Compared to the centralized IMM estimator, the local agents, especially the ones that are more "distant" from the agents directly sensing the target, have slower reaction to the mode switching. This is due to the weak connectivity of the communication graph and poor local joint observabilities at each agent.

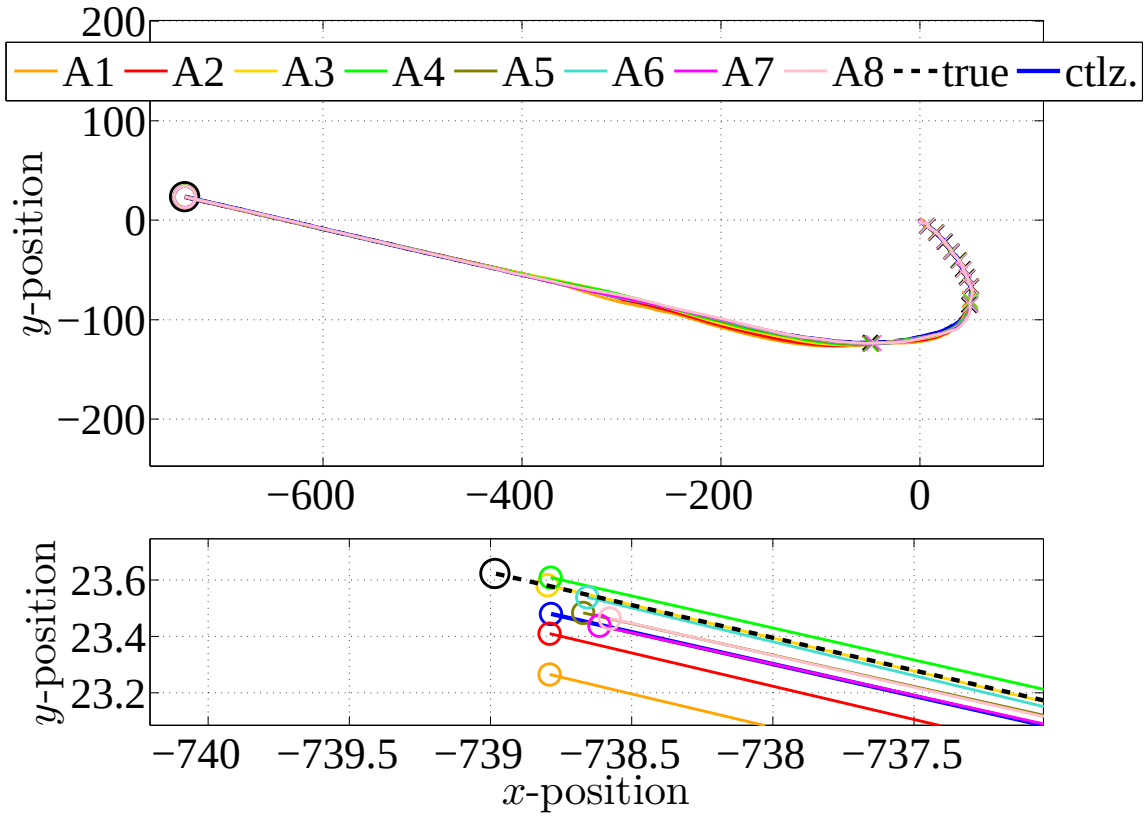


Figure 11.5: True trajectory as well as the trajectories estimated by the centralized IMM and the IMM-DHIF algorithm: overview (top) and zoomed-in view at the final location.

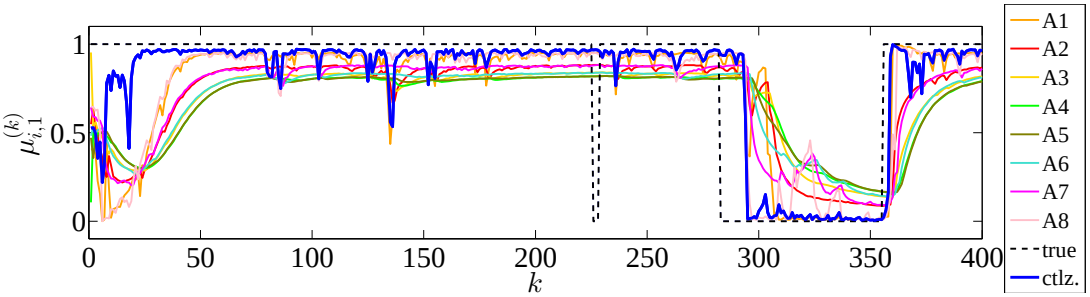


Figure 11.6: Probability of mode 1 computed by the centralized IMM and by the IMM-DHIF algorithm

## 11.5 Conclusion

This chapter extends the DHIF algorithm proposed in Chapter 9 to the scenario where the process model (respectively, models) of interest is (respectively, are) uncertain. Two algorithms are extended and shown to have the advantages of being fully distributed, robust against agents not directly sensing the target and require only a single communication iteration during each sampling interval. When the underlying model is unknown but fixed, all local agents are analytical shown to asymptotically identify the true underlying mode and hence come up with consistent output local estimates with sufficient conditions proposed. Simulations are used to illustrate the effectiveness of the proposed algorithms.

# Chapter 12

# Conclusion & Future Work

## 12.1 Conclusion

Part II studies the problem of distributed dynamic state estimation using networked local multi-agents. The scenario where the process and sensing models are both linear, is first considered in Chapter 9. The proposed distributed hybrid information fusion (DHIF) algorithm has the advantages of being unified, being robust against the presence of local agents sensing no target, and requiring no global information and only a single communication iteration during each time interval. It is also explored in this work the very mild conditions on general directed switching graphs and joint network observability/detectability to guarantee the stochastic stability of the proposed algorithm.

Then the DHIF algorithm is extended to two more general scenarios, namely, the scenario with nonlinearities involved in both the process and the sensing models, and the scenario with uncertain process models. In the former scenario, a nonlinear DHIF algorithm is proposed by adopting the unscented transformation approach. In the latter one, two algorithms are proposed by following

the two well-known multiple model (MM) paradigms, namely, the first order generalized pseudo Bayesian and the interacting MM approaches. The extended algorithms in both scenarios inherit the advantages of the original DHIF algorithm. The stability is also rigorously analyzed in each extended case.

## 12.2 Future Work

There are several potential directions for the future work. First of all, it would be interesting to analytically look into how the network topologies affects the performance difference between the DHIF algorithm and the centralized Kalman filter. This would be useful in designing the sensor network that works efficiently yet keeps a low cost. Secondly, it would be useful to analytically show the time invariance property of the local approximated estimate error covariance given arbitrary initial conditions in the case with LTI models and time-invariant communication graph. This would be the counterpart of the discrete algebraic Riccati equation of the centralized Kalman filter, in the distributed scenario. Thirdly, the stability analyzes for the IMM-based DHIF algorithm and the nonlinear-DHIF algorithm with nonlinear sensing model, are still to be explored. Last, it is also possible to consider the scenario with multiple nonlinear process models, and to combine the proposed MM-DHIF algorithm with the nonlinear-DHIF algorithm for such a scenario. It would be interesting yet very challenging to rigorously analyze the stability properties of the combined algorithm.

# Bibliography


[1] Ali Abur and Antonio Gomez Exposito. *Power system state estimation: theory and implementation*. CRC Press, 2004.

[2] M. Alighanbari and J.P. How. An unbiased Kalman consensus algorithm. In *Proc. American Control Conf.*, pages 3519–3524, Minneapolis, MN, June 2006.

[3] Badr N Alsuwaidan, John L Crassidis, and Yang Cheng. Generalized multiple-model adaptive estimation using an autocorrelation approach. *IEEE Transactions on Aerospace and Electronic Systems*, 47(3):2138–2152, 2011.

[4] Brian DO Anderson and John B Moore. *Optimal filtering*. Courier Corporation, 2012.

[5] He Bai, Randy A Freeman, and Kevin M Lynch. Distributed Kalman filtering using the internal model average consensus estimator. In *Proc. American Control Conf.*, pages 1500–1505, San Francisco, CA, 2011.

[6] Yaakov Bar-Shalom, Xiao-Rong Li, and Thiagalingam Kirubarajan. *Estimation with applications to tracking and navigation*. John Wiley & Sons, Inc. cop., New York (N.Y.), Chichester, Weinheim, 2001.

[7] G. Battistelli, L. Chisci, and C. Fantacci. Parallel consensus on likelihoods and priors for networked nonlinear filtering. *Signal Processing Letters, IEEE*, 21(7):787–791, July 2014.

[8] G. Battistelli, L. Chisci, G. Mugnai, A. Farina, and A. Graziano. Consensus-based linear and nonlinear filtering. *Automatic Control, IEEE Transactions on*, 60(5):1410–1415, May 2015.

[9] Giorgio Battistelli and Luigi Chisci. Kullback–Leibler average, consensus on probability densities, and distributed state estimation with guaranteed stability. *Automatica*, 50(3):707–718, 2014.

[10] Giorgio Battistelli and Luigi Chisci. Stability of consensus extended Kalman filter for distributed state estimation. *Automatica*, 68:169 – 178, 2016.

[11] Henk AP Blom and Yaakov Bar-Shalom. The interacting multiple model algorithm for systems with markovian switching coefficients. *IEEE Transactions on Automatic Control*, 33(8):780–783, 1988.

[12] Rakesh B Bobba, Katherine M Rogers, Qiyan Wang, Himanshu Khurana, Klara Nahrstedt, and Thomas J Overbye. Detecting false data injection attacks on dc state estimation. In *In Proceedings of the First Workshop on Secure Control Systems, CPSWeek*, volume 2010, April 2010.

[13] Stephen Boyd and Lieven Vandenberghe. *Convex optimization*. Cambridge university press, 2004.

[14] David W Casbeer and Randy Beard. Distributed information filtering using consensus filters. In *Proc. American Control Conf.*, pages 1882–1887, St. Louis, MO, June 2009.

[15] F.S. Cattivelli and A.H. Sayed. Diffusion strategies for distributed Kalman filtering and smoothing. *IEEE Transactions on Automatic Control*, 55(9):2069–2084, September 2010.

[16] G. Dan and H. Sandberg. Stealth attacks and protection schemes for state estimators in power systems. In *IEEE International Conference on Smart Grid Communications*, pages 214–219, October 2010.

[17] Ruilong Deng, Jiming Chen, Xianghui Cao, Yan Zhang, S. Maharjan, and S. Gjessing. Sensing-performance tradeoff in cognitive radio enabled smart grid. *IEEE Transactions on Smart Grid*, 4(1):302–310, 2013.

[18] Oliver E Drummond, Albert J Perrella Jr, and Steven Waugh. On target track covariance consistency. In *Signal and Data Processing of Small Targets*, volume 6236, pages 623615.1–623615.14, Kissimmee, FL, 2006.

[19] C. Fantacci, G. Battistelli, L. Chisci, A. Farina, and A. Graziano. Multiple-model algorithms for distributed tracking of a maneuvering target. In *Information Fusion (FUSION), 2012 15th International Conference on*, pages 1028–1035, July 2012.

[20] Marcello Farina, Giancarlo Ferrari-Trecate, Riccardo Scattolini, et al. Distributed moving horizon estimation for linear constrained systems. *IEEE Transactions on Automatic Control*, 55(11):2462–2475, 2010.

[21] Jay A Farrell. *Aided navigation: GPS with high rate sensors*. McGraw-Hill, New York City, NY, 2008.

[22] Dietrich Franken and Andreas Hupper. Improved fast covariance intersection for distributed data fusion. In *Proceedings of the International Conference on Information Fusion*, pages 25–28, Philadelphia, PA, 2005.

[23] Michael Grant and Stephen Boyd. Cvx: Matlab software for disciplined convex programming, version 2.1. `http://cvxr.com/cvx`, March 2014.

[24] Jonathan L Gross and Jay Yellen. *Handbook of graph theory*. CRC press, 2003.

[25] Nikos Hatziargyriou, Hiroshi Asano, Reza Iravani, and Chris Marnay. Microgrids. *IEEE Power and Energy Magazine*, 5(4):78–94, 2007.

[26] Jinwen Hu, Lihua Xie, and Cishen Zhang. Diffusion Kalman filtering based on covariance intersection. *Signal Processing, IEEE Transactions on*, 60(2):891–902, February 2012.

[27] Andrew H Jazwinski. *Stochastic Processes and Filtering Theory*. Academic Press, 1970.

[28] Liyan Jia, R.J. Thomas, and Lang Tong. Impacts of malicious data on real-time price of electricity market operations. In *45th Hawaii International Conference on System Science*, pages 1907–1914, January 2012.

[29] Simon J. Julier and Jeffrey K. Uhlmann. New extension of the kalman filter to nonlinear systems, 1997.

[30] S.J. Julier and J.K. Uhlmann. A non-divergent estimation algorithm in the presence of unknown correlations. In *Proc. American Control Conf.*, pages 2369–2373, Albuquerque, NM, 1997.

[31] Rudolph Emil Kalman. A new approach to linear filtering and prediction problems. *Transactions of the ASME, Journal of Fluids Engineering*, 82(1):35–45, 1960.

[32] A. Kamal, J. Bappy, J. Farrell, and A. Roy-Chowdhury. Distributed multi-target tracking and data association in vision networks. *IEEE Transactions on Pattern Analysis and Machine Intelligence*, PP(99):1–1, 2015.

[33] Ahmed Tashrif Kamal, Chong Ding, Bi Song, Jay A Farrell, and AK Roy-Chowdhury. A generalized Kalman consensus filter for wide-area video networks. In *Proc. IEEE Conf. on Decision and Control*, pages 7863–7869, Orlando, FL, 2011.

[34] Ahmed Tashrif Kamal, Jay A Farrell, and Amit K Roy Chowdhury. Information consensus for distributed multi-target tracking.

[35] Ahmed Tashrif Kamal, Jay A Farrell, and Amit K Roy Chowdhury. Information weighted consensus. In *CDC*, pages 2732–2737, 2012.

[36] Ahmed Tashrif Kamal, Jay A Farrell, and Amit K Roy Chowdhury. Information weighted consensus filters and their application in distributed camera networks. *IEEE Transactions on Automatic Control*, 58(12):3112–3125, 2013.

[37] U.A Khan and A Jadbabaie. On the stability and optimality of distributed Kalman filters with finite-time data fusion. In *American Control Conference (ACC), 2011*, pages 3405–3410, June 2011.

[38] U.A Khan and J.M.F. Moura. Distributing the Kalman filter for large-scale systems. *Signal Processing, IEEE Transactions on*, 56(10):4919–4935, Oct 2008.

[39] Derek B. Kingston and Randal W. Beard. Discrete-time average-consensus under switching network topologies. In *Proc. American Control Conf.*, Minneapolis, MN, June 2006.

[40] D. Kleinman and M. Athans. The design of suboptimal linear time-varying systems. *IEEE Transactions on Automatic Control*, 13(2):150–159, Apr 1968.

[41] Oliver Kosut, Liyan Jia, Robert J Thomas, and Lang Tong. Malicious data attacks on the smart grid. *IEEE Transactions on Smart Grid*, 2(4):645–658, 2011.

[42] Benjamin Kroposki, Robert Lasseter, Toshifumi Ise, Satoshi Morozumi, S Papatlianassiou, and Nikos Hatziargyriou. Making microgrids work. *IEEE Power and Energy Magazine*, 6(3):40–53, 2008.

[43] D. J. Lee. Nonlinear estimation and multiple sensor fusion using unscented information filtering. *IEEE Signal Processing Letters*, 15:861–864, 2008.

[44] William S Levine. *The control handbook*. CRC press, 1996.

[45] W. Li and Y. Jia. Consensus-based distributed multiple model ukf for jump markov nonlinear systems. *IEEE Transactions on Automatic Control*, 57(1):227–233, Jan 2012.

[46] W. Li, G. Wei, F. Han, and Y. Liu. Weighted average consensus-based unscented kalman filtering. *IEEE Transactions on Cybernetics*, 46(2):558–567, Feb 2016.

[47] Wenling Li and Yingmin Jia. Consensus-based distributed multiple model UKF for jump markov nonlinear systems. *IEEE Transactions on Automatic Control*, 57(1):227–233, Jan 2012.

[48] X Rong Li and Vesselin P Jilkov. Survey of maneuvering target tracking. part i. dynamic models. *IEEE Transactions on Aerospace and Electronic Systems*, 39(4):1333–1364, 2003.

[49] G. Liu, F. Worgotter, and I. Markelic. Square-root sigma-point information filtering. *IEEE Transactions on Automatic Control*, 57(11):2945–2950, Nov 2012.

[50] Yao Liu, Peng Ning, and Michael K Reiter. False data injection attacks against state estimation in electric power grids. *ACM Transactions on Information and System Security (TISSEC)*, 14(1):13, 2011.

[51] K. Ma, G. Hu, and C. J. Spanos. Energy consumption control via real-time pricing feedback in smart grid. *IEEE Transactions on Control Systems Technology*, 22(5):1907–1914, 2014.

[52] Ion Matei and John S Baras. Consensus-based linear distributed filtering. *Automatica*, 48(8):1776–1782, 2012.

[53] Pablo Millán, Luis Orihuela, Carlos Vivas, and Francisco R Rubio. Distributed consensus-based estimation considering network induced delays and dropouts. *Automatica*, 48(10):2726–2729, 2012.

[54] Yilin Mo, T.H.-H. Kim, K. Brancik, D. Dickinson, Heejo Lee, A Perrig, and B. Sinopoli. Cyber physical security of a smart grid infrastructure. *Proceedings of the IEEE, Special Issue on Cyber-Physical Systems*, 100(1):195–209, January 2012.

[55] A. Mohammadi and K.N. Plataniotis. Distributed widely linear multiple-model adaptive estimation. *IEEE Transactions on Signal and Information Processing over Networks*, 1(3):164–179, September 2015.

[56] J Nanda, Lakshman Hari, and ML Kothari. Economic emission load dispatch with line flow constraints using a classical technique. *IEE Proceedings-Generation, Transmission and Distribution*, 141(1):1–10, 1994.

[57] W. Niehsen. Information fusion based on fast covariance intersection filtering. In *Proceedings of the International Conference on Information Fusion*, volume 2, pages 901–904, Annapolis, MD, 2002.

[58] R. Olfati-Saber and R. M. Murray. Consensus problems in networks of agents with switching topology and time-delays. *IEEE Transactions on Automatic Control*, 49(9):1520–1533, Sept 2004.

[59] Reza Olfati-Saber. Distributed Kalman filter with embedded consensus filters. In *Decision and Control, 2005 and 2005 European Control Conference. CDC-ECC'05. 44th IEEE Conference on*, pages 8179–8184. IEEE, 2005.

[60] Reza Olfati-Saber. Distributed Kalman filtering for sensor networks. In *Proc. IEEE Conf. on Decision and Control*, pages 5492–5498, New Orleans, LA, December 2007.

[61] Reza Olfati-Saber. Kalman-consensus filter: Optimality, stability, and performance. In *Proc. IEEE Conf. on Decision and Control*, pages 7036–7042, Shanghai, China, December 2009.

[62] Francesco Palmieri, Sergio Ricciardi, Ugo Fiore, Massimo Ficco, and Aniello Castiglione. Energy-oriented denial of service attacks: an emerging menace for large cloud infrastructures. *The Journal of Supercomputing*, 71(5):1620–1641, 2013.

[63] Md Rahman and Hamed Mohsenian-Rad. False data injection attacks with incomplete information against smart power grids. In *IEEE Global Communications Conference*, pages 3153–3158. IEEE, 2012.

[64] Konrad Reif, Stefan Günther, Engin Yaz, and Rolf Unbehauen. Stochastic stability of the discrete-time extended kalman filter. *IEEE Transactions on Automatic control*, 44(4):714–728, 1999.

[65] Wei Ren, Randal W. Beard, and Derek B. Kingston. Multi-agent Kalman consensus with relative uncertainty. In *Proc. American Control Conf.*, pages 1865–1870, Portland, OR, June 2005.

[66] Henrik Sandberg, André Teixeira, and Karl H Johansson. On security indices for state estimators in power networks. In *Preprints of the First Workshop on Secure Control Systems*, Stockholm, Sweden, 2010.

[67] Kin Cheong Sou, H. Sandberg, and K.H. Johansson. Computing critical $k$-tuples in power networks. *IEEE Transactions on Power Systems*, 27(3):1511–1520, 2012.

[68] Kin Cheong Sou, H. Sandberg, and K.H. Johansson. Detection and identification of data attacks in power system. In *Proc. American Control Conf.*, pages 3651–3656, June 2012.

[69] Kin Cheong Sou, Henrik Sandberg, and Karl Henrik Johansson. On the exact solution to a smart grid cyber-security analysis problem. *IEEE Transactions on Smart Grid*, 4(2):856–865, 2013.

[70] Marco H Terra, João Yoshiyuki Ishihara, Gildson Jesus, et al. Information filtering and array algorithms for discrete-time markovian jump linear systems. *IEEE Transactions on Automatic Control*, 54(1):158, 2009.

[71] Yongge Tian. The dimension of the intersection of k subspaces. *Missouri Journal of Mathematical Science*, 14(2):2, 2002.

[72] S. Y. Tu and A. H. Sayed. Diffusion strategies outperform consensus strategies for distributed estimation over adaptive networks. *IEEE Transactions on Signal Processing*, 60(12):6217–6234, Dec 2012.

[73] V. Ugrinovskii. Distributed robust filtering with $h_\infty$ consensus of estimates. *Automatica*, 47(1):1 – 13, 2011.

[74] V. Ugrinovskii. Conditions for detectability in distributed consensus-based observer networks. *IEEE Transactions on Automatic Control*, 58(10):2659–2664, Oct 2013.

[75] V Ugrinovskii. Detectability of distributed consensus-based observer networks: An elementary analysis and extensions. In *Control Conference (AUCC), 2014 4th Australian*, pages 188–192. IEEE, 2014.

[76] Valery Ugrinovskii. Distributed robust estimation over randomly switching networks using $h_\infty$ consensus. *Automatica*, 49(1):160–168, 2013.

[77] S. Wang, J. Feng, and C. K. Tse. A class of stable square-root nonlinear information filters. *IEEE Transactions on Automatic Control*, 59(7):1893–1898, July 2014.

[78] Shaocheng Wang and Wei Ren. Stealthy attacks in power systems: Limitations on manipulating the estimation deviations caused by switching network topologies. In *Proc. IEEE Conf. on Decision and Control*, pages 217–222, Los Angeles, CA, December 2014.

[79] Shaocheng Wang and Wei Ren. Stealthy false data injection attacks against state estimation in power systems: Switching network topologies. In *Proc. American Control Conf.*, pages 1572–1577, Portland, OR, June 2014.

[80] Shaocheng Wang and Wei Ren. On the consistency and confidence of distributed dynamic state estimation in wireless sensor networks. In *Proc. IEEE Conf. on Decision and Control*, pages 3069–3074, Osaka, Japan, December 2015.

[81] Shaocheng Wang and Wei Ren. On the convergence of distributed estimation of LTV dynamic system with switching directed topologies and time-varying sensing models. In *Proc. American Control Conf.*, pages 5437–5442, Boston, MA, July 2016.

[82] Shaocheng Wang, Wei Ren, and Jie Chen. Fully distributed state estimation with multiple model approach. In *Proc. IEEE Conf. on Decision and Control*, Las Vegas, NV, December 2016. to appear.

[83] Yimin Wang and X.R. Li. A fast and fault-tolerant convex combination fusion algorithm under unknown cross-correlation. In *12th International Conference on Information Fusion*, pages 571–578, Seattle, WA, July 2009.

[84] Allen J Wood and Bruce F Wollenberg. *Power generation, operation, and control*. John Wiley & Sons, 2012.

[85] Lin Xiao, Stephen Boyd, and Sanjay Lall. Distributed average consensus with time-varying metropolis weights. *Automatica*, 2006.

[86] Le Xie, Yilin Mo, and Bruno Sinopoli. Integrity data attacks in power market operations. *IEEE Transactions on Smart Grid*, 2(4):659–666, 2011.

[87] K Xiong, HY Zhang, and CW Chan. Performance evaluation of ukf-based nonlinear filtering. *Automatica*, 42(2):261–270, 2006.

[88] Ray Daniel Zimmerman, Carlos Edmundo Murillo-Sánchez, and Robert John Thomas. Matpower: Steady-state operations, planning, and analysis tools for power systems research and education. *IEEE Transactions on Power Systems*, 26(1):12–19, 2011.